

ÉCOLE DE TECHNOLOGIE SUPÉRIEURE  
UNIVERSITÉ DU QUÉBEC

THESIS PRESENTED TO  
ÉCOLE DE TECHNOLOGIE SUPÉRIEURE

IN PARTIAL FULFILLMENT OF THE REQUIREMENTS FOR  
THE DEGREE OF DOCTOR OF PHILOSOPHY  
Ph. D.

BY  
Pradeep Kumar THALLA

BIOACTIVE COATING WITH LOW-FOULING POLYMERS FOR THE  
DEVELOPMENT OF BIOCOMPATIBLE VASCULAR IMPLANTS

MONTREAL, NOVEMBER 14, 2014



Pradeep Kumar Thalla, 2014



This Creative Commons licence allows readers to download this work and share it with others as long as the author is credited. The content of this work may not be modified in any way or used commercially.

**BOARD OF EXAMINERS (THESIS PH.D.)**

THIS THESIS HAS BEEN EVALUATED

BY THE FOLLOWING BOARD OF EXAMINERS

Prof. Sophie Lerouge, Thesis Supervisor  
Department of Mechanical Engineering at École de technologie supérieure

Prof. Gregory De Crescenzo, Thesis Co-supervisor  
Department of Chemical Engineering at École Polytechnique de Montreal

Prof. Nicola Hagemeister, Chair, Board of Examiners  
Department of Automated Production at École de technologie supérieure

Prof. Robert Hausler, Member of the jury  
Department of Construction Engineering at École de technologie supérieure

Prof. Maud Gorbet, External Evaluator  
Department of Systems Design Engineering at University of Waterloo

THIS THESIS WAS PRESENTED AND DEFENDED

IN THE PRESENCE OF A BOARD OF EXAMINERS AND THE PUBLIC

ON OCTOBER 8, 2014

AT ECOLE DE TECHNOLOGIE SUPERIEURE



## ACKNOWLEDGEMENTS

First and foremost, I would like to express my profound thanks and appreciation to my supervisors. I am extremely grateful to Dr. Sophie Lerouge for always being there with valuable guidance and encouragement. Her support, helpful advice and patience played a key role enabling me to reach this point. I would like to express my gratitude to my co-supervisor, Dr. Gregory De Crescenzo for his constant support throughout my journey in completing this work. Having two highly accomplished researchers in the field of biomaterials as my supervisors enabled me to learn a lot about not only the field but also how to tackle research problems in general.

Since this is a multidisciplinary project, I had the support and cooperation of other research labs. Therefore, I would like to extend my sincere gratitude to Dr. Yahye Merhi for his expertise in thrombosis experiments, valuable suggestions on my research and support for completing this work. I would also like to thank Professor Michael R. Wertheimer for his expertise in plasma polymerization and support during this project. I would like to continue by acknowledging the researchers of Sophie Lerouge's and Gregory De Crescenzo's labs. Many thanks to Marion Marie for valuable assistance in the lab, particularly for cell culture experiments. I would like to thank my co-authors who contributed to papers and provided support by preparing samples; Benoit for his guidance on chemical grafting, Hicham for his help with perfusion assays, Angel, Bachir and Houman for LP depositions and Pauline for cell culture experiments. Finally, I would also like to thank all of my colleagues (Elias, Audrey, Caroline, Fatemeh and Matthew) at our research lab, Laboratoire de biomatériaux endovasculaires (LBeV), for their encouragement, scientific discussions and help with translation (French to English) when I had difficulties understanding French.

I am deeply grateful to jury members Professor Nicola Hagemester, Professor Maud Gorbet, and Professor Robert Hausler for taking the time to review my doctoral thesis.

Last but not least, I would like to thank my family, whose support was contributed so much to the completion of this project. My wife, Tarangini Reddy, has been an infinite source of inspiration, encouragement and understanding during my time as a PhD student, and this has made me realize that together anything is possible. My mother Vijaya Thalla, my sister Sindhura and my in-laws Rohini Kumar, Vijaya Laxmi, Uday Bhaskar, and Vasanth Reddy have continually supported me, stood behind me over the years and fostered my desire to take on new challenges. I would also like to mention the names of my well-wishers Jyothi, Raju, Shruthi and Venu, for their constant encouragement and support during my time as a PhD student.

Finally, I would like to dedicate this thesis to my late father Venkat Reddy Thalla and my spiritual guru Shri Parthasaradhi Rajagopala Chariji.

# REVÊTEMENT BIOACTIF AVEC POLYMÈRES DE LOW-FOULING POUR LE DÉVELOPPEMENT DES IMPLANTS VASCULAIRES BIOCOMPATIBLES

Pradeep Kumar THALLA

## RÉSUMÉ

Le remplacement de vaisseaux sanguins occlus et la réparation endovasculaire des anévrismes de l'aorte abdominale (EVAR) effectués respectivement à l'aide de prothèses vasculaires synthétiques et d'endoprothèses couvertes, mènent tous deux à de fréquentes complications cliniques due à une problématique similaire : les matériaux utilisés (généralement le polyéthylène téréphthalate (PET) et le polytétrafluoroéthylène expansé (ePTFE) n'ont pas les propriétés de surface permettant de réduire les réactions biologiques indésirables tout en favorisant les interactions cellulaires requises pour la croissance des tissus biologiques. Par conséquent, l'objectif principal de cette thèse consistait à créer un revêtement bioactif sur les biomatériaux vasculaires pour réduire la thrombose tout en favorisant la croissance cellulaire.

Le premier objectif a consisté à mettre au point une surface empêchant l'adsorption des protéines (communément appelée « low-fouling ») à l'aide de polyéthylène glycol (PEG) à bras multiples. Un revêtement polymérisé par plasma riche en amine primaire (LP) a été utilisé comme substrat afin d'obtenir un revêtement polyvalent, pouvant être recréé sur n'importe quel type de biomatériaux ou de surface, ce qui n'est pas le cas des méthodes actuelles qui requièrent d'optimiser la technique de greffage pour chaque nouveau biomatériau. Tel que démontré par microbalance à cristal de quartz avec dissipation (QCM-D), par mesure directe de fluorescence ainsi que lors d'essais de perfusion sanguins, les revêtements de PEG créés génèrent une très faible adsorption de protéine et presque pas l'adhésion des plaquettes après 15 min de perfusion dans le sang total. Bien que l'adsorption des protéines ne soit pas empêchée à 100% et que les propriétés anti-plaquetaires ne permettent pas de conclure sur l'absence de thrombogénicité à long terme in vivo du revêtement, les propriétés de ce dernier peuvent être exploitées pour y coupler des molécules bioactives. Par conséquent, le second objectif consistait à développer un revêtement bioactif innovant et polyvalent en utilisant la combinaison de peptide d'adhésion (KQAGDV/RGD) et de facteur de croissance épidermique (EGF) greffé par le biais de coils électrostatiques. Le dextran carboxyméthylé (CMD) a été choisi comme une alternative possible au PEG en raison de ses meilleures propriétés « low-fouling » et la présence de groupes terminaux carboxyl abondants. Bien que la technique QCM-D nous ait permis d'optimiser la combinaison de l'immobilisation KQAGDV / RGD et EGF, les essais cellulaires n'ont pas montré d'amélioration de l'adhésion des cellules musculaires lisses vasculaires (CMLV) sur les surfaces PEG ou CMD modifiées par les peptides.

Ce résultat met en évidence, parmi d'autres facteurs, le difficile compromis à trouver pour empêcher l'adsorption des protéines sans empêcher l'adhésion cellulaire. Des travaux

## VIII

antérieurs du laboratoire suggéraient que la chondroïtine sulfate (CS), un glycoaminoglycan sulphaté, permettait de trouver ce compromis. Pour cette raison, le dernier objectif de cette thèse a consisté à étudier les propriétés de revêtements de CS comparativement aux deux polymères « low-fouling », le PEG et le CMD. Il a été démontré que la CS présente des propriétés anti-fouling sélectives puisque l'adsorption du fibrinogène est presque totalement supprimée tandis que d'autres protéines (et notamment certains facteurs de croissance connus pour interagir avec la CS) sont favorisées. La CS, comme le PEG et le CMD, diminue nettement l'adhésion plaquettaire en deça du niveau observé sur le PET. Par contre, alors que l'adhésion cellulaire sur le PEG et le CMD est très limitée, la CS favorise un attachement cellulaire prononcé, avec adhésion focale et résistance au cisaillement. Au contraire, les cellules endothéliales se détachent facilement du PET non modifié. Ainsi, les revêtements de CS forment une surface peu thrombogène favorisant la croissance d'une couche endothéliale complète et stable qui pourra agir comme surface anti-thrombotique active. Ensemble, l'utilisation du polymère plasma et de la CS greffée, suivie éventuellement d'immobilisation de facteurs de croissance, semble avoir un fort potentiel comme revêtement bioactif pour optimiser la biocompatibilité et les résultats cliniques des implants, en particulier des prothèses vasculaires.

**Mots-clés:** revêtement bioactif, prothèse vasculaire, endoprothèse, low-fouling, non thrombogénique, adhésion de peptides, facteur de croissance épidermique, microbalance à cristal de quartz avec dissipation.

# BIOACTIVE COATING WITH LOW-FOULING POLYMERS FOR THE DEVELOPMENT OF BIOCOMPATIBLE VASCULAR IMPLANTS

Pradeep Kumar THALLA

## ABSTRACT

The replacement of occluded blood vessels and endovascular aneurysm repair (EVAR) are performed with the use of synthetic vascular grafts and stent grafts, respectively. Both implants lead to frequent clinical complications that are different but due to a similar problem, namely the inadequate surface properties of the polymeric biomaterials used (generally polyethylene terephthalate (PET) or expanded polytetrafluoroethylene (ePTFE)). Therefore the general objective of this thesis was to create a versatile bioactive coating on vascular biomaterials that reduce material-induced thrombosis and promote desired cell interactions favorable to tissue healing around implants. The use of low-fouling backgrounds was decided in order to reduce platelet adhesion as well as the non-specific protein adsorption and thus increase the bioactivity of immobilized biomolecules.

As part of the preliminary objective, a multi-arm polyethylene glycol (PEG) was chosen to create a versatile low-fouling surface, since the current coating methods are far from being versatile and rely on the availability of compatible functional groups on both PEG and the host surface. This PEG coating method was developed by taking advantage of novel primary amine-rich plasma polymerized coatings (LP). As demonstrated by quartz crystal microbalance with dissipation (QCM-D), fluorescence measurements and platelet adhesion assays, our PEG coatings exhibited low protein adsorption and almost no platelet adhesion after 15 min perfusion in whole blood. Although protein adsorption was not completely abrogated and short-term platelet adhesion assay was clearly insufficient to draw conclusions for long-term prevention of thrombosis *in vivo*, the low-fouling properties of this PEG coating were sufficient to be exploited for further coupling of bioactive molecules to create bioactive coatings. Therefore, as a part of the second objective, an innovative and versatile bioactive coating was developed on PEG and carboxymethylated dextran (CMD), using the combination of an adhesive peptide (KQAGDV/RGD) and epidermal growth factor (EGF). CMD was chosen as an alternative to PEG due to its better low-fouling properties and the presence of abundant carboxyl terminal groups. Although the QCM-D technique enabled us to optimize the combined immobilization of KQAGDV/RGD and EGF, cell adhesion assay results did not show improvement of vascular smooth muscle cell (VSMC) adhesion on peptide-modified PEG or CMD surfaces.

Among the reasons explaining low cell adhesion on peptides grafted low-fouling surfaces is the difficulty of preventing protein adsorption/platelet adhesion without significantly reducing cell adhesion. Preliminary data in our laboratory indicated that CS could be an ideal substrate to find this compromise. For that reason, the final objective of this PhD consisted in evaluating the potential of chondroitin sulfate (CS) coating by comparing its properties with well-known low-fouling polymers such as PEG and CMD. It was shown

that CS presents selective low-fouling properties, low-platelet adhesion and pro-endothelial cell (EC) adhesive properties. As demonstrated by QCM-D and fluorescence measurements, CS was as effective as PEG in reducing fibrinogen adsorption, but it reduced adsorption of bovine serum albumin (BSA) and fetal bovine serum (FBS) to a lower extent than PEG and CMD surfaces. Whole blood perfusion assays indicated that all three surfaces drastically decreased platelet adhesion and activation to levels significantly lower than PET surfaces. However, while EC adhesion and growth were found to be very limited on PEG and CMD, cell attachment on CS was strong, with focal adhesion points and resistance to shear stress. CS coatings therefore form a low-thrombogenic background promoting the formation of a confluent endothelium layer, which may then act as an active anti-thrombogenic surface. CS coating can also be used to further graft biomolecules. Combination of LP, CS coating followed by GF immobilization shows great promise as a bioactive coating to optimize the biocompatibility and clinical outcome of vascular implants, in particular vascular grafts.

**Key words:** bioactive coating, vascular graft, stent-graft, low-fouling, non-thrombogenic, adhesion peptide, epidermal growth factor, QCM-D.

## TABLE OF CONTENTS

	Page
INTRODUCTION .....	1
CHAPTER 1 LITERATURE REVIEW .....	5
1.1 Clinical problematic.....	5
1.1.1 Morphology of arteries .....	5
1.1.2 Vascular injury.....	6
1.1.3 Vascular prostheses and their limitations .....	8
1.2 Blood-material interactions.....	12
1.2.1 Protein-surface interactions and their influence on protein adsorption ....	13
1.2.2 Thrombus formation .....	18
1.2.3 Blood coagulation .....	19
1.2.4 Regulation of thrombosis by endothelium.....	21
1.3 Surface modification for blood compatibility.....	23
1.3.1 Low-fouling coatings.....	23
1.3.2 Surface modification with anticoagulants.....	33
1.4 Modifying surface physico-chemical properties to promote cell adhesion .....	37
1.5 Bioactive coatings to promote cell adhesion and growth .....	39
1.5.1 Coatings made of ECM proteins.....	39
1.5.2 Surface modification with peptides .....	44
1.5.3 Surface modification with growth factors.....	54
1.5.4 Combination of peptide and growth factor .....	64
1.6 QCMD- technique.....	68
1.6.1 Introduction.....	68
1.6.2 Fundamental principles of the QCM-D technique.....	68
CHAPTER 2 OBJECTIVES AND HYPOTHESIS.....	75
CHAPTER 3 MATERIALS AND METHODS .....	79
3.1 Surface preparation and coating methods .....	79
3.1.1 Cleaning samples .....	79
3.1.2 Plasma polymerization.....	80
3.1.3 Chemical grafting of PEG, CMD and CS.....	81
3.1.4 Covalent immobilization of peptides and epidermal growth factor (EGF).....	85
3.2 Surface characterization.....	87
3.2.1 X-ray photoelectron spectroscopy (XPS) .....	87
3.2.2 Static Water Contact Angle .....	88
3.3 QCM-D measurements .....	89
3.3.1 QCM-D system .....	89
3.3.2 QCM-D measurements .....	92
3.3.3 Combined immobilization .....	94

3.3.4	Measuring cell adhesion .....	96
3.4	Protein adsorption studies by fluorescence measurements .....	96
3.4.1	Protein adsorption studies on PEG, CMD and CS surfaces.....	97
3.4.2	Micro -patterning .....	97
3.5	Platelet adhesion assays .....	98
3.5.1	Perfusion system .....	99
3.5.2	Platelet adhesion assay with radio-labeled platelets .....	100
3.5.3	Platelet adhesion assay using fluorescence staining .....	101
3.5.4	Scanning electron microscopy .....	102
3.6	Cell culture experiments .....	103
3.6.1	HUVEC adhesion and growth .....	103
3.6.2	VSMC adhesion assay on peptide grafted surfaces .....	105
3.7	Statistical Analysis.....	105
CHAPTER 4 RESULTS AND DISCUSSION.....		107
4.1	Develop a low-fouling and low-thrombogenic coating that can be applicable to a wide variety of biomaterial surfaces.....	107
4.1.1	Rationale .....	107
4.1.2	Results.....	108
4.1.3	Discussion .....	118
4.2	Develop a bioactive coating with the combination of peptide and GF on low- fouling background.....	121
4.2.1	Rationale .....	121
4.2.2	Results.....	122
4.2.3	Discussion.....	132
4.3	Evaluate the advantages and limitations of using CS coating for vascular grafts ....	139
4.3.1	Rationale .....	139
4.3.2	Results.....	140
4.3.3	Discussion.....	150
CHAPTER 5 GENERAL DISCUSSION .....		155
CONCLUSION .....		167
BIBLIOGRAPHY.....		169

## LIST OF TABLES

	Page
Table 1.1.	Major constituents of human blood serum and their biological functions. Taken from (David Richard Schmidt, 2009). .....18
Table 1.2.	Selective synthetic peptide sequences of extracellular matrix proteins and their functions. Taken from (Shin, Jo et Mikos, 2003). .....46
Table 4.1.	Surface elemental concentration (in At. %) of C, O, Si and N, as determined by XPS on amino-coated glass and PEG-modified surfaces using various star PEG coupling concentrations. ....111
Table 4.2.	Summarized observations of various experiments (at least 4 samples tested for each condition) performed to investigate the influence of immobilized peptides on VSMC adhesion .....131
Table 4.3.	Mean percentage reduction of protein-adsorbed mass compared to LP surface, based on QCM-D results (mean $\pm$ SD; $n \geq 3$ ). .....143



## LIST OF FIGURES

	Page
Figure 1.1. Schematic view of the organization of the three layers (intima, media and adventitia) of an artery. Taken from (Muscle anatomy of the body, 2014). .....	6
Figure 1.2. Schematic view of narrowing artery due to atherosclerotic plaque. Taken from (Merck, 2014). .....	7
Figure 1.3. Schematic of (A) commercially available ePTFE vascular grafts (GORE-TEX) for coronary artery bypass and (B) stent graft placement for the repair of EVAR (Biotextiles, 2014). .....	9
Figure 1.4. Schematic shows a simplified view of the interaction of blood elements with biomaterial surface. Taken from (Courtney et Forbes, 1994). ...	13
Figure 1.5. Schematic view of protein conformational changes upon adsorption on the material surfaces. Taken from (David Richard Schmidt, 2009). ...	15
Figure 1.6. A schematic view of protein-surface interactions. Both the surface and the protein have a number of interacting domains with charged, hydrophobic and polar character. Image taken from (Andrade et Hlady, 1986). .....	16
Figure 1.7. Schematic diagram of a simplified view of the blood coagulation cascade that includes intrinsic and extrinsic pathways. Taken from (Gorbet et Sefton, 2004). .....	21
Figure 1.8. (a) EC regulation of coagulation and (b) platelet adhesion and activation. Taken from (Li et Henry, 2011b). .....	23
Figure 1.9. Schematic shows hydrogen bonding between ether oxygen atoms. Image adapted and modified from (Andrade et Hlady, 1986). .....	25
Figure 1.10. Schematic view of (a) protein repulsion on hydrated polymer chains and (b) prevention of protein adsorption on PEG layer by excluded volume-steric repulsion. Image adapted from (Andrade et Hlady, 1986). .....	26
Figure 1.11. Schematic shows three different PEG regimes, depending on the PEG chain density. The PEG conformation on the surface changes from non-overlapping "mushrooms" to fully extended "brushes" at different grafting densities. Image adapted and slightly modified from (Unsworth et al., 2005). .....	28

Figure 1.12.	Schematic diagram of a) a linear PEG molecule and b) an end-functionalized 4-arm star PEG. The circles represent end functional groups by which the molecules may tether to surfaces. Image adapted from (Irvine et al., 1998). .....	29
Figure 1.13.	Schematic view of the possible interactions and orientations of biomolecules when they are immobilized on (a) an amine-functionalized surface vs. (b) a 4-arm star PEG modified surface .....	31
Figure 1.14.	Schematic shows (a) the chemical structure of dextran and (b) the configuration of surface-bound dextran polymer. Image adapted from (Massia, Stark et Letbetter, 2000).....	33
Figure 1.15.	Schematic view of mechanism of action of immobilized heparin, hirudin, thrombomodulin (TM) and tissue factor pathway inhibitor (TFPI) to inhibit coagulation. Taken from (Li et Henry, 2011b).....	36
Figure 1.16.	Schematic view of progression of anchorage dependent cell adhesion. (A) Initial contact of cell with solid substrate that has multiple binding domains. (B) Formation of bonds between cell surface receptors and ligands. (C) Cytoskeletal reorganization for increased adhesion strength. Taken from (Massia, 1999).....	41
Figure 1.17.	The chemical structure and nomenclature of RGD peptide. Image adapted from (Hersel, Dahmen et Kessler, 2003).....	47
Figure 1.18.	Coupling of a protected RGD peptide through its N-terminus to a surface carboxyl group and deprotection of the blocking groups. Image adapted from (Hersel, Dahmen et Kessler, 2003).....	48
Figure 1.19.	Reaction scheme between maleimide group on the surface and thiol functional group on peptide. Image adapted from (Hersel, Dahmen et Kessler, 2003; Lateef et al., 2002).....	49
Figure 1.20.	Schematic representation of how integrin-mediated activation regulates the cell/substrate interaction (Owen et al., 2005). .....	52
Figure 1.21.	Schematic illustration of RGD presentation on star polymers. (A) The same amount of ligands presented in homogeneous (top) versus ligands presented in discrete clusters (bottom).Image adapted from (Maheshwari et al., 2000). .....	53
Figure 1.22.	Cross talk between cells mediated by growth factors and ECM. Insert illustrates how ECM can control growth factor presentation in a temporal and spatial fashion. Taken from (Lee, Silva et Mooney, 2011). .....	55

Figure 1.23.	Primary structure of human epidermal growth factor (EGF). Adapted from (Carpenter et Cohen, 1979). ....	57
Figure 1.24.	(A) Schematic representation of EGFR domain structure of the extracellular and intracellular regions. (B) Hetero-dimerization of the EGFR and Erb B <sub>2</sub> upon receptor activation. Image adapted and redrawn from (McInnes et Sykes, 1997).....	58
Figure 1.25.	Schematic representing the pathways which lead to the activation of anti-apoptotic proteins (white) and the inactivation of pro-apoptotic proteins (black). Taken from (Srokowski et Woodhouse, 2013).....	59
Figure 1.26.	Schematic illustration of the interaction between cells and native (a) and immobilized (b) growth factors (Ito, Kajihara et Imanishi, 1991).....	60
Figure 1.27.	Schematic illustration of EGF accessibility to the cellular receptor when it is tethered to a substrate material via flexible polyethylene glycol chains. Taken from (Ito, 1998). ....	61
Figure 1.28.	Helical wheel representation of the heterodimeric parallel E/K coiled-coil, which shows hydrophobic interaction between V and L residues (at positions a, a', d and d') and electrostatic interchain interactions between E and K residues (at positions e-g' and g-e') that forms E/K salt bridge. Taken from (Chao et al., 1998). ....	63
Figure 1.29.	Schematic diagram of an oriented immobilization of EGF onto an amine-displaying surface through coiled-coil interaction (Boucher et al., 2009).....	64
Figure 1.30.	Schematic diagram of collaborative signaling of growth factor and integrin receptors. Taken from (Yamada et Even-Ram, 2002).....	65
Figure 1.31.	Schematic diagram of FAK function that integrates growth factor and integrin signals to promote cell migration (Sieg et al., 2000). ....	67
Figure 1.32.	Schematic illustration of relative changes in the crystal oscillation upon adsorption of mass (m). Initially, the frequency is constant at its fundamental overtone. When the mass is added to the crystal, the frequency decreases but remains constant. Finally, when the driving power is switched off, the frequency decays and the dissipation can be calculated (image adapted from Q-Sense reported data). ....	71
Figure 1.33.	Schematic diagram of the geometry of a quartz crystal covered with a viscoelastic protein film. The film is represented by various parameters such as density ( $\rho_f$ ), viscosity ( $h_f$ ), elastic shear modulus ( $\mu_f$ ), and thickness ( $t_f$ ). The parameters for bulk liquid are represented	

	by a density ( $r_l$ ), and a viscosity ( $h_l$ ) and for the crystal are represented by density ( $r_Q$ ), elastic shear modulus ( $m_Q$ ), and thickness ( $t_Q$ ). Taken from (Höök et al., 2001).....	74
Figure 3.1.	Schematic views of the low-pressure, capacitively coupled radio-frequency plasma reactor. Taken from (Truica-Marasescu et al., 2008)...	81
Figure 3.2.	Chemical structure of polyethyleneglycol (PEG), carboxymethyl dextran (CMD) and chondroitin-4-sulfate (CS).....	83
Figure 3.3.	Schematic diagram of star PEG covalent binding reaction. Either one or two N- hydroxyl succinamide (NHS) terminal groups of star PEG react directly with primary amines through ester-amine reactions to form stable amide bonds; the remaining terminal groups do not participate in coupling, due to steric constraints (Park, Mao et Park, 1990) and hydrolyze to carboxylic acid groups during the reaction. ....	84
Figure 3.4.	Schematic of KQAGDV and K coil peptide grafting using EMCH linker and E coil EGF tethering through coiled-coil interaction.....	86
Figure 3.5.	Schematic diagram of the contact angle and interfacial tensions at three phase boundaries.....	89
Figure 3.6.	Schematic picture of (A) complete setup of the QCM-D equipment (B) four flow modules chamber and their setup and (C) flow module with a crystal, dimensions and o-ring position. ....	90
Figure 3.7.	Schematic shows the viscous penetration depth as function of the overtone number (Q-Sense reported data). ....	91
Figure 3.8.	Example of QCM-D data for simultaneous measurements of frequency ( $\Delta f$ ) and ( $\Delta D$ ) dissipation changes (for various over tones) during fibrinogen (0.5 mg/mL) adsorption on LP deposited surface. Arrows refer to injection (left) of fibrinogen and rinsing (right) with PBS solution. ....	93
Figure 3.9.	Schematic diagram of serial immobilization of KQAGDV peptide, K coil, Cysteine and E coil EGF, with QCM-D. ....	96
Figure 3.10.	Image of electron microscopy grids consisting of 184- $\mu\text{m}$ wide parallel bars separated by 92 $\mu\text{m}$ . ....	98
Figure 3.11.	Schematic picture of (a) perfusion chamber (b) sample holder and (c) perfusion system setup along with thermostatically controlled water bath.....	100

Figure 3.12.	Typical smooth discoid shape of platelets (left) and spherical shape of activated platelets (right) (Harrison, 2005). ....	103
Figure 4.1.	Static water contact angles on unmodified amino-coated glass (left) and LP (right), and after PEG coating at various coupling concentrations (0.55, 1.66, 5, and 15% w/v). Results are expressed as mean $\pm$ SD, n=3. *Significantly different from amino-coated glass and LP surfaces (P<0.001), # significantly different from 5% PEG (P<0.001). ....	108
Figure 4.2.	XPS high-resolution C1s scans of amino-coated glass (a) before and (b-e) after star PEG grafting at various coupling concentrations (0.55, 1.66, 5, and 15% w/v). Note that the relative intensity of the C–O peak increased with the PEG coupling concentration; (f) Overlay spectra of 15% PEG-modified on unmodified amino-coated surface.....	110
Figure 4.3.	QCM-D real-time change in resonance frequency ( $\Delta f$ ) and dissipation ( $\Delta D$ ) related to modified (5% PEG) and unmodified LP surfaces upon exposure to fibrinogen solution (0.5 mg/mL; (1)) followed by rinsing with PBS (2).....	112
Figure 4.4.	Time-resolved effect of various PEG coupling concentrations on fibrinogen (0.5 mg/mL) adsorption. QCM-D data were analyzed according to the Voigt model. Time of fibrinogen injection (1) and rinsing with PBS (2) are indicated. This is an example figure that shows data from one experiment. ....	113
Figure 4.5.	Calculated mass of adsorbed fibrinogen (0.5mg/mL) on LP and after PEG grafting at various coupling concentrations. QCM-D data were analyzed using the Voigt model. Results are expressed as mean $\pm$ SD, n=4 (* result expressed as a mean; n=2 only).....	113
Figure 4.6.	Example curves for fibrinogen (0.5 mg/mL) adsorption on LP and on PEG modified surfaces immersed in PBS over a period of 1 or 28 days. QCMD data were analyzed according to the Voigt model. Time of fibrinogen injection (1) and rinsing with PBS (2) are indicated. ....	114
Figure 4.7.	Fluorescence detection of adsorbed Texas red labeled albumin (0.2 mg/mL) on bare PET, LP alone and LP-PEG coated PET. Results are expressed as mean $\pm$ SD (n=4). Background was subtracted from each surface. *Significantly different from PET (P<0.001), # significantly different from LP+ 5% PEG (P<0.001). ....	115

Figure 4.8.	Fluorescence microscopy images of LP micro-patterns on PET surfaces after exposure to albumin Texas red conjugate. Parallel pattern surface (a) without PEG grafting and (b) modified with PEG. ...	116
Figure 4.9.	Platelet adhesion on an intact artery (native artery), injured artery, PET film, LP and 5% PEG- modified substrates. Results are expressed on a logarithmic scale, as mean $\pm$ SD (n=4). * significantly different from PET (P<0.001), # significantly different from LP + 5% PEG (P<0.001). .....	117
Figure 4.10.	SEM visualization of platelet adhesion on LP (a, b), PET (c, d) and LP + 5% PEG (e, f) grafted surfaces. ....	118
Figure 4.11.	QCM-D frequency shift due to K coil, cysteine and E coil EGF serial injections on EMCH and PDPH modified CMD surfaces. Arrows refer to the PBS rinsing.....	123
Figure 4.12.	QCM-D frequency shift due to K coil, cysteine and E coil EGF serial injections on EMCH activated PEG and CMD surfaces. PEG + Cysteine and CMD + cysteine control surfaces corresponds to surface where K coil had not been immobilized. Arrows refer to the PBS rinsing. ....	124
Figure 4.13.	QCM-D frequency changes due to immobilization of various concentrations of KQAGDV and serial immobilization of K coil, Cysteine and E coil EGF on CMD surfaces. Arrows refer to PBS rinsing. ....	125
Figure 4.14.	Mass increase corresponding to KQAGDV, K coil grafting and E coil EGF recruitment on CMD surfaces (previously modified with EMCH linker), as a function of KQADGV concentration that had been initially injected (n $\geq$ 3). Cys only surface corresponds to negative control surface, on which reactive sites are blocked with cysteine. ....	126
Figure 4.15.	The frequency (left panel) and dissipation (right panel) changes due to VSMC adhesion on LP, PEG and CMD. Arrows refer to the injection of VSMCs (left) and DMEM rinsing (right).....	127
Figure 4.16.	The frequency (left) and dissipation (right) changes due to VSMC adhesion on LP, CMD and CMD + KQAGDV surfaces.....	129
Figure 4.17.	The frequency changes due to RGD (38 $\mu$ M) grafting (first arrow) on CMD + EMCH and CMD surfaces (left). VSMC adhesion on LP, CMD and CMD + RGD surfaces (right).....	129

Figure 4.18.	VSMC density observed (after 4 h adhesion in serum-free medium) by crystal violet staining on KQAGDV peptide modified and unmodified LP, CMD and EMCH surfaces. Scale bar corresponds to 200 $\mu$ m. ....	130
Figure 4.19.	Static water contact angle measurements of unmodified LP and LP coated with PEG, CMD and CS (mean $\pm$ SD; $n \geq 10$ ); * $p < 0.0001$ vs. LP. ....	141
Figure 4.20.	Static water contact angle measurements of unmodified and modified amino-coated glass surfaces with PEG, CMD and CS (mean $\pm$ SD; $n = 7$ ). ....	141
Figure 4.21.	QCM-D frequency ( $\Delta f$ , panel a) and dissipation ( $\Delta D$ , panel b) versus time for fibrinogen (0.5 mg/mL) adsorption on a CMD modified and an LP surface. The arrows refer to the injection of the protein solution (left) and PBS rinsing (right). ....	142
Figure 4.22.	The adsorption and desorption kinetics of BSA (a) and 10% (w/v) FBS (b) on PEG, CMD and CS modified and unmodified LP surfaces. Arrows indicate the start of the protein (left) and PBS (right) injections. ....	143
Figure 4.23.	Fluorescence intensity of adsorbed Texas Red labeled albumin (0.2 mg/mL) on PEG-, 2 CMD- and CS-modified and unmodified LP surfaces, as well as on bare PET control (mean $\pm$ 3 SD; $n = 8$ ); * $p < 0.0001$ vs. PET; # $p < 0.0001$ vs. CS. ....	144
Figure 4.24.	Typical images of crystal violet staining after 2 day HUVEC growth on each surface (scale bar = 200 $\mu$ m). ....	145
Figure 4.25.	HUVEC density after 4h (adhesion) and 2 days (growth) (mean $\pm$ SD ; $n = 12$ ); * $p < 0.0001$ . ....	145
Figure 4.26.	Immunostaining of vinculin (red), actin (green), and the nucleus (blue) after 24 h of HUVEC adhesion on PET, LP, LP-CS and LP-CMD surfaces. ....	146
Figure 4.27.	Percentage of surface area covered by platelets after perfusion with whole blood for 15 min (mean $\pm$ SD; $n \geq 5$ ); * $p < 0.0001$ vs. LP; # $p < 0.0001$ vs. PET. ....	147
Figure 4.28.	Representative images of SEM (a, c, e) and confocal microscopy (b, d, f, g, h: labeling with CD 61/FITC) for platelet adhesion on LP (a, b), PET (c, d), CS (e, f), PEG (g) and CMD (h) surfaces after perfusion with whole blood. ....	147

Figure 4.29. Cell density on the different surfaces (bare PET and LP +/-CS coating) not perfused (-Perfusion) and after perfusion (+Perfusion) of whole blood (mean ± SD; *n* = 7); \* *p* < 0.0001 vs. all other surfaces. Confocal microscopy images (right side) of HUVEC growth (7 d; labeled with CellVue Maroon (in blue color)) on PET, before and after 15 min of perfusion. Data adapted from Fadlallah's thesis (Fadlallah, 2013).....149

Figure 4.30. (a) Percentage of LP and CS surfaces covered by platelets after perfusion with whole blood in the absence (-HUVEC) and presence (+HUVEC) of previously seeded HUVEC (mean ± SD; *n* = 7; \* *p* < 0.0001 vs. other surfaces). (b) Representative images of HUVECs and platelets on LP and CS surfaces after perfusion (HUVEC membranes colored with CellVue® Maroon (blue) and platelets stained with anti-CD61/FITC antibody (green)). Scale bar corresponds to 200 μm. Data adapted from Fadlallah's thesis (Fadlallah, 2013).....149

## LIST OF ABBREVIATIONS

AAA	Abdominal Aortic Aneurysm
ADP	Adenosine Diphosphate
AFM	Atomic Force Microscopy
AT	Antithrombin
ATP	Adenosine Triphosphate
BSA	Bovine Serum Albumin
CMD	Carboxymethylated dextran
CS	Chondroitine-4-sulfate
ECM	Extracellular matrix
EC	Endothelial Cells
EDC	1-Ethyl-3-(3-dimethylaminopropyl) carbodiimide
EGF	Epidermal Growth Factor
EGFR	Epidermal Growth Factor Receptor
ERK	Extracellular signal-regulated kinases
EVAR	Endovascular Aneurysm Repair
ePTFE	expanded Polytetrafluoroethylene
FAK	Focal Adhesion Kinase
FBS	Fetal Bovine Serum
bFGF	basic Fibroblast Growth Factor
Fg	Fibrinogen
Fn	Fibronectin
FTIR	Fourier Transform Infrared Spectroscopy

GAG	Glycosaminoglycan
GF	Growth Factor
HA	Hyaluronic acid
HEMA	Hydroxyethyl Methacrylate
HMWK	High Molecular Weight Kininogen
HUVEC	Human umbilical vein endothelial cells
IgG	Immunoglobulin
LMWH	Low Molecular Weight Heparin
NHS	N-hydroxysuccinimide
PBS	Phosphate buffered saline
PEG	Polyethylene Glycol
PEO	Polyethylene Oxide
PET	Polyethylene Terephthalate
PLL	Poly L-lysine
PTFE	Polytetrafluoroethylene
PU	Polyurethane
PUU	Polyurethaneurea
QCM-D	Quartz Crystal Microbalance with Dissipation
SAMs	Self-Assembled Monolayers
SEM	Scanning Electron Microscope
SG	Stent Grafts
TF	Tissue Factor
t-PA	Tissue Plasminogen Activator

VEGF	Vascular Endothelial Growth Factor
Vn	Vitronectin
VSMC	Vascular Smooth Muscle Cell
VG	Vascular Grafts
vWF	von Willebrand Factor
XPS	X-Ray Photoelectron Spectroscopy



## INTRODUCTION

Cardiovascular disease (CVD) is one of the leading causes of mortality and morbidity worldwide. In 2008, 17.3 million people died from cardiovascular diseases (CVDs), which accounted for 30% all global deaths. Of these deaths, 7.3 million deaths were due to coronary heart disease alone, according to the World Health Organization (ThomasWHO, 2013). As per recent statistics of the Heart and Stroke Foundation of Canada, cardiovascular diseases cause the death of one Canadian every seven minutes and cost the Canadian economy \$ 20.9 billion every year (2011, statistics Canada).

Vascular occlusive disease is the greatest risk factor affecting the coronary arteries, and ultimately leads to complete heart failure. To date the standard clinical approach involves angioplasty, stenting, and bypass graft surgery depending on the degree of occlusion. More than 70% of patients with occluded arteries require treatment with bypass grafts. Autografts (such as saphenous vein, arm vein, mammalian artery, or radial artery) are preferred for primary revascularisation to replace small diameter vessels (Desai, Seifalian et Hamilton, 2011). However, 3–30% patients presented with no autologous vessels due to previous disease conditions or previous organ harvesting (L'Heureux et al., 2007; Rathore et al., 2012).

Synthetic vascular grafts (VG), made of polyethylene terephthalate (PET) and expanded polytetrafluoroethylene (ePTFE), are successfully used for the replacement of medium or large diameter blood vessels ( $> 6\text{mm}$ ). However, the use of PET and ePTFE based vascular grafts for small diameter vessels ( $<6\text{ mm}$ ) have been restricted due to unacceptable patency rates in the long term. This could be due to the fact that small diameter vascular grafts encounter low blood flow and high shear rate conditions that lead to several complications such as acute thrombosis (leads to early failure; within 30 days after the implantation), intimal hyperplasia (leads to midterm failure; 3 months to 2 years after the implantation), and atherosclerosis (leads to late failure after 2 years) (Conte et al., 2002). Similarly, the use of PET and ePTFE based stent grafts (SG) for the treatment of

endovascular aneurysm repair (EVAR) is limited by risk of thrombosis, undesirable blood-material interactions and most importantly inadequate healing around implants. Therefore, there is an urgent clinical need for developing improved vascular implants (Zhang et al., 2007). Current VGs and SGs made of PET and e PTFE tend to fail because they are ineffective in preventing surface-induced thrombosis and lack favorable surface properties that promote confluent cell adhesion growth and survival.

Several attempts were already made to improve surface properties and thereby enhance the patency rates of vascular implants. However, two main issues still need to be addressed. The first is that current bioactive coating methods fail to find a good compromise between preventing thrombus formation and promoting desirable cell-adhesive properties. The second is that most techniques lack versatility, which compromises their commercial use since the coating process must be optimized for each material and application. Therefore, the multidisciplinary work of this PhD thesis involves the growing field of surface modification in biomaterial research. More specifically, it aims to develop an innovative and versatile bioactive coating for vascular grafts and stent grafts that can induce desired cell interactions while preventing undesirable protein and blood-material interactions.

Chapter 1 of this thesis includes a literature review, detailing the current vascular implants, blood-material interactions and the scientific approach leading to the design of bioactive coatings. More specifically, this section describes the structure and function of arteries, vascular disease, the uses of current vascular implants and limitations, protein-surface interactions and their consequences such as thrombosis and blood coagulation. Surface modifications with low-fouling coatings and anticoagulants that reduce protein adsorption and thrombosis, and finally bioactive coatings using peptides and growth factors that improve cell interactions with the material surface are also presented. The potential advantage of using low-fouling backgrounds or spacers for biomolecules immobilization is explained, as well as the use of the hydrophilic polymers polyethyleneglycol (PEG) and carboxymethylated dextran (CMD) to obtain such low-fouling background.

Based on the literature review, several hypotheses were made and three main objectives were defined for this thesis. In addition, the most promising bioactive molecules were chosen to create a low-fouling and non-thrombogenic bioactive coating that promotes cell growth. The specific objectives and their rationale are presented in Chapter 2, while Chapter 3 covers the materials and methods used for the project. Chapter 4 comprises the results and discussion section of PhD thesis, which was divided into three subsections based on the specific objectives. The general discussion and the resulting recommendations and limitations are presented in Chapter 5 followed by the conclusions.



## CHAPTER 1

### LITERATURE REVIEW

#### 1.1 Clinical problematic

##### 1.1.1 Morphology of arteries

The walls of large vessels such as arteries consist of three concentric layers: an inner intima, an intermediate media and an outer adventitia (Figure 1.1). Regardless of the organization of these layers, the main constituents of blood vessel walls are endothelial cells (ECs), smooth muscle cells (SMCs) and the extracellular matrix (ECM). The intimal layer is attached to the basement membrane rich in collagen IV and laminin. This layer consists of a monolayer of specialized ECs, which forms a tight non-thrombogenic/anti-thrombogenic barrier between the lumen and the rest of the vessel wall. Vascular ECs experience shear stress *in vivo*, which ranges between 10 and 20 dynes/cm<sup>2</sup> for straight arteries of uniform geometry. For non-uniform geometries (branches and arches), the shear stress can be as high as 50 dynes/cm<sup>2</sup> with pulsatile flow (Papaioannou et Stefanadis, 2005). The intimal layer plays a role not only in preventing unwanted clot formation, but also prevents infection and inflammation of the underlying tissue.

The acellular and dense elastin layer, also known as the internal elastic lamina, separates the intimal layer from the medial layer. This muscular layer of the artery consists mainly of SMCs, collagen Type I and III, and a lesser amount of other proteins and proteoglycans. The collagen matrix and the SMCs in the intermediate media are aligned circumferentially along the axis of the blood vessel. Vessel contraction or dilation is caused by the stimulation of SMCs by signals from ECs of the lumen or directly by cytokines. Another dense elastin layer, the external elastic lamina, separates the intermediate media from the outermost layer of the vessel wall, i.e. the outer adventitia. The adventitia consists of a loose collagen matrix with embedded fibroblasts and vasa vasorum, which serves to anchor the blood vessel to the surrounding tissue and to provide additional structural support.

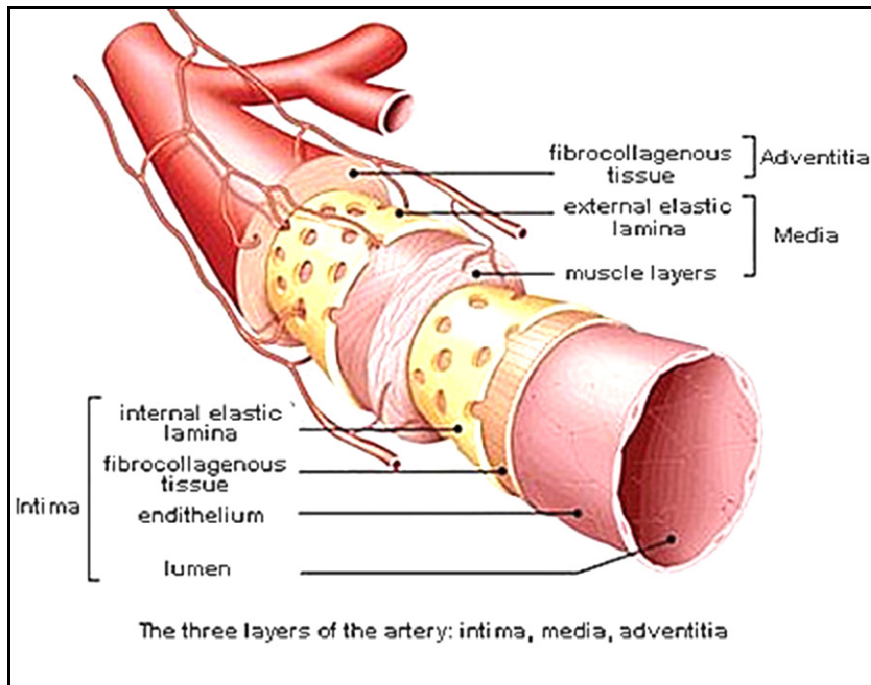


Figure 1.1. Schematic view of the organization of the three layers (intima, media and adventitia) of an artery. Taken from (Muscle anatomy of the body, 2014).

### 1.1.2 Vascular injury

The most common reason for vessel failure is atherosclerosis, which is an inflammatory disease that causes plaque build-up beneath the intimal layer of the vessel wall. This plaque is formed by the infiltration of monocytes into the intima, and a resulting increase in the migration, proliferation, and secretory activity of the vascular SMCs. The blood vessel lumen narrows as the plaque grows (see Figure 1.2) and calcifies, leading to a decrease in blood flow to the downstream tissues. Plaque rupture and subsequent clot formation can eventually lead to infarction of the downstream tissue (Stary et al., 1995).

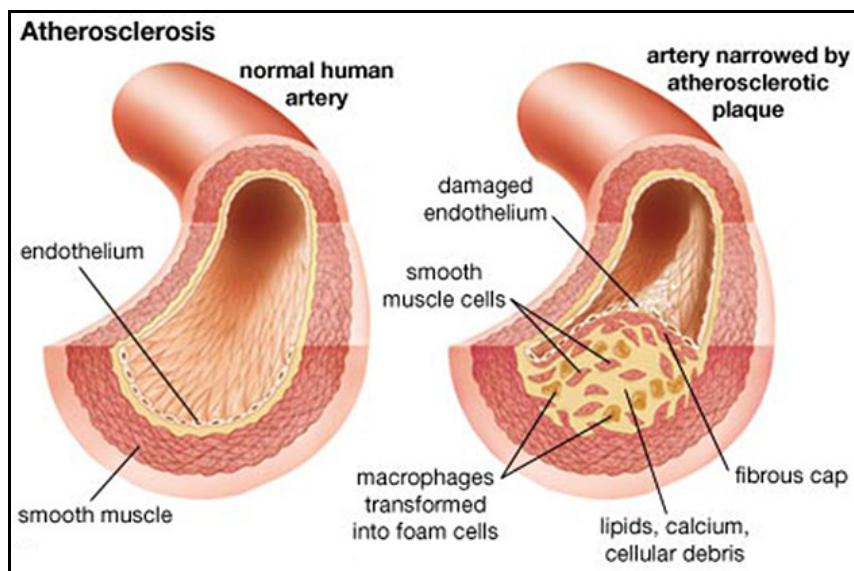


Figure 1.2. Schematic view of narrowing artery due to atherosclerotic plaque. Taken from (Merck, 2014).

Another possible result of atherosclerosis is the abnormal permanent dilation of the aorta, which leads to the formation of an aneurysm (Sakalihasan, Limet et Defawe, 2005; Zankl et al., 2007). Aortic aneurysms commonly occurred in three different locations, which are classified as abdominal aortic aneurysm (AAA), thoracic aneurysm and thoracic abdominal aneurysm. Of those aneurysms, AAA is leading cause of death in the aging population. It is typically either fusiform or saccular. Fusiform aneurysms present as a fairly uniform shape with symmetrical dilation that involves the full circumference of the aortic wall while saccular aneurysms present as localized dilation that appear as an outpouching of only a portion of the aortic wall (Adam van der Vliet et Boll, 1997).

There are three main pathophysiological mechanisms, such as inflammation, proteolysis and apoptosis, involved in the development of abdominal aortic aneurysms. AAA is mostly associated with severe atherosclerosis, which is characterized by the presence of inflammatory cells (Jonasson et al., 1986) that are recruited from blood and neovascularization processes in the media layer forming a lymphomonocytic infiltrate (Herron et al., 1991; Holmes et al.; Shah, 1997). The second mechanism for the development of AAA involves proteolytic degradation of elastin fibers and collagen by matrix

metalloproteinases (MMPs) that are either activated by other MMPs or plasmin (Carrell et al., 2002; Defawe et al., 2003; Rao, Reddy et Cohen, 1996; Thompson et Parks, 1996). The third and most significant mechanism leading to AAA involves the reduction of the density of smooth muscle cells in the media layer by the apoptotic process (Lopez-Candales et al., 1997). Altogether, the mechanisms leading to AAA suggest that the presence of a smooth muscle cell layer in the aortic wall is important, since VSMCs protect against inflammatory and proteolytic processes and also play a key role in repair processes of the aneurysms through localized expression of numerous extracellular matrix proteins and protease inhibitors (Allaire et al., 2002).

### **1.1.3 Vascular prostheses and their limitations**

When stenting is not an option, the use of autologous vessels, including saphenous veins and mammary arteries, remains the standard procedure for the replacement of coronary arteries. However, one third of patients do not have veins suitable for grafting due to pre-existing vascular disease and vein stripping or vein harvesting for prior vascular procedures (Edwards, Holdefer et Mohtashemi, 1966; Veith et al., 1979). Finally, the harvest of autologous vessels causes significant morbidity and surgical costs. All of these factors contribute to a clinical requirement for readily available and functional synthetic small-diameter vascular grafts. Therefore, there is an increasing need to develop small-diameter vascular vessels for bypass surgery and other vascular reconstructive procedures. In addition, vascular grafts are needed for surgery performed for vascular trauma, aneurysms, and organ transplantation.

The most common method for the treatment of AAA involves traditional open surgery and endovascular aneurysm repair (EVAR). Surgical procedure involves the replacement of the walls of the aneurysm with a synthetic graft, whereas EVAR using stent grafts is an alternative to surgical procedure (see Figure 1.3 B). SGs, also called covered stents, are made of a polymeric tubular structure supported by metallic struts and are inserted by catheter to exclude blood flow from the aneurysmal sac and therefore prevent further enlargement or aneurysm rupture. EVAR is increasingly being used due to several

advantages such as its minimally invasive nature, reduced expense compared to conventional surgery and reduced recovery time and morbidity. However, this procedure is not free of complications that potentially occur during and after the EVAR procedure, which are mainly due to poor healing around the SG and lack of fixation into the surrounding vessel.

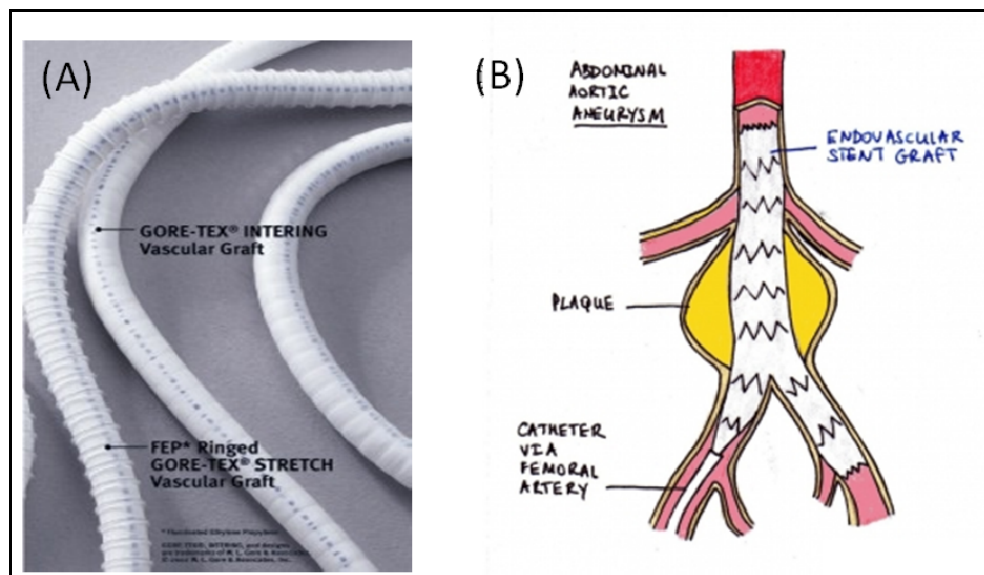


Figure 1.3. Schematic of (A) commercially available ePTFE vascular grafts (GORE-TEX) for coronary artery bypass and (B) stent graft placement for the repair of EVAR (Biotextiles, 2014).

Current vascular grafts and stent grafts are generally made of woven polyethylene terephthalate (PET, Dacron) or expanded polytetrafluoroethylene (ePTFE) (see Figure 1.3).

**PET:** Poly (ethylene terephthalate), chemical structure represented as  $[O-C(=O)-C_6H_4-O-C(=O)-CH_2CH_2]_n$ , is a semi-crystalline polymer from the family of polyesters patented by DuPont (Dacron ®) in 1950; (Chlupac, Filova et Bacakova, 2009)). PET's long chains are obtained from polycondensation of terephthalic acid and ethylene glycol. When PET is made into fibers, it is referred to commercially as Dacron. Dacron can be manufactured in either knitted or woven designs. Woven grafts have small pores, while knitted grafts have larger pores that promote greater tissue ingrowth and are more compliant. This polymer is generally strong, with a tensile strength of 170 MPa-180 MPa and a tensile modulus of 14,000 MPa.

These properties confer non-biodegradability and are stable for up to 30 years. However, Dacron grafts have been found to dilate over time (Boss et Stierli, 1993; Sporn et al., 2008).

**PTFE:** ePTFE, or Teflon, is a crystalline polymer composed of saturated carbon and fluorine atoms (-CF<sub>2</sub>-CF<sub>2</sub>-) patented by Gore (Gore-Tex) in 1969 (Chlupac, Filova et Bacakova, 2009). ePTFE is an expanded polymer that is obtained by a heating, stretching, and extruding process resulting in a non-textile porous tube composed of random-shaped solid membranes (nodes). This polymer is considered to be chemically inert and hydrophobic. ePTFE has a very low coefficient of friction, medium stiffness with a tensile strength of 21 MPa and tensile modulus of 413 MPa, and is much less flexible than PET (Palmaz, 1998; Ruben Y. Kannan et al., 2005). This polymer is relatively less prone to deterioration in biological environments compared to PET (Guidoin et al., 1993). The electronegative character of ePTFE is known to be helpful in minimizing its reaction with blood components (Palmaz, 1998; Ruben Y. Kannan et al., 2005).

These two materials were chosen for designing vascular prostheses due to their mechanical properties and relatively good hemocompatibility, which help to prevent thrombus formation. The current VG perform well as large-caliber substitutes, but their long-term patency is not satisfactory for small-caliber applications (<6 mm) such as in coronary and microvessel surgery (Hoenig et al., 2005; Kakisis et al., 2005; Kannan et al., 2005; Salacinski et al., 2001). This failure is mainly the result of an unfavorable healing process, surface thrombogenicity, lack of endothelial cells and anastomotic intimal hyperplasia caused by hemodynamic disturbances. Therefore, the use of synthetic small-diameter vascular grafts made of PET and ePTFE remain unsuccessful (Burkel, 1988; Greisler, 1990; Yeager et Callow, 1988; Zilla, von Oppell et Deutsch, 1993). Similarly, the use of current stent grafts for EVAR is limited by postoperative complications, which mainly arises due to surface-induced thrombosis, incomplete healing and lack of vascular tissue growth around the implant. These complications are mainly related to lack of favorable surface properties of implants for promoting VSMC adhesion, growth and resistance to apoptosis.

The comparison of Dacron vs. ePTFE by systematic evaluation and meta analysis of randomized controlled trials showed no evidence of an advantage of one material over the other (Roll et al., 2008). Host reactions to the synthetic vascular prosthesis start immediately after contact with blood circulation. The physico-chemical properties of the material surface, such as charge, energy, wettability and roughness, play a key role for the graft's patency. It was demonstrated that the first event is the plasma protein adsorption/desorption process typical for any blood/material interface (Vroman et Adams, 1969). This process is followed by platelet recruitment, white blood cell and erythrocyte adhesion, and eventually endothelial and smooth muscle cell migration. Fibrin deposits (containing platelets and blood cells) usually form during the first few hours to days after implantation and are stabilized for 18 months with the formation of an inner compacted fibrin layer. Furthermore, fibrin is known to fill the interstices within the graft wall. Unfortunately, these steps are not followed by spontaneous endothelialisation, which would be required to reproduce the anti-thrombotic properties as described above. Only a few dispersed small islands of endothelialisation appeared on woven excised Dacron grafts (Wu et al., 1995) and knitted Dacron grafts during 1-11 years after implantation (Shi et al., 1997). ePTFE-based grafts face the same complications as Dacron when used for small-diameter blood vessels (Wu et al., 1995).

The presence of adsorbed proteins from blood plasma greatly influences cell attachment to synthetic surfaces. Proteins bind to surfaces depending on surface physico-chemical properties (Roach, Farrar et Perry, 2006) such as wettability, chemical composition and surface charge. These properties can determine the composition, surface density and conformation of the adsorbed protein layers. A combination of interactions such as hydrophobic forces, electrostatic forces, hydrogen bonding and van der Waals forces is responsible for protein adsorption on material surfaces (Brash, 1996). Changing surface properties, for example increasing surface hydrophilicity, results in quantitative and qualitative variation in the composition of the adsorbed protein layer. Proteins usually adhere irreversibly on hydrophobic surfaces since such surfaces exert strong interaction with hydrophobic parts of the protein. This interaction causes protein deformation or denaturation or disruption of native conformation and therefore the exposition of cell-binding regions on proteins is altered. It has been recognized that albumin and fibrinogen (Wu et al., 2005)

adsorbs to hydrophobic surfaces, while adhesive proteins (Fn and Vn) preferentially adsorb to hydrophilic surfaces when surfaces are exposed to blood plasma or serum (Koenig, Gambillara et Grainger, 2003a; Kottke-Marchant, Veenstra et Marchant, 1996). It is generally observed that ECs adhere and spread moderately on hydrophilic surfaces, whereas EC adhesion is reduced or even absent on hydrophobic surfaces (Absolom, Hawthorn et Chang, 1988; van Wachem et al., 1987). Both Dacron and ePTFE grafts are hydrophobic, however ePTFE is more hydrophobic than PET (Chlupac, Filova et Bacakova, 2009). Therefore, these materials are prone to adsorb fibrinogen and albumin and unfavorable for the adsorption of cell-adhesive proteins, which may lead to platelet adhesion and activation with poor or no EC adhesion. Therefore it is important to improve surface chemical and biological properties to reduce thrombosis and promote desired cell adhesion and growth (ECs for vascular grafts and VSMCs for sent grafts). In the following sections various surface modification methods will be described.

## **1.2 Blood-material interactions**

The majority of biomaterials used in blood-contacting devices are associated with many complications due to the interactions between blood and the material surface. Such interactions can ultimately lead to the failure of the device. This section will describe the mechanisms implicated in thrombus formation on biomaterials surfaces. As mentioned earlier, the introduction of foreign material into the body or blood causes immediate adsorption of blood proteins onto the surface and usually form a monolayer within seconds (Brash et Ten Hove, 1993; Courtney et Forbes, 1994). These interactions usually followed by platelet adhesion and activation, leukocyte adhesion, activation of the complement system, activation of blood coagulation and therefore thrombus formation (Eckmann et al., 2013; Gorbet et Sefton, 2004; Ratner et Bryant, 2004). As shown in Figure 1.4 (Courtney et Forbes, 1994), the body reacts to the layer of adsorbed proteins rather than the surface itself. Since the protein adsorption is the initial step of blood-material interactions, the protein adsorption phenomenon is also described in the following sections.

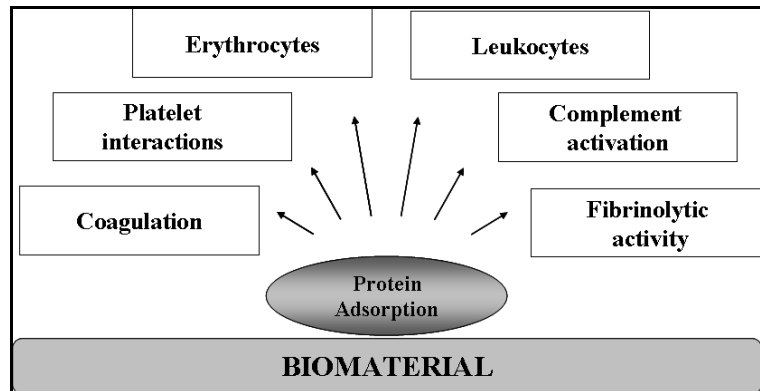


Figure 1.4. Schematic shows a simplified view of the interaction of blood elements with biomaterial surface. Taken from (Courtney et Forbes, 1994).

### 1.2.1 Protein-surface interactions and their influence on protein adsorption

Proteins consist of long chain amino acids that are linked together by peptide bonds formed between the amino and carboxyl groups of adjacent amino acid residues. Proteins are also referred to as polypeptides, since amino acids polymerize to form protein through peptide bonds. The net charge on proteins can be positive, negative or neutral, depending on the composition of amino acids, pH of the solution and protein's isoelectric point. Protein adsorption can be described as the "accumulation" of protein at the material interface. Normally, protein adsorption on the surface takes place in a non-specific way, which means that the proteins are only "physically" attached to the surface. The amount of adsorbed protein on the surface depends on its concentration as well as protein-surface affinity (Barnthip et al., 2008).

Both the affinity and the rate of transport to the surface influence protein adsorption kinetics. The rate of protein diffusion is influenced by the size of proteins, with smaller proteins diffusing faster than larger ones. The size of the protein also determines the affinity of protein molecules. For example, larger proteins may readily adsorb to the material surface since they have more binding sites to interact with the surface. A number of other factors come into play to influence the affinity of protein adsorption, since proteins are composed of sequences of amino acids and they exhibit different properties. Protein properties such as

charge (depending on the pH of their environment), hydrophilicity, hydrophobicity and internal structure influence protein-surface affinity (David Richard Schmidt, 2009). For example, larger "soft" proteins (e.g. immunoglobulin (IgG),  $\alpha$ -lactalbumin,  $\beta$ -casein and hemoglobin) that have a low structural stability are known to interact with higher affinity than smaller "hard" ones ( $\alpha$ -chymotrypsin, ribonuclease, lysozyme and  $\beta$ -lactoglobulin) that have greater structural stability (Norde, 1996).

The structure of a protein also plays a key role in protein adsorption because specific conformation may expose specific binding domains to interaction with the surfaces. Protein may lose its specific activity when it undergoes a conformational change upon adsorption to a material surface; over a period of time pertinent protein unfolding and changes in protein activity may also occur as shown Figure 1.5. This schematic illustrates that; (a) the protein has a binding site that requires a specific structure, (c) upon protein adsorption, these conformational epitopes are no longer functional as they are far apart, (d) over a period of time, the adsorbed protein may continue to unfold, thereby exposing additional binding sites. and (b) the hidden binding site of protein may have been revealed but it becomes available for binding to another molecule once the protein has unfolded upon adsorption on the material surface (David Richard Schmidt, 2009).

In a multi-protein system, for example blood plasma, many proteins compete for the adsorption sites on the material surface. Initially, protein adsorption is controlled by protein diffusion. Therefore, in the early stages, the protein concentration and size play a critical role (Barnthip et al., 2009; Krishnan, Siedlecki et Vogler, 2004; Noh et Vogler, 2007); smaller proteins present at higher concentration adsorb more than larger ones at lower concentration. However, over a period of time, proteins of higher surface affinity will displace those of lower affinity regardless of protein concentration and size. This exchange phenomena is known as the Vroman effect (Leonard et Vroman, 1991; Noh et Vogler, 2007). For example, when this phenomenon was verified for plasma proteins containing albumin, IgG and fibrinogen (Fg) (Brash, 1996; Jung et al., 2009; Noh et Vogler, 2007), it was noticed that initially adsorbed Fg had been displaced over time by other higher affinity and low concentration proteins such as high molecular weight kininogen (Brash et Ten Hove, 1993).

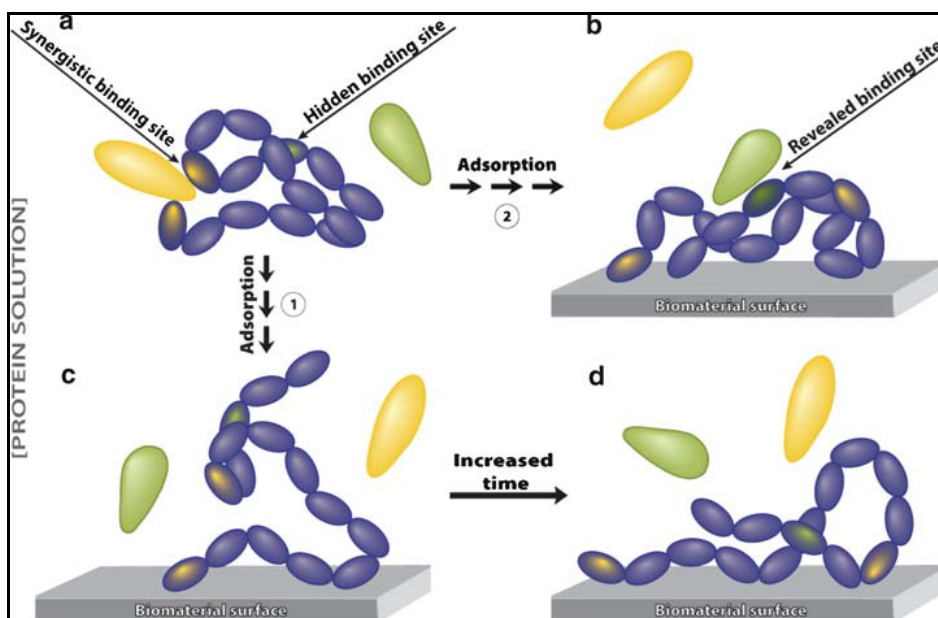


Figure 1.5. Schematic view of protein conformational changes upon adsorption on the material surfaces. Taken from (David Richard Schmidt, 2009).

While the properties of individual proteins are important for protein adsorption, material surface properties such as hydrophilicity, hydrophobicity, topography, surface charge and chemistry (Andrade et Hlady, 1986) also decide the fate of protein adsorption. Figure 1.6 shows the interactions between a protein and the surface that have different binding domains. It is worth noting that water molecules adsorb to the material surface prior to protein adsorption. In the case of hydrophobic surfaces, a shell of water molecules forms in which water molecules prefer to interact with each other rather than interacting with the hydrophobic surface. *One hypothesis postulates that the shell of these surrounding water molecules represents a fairly ordered scenario with a decreased level of entropy; disruption of this layer with proteins is energetically favorable due to a concomitant increase in entropy* (David Richard Schmidt, 2009). The increase in entropy is the primary driving force for protein adsorption on hydrophobic surfaces. Although it is difficult to predict how surface hydrophobicity affects protein adsorption for a specific system, in general, enhanced protein adsorption and conformational changes are observed as surface hydrophobicity increases (Gray, 2004). Depending on the charged areas of both the surface

and the protein, surface charge has an effect of either attracting or repelling proteins. For example, a net negative charge on the material surface reduces the adsorption of serum proteins, since the majority of blood serum proteins are negatively charged (in physiological condition).

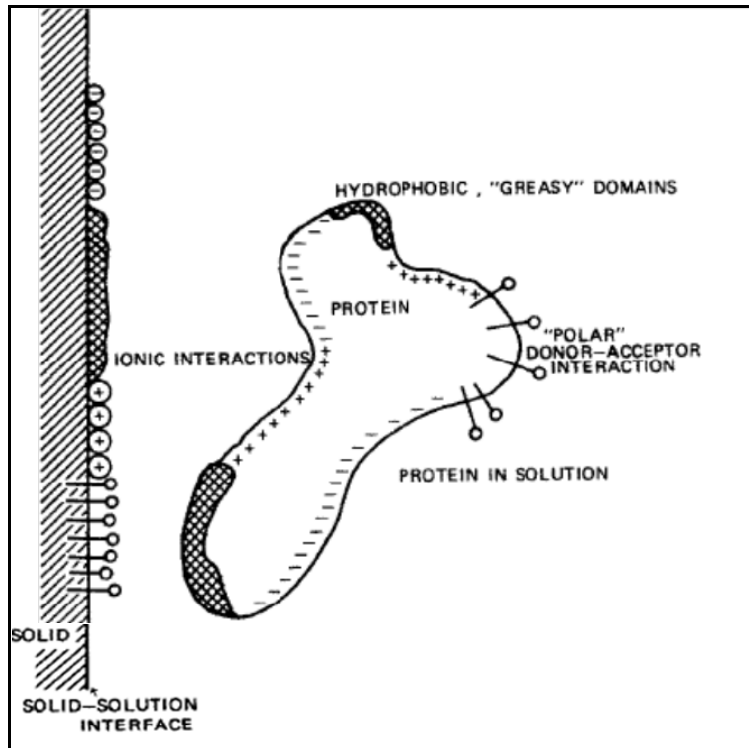


Figure 1.6. A schematic view of protein-surface interactions. Both the surface and the protein have a number of interacting domains with charged, hydrophobic and polar character. Image taken from (Andrade et Hlady, 1986).

Protein adsorption is also strongly influenced by topographical features on a material surface. Increased surface roughness may lead to a net increase in protein adsorption on the material surface, since roughness provides more surface area for protein adsorption (Rechendorff et al., 2006). Finally, changes in surface chemistry dictate the types of bonds between protein and material surface and thus affect protein adsorption. In the literature, the impact of several surface functional groups on protein adsorption was mentioned. Non-polar

and hydrophobic groups such as methyl ( $\text{CH}_3$ ) groups are known to tightly bind fibrinogen (a key protein involved in platelet adhesion and thrombus formation) and immunoglobulin (IgG; an antibody protein involved in the immune response). A material surface that functionalized with  $-\text{OH}$  groups is known to increase surface hydrophilicity and thus reduce the affinity of plasma proteins. Amine ( $\text{NH}_2$ ) groups are found to strongly bind fibronectin and other proteins and induce adhesion of platelets and several cell types. These functional groups are also known to trigger acute inflammatory reactions *in vivo*. (Wang et al., 2004). Carboxyl ( $-\text{COOH}$ ) groups are negatively charged in the presence of blood serum and aqueous protein solutions and are hydrophilic. These groups are known to interact preferentially with vitronectin and albumin (Wang et al., 2004; Weis et al., 2004). It is important to note that these generalized observations may not be true for all cases and may vary depending on experimental conditions and the type of protein solutions. For example, a surface that is activated with multiple functional groups may have a different effect on protein adsorption compared to individual functional groups. In the case of mixed SAMs of  $-\text{NH}_2$  and  $-\text{COOH}$  functional groups (at equal molar fractions), reduced fibrinogen adsorption (Chuang et Lin, 2007) and therefore the lowest platelet adhesion was observed (Thevenot, Hu et Tang, 2008; Wang et al., 2004). It is also important to note that, over time, the presence of water and other molecules in the surrounding environment may modify the activity of functional groups on the material surface (Wang et al., 2004; Weis et al., 2004).

The environment in which protein adsorption occurs is also an important factor that may alter protein adsorption and conformation. Temperature significantly above room temperature can increase protein adsorption. Another important factor is pH condition, which can affect protein adsorption because changes in the charge of both the material surface and the protein molecule may lead to variations in electrostatic interactions (Brash et Ten Hove, 1993).

### 1.2.1.1 Adsorption of serum proteins

The adsorption of serum proteins plays a critical role in promoting platelet and cell adhesion and other biological functions. There are more than 150 varieties of proteins found in human blood serum. The most widely studied proteins and their biological function are listed in the following Table 1.1. Some studies in the literature reported that serum protein adsorption on glass surfaces follows the sequence as albumin first, followed by IgG, fibrinogen, fibronectin, factor XII, and high molecular weight kininogen (Boland et Weigel, 2006; Ellis et al., 1999). Since albumin is the smallest protein and present in high concentration in serum, it adsorbs first on the material surface. Albumin, however, has a relatively low affinity compared to other proteins present in the serum, therefore, over a period of time, it is partially replaced by larger and higher-affinity proteins such as fibrinogen (which is a key molecule in promoting platelet recruitment) (Boland et Weigel, 2006; Ellis et al., 1999).

Table 1.1. Major constituents of human blood serum and their biological functions.  
Taken from (David Richard Schmidt, 2009).

Blood serum proteins	Concentration in normal human blood (mg/ml)	Major function
Albumin	40	Maintains osmotic pressure; forms complexes with, and thus "carries," other serum molecules
Complement C3	1.6	Participates in complement system activation and function
Hemoglobin	0.01	Transports oxygen
High molecular weight kininogen	0.08	Participates in blood clotting
Immunoglobulin (IgG)	15	Participates in the immune response
Fibrinogen	3	Participates in blood clotting
Fibronectin	0.3–0.4	Mediates cell adhesion
Factor XII	0.03	Participates in blood clotting
Vitronectin	0.3	Mediates cell adhesion

### 1.2.2 Thrombus formation

The blood circulatory system is a closed-loop system and it is responsible for the distribution of essential nutrients throughout the body. Injury to the healthy blood vessel leads to immediate thrombus formation to seal the damaged site and therefore to prevent

blood leakage. This process is an essential mechanism to maintain circulation integrity. The accumulation of circulating platelets will take place at the site of injury during thrombus formation and the coagulation system produces thrombin and fibrin to stabilize the clot.

In the native vasculature, after vessel injury, platelet aggregation occurs by the adhesion of exposed collagen in the sub-endothelial matrix. The initial platelet adhesion is mediated by membrane receptors, such as glycoprotein VI and glycoprotein Ib, that bind to collagen and von Willebrand factor, respectively (Fressinaud et al., 1994; Mackman, 2008; Ruggeri, 1997). Platelet adhesion is also known to be mediated by integrin receptors  $\alpha 2\beta 1$  and  $\alpha \text{IIb}\beta 3$ , which bind to collagen and fibrinogen/fibrin, respectively (Bennett, Berger et Billings, 2009; Mackman, 2008; McCarty et al., 2004). The adsorption of these proteins to blood-contacting devices or materials initiates platelet adhesion and therefore platelet activation will occur. Alternatively, soluble factors can activate platelets through binding to its receptors. For example, the tissue factor (TF) pathway leads to thrombin production, and subsequently thrombin cleaves protease-activated receptor 1 (Par-1) on the platelet surface and ultimately activates platelets. Another example is that thromboxane A2 (TXA2) and ADP can bind to their respective receptors on platelets and activate platelets (Davie, Fujikawa et Kisiel, 1991; Furie et Furie, 2008; Mackman, 2008). Both mechanisms (platelet adhesion and the exposure to soluble agonists) are known to be capable of initiating platelet activation individually. However, the relative contribution of each mechanism is still unknown. In general, platelet activation can be recognized by a rapid change in platelet geometry and the release of platelet granules containing a variety of strong chemical agonists that amplify the activation and aggregation of platelets (Blockmans, Deckmyn et Vermylen, 1995; Ruggeri, 2009). The activation of platelets leads to thrombus formation as well as inflammatory responses.

### **1.2.3 Blood coagulation**

Blood coagulation involves a series of cascading events that leads to formation of thrombin and therefore fibrin clot. Blood coagulation follows two separate pathways, namely, the intrinsic pathway (or contact phase pathways) and the extrinsic pathway. Both

pathways lead to a common pathway for thrombin generation (as shown in Figure 1.7). The intrinsic pathway is a series of cascading events that occurs immediately (within 100-200 s) after the surface comes into contact with blood. The Factor XII, kallikrein, high-molecular-weight kininogen, and Factor XI are known as primary components for the intrinsic pathway (Davie, Fujikawa et Kisiel, 1991; Schmaier, 1997). However, it was found that patients deficient in activated Factor XII still produce elevated levels of thrombin during vascular bypass procedures. Therefore it was suggested that the intrinsic pathway may not be required for thrombus formation on implantable material surfaces (Burman et al., 1994).

The extrinsic pathway of blood coagulation, also referred to as the TF dependent pathway, is initiated by the exposure of TF to blood. The physiological coagulation process involves the expression of TF to damaged cells at the site of vascular injury. Initially it was believed that TF resides on the adventitial and medial tissue layers of blood vessels (Wilcox et al., 1989). However, a significant amount of evidence from several research groups suggests that TF presents in the circulating blood secreted by monocytes and neutrophils (Coughlin, 2000; Furie et Furie, 2008; Giesen et al., 1999). Thus TF in blood plays a key role in biomaterial-induced thrombus formation (Jensen et al., 2007; Tomizawa, 1995). Once exposed, plasma Factor VII (FVII) binds to TF on the cell membranes and forms TF-VIIa complex, which is also known as the tenase complex. This tenase complex cleaves Factor X to produce activated Factor Xa and then Factor Xa is able to activate and interact with Factor V. This process leads to the formation of Factor Xa–Factor Va complex, which is also known as the prothrombinase complex. Finally, prothrombinase complex converts prothrombin to thrombin (Coughlin, 2000; Davie, Fujikawa et Kisiel, 1991; Furie et Furie, 2008).

Thrombosis is necessary for the maintenance of hemostasis, but to maintain the function of cardiovascular implants (such as vascular and stent grafts) it is important to prevent thrombosis on implant surfaces. Endothelium is known to be an effective cellular layer that inhibits the adhesion and activation of platelets and also inhibits thrombin generation by expressing several thrombin inhibitors, and therefore blocks the coagulation process and mediates clot dissolution, which is described in the following section. With the

understanding of these molecular mechanisms, one can design bioactive surfaces that mimic natural antithrombogenic properties locally or systemically.

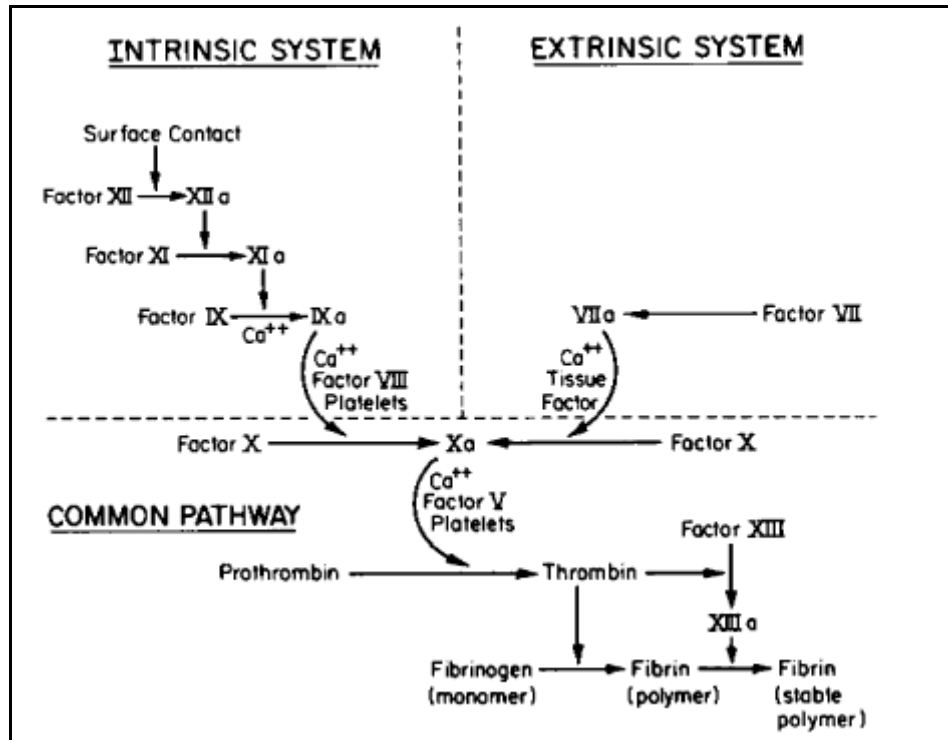


Figure 1.7. Schematic diagram of a simplified view of the blood coagulation cascade that includes intrinsic and extrinsic pathways. Taken from (Gorbet et Sefton, 2004).

#### 1.2.4 Regulation of thrombosis by endothelium

The endothelium acts as a physical barrier that separates circulating blood from thrombogenic tissue components within the vascular wall. Moreover, the endothelium is known to play a multifaceted role in hemostasis and actively regulates thrombotic events. Therefore, biomaterial research has largely focused on achieving EC coverage and/or mimicking specific antithrombotic elements inherent to ECs. Here we give a brief overview of the key mechanisms of EC regulation of thrombus formation.

ECs synthesize several key molecules that inhibit blood coagulation events and act as an antithrombotic layer. The EC layer expresses heparan sulfate proteoglycan (HSPG) that serves as a cofactor of antithrombin-III (AT-III) to facilitate thrombin inhibition (Bernfield et al., 1999; Bernfield et al., 1992). Additionally, ECs express thrombomodulin (TM), which binds to thrombin and converts protein C to its active form (activated protein C; APC), which in turn inhibits Factor Va and Factor VIIa (Stearns-Kurosawa et al., 1996). ECs are also known to be responsible for synthesizing TF pathway inhibitor (TFPI), which binds to both Factor VIIa and Factor Xa. Therefore, TFPI limits TF-induced activation of the extrinsic coagulation pathway (Hackeng et al., 2009) (Figure 1.8).

The endothelium also plays a key role in inhibiting or regulating thrombus formation. ECs synthesize and release nitric oxide (NO) and prostacyclin (PGI<sub>2</sub>), both known to suppress platelet adhesion and activation (Figure 1.8 b) (Best et al., 1977; de Graaf et al., 1992). The level of expression of NO and prostacyclin is modulated by ECs in response to fluid shear stress and chemical stimuli (Knudsen et Frangos, 1997; Radomski et al., 1993). The ECs also bind to ectonucleotidases that hydrolyze ADP, which is an agonist of platelet activation (Michiels, 2003; Pearson, Carleton et Gordon, 1980). The EC surface has a brush-like glycocalyx layer (0.4–0.5  $\mu\text{m}$  in thickness), which consists of proteoglycans with glycosaminoglycan (GAG) side chains and glycoproteins bearing acidic oligosaccharides. The GAGs, such as chondroitin/dermatan sulfate proteoglycans and hyaluronic acid/hyaluronan (HA), are expressed by ECs, with heparan sulfate accounting for 50%– 90% of side chains. These molecules are negatively charged and effectively retain water and form a lubrication layer on the EC surface. There is evidence that heparin sulfate proteoglycans (HSPGs) can resist platelet adhesion (Hashi et al., 2007). Overall, the literature suggests that the healthy ECs exert antithrombotic activity by inhibiting coagulation and suppressing platelet aggregation.

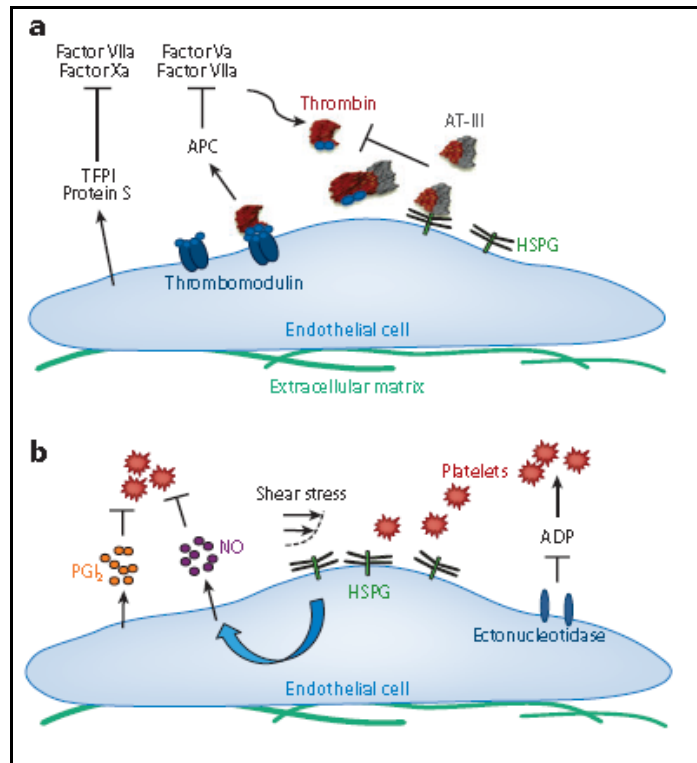


Figure 1.8. (a) EC regulation of coagulation and (b) platelet adhesion and activation. Taken from (Li et Henry, 2011b).

### 1.3 Surface modification for blood compatibility

#### 1.3.1 Low-fouling coatings

Biological "inertness" is a desired feature for designing implantable devices used in research and clinical applications (Boland et Weigel, 2006). The main principle of biological inertness is to reduce unfavorable immune responses to the foreign body or implantable device to the absolute minimum. Since surface-induced thrombosis continues to be a major problem, biomedical materials that prevent non-specific protein adsorption and cellular interactions are considered to be advantageous. Protein adsorption is the initial event that occurs when the material surface comes into contact with the biological environment and plays a critical role leading to thrombus formation. Therefore it is important to passivate the surface to reduce non-specific protein adsorption. Such protein-resistant surfaces also referred to as low-fouling or non-fouling surfaces.

As mentioned in the previous section, protein adsorption to synthetic materials is largely dependent on the material's surface chemistry. Over the past decades, various efforts were made to develop protein-resistant properties by chemical modification of the material surface (Kingshott et Griesser, 1999; Lee, Lee et Andrade, 1995; Roach, Farrar et Perry, 2005; Shen et al., 2003). Whiteside's group and others extensively investigated the effect of surface functional groups on protein adsorption using self-assembled monolayers (SAMs). They described that the surface should possess four different surface characteristics to prevent protein adsorption: the surface should (1) be polar, (2) have hydrogen-bond acceptors, (3) have no hydrogen-bond donors and (4) be electrically neutral (Chapman et al., 2000; Love et al., 2005; Ostuni et al., 2001). Although all the inert surfaces that they examined match these characteristics, not all inert surfaces do (Love et al., 2005). Since the interactions between protein and material surface are diversified, various methods have been developed to design protein-repellent surfaces (Higuchi et al., 2002; Zhao et al., 2003; Zhou et al., 2005). The most common strategy involves producing well-solvated polymer brushes on the surface and thus creating a high activation barrier for protein adsorption (Leckband, Sheth et Halperin, 1999). Several protein-resistant polymers were identified, including: Polyethylene glycol (PEG) (also referred as polyethylene oxide (PEO)) (Lee, Lee et Andrade, 1995), poly 2-hydroxyethylmethacrylate (PHEMA), poly sulfobetaine and poly carboxybetaine methacrylate (Zhang et al., 2006), poly 2-methoxyethylacrylate (poly(MEA)) (Jin et al., 2009), polyacrylic acid (PAA) (Vermette et Meagher, 2002), polysaccharides (Osterberg et al., 1995), and poly(methacrylates) (Zhang et al., 2006). Of those polymers, PEG is the most widely used and investigated polymer for developing non-fouling or low-fouling surfaces. Moreover, depending on surface charge and functional groups, PEG is known to possess most of the characteristics described by Whiteside's group (as described above). Since we use this polymer for creating low-fouling surfaces in this PhD thesis, PEG and its low-fouling mechanism is described in the following section.

### 1.3.1.1 Polyethylene glycol (PEG)

Polyethylene glycol (PEG) is crystalline, water-soluble (in room temperature), non-toxic and a synthetic polymer and is available in a wide range of molecular weights. It is available in both linear and branched conformations, with a repeat unit of  $-\text{CH}_2-\text{CH}_2-\text{O}-$  and usually terminated on each end of the molecule by an  $-\text{OH}$  group. However, PEG is also synthesized with several other terminal groups, for example  $-\text{OCH}_3$ ,  $-\text{OCH}_2$ ,  $-\text{NHS}$ , and  $-\text{COOH}$ . These terminal groups are helpful and important for covalent grafting onto biomaterial surface or conjugating with other molecules. Since PEG is highly water-soluble, it has a good structural fit with water molecules. As shown Figure 1.9, a strong hydrogen bonding exists between the ether oxygen atoms of PEG and hydrogen atoms of two water molecules.

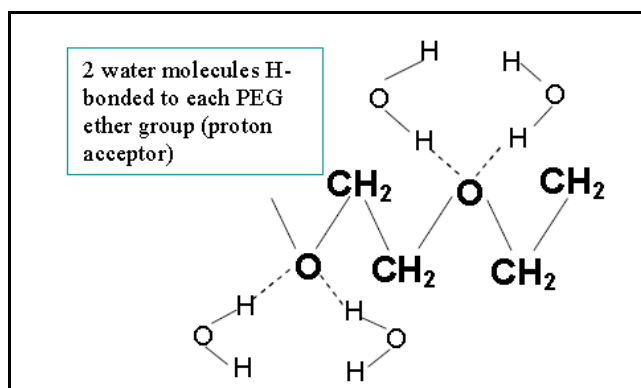


Figure 1.9. Schematic shows hydrogen bonding between ether oxygen atoms.  
Image adapted and modified from  
(Andrade et Hlady, 1986).

### PEG low-fouling mechanism

As explained earlier, surface modification with hydrophilic polymers, such as PEG, is a widely used method to reduce protein adsorption. Although several factors have been hypothesized for protein-resistant properties, two main mechanisms are described more often in the literature to explain PEG non-fouling properties.

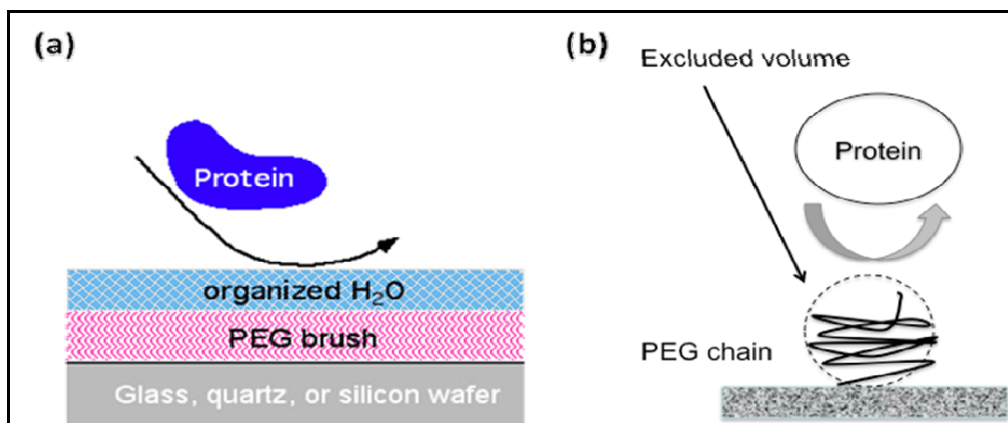


Figure 1.10. Schematic view of (a) protein repulsion on hydrated polymer chains and (b) prevention of protein adsorption on PEG layer by excluded volume-steric repulsion. Image adapted from (Andrade et Hlady, 1986).

The first mechanism involves steric repulsion, especially for long chain polymers, which arises due to conformational freedom of the -C-C-O backbone of PEG and unrestricted rotation around the C-O bonds. When protein approaches the PEG-modified surface, the compression of the polymer chains causes an entropy loss and generates steric repulsion against proteins, and therefore polymer chains, effectively pushing proteins away from the surface (see Figure 1.10 b) (Jeon et Andrade, 1991; Jeon et al., 1991). The second mechanism is related to the hydration layer near the surface and the low interfacial energy at the PEG-water interface (Chen et al., 2000; Herrwerth et al., 2003; Zheng et al., 2005). The tightly bound water layer around polymer chains forms a physical and energetic barrier to protein adsorption. Expulsion of the water molecules from the polymer chain is the obligatory step to allow protein adsorption by reducing the free energy barrier arising from dehydration entropic effects (Chen et al., 2000). Although most of hydrophilic polymers are able to reduce protein adsorption, the best non-fouling ability can only be achieved when surface hydration and steric repulsion work together. It was speculated that both the steric repulsion and the hydration properties of PEG make it ideal for creating a non-fouling surface.

However, many other parameters influence protein adsorption on PEG-modified surfaces, such as polymer chain density, chain length, chain terminal groups-protein

interaction, protein-surface interaction and so on (Currie, Norde et Cohen Stuart, 2003). Among these, both PEG chain length and surface coverage are considered to be very important parameters affecting protein resistance (Currie, Norde et Cohen Stuart, 2003). Therefore, a surface modified with sufficiently high density and long PEG chains is able to resist protein adsorption very effectively.

### **1.3.1.2 PEG immobilization**

Several strategies have been proposed for PEG immobilization on material surfaces, including simple direct adsorption (Davis et Illum, 1988), radiation and chemical cross-linking approaches (Graham et McNeill, 1984), and self-assembled monolayers (Yang, Galloway et Yu, 1999). Of those methods, the simple adsorption method is flexible and convenient, but its efficacy is limited by the tendency of PEG to elute off the surface (Gombotz et al., 1991). It has been demonstrated that a stable and efficient PEG coating can be achieved by covalent chemical grafting onto substrates (Demming et al., 2011). When PEG is covalently grafted onto the substrate through its terminal groups, depending on PEG density, three surface "regimes" may be distinguished (Gasteier et al., 2007), as shown in Figure 1.11. If the PEG grafting density is too low, the PEG will be grafted and displayed in a random coil conformation, known as the "mushroom regime", where the PEG chains do not overlap. In this case, empty spaces exist between PEG molecules and therefore protein will adsorb on these open spaces. As the density increases, random coil conformation no longer exists, and PEG molecules must stretch to be accommodated in a given space. At a higher PEG grafting density, the distance between the chains is smaller than the radius of gyration and PEG chains will be completely stretched, and therefore the surface will be displayed in the "brush regime" (Figure 1.11). In this case, protein adsorption is prevented more effectively. However, it depends on the type of PEG used for grafting. For example, if the PEG is a homobifunctional polymer, there are great chances of both terminal groups interacting with the substrate.

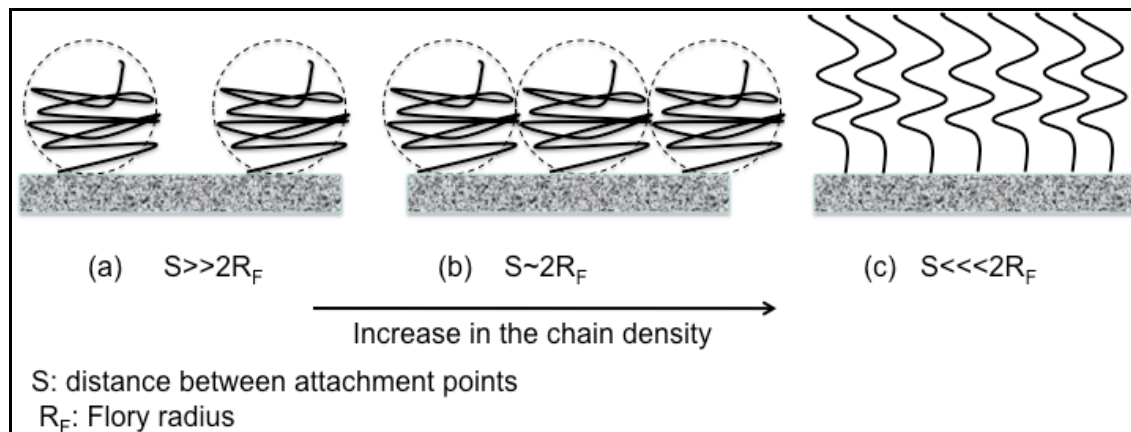


Figure 1.11. Schematic shows three different PEG regimes, depending on the PEG chain density. The PEG conformation on the surface changes from non-overlapping "mushrooms" to fully extended "brushes" at different grafting densities. Image adapted and slightly modified from (Unsworth et al., 2005).

### 1.3.1.3 Linear vs. branched polymers

As mentioned earlier, PEG can be synthesized in both linear and branched conformations or star-shaped structures (Irvine et al., 1998). Star-shaped molecules are defined as species consisting of a central core region with linear "arms" that are radiating outward from that core (Sofia, Premnath et Merrill, 1998). Star-shaped structures usually form at the junction of various linear molecules, which are referred to as the star arms (see Figure 1.12b). This junction forms the star core with arms extending out from the higher-density core and the number and length of these arms can vary. Various groups synthesized a wide range of molecular weight star PEGs, with a great variety of arms per molecule (ranges from 4 arms to 70 arms/molecule) (Groll et Moeller, 2010; Irvine et al., 1998; Keys, Andreopoulos et Peppas, 1998; Kuhl et Griffith-Cima, 1996; Sofia Susan et Merrill Edward, 1997). The structural variation of star PEG compared to linear PEG is advantageous for low-fouling and bioactive coating on biomaterial surfaces.

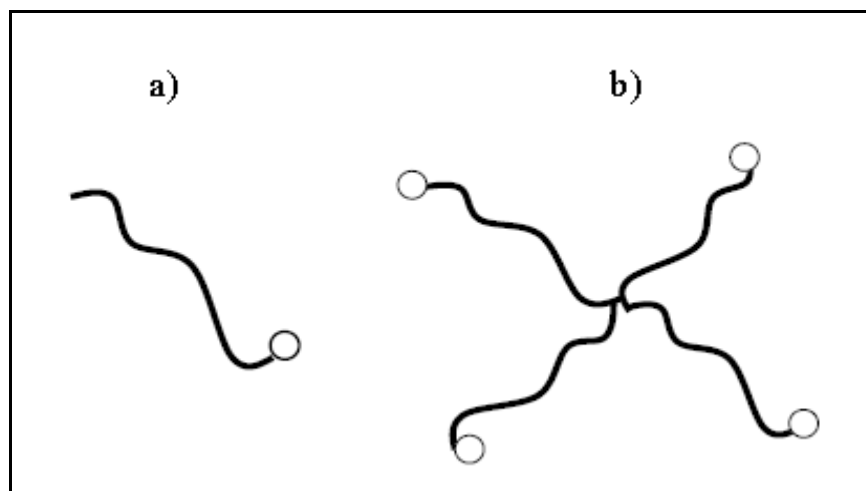


Figure 1.12. Schematic diagram of a) a linear PEG molecule and b) an end-functionalized 4-arm star PEG. The circles represent end functional groups by which the molecules may tether to surfaces. Image adapted from (Irvine et al., 1998).

The presence of greater number of chains or arms, terminal groups and long chain length on star PEG enable higher surface grafting density compared to linear PEG. (Groll et Moeller, 2010; Kuhl et Griffith-Cima, 1996; Sofia Susan et Merrill Edward, 1997). Irvine and coworkers compared the effect of polymer architecture on surface concentration and protein adsorption using different molecular weights of star-shaped and linear PEGs. The grafting density for star PEG was found to be significantly higher than that of linear molecules (Irvine, Mayes et Griffith-Cima, 1996). It was also noted that, for similar chain lengths and molecular weights, star-shaped polymers possess higher grafting density compared to linear PEGs. Star PEGs are known to prevent the adsorption of large proteins (for example fibrinogen and albumin) more effectively compared to linear PEGs, which is due to greater steric repulsion arising from the large number of arms in star PEG (Sofia, Premnath et Merrill, 1998). However, star PEGs were also shown to allow a small amount of protein adsorption, especially smaller size proteins (for example cytochrome-c) (Sofia, Premnath et Merrill, 1998). It was suspected that this was due to lack of overlapping between star molecules, creating open spaces between star molecules that allowed the adsorption of smaller size proteins in small amounts (Sofia, Premnath et Merrill, 1998). It was suggested that increasing star PEG coupling concentrations during grafting would overcome steric

repulsion between star molecules and help to achieve tight packing of star PEG molecules on the surface and therefore achieve complete prevention of protein adsorption (Groll et al., 2004a; Irvine et al., 2002; Satulovsky, Carignano et Szleifer, 2000). It was also demonstrated that a monolayer coverage of star PEG polymers with sufficient grafting density on the surface is able to prevent complete protein adsorption (Groll et al., 2004a; Groll et al., 2005c), which may not be possible using linear PEG as most systems are using PEG SAMs to create complete low-fouling surfaces.

#### **1.3.1.4 Low-fouling polymers for bioactive coatings**

In the last few years, there has been increasing interest in using low-fouling polymer as a spacer for the immobilization of small peptide sequences, growth factors and other biomolecules. The bioactivity of immobilized biomolecules can be increased on low-fouling surfaces compared to those immobilized on fouling surfaces. This is due to several reasons (see Figure 1.13): (i) It prevents non-specific adsorption of biomolecules and of proteins which would cover and hide the bioactive molecule. (ii) It prevents interaction of the other end of tethered biomolecule with the substrate. (iii) Tethered biomolecules stand out from the surface and are accessible for receptor binding due to the sterical hindrance effect of low-fouling polymers (for example star PEG as shown in Figure 1.13). (iv) It offers conformational flexibility to the tethered biomolecules and makes them accessible to the receptors. As shown in Figure 1.13, the arms of star PEG always emanate outward from the core of the molecule due to the steric hindrance effect. Therefore the terminal groups are still available for further coupling with other molecules. This makes it possible to tether a greater number of biomolecules per star molecule (Groll et Moeller, 2010; Kuhl et Griffith-Cima, 1996), which is not possible using linear PEG as it has only one end group available for coupling. Moreover, if the linear PEG is a homobifunctional polymer, it is possible that both the terminal groups would interact with the surface, leaving no available groups for further coupling.

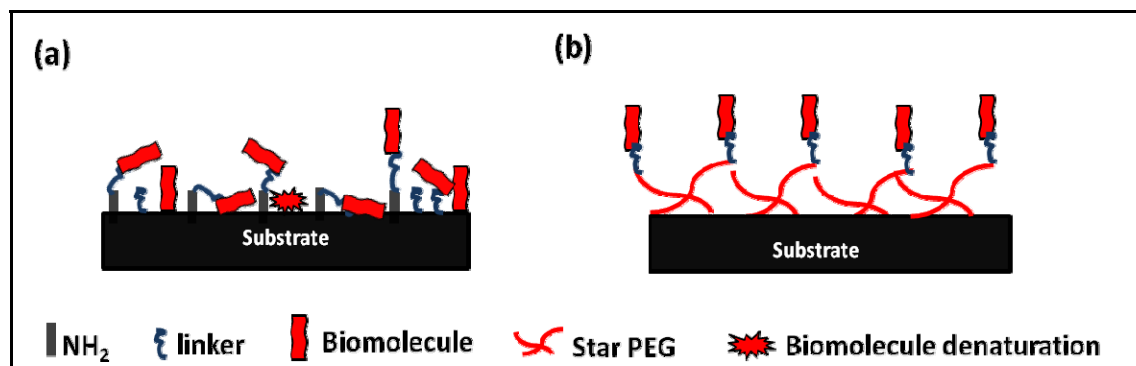


Figure 1.13. Schematic view of the possible interactions and orientations of biomolecules when they are immobilized on (a) an amine-functionalized surface vs. (b) a 4-arm star PEG modified surface

Several studies have demonstrated improved bioactivity of immobilized biomolecules on PEG coated surfaces. Kim and co-workers immobilized heparin on a PEG spacer and showed improved bioactivity of heparin in terms of antithrombin binding compared to those surfaces prepared by direct immobilization of heparin (Byun, Jacobs et Kim, 1994). Others also showed high antithrombin binding of heparin and reduced fibrinogen adsorption when it is immobilized through a PEG spacer (Chen et al., 2005a; Xu et al., 2005). In another studies, a PEG spacer was used to improve the bioactivity of antibodies to detect antigens for biosensor applications (Sebra et al., 2005) and similarly for DNA hybridization in microarrays (Del Campo et Bruce, 2005). Several other studies also used PEG coatings to promote specific cell adhesion (Groll et al., 2005b; Hoffmann et al., 2006) and investigate cell interactions (Maheshwari et al., 2000) by immobilizing small peptide sequences such as RGD peptides and growth factors (Klenkler et al., 2008). Overall, the literature suggests that PEG coatings are useful for preparation of bioactive surfaces, which are helpful in developing biocompatible biomaterials for vascular graft applications.

### 1.3.1.5 Limitations of PEG coatings

There are some limitations using PEG surfaces for low-fouling and bioactive coatings, which include: (i) PEG is very expensive to synthesize (ii) PEG coatings exhibit poor stability due to the rapid oxidization of PEG in the presence of oxygen and transition

metal ions. (iii) Some studies have shown that despite low protein adsorption on PEG surfaces, blood coagulation still occurs on these surfaces (Hansson et al., 2005a; Zhang et al., 2008a). *In vitro* and *in vivo* studies by several groups have proved that PEG-coated cardiovascular materials significantly reduce platelet adhesion (Bernacca et al., 1998; Deible et al., 1999; Park et al., 2000; Ritter et al., 1998). However, most *in vivo* studies of PEG-modified implants have been unsuccessful in limiting blood clot formation (Hansson et al., 2005b; Nojiri et al., 1990a; Park et al., 2000). One explanation is that the PEG layers limit only individual platelet adhesion but not platelet aggregates that might form in blood away from the material surface (Park et al., 2000). Moreover, PEG coatings do not prevent material induced complement activation and blood coagulation (Andersen et al., 2013b). (iv) The non-adhesive nature of high-density PEG coatings may be unfavorable for promoting confluent cell growth on the biomaterial surface (Klenkler et al., 2008). Altogether these limitations suggest that PEG coatings alone are not enough to improve patency of vascular implants; they must combine with biomolecules that promote desired cell adhesion and prevent blood clotting.

#### **1.3.1.6 Dextran for low-fouling coatings**

Among low-fouling coatings, PEG polymers have attracted particularly strong attention because of their hydrophilic nature as well as their steric repulsion properties. Another class of molecules, such as polysaccharides (alginic acid, dextran and chondroitin sulphate, etc), was also found to be highly wettable and able to produce low-fouling coatings (McArthur et al., 2000). These polymers are heavily hydrated, and hydrogels like structure and mobile molecular chains that offer a steric repulsion towards protein adsorption. Among polysaccharides, dextran coatings were found to be a good alternative to PEG coatings and its low-fouling properties were as good as PEG (Dubois, Gaudreault et Vermette, 2009; Michel et al., 2014; Monchaux et Vermette, 2007). These coatings have been investigated for a variety of biomaterials and biosensor applications (Marchant, Yuan et Szakalas-Gratzl, 1994; Österberg et al., 1993; Toufik et al., 1995). The low-fouling mechanisms for dextran polymers are similar to the mechanisms described for PEG. Carboxymethylated dextrans

(CMDs) have been widely studied as their carboxylic terminal groups enable reaction either with surfaces or with bioactive molecules (Dubois, Gaudreault et Vermette, 2009; Liberelle et al., 2010; Massia, Stark et Letbetter, 2000). The most common methods of CMD grafting include covalent immobilization of carboxyl terminal groups onto the surface. This strategy was found to be efficient against protein adsorption and cell adhesion (Massia, Stark et Letbetter, 2000). Surface-bound CMD is known to provide more sites than PEG for further immobilization of biomolecules (for example small peptide sequences). However, CMD has random polymer chains, unlike star PEG (see Figure 1.14). Several studies used CMD as a spacer for the immobilization of RGD (to enhance HUVEC adhesion) (Hadjizadeh et Doillon, 2010; Hadjizadeh, Doillon et Vermette, 2007), antibodies (for ELISA test) (Liberelle, Merzouki et Crescenzo, 2013) and fibronectin (Dubiel et Vermette, 2012).

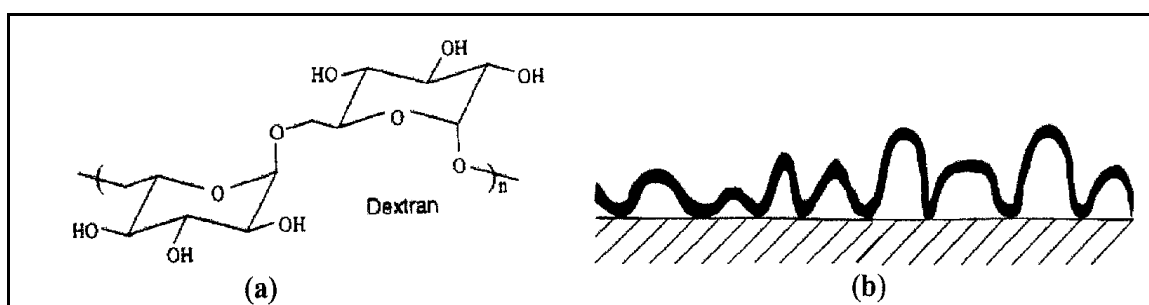


Figure 1.14. Schematic shows (a) the chemical structure of dextran and (b) the configuration of surface-bound dextran polymer. Image adapted from (Massia, Stark et Letbetter, 2000).

### 1.3.2 Surface modification with anticoagulants

While the low-fouling polymers such as PEG, CMD and other hydrophilic polymers are known to prevent protein adsorption and therefore reduce platelet adhesion and activation, they clearly do not reproduce the anti-thrombotic activity of EC. Alternatively, surface coating with anticoagulant molecules became a popular choice for inhibiting biomaterial-induced thrombosis and blood clotting. In particular, in the last few decades, heparin-coated surfaces have been widely investigated for the development of biomedical

materials with anticoagulant function. Therefore, here we focussed on surface modification using heparin molecules and other thrombin inhibitors.

Heparin sulfate is a linear polysaccharide with repeating units of alpha-D-glucosamine and uronic acid (Mulloy, Mourão et Gray, 2000) containing clusters of O- and N-sulphated groups. Heparin is able to bind AT-III and causes a conformational change in the reactive center of AT-III to allow the inhibition of thrombin (see Figure 1.15). To some extent, heparin-AT-III complexes are also known to inhibit other coagulation factors such as Factors XIa, Xa, and IXa (Holmer, Kurachi et Soderstrom, 1981).

Several studies showed that surface modification with heparin could substantially reduce thrombus formation, both *in vitro* and *in vivo* (Huynh et al., 1999; Ritter et al., 1998; Walpoth et al., 1998). The heparinized vascular implants generally showed improved anticoagulant properties compared to unmodified implants. Several studies also showed prolonged blood clotting on heparin-modified synthetic polymers (e.g. poly(hydroxyethyl methacrylate) (PHEMA) and vinyl copolymers) (Baldwin et Kiick, 2010; Jao et al., 2010; Marconi, Benvenuti et Piozzi, 1997; Wang et al., 2011a). Heparin coatings are also currently being used for commercially available medical devices such as stents, oxygenators and vascular grafts, and many of these devices have been developed using the coating method developed by Larm et al. (Larm, Larsson et Olsson, 1983) (for example Carmeda® BioActive Surfaces (CBAS)).

Although the above-mentioned heparinized surfaces have been found to prolong clotting time, they do not prevent clotting completely, and it was also demonstrated that clinical success of heparin-coated surfaces has been rather limited (Gorman et al., 1996; Jain et al., 2009; Palatianos et al., 1983). These mitigated results for heparin could be explained by two reasons; (i) The antithrombotic action of heparin is based on its ability to bind antithrombin and its strong stimulatory effect on the neutralization of thrombin and Factor Xa (E. Niklason et S. Langer, 1997; Sacks, Schoen et Mayer, 2009). Therefore, maintaining the biological activity of heparin (i.e. the AT-III binding should remain accessible) is an important concern. Variations in heparin immobilization strategies may result in different

efficacy and clinical outcomes. (ii) The anticoagulant response to heparin is unpredictable, since the heparin–antithrombin complex is not able to inhibit fibrin-bound thrombin (Lytle et al., 1985).

Other sulfated glycoaminoglycans have also shown to exhibit anticoagulant properties. It is the case of chondroitin sulfate (CS) and sulfated hyaluronic acid which were shown to prevent thrombosis. (Keuren et al., 2003). Little is known about this question and the mechanism of action is not completely known, but it was found that the removal of sulfated groups decreased their anticoagulant activity (Mulloy, Mourão et Gray, 2000). It is thus suspected that the negative charge induced by sulfated groups causes electrostatic repulsion towards negatively charged blood components while wettability diminishes protein adsorption.

Several different strategies have been used for the immobilization of anticoagulant on biomaterials surfaces. They include ionic bonding, physical adsorption, bulk material incorporation, and covalent linkage. Stability of heparin coatings were found to be much higher for a covalent immobilization compared to other immobilization strategies. Covalent grafting can be achieved on a biomaterial surface by cross-linking reactions involving one of several functional groups (such as hydroxyls, carboxyls, or amines) that reside on the heparin chain. Covalent immobilization of heparin using a PEG spacer was shown to enhance the AT-III binding activity of heparin (Park et al., 2000; Tay et al., 1989) and maintain the patency of vascular grafts for 3 months in a canine model (Nojiri et al., 1990b). The improved biological activity of heparin when using a PEG spacer is most probably due to the reduction of non-specific protein adsorption and conformational flexibility. Therefore, the use of low-fouling spacers such as PEG or other polymers seems to be a more promising strategy for heparin immobilization and thus reducing blood clotting.

Despite widespread use of heparin to coat blood-contacting materials, it has a few limitations; (i) Heparin is unable to inhibit fibrin-bound thrombin. (ii) Heparin relies on the local presence of AT-III to exert its activity. (iii) Heparin has the ability to bind a wide range

of biomolecules that includes growth factors and matrix proteins, which could lead to other side effects and adverse immune reactions (Fairbrother et al., 1998; Neufeld et al., 1999a; Sakiyama-Elbert et Hubbell, 2000). It was thus demonstrated that heparin-coated stents could induce neointima formation due to the inflammatory response caused by heparin coating (De Scheerder et al., 1997; Goodwin et al., 2003).

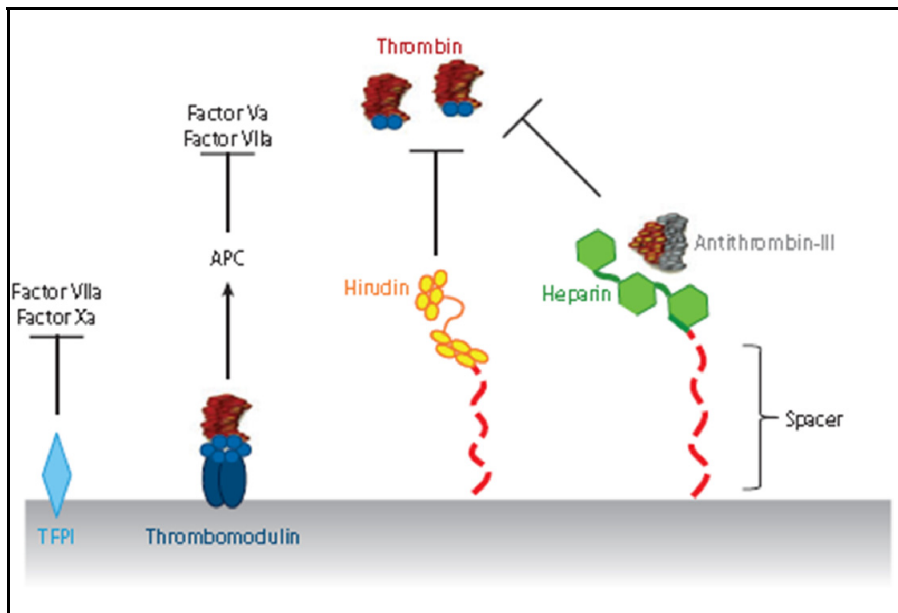


Figure 1.15. Schematic view of mechanism of action of immobilized heparin, hirudin, thrombomodulin (TM) and tissue factor pathway inhibitor (TFPI) to inhibit coagulation. Taken from (Li et Henry, 2011b).

In order to overcome the limitations of heparin, many groups have explored surface modifications using factors that directly inhibit thrombin or thrombin production. Among direct thrombin inhibitors, hirudin was found to be the most potent natural inhibitor. Hirudin is a small protein consisting of only 65 amino acids and originally derived from the medicinal leech. It forms a tight bivalent complex with thrombin, and this complex blocks both the active site and the fibrinogen-binding exosite of thrombin (Grutter et al., 1990; Schmitz, Rothe et Dodt, 1991). Furthermore, it is capable of inhibiting soluble thrombin as well as fibrin-bound thrombin (Figure 1.15). Several studies covalently attached recombinant hirudin (r-hirudin) to biomaterial surfaces and succeeded in significantly reducing thrombus

formation *in vitro* (Phaneuf et al., 1997; Seifert, Romaniuk et Groth, 1997; Wyers et al., 1999). However, direct immobilization (without using any spacer) of hirudin through its N terminus has resulted in significantly reduced bioactivity compared to soluble hirudin. Selective attachment using the  $\epsilon$ -amino acids was shown to be a good alternative to preserve the bioactivity of immobilized hirudin (Lahann et al., 2001). Again, the use of a PEG spacer and covalent immobilization through the C-terminus showed improved bioactivity of r-hirudin and overall reduction of adherent and activated platelets. *In vivo* performance of the PEG-hirudin-treated vascular graft was shown to increase in patency at 6 months after implantation into rat carotid arteries (Hashi et al., 2010). The effect of immobilized hirudin on late stent thrombosis still needs to be investigated. Although hirudin coatings through the use of a PEG spacer seems to be a promising strategy, the complete prevention of blood clot formation has not yet been achieved. Alternatively, some groups are investigating (Sun et al., 2001; Tseng et al., 2006) the use of TM and TFPI coatings to limit thrombin production (Figure 1.15) and further enhance the antithrombogenic properties of tissue-engineered implants

Overall the literature shows an interesting development towards bioactive anti-thrombogenic surfaces and suggests that the use of a low-fouling spacer could help to improve the biological activity of anticoagulants such as heparin and hirudin. However, these surfaces do not reproduce the complete set of bioactivity observed with the native endothelium, as described in section 1.2.4. Moreover their long term efficiency is a concern. An alternative approach is to directly promote the growth of an endothelial layer for achieving perfect antithrombogenic surfaces because endothelium has the advantage of multifaceted activity in regulating thrombus formation and blood clotting.

#### **1.4 Modifying surface physico-chemical properties to promote cell adhesion**

In order to improve surface properties of vascular materials, several research groups focussed on increasing surface hydrophilicity either by chemical (UV exposition or alkaline hydrolysis) (Mikulikova et al., 2005) or plasma treatments (ammonia or oxygen plasma

treatment) (Gigout et al., 2011; Lerouge et al., 2007; Pompe et al., 2007; Pu et al., 2002b; Ratner, 1995). These treatments introduce polar groups and charges on the surface. For example, TCPS and Primaria (routinely used for cell culture) are made by plasma treatments in order to create cell-adhesive surfaces. Such plasma-modified surfaces are hydrophilic and allow adsorption of adhesive proteins and can promote cell adhesion, spreading and growth (Gigout et al., 2011; Qu et al., 2005; Steele et al., 1994). Oxygen-rich surfaces exhibit negatively charged groups, while nitrogen-rich surfaces are positively charged at any physiological pH. In the presence of serum or blood plasma, the adsorption of Fn is responsible for initial cell attachment on nitrogen-rich surfaces (e.g, Primaria), whereas cell adhesion on oxygen-rich surfaces (e.g. TCPS) is mediated by Vn adsorption alone, because Fn is a negatively charged acidic protein that can abundantly adsorb on positively charged surfaces (Boura et al., 2005; Ertel, Ratner et Horbett, 1990; Steele et al., 1994).

Plasma treatments, particularly amine plasma polymerization, are widely used to alter biomaterial surface properties. In general, plasma depositions can change a variety of surface characteristics, including chemical, electrical, and mechanical properties (Siow et al., 2006). These treatments can provide sterile surfaces and can be scaled up to industrial productions (Ohl et Schröder, 1999). Nitrogen- and oxygen-based plasma depositions are commonly used to introduce a variety of functional groups such as hydroxyl, carboxyl, amine and aldehyde. There are two main advantages to using these techniques in the context of vascular graft applications: (i) improved cell-adhesive properties due to alteration of surface charge and increase in surface hydrophilicity; (ii) introduction of functional groups allowing chemical coupling of a variety of molecules such as hydrophilic polymers and biomolecules.

More recently, the team of professor Wertheimer (École Polytechnique) and Lerouge has developed a new range of primary amine-rich organic coatings via polymerization of ethylene ( $C_2H_2$ ) and ammonia ( $NH_3$ ) operating at low-pressure (L-PPE: N) or atmospheric pressures (“high”, “HPPE:N”) (Truica-Marasescu et al., 2008). These coatings possess several advantages compared to simple plasma functionalization techniques; i) very versatile i.e. coatings can be deposited on any biomaterial surface, (ii) high nitrogen and primary

amine concentration (about 7%), iii) relatively low aging and iv) very good surface uniformity (Ruiz et al., 2010; Truica-Marasescu et al., 2008). L-PPE: N or H-PPE: N coatings on biomaterial surfaces, such as PET and ePTFE, were shown to promote HUVEC adhesion and retention for vascular graft applications (Gigout et al., 2011). These coatings were also used to promote VSMC adhesion and growth for stent graft applications (Lerouge et al., 2007). However such physico-chemical modifications of the surfaces promote non-specific interactions through the adsorbed protein layer, leading to uncontrolled and unwanted interactions with blood and biological compounds. Therefore, many attempts are now made to promote more specific surface modification using bioactive biomolecules known to directly interact with cells and promote specific behavior. Thus, in Lerouge's lab, the primary amine-rich L-PPE:N was used for the covalent immobilization of anti-apoptotic molecules, namely CS and Epidermal Growth Factor (EGF). These coatings showed enhanced VSMC adhesion, growth and resistance to apoptosis (Charbonneau et al., 2012). Other experiments showed that, interestingly, CS promotes VSMC adhesion while preventing EGF non-specific adsorption during grafting, indicating probable low-fouling properties (Lequoy et al. 2014).

More generally, there is a clear trend towards bioactive coatings to foster specific cell-surface interactions. In the following section, we discuss in detail the possibilities of improving surface biocompatibility using bioactive coatings. These can be combined with low-fouling coatings to help improving the biocompatibility of materials used for vascular implants.

## **1.5 Bioactive coatings to promote cell adhesion and growth**

### **1.5.1 Coatings made of ECM proteins**

#### **1.5.1.1 ECM and cell interactions**

The ECM provides mechanical support and biochemical cues for cell adhesion and influences major cellular events such as migration, proliferation, differentiation and

apoptosis. The composition of the ECM ultimately determines which program will be selected for cellular events. ECM proteins, more particularly cell adhesive proteins (fibronectin (Fn), laminin (Ln) and vitronectin (Vn)), have many binding domains that can interact with cell surface receptors (see Figure 1.16) as well as with other ECM proteins. The specific amino acid sequence present within ECM molecules is responsible for binding with cell surface receptors and triggering intracellular pathways. Cell-ECM adhesions are mediated primarily by heterodimer proteins, known as integrins, which consist of  $\alpha$  and  $\beta$  subunits. To date 18  $\alpha$  and 8  $\beta$  subunits are known, which can associate to form 24 different heterodimers. The formation of different heterodimers from these complexes depends on the signals found on the ECM. However, each amino sequence present on the ECM is a signal for a specific integrin complex attachment site. For example endothelial cells (ECs) are found to interact with fibronectin through  $\alpha\text{v}\beta\text{3}$  and  $\alpha\text{5}\beta\text{1}$  integrins (Brooks, Clark et Cheresch, 1994; Stupack et Cheresch, 2004) whereas collagen type 1 and IV interact through  $\alpha\text{1}\beta\text{1}$  and  $\alpha\text{2}\beta\text{1}$  integrins (Panetti et al., 2004; Plow et al., 2000).

Once the ligand interacts with its specific receptor on the cell, it begins to spread or flatten on the interface. Integrins then form adhesion structures and relay signals to the cell nucleus by bridging proteins and actin fibres. If these signals are positive, integrin molecules that are attached to both the ligand outside of the cell and the cytoskeleton inside the cells (stress fibers and a number of other cell proteins, such as focal adhesion kinase, vinculin, talin, and tensin) cluster together in the plasma membrane and thus increase the area of cell adhesion to the substrate. The cascade of events finally leads to formation of focal adhesion contacts (Geiger et Bershadsky, 2001b; Petit et Thiery, 2000; Zamir et Geiger, 2001b). It is worth noting that the interaction between peptide ligands and integrins not only ensures the structural integrity of living cells, but also influences many aspects of cell responses such as migration, growth, differentiation and survival (Petit et Thiery, 2000). The coordination between integrin receptors and other receptors and their synergistic effects is further discussed in the combined immobilization section.

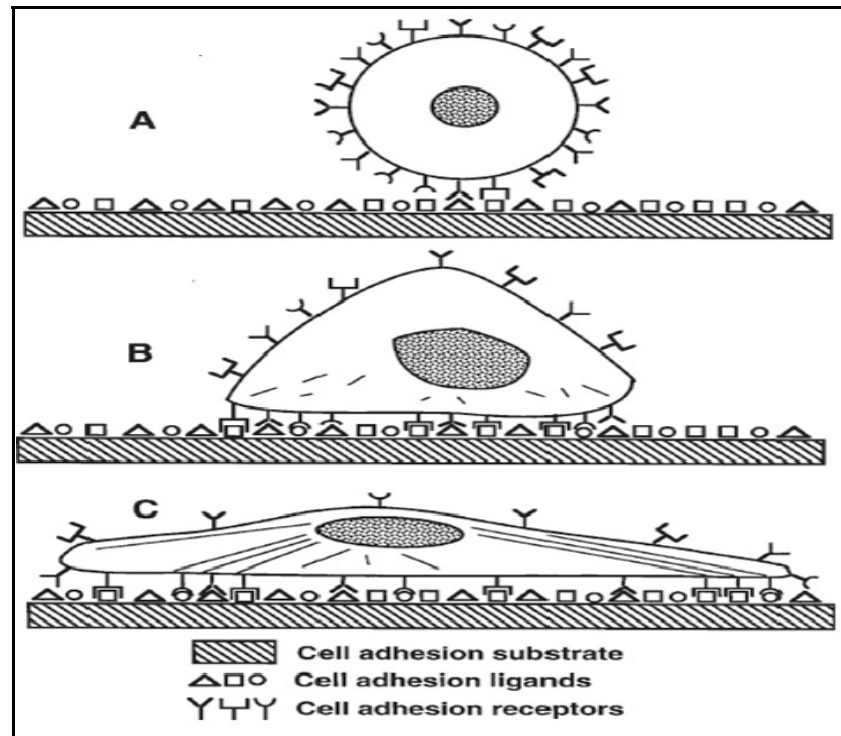


Figure 1.16. Schematic view of progression of anchorage dependent cell adhesion. (A) Initial contact of cell with solid substrate that has multiple binding domains. (B) Formation of bonds between cell surface receptors and ligands. (C) Cytoskeletal reorganization for increased adhesion strength. Taken from (Massia, 1999).

### 1.5.1.2 Surface coating with cell adhesive proteins

Surface coating with the adsorption of several ECM proteins may promote cell adhesion, but it is an exceedingly complex phenomenon, the exact composition is not known and it is very difficult to control or reproduce (Ratner, 1993). Moreover, the adsorbed protein layer can undergo denaturation and proteolysis, which may affect the long-term performance of implanted biomaterials (Andrade et Hlady, 1986; Thomas et John, 1987). Hence, the use of individual components of the ECM such as Fn, collagen type I and IV would be more controllable and beneficial in designing or developing biocompatible materials. Surface coating with such individual proteins may be adequate enough to mimic physico-chemical features of tissue ECM and to promote cell interactions with the material surface. Since ECM proteins are large molecules and have several binding domains to interact with the surface,

surface coatings are usually performed via direct adsorption. Although covalent binding allows stable coupling, most systems rely on direct adsorption of ECM proteins. This might be due to the fact that it is difficult to control the orientation of proteins through covalent bonding (due to the presence of several binding groups on ECM proteins for coupling) (Petersen, Gattermayer et Biesalski, 2011), which leaves a significant fraction of binding sites inaccessible to cells and therefore loss of protein biological activity. Several ECM protein coatings on a different variety of surfaces and their influence on promoting cellular interactions are thus discussed in the following paragraph.

Fn is a widely used and investigated ECM protein for surface coating that was shown to enhance several types of cell adhesion, spreading and proliferation (Koenig, Gambillara et Grainger, 2003b). Such Fn coating was shown to promote the formation of focal adhesions and the organization of actin filaments into stress fibers through the interaction of integrin receptors such as  $\alpha 5\beta 1$  and  $\alpha v\beta 3$  (Underwood et Bennett, 1993). Similarly, collagen type I and type IV coating on PTFE was shown to promote EC adhesion and retention (Feugier et al., 2005; Ludwig et al., 2006) and induce EC migration to a higher extent than Fn (van Horssen et al., 2006), which is known to interact with integrin receptors  $\alpha 1\beta 1$  and  $\alpha 2\beta 1$  (Underwood et Bennett, 1993). Another ECM protein, Laminin, was also shown to support EC adhesion and spreading, but to a lesser extent than Fn and collagen (Underwood et Bennett, 1993), with no formation of focal or even fibrillar adhesions (Vainionpaa et al., 2006).

Although these proteins enhance the cell interactions with the surface, the underlying surface chemistry is known to influence protein density, conformation and spatial organization, which in turn affect cell attachment and subsequent cell behavior. Fn adsorbed on a hydrophilic surface supports higher EC adhesion and retention than when adsorbed on a hydrophobic surface. It has been reported that the protein exposes to a higher density of cell binding sites when bound to a hydrophilic substrate, therefore cells may form more bonds with the surface and lead to a higher cell adhesion strength (Burmeister et al., 1999; Iuliano, Saavedra et Truskey, 1993; Ugarova et al., 1995). Cell adhesion studies on Fn coating using

various surface chemistries (such as neutral, positive and negatively charged surfaces) showed that it can alter Fn conformation and influences subsequent integrin binding and its ability to support cell adhesion (Keselowsky, Collard et García, 2003). Changes in Fn conformation showed different binding affinity levels with  $\alpha 5\beta 1$  and/or  $\alpha \nu\beta 3$  integrins (Garcia, Vega et Boettiger, 1999; Keselowsky, Collard et García, 2005). Fn was found to be weakly bound and can be rearranged when it is adsorbed on hydrophilic negatively charged surfaces, which in turn allowed the N-terminal domain of Fn to interact with  $\alpha 5\beta 1$  integrins on EC and therefore increased focal adhesion. On the contrary, Fn was found to strongly interact with the surface and could not be rearranged when it was covalently attached or adsorbed onto a hydrophobic surface (Pompe et al., 2003). EC attached on strongly bound Fn presented fewer focal adhesions than on weakly bound Fn (Pompe et al., 2007; Pompe et al., 2003). The integrin binding ability of Fn and resulting cell behavior depended on surface pliability (Katz et al., 2000). For example, fibroblasts were attached to Fn through  $\alpha 5\beta 1$  integrin when they were exposed to strongly bound Fn, whereas in the case of weakly bound Fn, cells were attached through  $\alpha \nu\beta 3$  integrin (Faucheux et al., 2006; Katz et al., 2000). Altogether, these studies suggest that it may be possible to improve cell interactions on ECM protein coated surfaces compared to unmodified biomaterial surfaces, but it is difficult to control and predict their orientation and their interactions with the cells.

### **Limitations of using ECM proteins**

Fibronectin coatings on ePTFE or Dacron were shown to be effective in enhancing endothelialization (Assmann et al., 2013; De Visscher et al., 2012). However, EC seeding should be performed *in vitro* before conduit implantation due to concerns regarding increased thrombogenicity (Parikh et Edelman, 2000). Similarly, collagen coatings were also shown to enhance EC attachment to ePTFE or Dacron (Kapadia, Popowich et Kibbe, 2008; Wissink et al., 2000b), but native collagen is intrinsically thrombogenic and it was shown to increase platelet attachment compared to uncoated ePTFE (Badimon et al., 1987). The other main limitation of ECM protein coatings is that it is difficult to reproduce surface coatings because their orientation and conformation is not predictable. Fibronectin or other ECM protein coating on biomaterials surfaces through the use of low-fouling polymers or spacers may

help to solve the issue of protein denaturation and nonspecific protein adsorption. However, it is not clear whether these immobilized proteins (via chemical coupling) are biologically active or not, since ECM proteins are large in size and possess multiple binding sites for chemical coupling that may lead to multiple interactions with low-fouling polymers or spacers (which may ultimately lead to abrogated biological activity) (Hersel, Dahmen et Kessler, 2003; Li et Henry, 2011b).

There are other limitations to using ECM proteins for vascular graft surface coatings. Since proteins have to be isolated and purified from other organisms, they may cause immune responses and infection risks. Proteins can undergo proteolytic degradation, which makes them impossible to use for long-term applications. The surface charge, wettability and topography may influence the conformation and orientation of the proteins, which causes a different presentation of cell reorganisation motifs (Altankov, Grinnell et Groth, 1996; Fields et al., 1998; Hlady et Buijs, 1996; Hyman, 1985; Iuliano, Saavedra et Truskey, 1993; Lewandowska et al., 1992; Lhoest et al., 1998; Underwood, Steele et Dalton, 1993). It was also recognized that the stochastic orientation of proteins on the surface means that only a part of the proteins have the proper orientation for cell adhesion (Elbert et Hubbell, 2001).

### **1.5.2 Surface modification with peptides**

Due to the limitations of protein immobilization on biomaterial surfaces, the use of smaller biomolecules, namely peptides and growth factors, has been proposed in order to elicit desired and defined cell interactions. Therefore, this section and the next section describes the rationale and methods for grafting peptides and growth factors on biomaterial surfaces.

Since the discovery that short peptide sequences within ECM protein are specifically recognized by cell receptors, small peptide fragments have been used for surface modification in several studies (Ferris et al., 1999; Ito, Kajihara et Imanishi, 1991; Mann et West, 2002; Patel et al., 2007; Petrie et al., 2008) in order to control elicited signals and subsequent cell behavior. In addition to providing binding specificity, the use of short peptide

fragments has several advantages over the use of native ECM proteins. Unlike native ECM proteins, the short peptide fragments are relatively more conformationally stable and they can be synthesized massively in laboratories more economically (Neff, Caldwell et Tresco, 1998). Moreover, the short peptide fragments exhibit higher stability under sterilization conditions (Weiß, Klee et Höcker, 2001), heat treatment, pH-variation (Ito, Kajihara et Imanishi, 1991) and storage conditions (Boxus et al., 1998). Small peptide fragments are known to be stable against enzymatic degradation and therefore they can be used for long-term applications. Since the peptide fragments need less space than ECM proteins, they can be packed with higher density on surfaces. Small peptide sequences represent only one motif that can selectively address a specific type of cell adhesion receptor, whereas ECM proteins have several binding domains that can address adhesion of several cell types.

As an alternative to whole ECM protein, the small peptide sequence Arg-Gly-Asp (RGD) was used in numerous studies to promote cell interactions on biomaterial surfaces. This peptide sequence is present in various adhesive proteins such as fibronectin (FN), vitronectin (VN) and laminin (LN). It has been recognized that about half of the 24 integrins ( $\alpha 3\beta 1$ ;  $\alpha 5\beta 1$ ;  $\alpha 8\beta 1$ ;  $\alpha 11\beta 3$ ;  $\alpha \nu\beta 1$ ;  $\alpha \nu\beta 3$ ;  $\alpha \nu\beta 5$ ;  $\alpha \nu\beta 6$ ;  $\alpha \nu\beta 8$ ; and to some extent  $\alpha 2\beta 1$  and  $\alpha 4\beta 1$ ) can bind with RGD sequences (Pfaff, 1997). Therefore RGD is known to promote adhesion of almost all cell types (Hersel, Dahmen et Kessler, 2003). Several other cell-adhesive motifs such as Tyr-Ile-Gly-Ser-Arg (YIGSR), Arg-Glu-Asp-Val (REDV), Lys-Gln-Ala-Gly-Asp-Va (KQAGDV) and Ile-Lys-Val-Ala-Val (IKVAV) are also able to stimulate adhesion of several cell types when immobilized on biomaterial surfaces (Ranieri et al., 1995). Interestingly, some of them are recognized to promote selective cell adhesion. For example, KQAGDV, used in this PhD thesis, is known to interact specifically with VSMC (Dong et al., 2012b; Mann et West, 2002). This is due to the fact that the cell adhesion of KQAGDV is mediated through the single motif,  $\alpha 2\beta 3$  integrin and it may be specific for the receptor of VSMCs (Dong et al., 2012a). Similarly, there are several other peptide sequences that promote selective cell adhesion. The selective synthetic peptide sequences and their specificity for cell adhesion are listed in Table 1.2.

Although small peptide sequences are known to promote cell adhesion, their presentation on biomaterials surface is an important factor in making them accessible for cell adhesion receptors. Therefore different immobilization methods are discussed in the following section.

Table 1.2. Selective synthetic peptide sequences of extracellular matrix proteins and their functions. Taken from (Shin, Jo et Mikos, 2003).

Synthetic sequences	Origin	Function
RGD	Fibronectin, Vitronectin	Cell adhesion
KQAGDV		Smooth muscle cell adhesion
YIGSR	Laminin B1	Cell adhesion
REDV	Fibronectin	Endothelial cell adhesion
IKVAV	Laminin	Neurite extension
RNIAEIIKDI	Laminin B2	Neurite extension
KHIFSDDSSSE	Neural cell adhesion molecules	Astrocyte adhesion
VPGIG	Elastin	Enhance elastic modulus of artificial ECM
FHRRIKA	Heparin binding domain	Improve osteoblastic mineralization
KRSR	Heparin binding domain	Osteoblast adhesion
NSPVNSKIPKACCVPTLSAI	BMP-2	Osteoinduction
APGL		Collagenase mediated degradation
VRN		Plasmin mediated degradation
AAAAAAAAA		Elastase mediated degradation

### 1.5.2.1 Peptide immobilization or coupling methods

A variety of materials such as glass (Dee, Andersen et Bizios, 1998; Dee, Anderson et Bizios, 1999; Mann et West, 2002), quartz, metal oxide (De Giglio et al., 2000; Dong et al., 2012a; Rezania et al., 1999), and polymers (Massia et Hubbell, 1990b; Sabra et Vermette, 2011; Tugulu et al., 2007) have been modified with small synthetic peptides and characterized to determine their interaction with cells. The covalent chemical coupling method is known to offer stable coating and is the most widely used method for modifying surfaces with peptides. It was also recognized that cell attachment on covalently linked RGD peptide leads to an increase in expression of integrins and focal contact formation (Cavalcanti-Adam et al., 2002; Grigoriou et al., 2005).

In the literature, several different coupling techniques have been employed. However, the most common approach involves stable covalent amide bonding between COOH functional groups on the material surface and the NH<sub>2</sub> functional group (N-terminus of the peptide) on peptides. This type of reaction is usually performed by either the single step or the two step method. The single step method involves activation of carboxylic groups using a water-soluble coupling reagent such as 1-ethyl-3-(3-dimethylaminopropyl)-carbodiimide (EDC). However, there are two problems using this method. Firstly, multiple reactive groups are present on the peptide, which leads to multiple binding with the surface, and the peptide may lose its biological activity. For example, as shown in Figure 1.17, RGD peptide has COOH functional groups on C- terminus as well as in the aspartic acid side chain. Similarly, it has NH<sub>2</sub> functional groups in the N-terminus as well as in the arginine side chain. The second problem is that the activated carboxylic groups (by EDC) can be deactivated quickly by hydrolysis. In order to overcome this problem, some studies proposed blocking the reactive amino acid side chains using protecting groups (which can be done prior to coupling with the substrate). This method was used successfully to bind RGD peptides on polymers (Lin et al., 1994; Lin et al., 1992; Quirk et al., 2001), as shown in Figure 1.18. However, the major drawback of using this method is that it requires harsh conditions for deprotection of blocking groups, which may hamper the biological activity of the peptide.

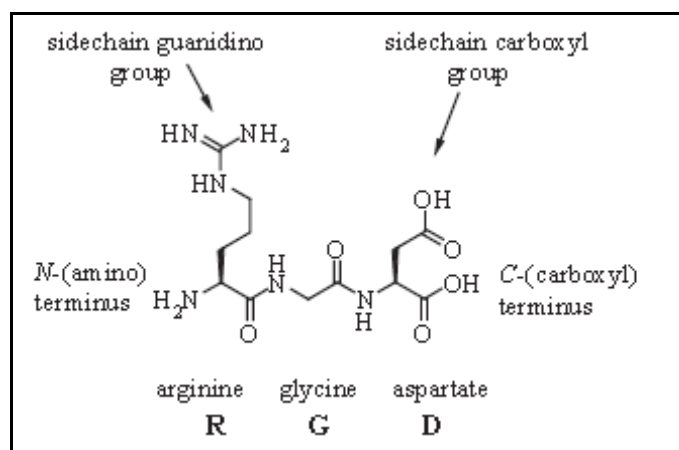


Figure 1.17. The chemical structure and nomenclature of RGD peptide. Image adapted from (Hersel, Dahmen et Kessler, 2003).

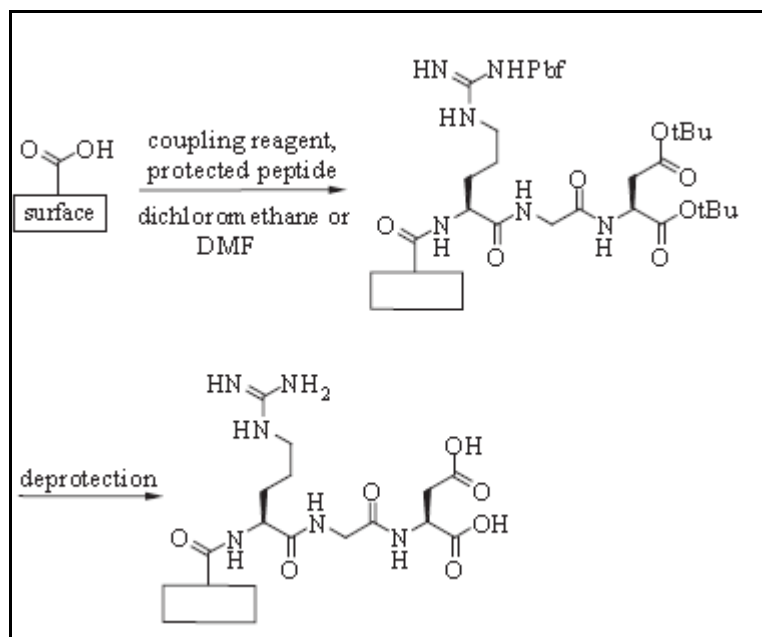


Figure 1.18. Coupling of a protected RGD peptide through its N-terminus to a surface carboxyl group and deprotection of the blocking groups. Image adapted from (Hersel, Dahmen et Kessler, 2003).

As an alternative to this method, a two-step method was proposed. This method involves the activation of carboxylic groups using DCC or EDC and subsequent reaction with NHS (Jo, Engel et Mikos, 2000). It prevents quick hydrolysis of activated carboxylic groups, since the half-life time of NHS active esters ranges between several minutes and an hour at neutral pH (Besselink, Beugeling et Bantjes, 1993; Morpurgo, Bayer et Wilchek, 1999). Such NHS-activated surfaces can also be stored (not in the presence of solution or exposure to air but in specific conditions) for several months and the best conditions for peptide coupling to this ester are at pH 8-9 using sodium bicarbonate or phosphate buffer (Hern et Hubbell, 1998; Morpurgo, Bayer et Wilchek, 1999). The peptide coupling using this procedure is usually for 1-2 h, however, more elevated pH conditions and high concentration buffers (or salts) can reduce the half-life time of NHS-activated ester to less than several minutes or even less than 1 minute (Morpurgo, Bayer et Wilchek, 1999). The advantage of using this method is that it does not require protecting groups when using COOH displaying surfaces. Since it is a two step procedure, the surface is activated with NHS/EDC prior to

RGD coupling. Therefore, in this procedure, the aspartate side chain carboxyl group is not activated for coupling and the nucleophilicity of the arginine side chain is nearly abolished due to protonation in water (Hermanson, 2008). In order to increase the yield of peptide bonding, in some studies coupling was performed at low pH conditions and long coupling times (Beer, Springer et Coller, 1992; Dai, Belt et Saltzman, 1994; Hirano et al., 1993; Jo, Engel et Mikos, 2000) and using excess peptide (Hern et Hubbell, 1998).

### Peptide immobilization using a spacer or linker

The use of spacers became a popular method for peptide immobilization, as it offers flexibility to the immobilized peptide in the biological environment (Rezania et al., 1999) and helps the cells to access the peptides. This method involves exploiting the heterobifunctional cross linker. In this approach, the thiol group (-SH) on peptide is usually linked to a maleimide functionalized surface (as shown in Figure 1.19) via a heterobifunctional linker (for example sulfosuccinimidyl 4-(N-maleinimidomethyl) cyclohexane-1-carboxylate (Sulfo-SMCC)) (Lateef et al., 2002; Stile et Healy, 2001), which enables peptide coupling through disulfide bonding. The major advantage of using this method is that it does not interrupt either N- or C-terminus of the peptide.



Figure 1.19. Reaction scheme between maleimide group on the surface and thiol functional group on peptide. Image adapted from (Hersel, Dahmen et Kessler, 2003; Lateef et al., 2002).

When peptides are directly grafted on biomaterials, peptides may be covered by a layer of adsorbed proteins, the same as for a normal surface. Thus minimizing non-specific protein adsorption is an important criterion while immobilizing a peptide or any other biomolecules in order to elicit the desired signals and subsequent cell responses. In such cases, peptides can usually be immobilized using low-fouling spacers that can limit non-

specific protein adsorption and enable peptide sequences to freely extend outward from the network. In order to achieve this, several studies performed peptide immobilization using various low-fouling polymers such as PEG (Fittkau et al., 2005; Hern et Hubbell, 1998), polysaccharides (Massia et Stark, 2001; Murugesan et al., 2002; Sagnella et al., 2004), and phospholipid bilayers (Dillow et al., 2001; Pakalns et al., 1999b). Again, covalent immobilization is the method of choice for peptide immobilization on low-fouling polymers. This is usually achieved by linking carboxyl groups or maleimide groups on low-fouling polymer and amine-displaying groups on the N-terminus of the peptide (as described above).

#### **1.5.2.2 The effect of peptide density and presentation on cell adhesion**

The peptide surface concentration may be related to the number of cells attached to the surface. Cell adhesion as a function of RGD peptide density showed a sigmoidal increase (Danilov et Juliano, 1989; Jeschke et al., 2002; Kantlehner et al., 2000; Neff, Tresco et Caldwell, 1999). It was also demonstrated that a higher peptide density is also related to cell spreading, focal contact formation, survival and to some extent cell proliferation (Kantlehner et al., 2000; Mann et West, 2002; Massia et Hubbell, 1990a; Neff, Tresco et Caldwell, 1999). Some studies showed the required minimum peptide concentration to induce cell attachment, cell spreading and focal contact formation by using substrates of covalently grafted peptides (Drumheller et Hubbell, 1994; Hubbell, Massia et Drumheller, 1992; Massia et Hubbell, 1991). One study indicated that at least 1 fmol/cm<sup>2</sup> of peptide density is necessary for fibroblast spreading and 10 fmol/cm<sup>2</sup> of surface density is required for cytoskeleton formation (Massia et Hubbell, 1991). However, the required concentrations were higher when RGD peptide was grafted on poly (acrylic acid) hydrogel via a PEG spacer, which was 12 fmol/cm<sup>2</sup> for cell spreading and 66 fmol/cm<sup>2</sup> for focal contact formation (Drumheller, Elbert et Hubbell, 1994). These results indicate that high peptide density is required when using low-fouling coatings. Some other study also investigated the relation between peptide density and cellular response using PEG-based hydrogels. These results showed that the intermediate concentrations (2.8-7  $\mu\text{mol/mL}$ ) of incorporated peptide promoted cell adhesion and spreading without hampering migration, proliferation and matrix production of smooth muscle cells (Mann et West, 2002). It seems a dose-dependent increase in cell response may

depend on the type of cell line and polymer used for peptide immobilization. Moreover, using low-fouling polymers may be unpredictable due to sterical hindrance effect of low-fouling polymers.

Surfaces with high peptide density may enhance cell adhesion, but they may impede cell migration and proliferation. EC adhesion, spreading and focal adhesion formation were shown to increase with RGD peptide density. However, EC migration was maximum at intermediate concentration of RGD (Hern et Hubbell, 1998; Lin et al., 2001; Mann et West, 2002; Murugesan et al., 2002; Pakalns et al., 1999a; Smith, Elkin et Reichert, 2006). This might be due to the fact that at low-peptide/ligand density cells cannot form new focal adhesion at leading edge efficiently, while at high density cells cannot break focal adhesion. Overall these observations suggest that it is not possible to generalize the impact of peptide density on promoting cell adhesion, but in general, high peptide density may be advantageous for cell attachment but not for cell migration and proliferation. It seems surfaces need to be activated with other factors such as growth factors, since GFs are known to promote cell migration and proliferation (Neufeld et al., 1999b; Nolan et al., 2004).

As mentioned earlier, low-fouling coatings help to improve the bioactivity of immobilized biomolecules. In addition, when using star shaped low-fouling polymers for peptide immobilization, they have been shown to promote integrin clustering. Before describing this advantage, it is important to understand the mechanism of integrin-mediated cell adhesion, which is explained in the following paragraph.

A cascade of four different overlapping events such as cell adhesion, organisation of cytoskeleton and focal contact formation are involved in the process of integrin-mediated cell adhesion (LeBaron et Athanasiou, 2000): (i) The initial cell attachment to the surface through ligand binding allows cells to withstand gentle shear forces. (ii) Then, the cell body begins to flatten and spread over the substrate. (iii) Cell spreading leads to actin organisation into microfilament bundles, also referred to as stress fibers. (iv) Finally, focal contact formation will occur, which will link ECM molecules of the actin cytoskeleton. The clustered integrins and more than 50 other transmembrane associated molecules are involved in focal adhesion

(see Figure 1.20), in which tetraspanins, growth factor receptors, syndecans, lipids, tensin, talin, vinculin, paxillin, and focal adhesion kinase (FAK) were identified (Geiger et Bershadsky, 2001a; Pande, 2000; Petit et Thiery, 2000; Zamir et Geiger, 2001a). These events describe the importance of integrin clustering for focal contact formation and therefore strong cell attachment on the surface.

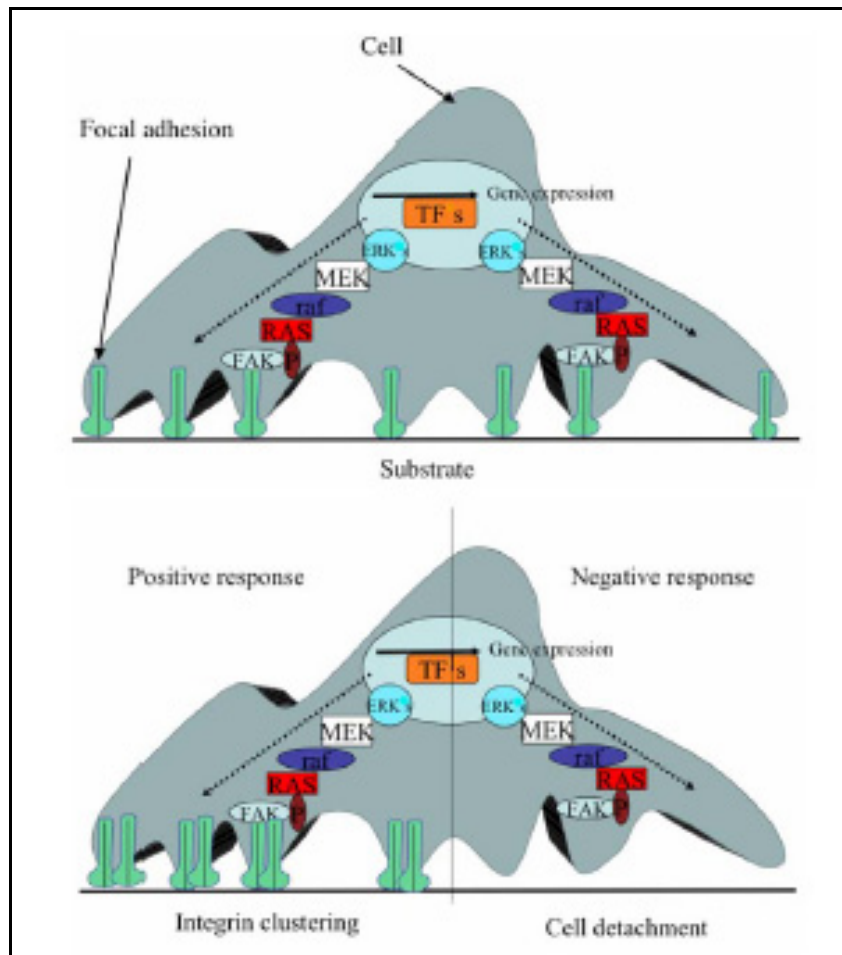


Figure 1.20. Schematic representation of how integrin-mediated activation regulates the cell/substrate interaction (Owen et al., 2005).

Therefore, integrin-mediated cell adhesion not only depends on receptor occupancy, but also depends on integrin clustering. The linked fibrils of the ECM account for a complex network conducive to receptor occupancy as well as integrin clustering. It was demonstrated that different cell responses on peptide-modified surfaces are not only due to different

surface concentrations, but also depend on the method of presentation (Irvine, Mayes et Griffith, 2000). Maheshwari et al. compared fibroblast cell response when peptides presented in a clustered versus random individual fashion (Maheshwari et al., 2000). In order to achieve controlled peptide density and controlled spatial ligand distribution, RGD peptides were functionalized on branched/star PEG polymer. An average of 1, 5 and 9 peptides per star molecule were immobilized to achieve an overall surface concentration range of 0.15-20.5 nmol/cm<sup>2</sup>. A significant fraction of fibroblasts showed enhanced shear stress resistance, well-formed stress fibers and focal contact formation on RGD clusters compared to the individual format. Few other studies also showed a similar trend when RGD was immobilized on embedded PPMA latex or comb polymers (Irvine, Mayes et Griffith, 2000; Irvine et al., 2001; Koo et al., 2002).

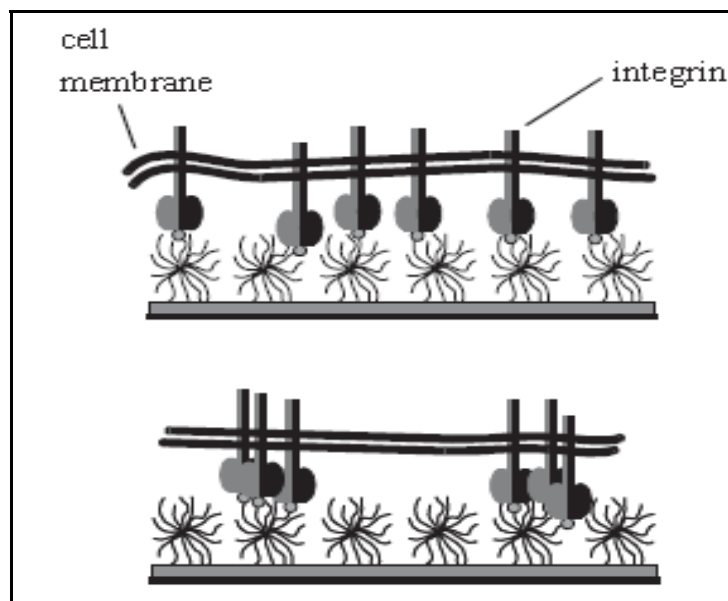


Figure 1.21. Schematic illustration of RGD presentation on star polymers. (A) The same amount of ligands presented in homogeneous (top) versus ligands presented in discrete clusters (bottom). Image adapted from (Maheshwari et al., 2000).

Overall the literature suggests that the presentation of peptide on the surface and its concentration are important factors for eliciting desired cell interactions. However, it is not clear whether high grafting densities have a negative impact on other cellular events such as

cell migration and proliferation. When using low-fouling surfaces, it is important to cover the surface with high peptide densities, otherwise complete cell coverage may not be achieved on these surfaces. If high peptide densities are problematic for promoting other cellular events such as cell migration and proliferation, co-immobilization of peptides and growth factors may help to achieve optimal cell interactions on biomaterial surfaces.

### **1.5.3 Surface modification with growth factors**

Growth factors are soluble polypeptides, produced naturally by many cell types, that are capable of instructing specific cellular responses in a biological environment. Growth factor signaling can result in a very wide range of cell actions such as cell survival, control over migration, and differentiation or proliferation of a specific subset of cells. These actions may occur through autocrine (produced by and acts on the same cell type) and juxtacrine (acts on neighbouring cells) or paracrine (produced by and acts on different cell types) mechanisms (Douglas A. Lauffenburger, 1993). The biological functions and roles of growth factors will be altered when they are present in the ECM, since ECM contain numerous components such as adhesive molecules, notch signaling molecules, and proteoglycan molecules, which can modulate the activity of a number of growth factors (Cao et al., 2009; Discher, Janmey et Wang, 2005; Ramirez et Rifkin, 2003). As shown in Figure 1.22, the producer cell secretes growth factors and initiates the signal transmission mechanism. The growth factor binds to specific transmembrane receptors (which are referred as transmembrane glycoproteins, belonging to either the receptor tyrosine kinase (RTK) or G-protein-coupled receptor (GPCR) families (Sorkin et Von Zastrow, 2002)) of the target cell and translates instructions to the cell nucleus through the cascade of events involving cytoskeleton protein phosphorylation, ion fluxes, changes in metabolism, gene expression, protein synthesis and ultimately an integrated biological response (Cohen, Ren et Baltimore).

The receptor activation may also lead to phosphorylation of Akt, a kinase involved in antiapoptotic signaling (Yanai et al., 2002), and alteration of cell morphology and motility through association with the actin cytoskeleton. Binding of growth factors to the ECM leads to sequestration or controlled release of growth factors and may regulate or enhance their

effect on cellular interactions (Dinbergs, Brown et Edelman, 1996). The growth factor stimulation induces cells to produce or alter the surrounding matrix, and promotes migration on the ECM through enhanced integrin expression or cytoskeletal interactions (Maldonado et Furcht, 1995).

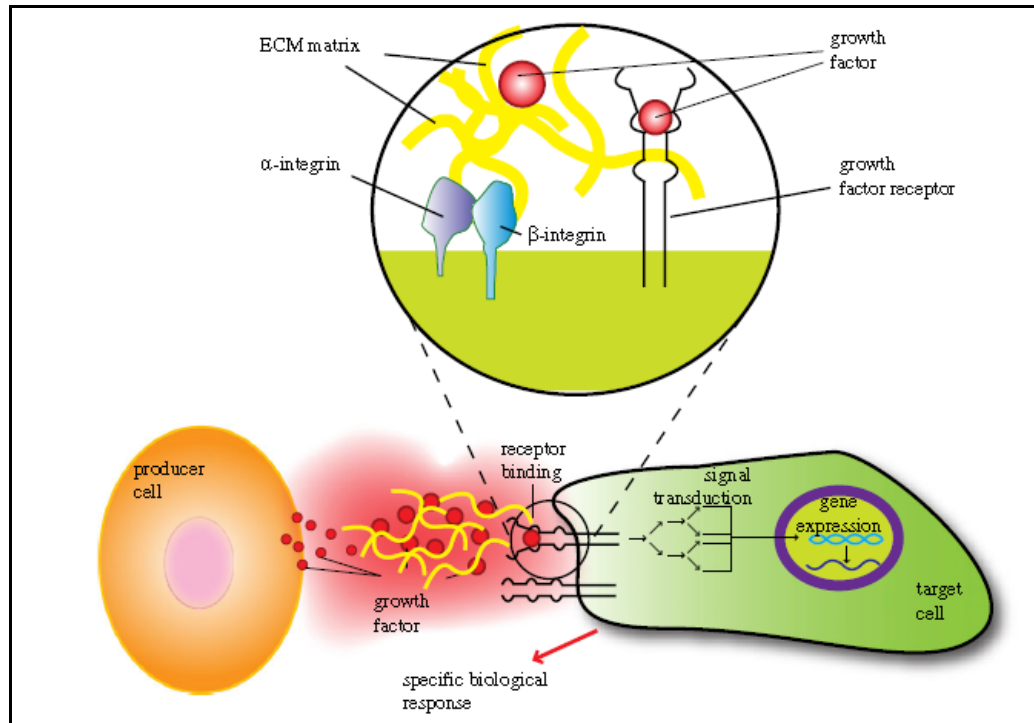


Figure 1.22. Cross talk between cells mediated by growth factors and ECM. Insert illustrates how ECM can control growth factor presentation in a temporal and spatial fashion. Taken from (Lee, Silva et Mooney, 2011).

The relationship between growth factor signaling and specific cellular response is not yet well understood. On the one hand, the same growth factor can convey different instructions, depending on the receptor type and cell type to which it binds. On the other hand, the same receptor can translate different messages depending on the intracellular transduction pathways, which can differ from one cell type to another (Lamallice, Le Boeuf et Huot, 2007; Lee, Silva et Mooney, 2011).

It was recognized that two waves of growth factor-dependent signaling events were required for a proliferative response, one occurring immediately after growth factor

stimulation and the other post stimulation (Jones et Kazlauskas, 2000). The former is known as acute burst signalling, which does not persist longer than 60 minutes. It was noted that the cell silences this signalling cascade in different ways, such as receptor internalization and degradation, as well as the appearance of enzymes (which antagonize the signaling enzyme). After completion of acute burst signaling, the post stimulation triggers the cell cycle program through the exposure of growth factor to the receptor for 8-10 h, which involves activation of cyclin-dependent kinases (Cdks). It was shown that fibroblasts require at least 8 h continuous exposure to growth factor to engage the cell cycle program (Pardee, 1989). It seems that early burst signaling is insufficient for cell cycle progression, and there must be additional inputs made by growth factor at later time points. Therefore it is important to note that cells require continuous exposure of growth factors at least for 8-10 h in order to complete cell cycle progression.

### **1.5.3.1 Epidermal Growth Factor (EGF)**

Among the various growth factors involved in vascular repair, epidermal growth factor (EGF) is of particular interest, since it was known as a potent mitogenic and chemotactic factor for VSMC (Miyagawa et al., 1995; Raab et Klagsbrun, 1997; Reape et al., 1997) and was previously shown to enhance VSMC growth (Major et Keiser, 1997; Reynolds et al., 2002). It is worth noting that promoting VSMC growth and resistance to apoptosis is prerequisite for developing stent grafts that are used to repair EVAR.

EGF is one of the most stable and biologically potent growth factors known to date. It is a globular, water-soluble and 6 kDa polypeptide comprised of a single chain consisting of 53 amino acids (Carpenter et Cohen, 1979; Holladay et al., 1976; Lee et Park, 2002). The primary structure of human EGF as shown in Figure 1.23. EGF has an isoelectric point of 4.6 and it is known to be negatively charged under physiological pH conditions (Taylor, Mitchell et Cohen, 1972).

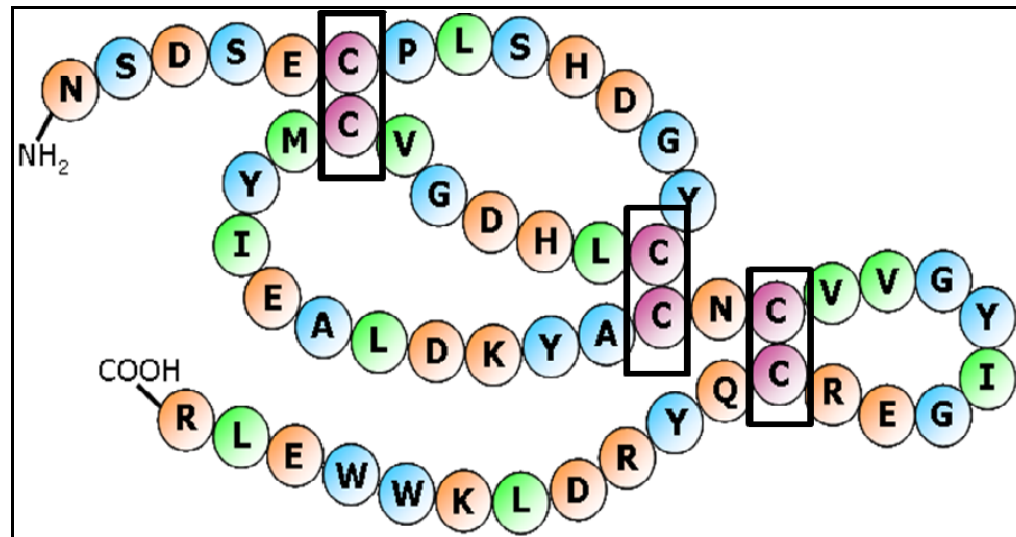


Figure 1.23. Primary structure of human epidermal growth factor (EGF).  
Adapted from (Carpenter et Cohen, 1979).

### EGF receptor binding and signaling pathways

EGF binds to both low and high affinity sites on cells expressing the EGF receptor (EGFR) (Jorissen et al., 2003). This receptor consists of the intracellular domain as well as the extracellular domain, which are linked in the native protein by a single membrane-spanning segment (Jorissen et al., 2003; Lax et al., 1991). The former is for expressing its protein tyrosine kinase activity and the latter is for binding its ligand (EGF). Signal transduction is initiated through the binding of EGF to the extracellular domain of the receptor that contains a two-cysteine-rich region (see Figure 1.24). The EGF receptor (ErbB) family consists of four closely related tyrosine kinase transmembrane receptors such as ErbB1/ EGFR, ErbB2/HER2/neu, ErbB3/HER3, and ErbB4/HER4 (Normanno et al., 2005). However, EGF binds exclusively with ErbB1 whereas ErbB2 acts as a co-receptor. Binding EGF to corresponding receptors leads to formation of a ligand-receptor complex and therefore leads to hetero-dimerization of the receptor.

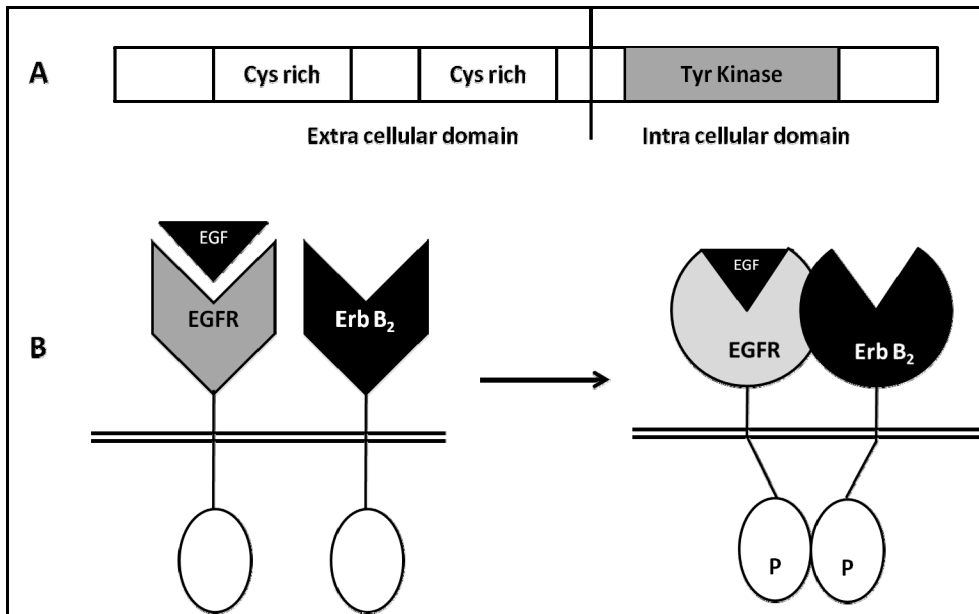


Figure 1.24. (A) Schematic representation of EGFR domain structure of the extracellular and intracellular regions. (B) Hetero-dimerization of the EGFR and Erb B<sub>2</sub> upon receptor activation. Image adapted and redrawn from (McInnes et Sykes, 1997).

This results in the activation of the intracellular kinase domain leads to autophosphorylation of tyrosine residues (Sherrill et Kyte, 1996). These (tyrosine phosphorylated) sites allow the binding of proteins containing the Src Homology 2 (SH2) domain, which consists of intracellular docking proteins or adaptor proteins such as Grb2, Nck and Shc. These proteins associate with other proteins, resulting in the activation of serine–threonine kinases that phosphorylates serine or threonine residues on transcription factors (Olayioye et al., 2000). This resulting kinase cascade leads to amplification of a network of signaling pathways, which eventually leads to changes in protein functions and activation of gene transcription. These changes also interact with the apoptotic signaling pathways (see Figure 1.25) preventing cell death. This cascade of events is crucial to a variety of cellular responses, such as cell proliferation, migration, and differentiation (Carpenter et Cohen, 1990; Earp et al., 1995).

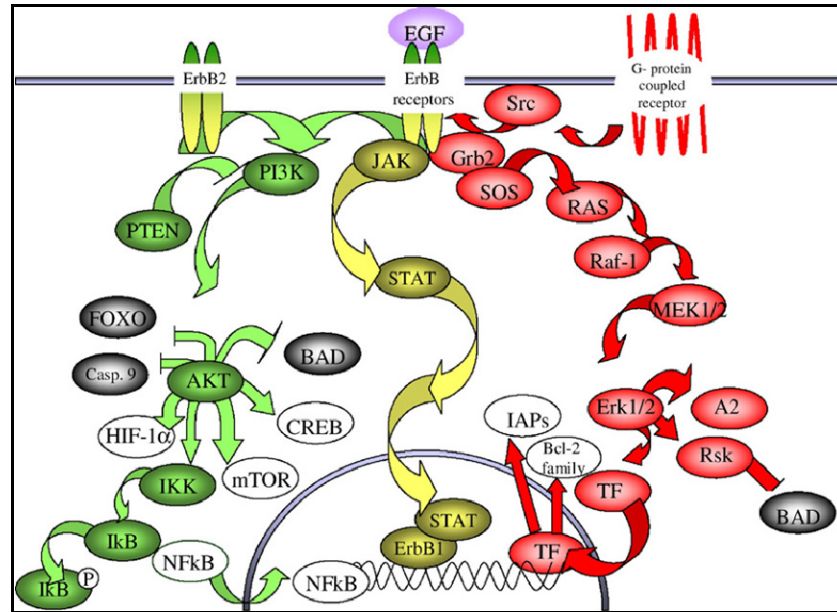


Figure 1.25. Schematic representing the pathways which lead to the activation of anti-apoptotic proteins (white) and the inactivation of pro-apoptotic proteins (black). Taken from (Srokowski et Woodhouse, 2013).

### 1.5.3.2 EGF tethering to implant surface

A suitable method is required to deliver EGF to the surrounding cells and therefore direct cellular response to a biomaterial surface. The delivery of growth factor can be achieved through different methods including from solution, by controlled release, simple adsorption and chemical immobilization to the biomaterial surface. The mechanism of delivery must allow the growth factor to occupy the receptor for a sufficient length of time to effect cell cycle progression (Douglas A. Lauffenburger, 1993; Jones et Kazlauskas, 2000), as mentioned above. Immobilization of growth factor is expected to result in improved control of its concentration and delivery compared to its soluble form because the immobilization procedure inhibits the internalization of growth factor as shown in Figure 1.26 (Ito, Kajihara et Imanishi, 1991). Normally cells decompose the biosignal molecules to reduce their stimulation. This phenomenon is called down-regulation. The immobilization method was considered to inhibit this down-regulation and therefore the stimulation continues for a long time.

It is worth noting that the simple adsorption method is convenient but not preferable, since it leads to changes in growth factor conformation and is therefore inaccessible to the receptors present on cells.

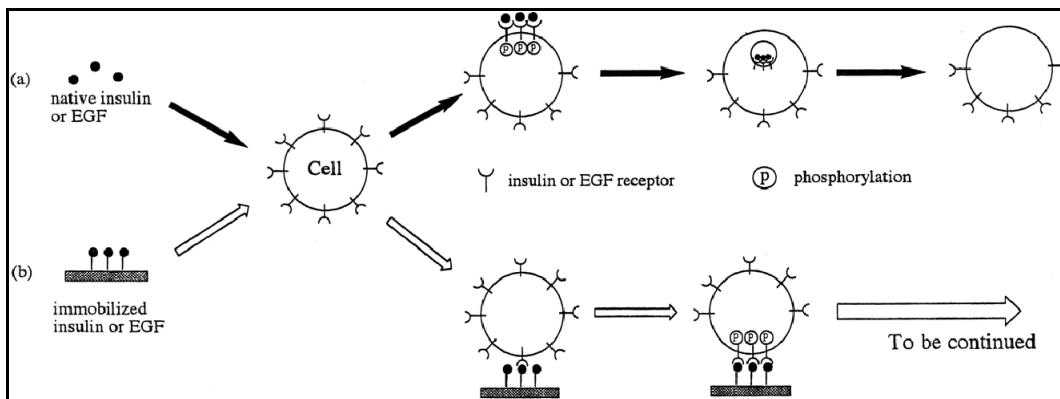


Figure 1.26. Schematic illustration of the interaction between cells and native (a) and immobilized (b) growth factors (Ito, Kajihara et Imanishi, 1991).

Growth factor attachment must be performed in a manner such that the receptor binding and resulting biological activity of the growth factor is preserved. This may be accomplished by the covalent immobilization method, which involves the creation of one or more covalent bonds between the growth factor and the surface, with or without using a polymer linker. Immobilization of growth factor on solid substrate via a polymer linker is known as tethering. Kuhl and Griffith-Cima showed that EGF retained its activity in promoting DNA synthesis in rat hepatocytes when EGF was tethered to glass substrates using a PEG spacer (Kuhl et Griffith-Cima, 1996). Other studies also showed enhanced growth factor activity when they immobilized on PEG hydrogels compared to growth factors in soluble form (Bentz, Schroeder et Estridge, 1998; Gobin et West, 2003a; Mann, Schmedlen et West, 2001). The use of a PEG spacer is believed to enhance the flexibility and therefore accessibility of the growth factor to the cellular receptor (as shown in Figure 1.27). However, PEG's steric hindrance effect and non-adhesive nature may hamper cell growth, as observed by Klenkler et al. studies (Klenkler et al., 2008).

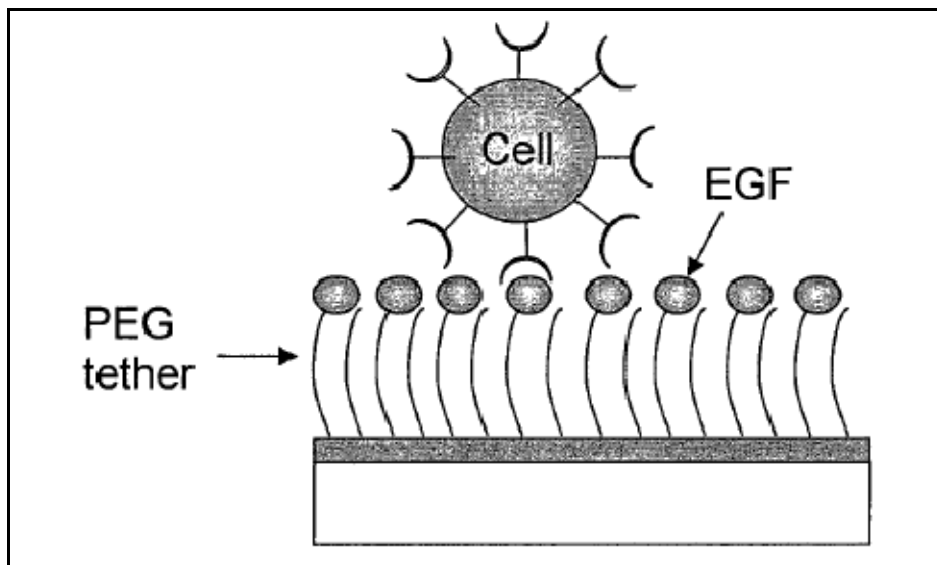


Figure 1.27. Schematic illustration of EGF accessibility to the cellular receptor when it is tethered to a substrate material via flexible polyethylene glycol chains. Taken from (Ito, 1998).

In the literature, the most common approach for covalent immobilization involves bonding through carbodiimide chemistry between carboxyl groups on the substrate and amine groups displayed on N-terminus or on the side chains of lysine residues of EGF. Although this approach is convenient, it causes improper orientation of EGF due to the presence of multiple amine-displaying groups (Carpenter et Cohen, 1990). This type of immobilization, also known as non-oriented or random immobilization, leads to heterogeneous ligand populations, poorly reproducible and therefore inefficient, and optimal cell interactions could not be achieved.

Other covalent immobilization alternatives involve exploiting thiol groups and disulfide bonding between ligand and surface functional groups (O'Shannessy, Brigham-Burke et Peck, 1992). This method is more common for the immobilization of small peptide sequences, where an engineered cysteine is added to the original peptide sequence during synthesis and the surface is activated with the cross linker that contains maleimide groups. However, this method is not appropriate for EGF tethering because it has a negative impact on bioactivity due to a wrong disulfide bridge during folding.

Another method of choice is exploiting the specific interaction between streptavidin and biotin reactive linkers. This strategy involves biotinylation of the protein and subsequent immobilization onto streptavidin coated surfaces. This method, also referred to as ligand affinity capture, is not strictly covalent, but high affinity interaction between biotin and streptavidin is irreversible (Blackburn et Shoko, 2011; De et al., 2000). This method is becoming a popular choice because it offers oriented and stable immobilization and homogeneity of ligand population .

The concept of oriented immobilization was also investigated by our team in De Crescenzo's lab, by taking advantage of a *de novo* designed coiled-coil system. The coiled-coil system is composed of two distinct peptides, namely E and K coils, that were originally designed by Hodges and Co-workers (Chao et al., 1998; Chao et al., 1996). The K peptide is made of a unique repeating heptad with the sequence K-V-S-A-L-K-E, and similarly the E peptide consists of repeating heptad with the sequence E-V-S-A-L-E-K. When the E and K peptides associate, they specifically heterodimerize to form a well-defined coiled-coil structure. The E and K coils were shown to interact through hydrophobic and electrostatic interactions with high affinity, and the resulting coiled-coil complex is stable at wide range of pH and salt concentrations. The hydrophobic residues V and L (at positions a, a', d and d') of E/K coils are responsible for hydrophobic interactions, which tend to favor a dimeric conformation and therefore formation of a stable coiled-coil complex. Electrostatic attraction (at positions g-e' or g'-e) further stabilizes the E/K coiled-coil through E and K interchain salt bridge formation as shown in Figure 1.28.

The main advantage of the coiled-coil system is that it is ideal for immobilizing proteins or growth factors in an oriented manner at the biomaterial surface. In order to achieve this, one E/K coil peptide should be chemically conjugated to growth factor or protein and subsequently immobilized onto the surface that is previously activated (via covalent immobilization using a cross-linker) with the other coil peptide. More recently, our team in De Crescenzo's lab has tested and successfully demonstrated EGF immobilization onto amine- and carboxyl-displaying surfaces using the coiled-coil system. To accomplish

this, E coil EGF was produced in human embryonic kidney (HEK) 293 cells and its bioactivity was confirmed on human epidermoid carcinoma (A-431) cell lines (Boucher et al., 2008a) and Cysteine tagged K coil (Cys-Gly-Gly-K coil) produced as described in (De Crescenzo et al., 2003) and was demonstrated to be efficient for the stable and oriented capture of coil tagged proteins. Thiol groups on the cysteine molecule of K coil were exploited for immobilization onto amine-displaying or carboxyl-displaying surfaces using an LC-SPDP or EMCH cross-linker. Therefore, E/K coiled-coil was achieved through high affinity interaction between K coil and E coil EGF (See Figure 1.29).

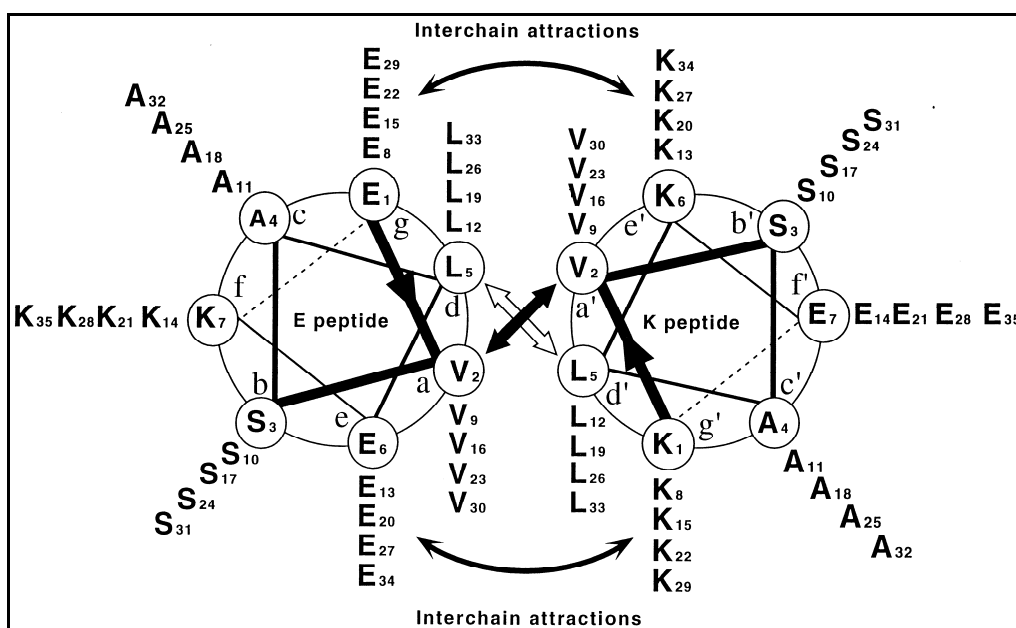


Figure 1.28. Helical wheel representation of the heterodimeric parallel E/K coiled-coil, which shows hydrophobic interaction between V and L residues (at positions a, a', d and d') and electrostatic interchain interactions between E and K residues (at positions e-g' and g-e') that forms E/K salt bridge. Taken from (Chao et al., 1998).

EGF oriented immobilization via coiled-coil interactions led to a strong and sustained EGFR autophosphorylation as compared to that observed on randomly immobilized (covalent immobilization via the reactive amine groups present at the EGF N-terminus or on its lysine side chain (at position 28 and 48 for human EGF)) or soluble EGF (Boucher et al., 2009). More recently, in our lab this strategy was applied to immobilize EGF on a CS

surface. This study showed that EGF bioactivity and therefore VSMC survival and resistance to apoptosis (in a serum-deprived environment) were enhanced when using the coiled-coil strategy as compared to random immobilization of EGF (Lequoy et al., 2014). As mentioned above, the coiled-coil capture system could also be applied to other growth factors or proteins. As an example, recently this system was successfully used for hVEGF capture on amine-displaying surfaces and confirmed its bioactivity (Murschel et al., 2013).

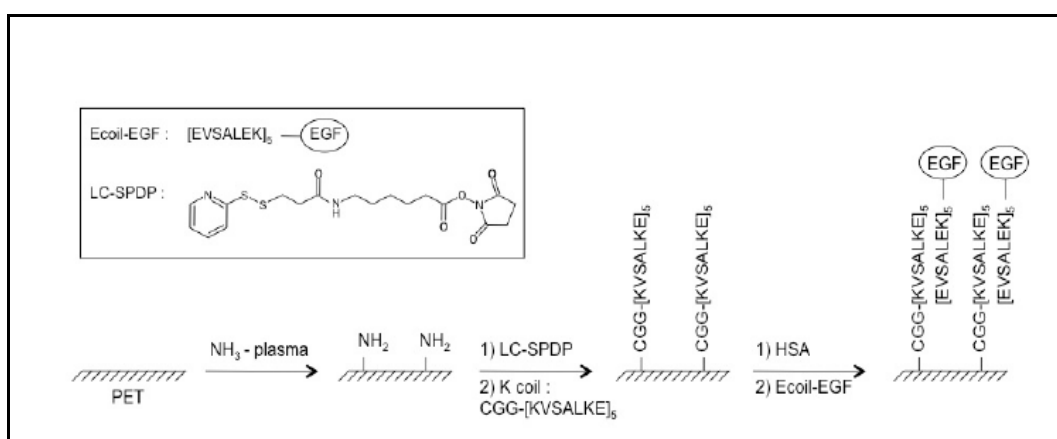


Figure 1.29. Schematic diagram of an oriented immobilization of EGF onto an amine-displaying surface through coiled-coil interaction (Boucher et al., 2009).

#### 1.5.4 Combination of peptide and growth factor

Achieving optimal cell interactions on a low-fouling background is a challenging task due to the non-adhesive nature of low-fouling polymers. Klenkler et al. observed poor cell coverage and growth when EGF immobilized on PEGylated surfaces (Klenkler et al., 2008). Similarly, poor VSMC response was observed when EGF tethered on CMD surface in oriented fashion (Lequoy et al., 2014). Klenkler concluded that additional factors that would promote initial cell adhesion on PEG surfaces were required. These concerns encouraged us to search in the literature for combined immobilization of growth factors and/or cell adhesive molecules and their possible synergistic effects.

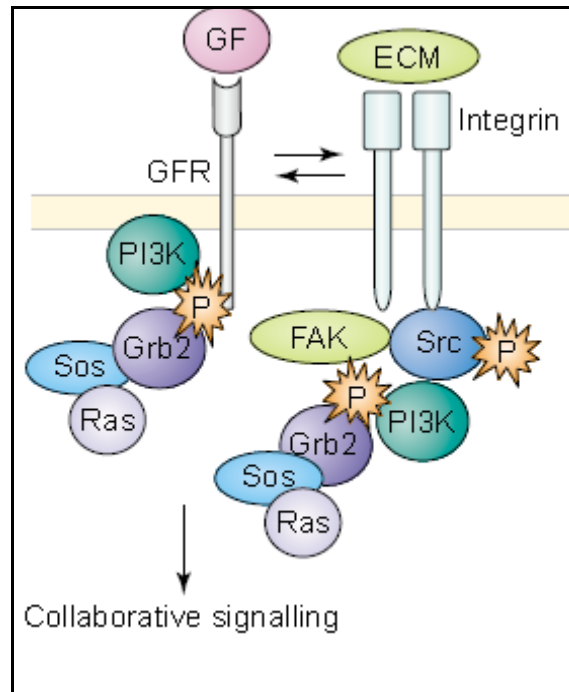


Figure 1.30. Schematic diagram of collaborative signaling of growth factor and integrin receptors. Taken from (Yamada et Even-Ram, 2002).

The cell adhesion receptors such as integrin and growth factor receptors are known to share common signaling pathways, and the mutual activation of both the receptors through their association results in signaling synergism and reciprocal potentiation (Comoglio, Boccaccio et Trusolino, 2003; Yamada et Even-Ram, 2002). The synergy between integrin and growth factor receptors is known to regulate cell differentiation, proliferation, and survival. A classic example of sharing common signaling pathways is the ability of integrins to engage ligands and subsequent activation of the Shc-Ras-Mitogen activated protein kinase pathway in a manner similar to growth factor receptors (Wary et al., 1996; Wary et al., 1998). The mechanism of synergy between integrin and growth factor signaling can be explained by collaborative signaling as shown in Figure 1.30. Integrin clustering takes place when ligands bind to integrins and the clustered integrins can associate with other surface receptors, including growth factor receptors (Yamada et Even-Ram, 2002). Signals triggered by growth factor and integrin binding to their respective receptors will follow parallel but superimposable pathways, with additive activation of signaling cascades that converge on

common downstream effectors. This type of collaboration is also known to exploit membrane proximal proteins to mediate (directly or indirectly) the formation of integrin-growth-factor-receptor complexes. For example, as shown in Figure 1.31, a membrane-proximal transducer such as FAK is able to integrate cytoplasmic tails of growth factor and integrin receptors through its amino and carboxyl termini, respectively (Sieg et al., 2000). This coordinated activity can be explained by the observation that fibroblasts lacking FAK are refractory to motility signals from platelet-derived growth factor (PDGF) and epidermal growth factor (EGF), and rescue of this defect was achieved by stable expression of FAK that is able to interact with the sites of kinase and integrin receptor clustering (Sieg et al., 2000). An increase in VEGFR-2 activation and EC proliferation was observed when VEGF receptor ((VEGFR)-2) physically associates with the  $\alpha\text{v}\beta\text{3}$  integrin (Soldi et al., 1999).

A question remains whether growth factor covalently/firmly linked to the surface promotes collaborative association with integrins. This can be explained by comparing the mechanism of action for soluble and immobilized growth factor. Soluble growth factors bind receptors on the apical side of the cell and form collaborative associations with integrins, but they are internalized and therefore immediately terminate the stimulated cell growth. However, immobilized growth factors are exposed to the basal side of the cell and can directly bind integrins. Due to increased local concentrations, immobilized growth factors may induce formation of integrin-growth factor-receptor complexes that do not form in the presence of soluble growth factors (Vlahakis et al., 2007). Moreover, immobilized growth factors are known to offer sustained activity since they are not internalized.

Very few studies to date have examined combined immobilization of growth factors and cell adhesion peptides or ECM proteins and their effect on cell growth. Ito and coworkers observed enhanced insulin growth factor activity and cell growth when it co-immobilized with ECM proteins or RGD peptides on a polymer surface (Ito, 1998). De Long et al (DeLong, Moon et West, 2005) noted enhanced fibroblast proliferation and migration when EGF tethered on RGD containing hydrogels. Similarly, Gobin et al (Gobin et West, 2003b) observed increased VSMC proliferation and migration when FGF co-immobilized

with RGD peptide. More recently Christopher M et al. developed a surface that presents both cell-adhesion factors (RGD) and growth factors (bFGF) at subcellular-length scales using PEG hydrogels. The results from this work showed enhanced HUVECs adhesion, spreading and formed focal adhesion assemblies through synergistic effects of integrin, and growth factor receptor signaling (Murray et Lopez, 1997).

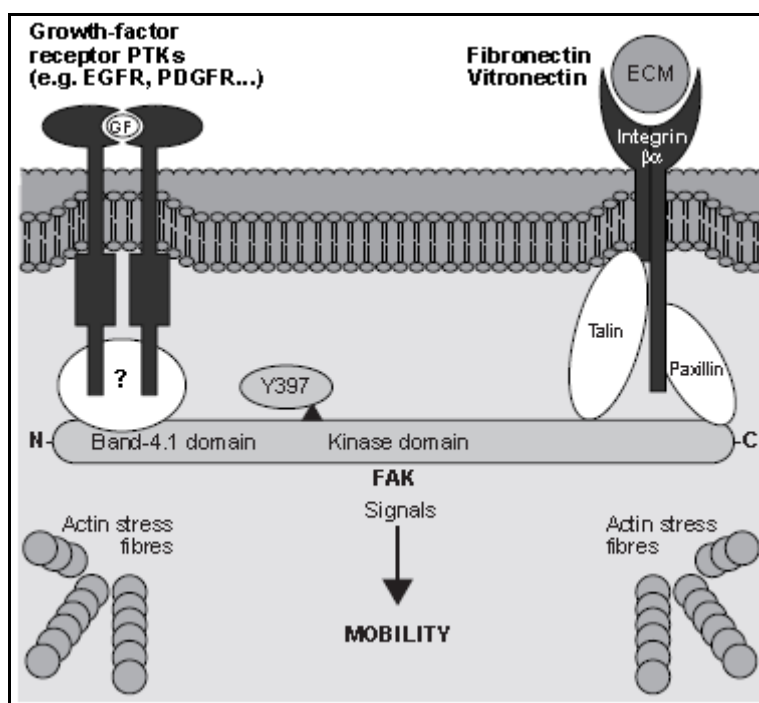


Figure 1.31. Schematic diagram of FAK function that integrates growth factor and integrin signals to promote cell migration (Sieg et al., 2000).

Overall, based on the literature, integrin receptor seems to collaboratively associate with other integrin receptors or growth factor receptors to potentiate their signals. There is a strong interest in developing methods that allow combined immobilization of an adhesive peptide with a growth factor to enhance cell proliferation and migration and therefore to achieve optimal cell interactions. However, several factors may need to be optimized, such as grafting density and required ratios of these biomolecules on the surface. The coiled-coil tethering method developed in De Crescenzo's lab may be helpful for combined immobilization of peptides and GFs and therefore modulate the ratios of these biomolecules.

In addition, the Quartz Crystal Microbalance (QCM-D) technique, which will be detailed in the next section, may help to achieve an interesting study of combined immobilization.

## **1.6 QCMD- technique**

### **1.6.1 Introduction**

The quartz crystal microbalance (QCM) was used for a long time as a weighting device to measure thin film deposition in vacuum as well as gas phases. In 1980, it was recognized that the QCM technique could be used in the liquid phase (Nomura et Hattori, 1980). Later, Hook constructed an experimental setup to follow frequency and dissipation of energy simultaneously in all three phases (vacuum, air and liquid) (Höök et al., 2002). Hook's technique was named quartz crystal microbalance with monitoring of dissipation (QCM-D), which is an extension of the traditional QCM method. Among others, QCM-D enables to study the kinetics of protein adsorption. Unlike QCM, the QCM-D technique can provide the unique and quantitative information of the viscoelastic properties of adsorbed protein layers (Hook et al., 2001). Thus this technique is known to allow a reliable protein adsorption study in biomaterial research (Andersson et al., 2005; Thompson, Arthur et Dhaliwal, 1986).

### **1.6.2 Fundamental principles of the QCM-D technique**

The QCM system consists of a piezoelectric quartz crystal sensor that is used to measure very small masses. This thin crystal is covered with gold electrodes on its two faces. When an AC voltage is applied across the electrodes, it causes the crystal to oscillate at a specific resonant frequency ( $f$ ). A change in frequency of the oscillating crystal will occur if the mass is adsorbed on the crystal and the resonant frequency will decrease proportionally to the mass of the film. This linear relation between increase in mass ( $\Delta m$ ) and decrease in resonance frequency ( $\Delta f$ ) was described in 1959 by Sauerbrey (Hemmersam et al., 2005; Höök et al., 1998; Sauerbrey, 1959), which can be explained as follows. The resonant frequency ( $f$ ) is given by the following Eq.1.1 (taken from (Sauerbrey, 1959)).

$$f = n \cdot v_q / 2 t_q = n \cdot f_0 \quad (1.1)$$

Where " $v_q$ " is the wave velocity and " $t_q$ " is the thickness of the quartz plate (Höök et Biophysics, 1997; Sauerbrey, 1959) and " $n$ " is the overtone number ( $n=1, 2, 3$  etc.). The resonant frequency for  $n=1$  is called the fundamental resonant frequency ( $f_0 (=v_q/2 \cdot t_q)$ ), and  $n=3$  for the third overtone and so on.

An increase in mass ( $\Delta m$ ) bound to the quartz crystal surface causes the oscillation frequency to decrease, obtaining a negative shift of the resonance frequency ( $-\Delta f$ ). It is described by the following Eq.1.2. (taken from (Sauerbrey, 1959))

$$df = \Delta f = -f / t_q \rho_q \cdot \Delta m = -n \cdot 2 \cdot f_0^2 / v_q \rho_q = -n \cdot 1/C \cdot \Delta m \quad (1.2)$$

Where  $C$  is the mass sensitivity constant ( $C=17,7 \text{ ng} \cdot \text{cm}^{-2} \cdot \text{Hz}^{-1}$  at 5MHz).

The Sauerbrey equation (Eq.1.2) is valid if: (i) the adsorbed layer is rigid, (ii) the added mass is smaller than the weight of the crystal, (iii) there is no slip in the metal/layer interface, and (iv) the layer is homogeneously distributed on the surface. Thus, for the Sauerbrey relation, it was concluded that the change in resonance frequency is proportional to the change in the adsorbed mass if the adsorbed mass is much smaller than the mass of the crystal (Hemmersam et al., 2005; Sauerbrey, 1959).

### 1.6.2.1 The dissipation factor

The QCM technique is a very sensitive tool that determines the mass of the analyte adsorbed, with sensitivity in the  $\text{ng}/\text{cm}^2$  regime (Rodahl et al., 1995; Thompson, Arthur et Dhaliwal, 1986; Weber, Wendel et Kohn, 2005a). However, it is not applicable to inelastic subjects such as cells and bimolecular systems, because there is an energy loss due to hydrated and viscous layers. In the case of protein solutions, the protein layer is not rigid and does not couple completely with the oscillating crystal, which leads to underestimation of the real mass when using the Sauerbrey relation. Therefore, in those cases, in addition to

resonant frequency, the dissipation factor (D) must be taken into consideration (Hemmersam et al., 2005; Rodahl et al., 1995). The dissipation factor is inversely proportional to the Q-factor of the oscillator (Höök et al., 2002), which is a dimensionless parameter that compares the time constant for decay of an oscillating physical system's amplitude to its oscillation period. This relation is described by the following Eq.1.3 (taken from (Voinova et al., 1999)):

$$D = 1/Q = E_{dissipated} / 2 \pi E_{stored} \quad (1.3)$$

Where  $E_{dissipated}$  refers to the energy dissipated during one period of oscillation, and  $E_{stored}$  refers to the energy stored in the oscillating system.

The QCM-D technique measures the dissipation factor (D) based on the fact that the voltage over the crystal ( $A(t)$ ) decays exponentially as a damped sinusoidal with the time ( $t$ ) when the driving power of a piezoelectric oscillator is switched off (Voinova et al., 1999) (as shown in Figure 1.32). This relation is described by the following Eq.1.4.

$$A(t) = A_0 \cdot e^{-t/\tau} \cdot \sin(2\pi ft + \phi) \quad (1.4)$$

Where " $A_0$ " is the amplitude of oscillation before switching off the driving power,  $\tau$  is the decay time constant,  $f$  the frequency and  $\phi$  is the phase angle.

The dissipation factor is related to the decay time constant and therefore it can be calculated using the following equation Eq.1.5

$$D = 1/\pi f \tau \quad (1.5)$$

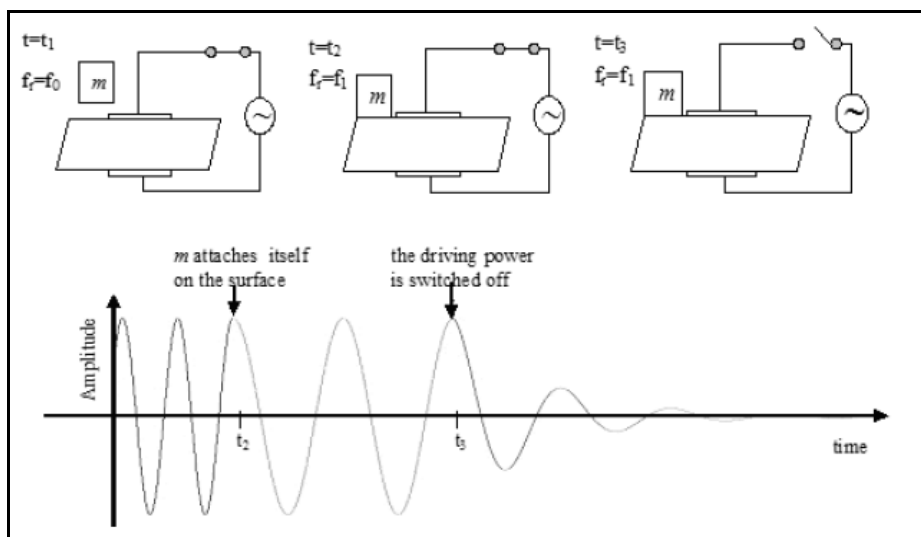


Figure 1.32. Schematic illustration of relative changes in the crystal oscillation upon adsorption of mass ( $m$ ). Initially, the frequency is constant at its fundamental overtone. When the mass is added to the crystal, the frequency decreases but remains constant. Finally, when the driving power is switched off, the frequency decays and the dissipation can be calculated (image adapted from Q-Sense reported data).

The loss of energy in the system depends on the medium surrounding the crystal and the properties of adsorbed mass onto the crystal. The possibilities of determining dissipation shift in real time gives additional valuable information about the adsorbed protein layer (when using protein solutions) on the surface. Since the dissipation is caused by the loss of energy within the protein layer, the changes in dissipation are believed to arise from protein conformational changes and/or the amount of liquid trapped inside the protein layer (Rodahl et al., 1997b).

QCM-D allows frequency ( $\Delta f$ ) and dissipation shift ( $\Delta D$ ) to be recorded simultaneously by applying alternating current (AC) across the quartz crystals. This technique can provide unique and quantitative information on the viscoelastic properties of adsorbed protein layers, which includes density, shear elastic modulus, and shear viscosity (Hook et al., 2001). As explained above, since the protein layer is not rigid, may slip on the moving electrodes surface and is not fully coupled to the crystal surface, the Sauerbrey relation underestimates the adsorbed mass. Therefore, when using protein solution the

Sauerbrey equation must be used cautiously. For viscoelastic films, the Sauerbrey equation can be applied if the protein layer has the following characteristics: (i) The dissipation shift should be less than  $1 \times 10^{-6}$  or dissipation should be less than 5% of a frequency shift of respective surface (Brewer et al., 2005). (ii) The film thickness should be less than 250nm, which is the extinction depth into the aqueous protein solution of the shear waves excited by the QCM-D crystal (Höök et al., 1998). Although Sauerbrey mass is not real for viscoelastic films, the calculated mass allows comparison between different surfaces.

If the protein layer possesses high dissipation values ( $>1 \times 10^{-6}$ ; as mentioned above), it is necessary to consider dissipation changes to calculate the adsorbed mass and to determine viscoelastic properties. In order to calculate adsorbed mass for such protein layers, theoretical modeling of QCM-D response is necessary. This can be achieved by introducing a shear viscosity coefficient ( $\eta$ ) and a shear elasticity modulus ( $\mu$ ) using either one of these two basic models: (i) Maxwell and (ii) Kelvin-Voigt. Polymer solutions can exhibit purely liquid-like behavior, at least for low shear rates, and therefore the Maxwell model is usually applicable. For polymers that conserve their shape and do not flow, however, the Voigt model is applied. (Voinova et al., 1999). The Voigt model was applied in this PhD thesis, since we used protein solutions and were unsure about purely liquid-like behavior for protein solutions. Moreover, in the literature, it is very common that protein adsorption studies were performed applying Voigt model.

The Voigt viscoelastic model is a mechanical model that uses a parallel combination of a spring and a dashpot to represent the elastic (storage) and inelastic (damping) part of a material. In the Voigt model, as shown in Eq 1.6, the viscoelastic element is described by a complex shear modulus ( $G$ ) in which the real part (storage modulus ( $G'$ )) is independent of frequency while the imaginary one (loss modulus ( $G''$ )) increases linearly with frequency (Voinova et al., 1999).

$$G = G' + iG'' = \mu_f + i2\pi f \eta_f \quad (1.6)$$

where " $\mu_f$ " is the elastic shear modulus, " $\eta_f$ " is the shear viscosity and " $f$ " is the oscillation frequency

Based on this approach, Voinova et al. analytically solved the wave equation describing the shear oscillation of a quartz crystal surface covered by a viscoelastic film (uniform thickness and density) that is in contact with a semi-infinite Newtonian liquid under no-slip conditions (Voinova et al., 1999). The general solution of this wave equation was referred to as the  $\beta$ -function. The change in resonance frequency ( $\Delta f$ ) and dissipation factor ( $\Delta D$ ) of the adsorbed film can be obtained from the imaginary and the real part of the  $\beta$ -function (referred in Eq. 1.7 and 1.8) (Hook et al., 2001; Voinova et al., 1999).

$$\Delta f = \text{Im}(\beta) / \pi f \rho_Q t_Q \quad (1.7)$$

$$\Delta D = \text{Re}(\beta) / \pi f \rho_Q t_Q \quad (1.8)$$

In the Voigt model, each protein film is represented by four unknown parameters (Figure 1.33), which includes density ( $\rho_f$ ), shear viscosity ( $\eta_f$ ), shear elastic modulus ( $\mu_f$ ), and the thickness ( $t_f$ ). Since viscous layers exhibit different penetration depths of harmonic acoustic frequencies, changes in frequency and dissipation can be measured simultaneously by considering several different overtones. It was suggested that frequency and dissipation changes be measured by considering the maximum number of overtones (there are 13 overtones in total;  $f=5\text{MHz}$ ,  $15\text{MHz}$ ,  $25\text{MHz}$ .etc.), which allows the Voigt model to better fit the data and to calculate the unknown parameters ( $\rho_f$ ,  $\mu_f$ ,  $t_f$ ).

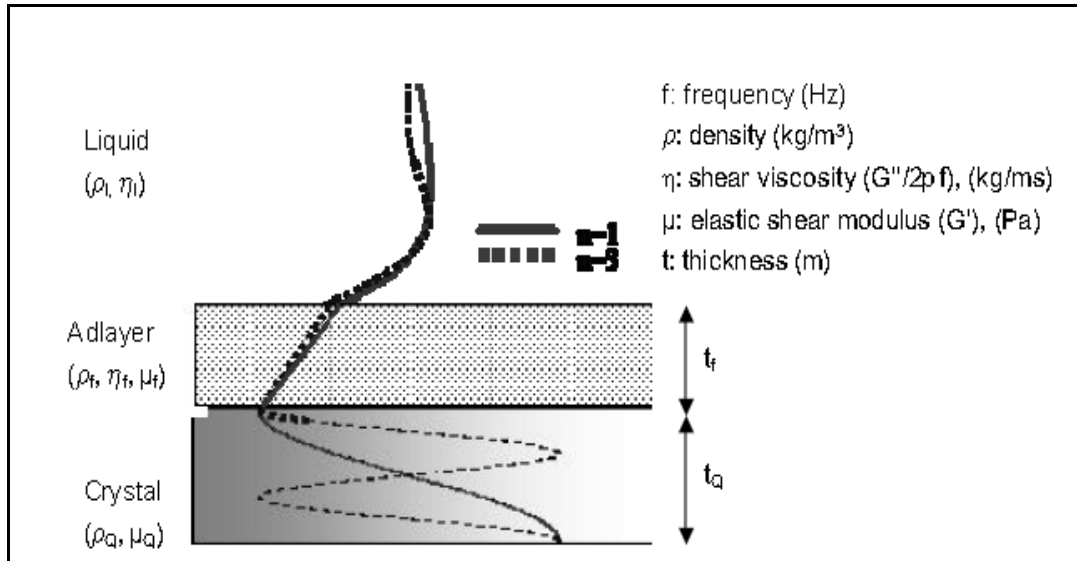


Figure 1.33. Schematic diagram of the geometry of a quartz crystal covered with a viscoelastic protein film. The film is represented by various parameters such as density ( $\rho_f$ ), viscosity ( $\eta_f$ ), elastic shear modulus ( $\mu_f$ ), and thickness ( $t_f$ ). The parameters for bulk liquid are represented by a density ( $\rho_l$ ), and a viscosity ( $\eta_l$ ) and for the crystal are represented by density ( $\rho_q$ ), elastic shear modulus ( $\mu_q$ ), and thickness ( $t_q$ ). Taken from (Höök et al., 2001).

## CHAPTER 2

### OBJECTIVES AND HYPOTHESIS

As seen in the literature review, small vascular implants made of PET and ePTFE fail due to thrombosis and neointima formation. These materials also show their limitations when used for the design of stent grafts, where they do not promote the tissue encapsulating the implant and ensuring its fixation into the vessel wall. Both cases show that those polymeric materials lack favorable properties for promoting cell adhesion and growth. A potential way to limit vascular graft failure would be to provide rapid, uniform, stable and complete endothelial cell coverage for vascular grafts. Similarly, it is essential to promote vascular smooth muscle cell growth around endovascular stent-graft materials to ensure better fixation into the vessel wall. **Therefore the general aim of this PhD thesis is to develop bioactive coatings on PET-based vascular grafts and stent grafts to promote confluent cell adhesion, survival and growth.**

Altering surface physical, chemical and biological properties of PET or ePTFE has shown some success, but the formation of a stable and confluent endothelial layer on the lumen side of vascular graft is still a challenge. Moreover, several strategies such as fibronectin or primary amine-rich plasma polymerized coatings previously developed by our team in Wertheimer and Lerouge's lab (Ruiz et al., 2010; Truica-Marasescu et al., 2008) do not only promote endothelial cell adhesion and retention (Gigout et al., 2011), but also platelet adhesion. Such thrombogenic underlayers could be problematic in case of cell detachment under blood flow. In contrast, it is known from the literature that low-fouling underlayers can reduce platelet adhesion as well as the non-specific protein adsorption and could increase the bioactivity of immobilized biomolecules (Chen et al., 2005b; Groll et al., 2004b; Sebra et al., 2005). ***General hypothesis: Based on the literature, we hypothesize that low-fouling coating combined with adequate immobilized biomolecule(s) allows to create a non-thrombogenic coating promoting cell and tissue growth on synthetic vascular prostheses.***

**Rationale 1:** Minimizing non-specific protein adsorption and platelet adhesion could help to reduce surface thrombogenicity. PEG coatings have previously been reported to exhibit a low degree of protein adsorption (Jeon et Andrade, 1991) and platelet and cell adhesion (Zhang, Desai et Ferrari, 1998). Multi-arm PEG coatings are known to offer relatively high grafting densities and better low-fouling properties compared to linear PEG (Groll et al., 2005a; Sofia Susan et Merrill Edward, 1997). Several studies have already proposed methods for PEG coatings (Davis et Illum, 1988; Demming et al., 2011; Gombotz et al., 1991; Graham et McNeill, 1984). However, current coating methods are far from being versatile since they rely on the availability of compatible functional groups on both PEG and the host surface.

*We hypothesize that the combination of LP coating and subsequent star PEG coating can offer low-protein adsorption and low-thrombogenic properties on any biomaterial surface.*

**Objective 1.** Develop low-fouling and low-thrombogenic coatings that can be applicable to a wide variety of biomaterial surfaces.

**Rationale 2:** The terminal groups of star PEG or CMD coatings enable subsequent coupling of peptide and/or growth factors at higher densities. Low-fouling polymers (PEG or CMD) offer conformational flexibility and minimize non-specific protein adsorption and therefore enhance the bioactivity of immobilized biomolecules (peptides or growth factors) (Groll et al., 2005b; Tugulu et al., 2007). However, based on the literature and previous studies in our lab (Lequoy et al., 2014), it was recognized that immobilization of growth factor alone is not sufficient to achieve cell confluence due to the non-adhesive nature and sterical hindrance effect of high density low-fouling underlayers (Klenkler et al., 2008). More generally, the literature (Crombez et al., 2005; Klenkler et al., 2008; Kolodziej et al., 2011) suggests that immobilization of EGF with the combination of cell-adhesive peptide (for example RGD or KQAGDV) on low-fouling background could help to increase VSMC adhesion and growth and optimal cell interactions could be achieved through positive synergistic effects. The coiled-coil technique for EGF immobilization, previously developed in De Crescenzo's lab (Boucher et al., 2008b) using K coil and E coil tags, was shown to enhance the bioactivity of

EGF and offers an interesting approach to combine EGF with adhesive peptides on low-fouling substrates.

*We hypothesize that the bioactivity of KQAGDV peptide and / or EGF is increased when they are immobilized on low-fouling polymers (PEG or CMD) and together they produce an additive or synergistic effect. This could aid to significantly enhance biological activities such as VSMC adhesion, survival and growth.*

**Objective 2:** Develop immobilization protocols allowing for the subsequent decoration of KQAGDV peptide and/or EGF (individually or combined) on low-fouling surfaces and evaluate their effect on vascular smooth muscle cells.

**Rationale 3:** CS coating has previously been developed in our lab (Charbonneau et al., 2012), and this polymer was shown to promote VSMC growth and resistance to apoptosis. CS exhibited a good cell growth when recent studies (from our lab) compared VSMC behavior on CS and CMD surfaces on which EGF had been grafted (Lequoy et al., 2014). Moreover, CS prevented EGF non-specific adsorption as effectively as CMD (Lequoy et al., 2014). It was also shown that sulfated polysaccharides can improve hemocompatibility by means of electrostatic repulsion toward negatively charged blood components (Keuren et al., 2003).

*Based on the literature and observations from previous studies in our lab, we hypothesize that CS exhibits selective low-fouling, low-thrombogenicity and pro-cell adhesive properties which could create an interesting compromise as a luminal surface for vascular grafts endothelialization.*

**Objective 3:** Evaluate the low-thrombogenic and low-fouling properties of various coatings (PEG, CMD and CS) and evaluate the advantages and limitations of using CS coating for the creation of low-thrombogenic surfaces for vascular graft applications.



## CHAPTER 3

### MATERIALS AND METHODS

#### 3.1 Surface preparation and coating methods

During this PhD thesis, various substrates were used for surface coatings. The nitrogen-rich plasma polymerized ethylene coatings (LP) were performed on microscope glass slides, PET films (Goodfellow, Huntingdon, England) and gold-plated QCM-D crystal surfaces (Q-Sense AB, Sweden). Such primary amine-rich coatings were used as an underlayer for covalent immobilization of multi-arm polyethyleneglycol (star PEG), carboxymethylated dextran (CMD) and chondroitine-4-sulfate (CS) polymers. However, amino-coated glass surfaces ( $10 \times 10 \text{ mm}^2$ ; Erie Scientific Co, Portsmouth, NH, USA) were also used for same purpose, in particular for specific experiments such as X-ray photoelectron spectroscopy (XPS) analysis and complementary protein adsorption studies using fluorescence measurements. For the second objective of this thesis, adhesive peptides and epidermal growth factor (EGF) molecules were further immobilized on PEG and CMD surfaces, as described in 3.1.4.

##### 3.1.1 Cleaning samples

The substrates were cleaned before and after surface coatings, as described in the following paragraphs.

**Before LP deposition:** PET films and microscope glass slides were cleaned with ethanol in an ultrasonic bath for few minutes and dried with a stream of nitrogen gas. Gold-plated sensor surfaces were cleaned using the cleaning protocol described below in the QCM-D section.

**Cleaning amino-coated glass surfaces:** Prior to chemical grafting, the glass slides were cleaned with chloroform (99% purity, Fisher Scientific) for 2 min using an ultrasonic bath

followed by rinsing twice with Milli-Q water, and finally drying with a stream of nitrogen gas.

**After chemical grafting of PEG, CMD and CS:** After completion of the reaction, the excess solution was removed from the surfaces, and the slides were rinsed for 2 min with PBS, followed by Milli-Q water (2 times) in an ultrasonic bath. Finally, the slides were dried with nitrogen gas stream.

### 3.1.2 Plasma polymerization

The low-pressure plasma polymerized (LP) coatings were deposited using a low-pressure radio-frequency (r.f.) glow-discharge plasma reactor developed by Wertheimer and Lerouge. LP deposition was performed as already described in (Ruiz et al., 2010; Truica-Marasescu et al., 2008). The coating was deposited in a cylindrical aluminium/steel vacuum chamber approximately 20 cm in diameter and 20 cm in height (Figure 3.1). A turbo-molecular pump, backed by a two-stage rotary vane pump, was used to evacuate the chamber and to maintain a base pressure of  $<10^4$  Pa (measured by an ionisation gauge). A mixture of anhydrous ammonia ( $\text{NH}_3$ ) and ethylene ( $\text{C}_2\text{H}_4$ ) (99.9% and 99.5% purity, respectively; Air Liquide Canada Ltd., Montreal, QC, Canada) was admitted into a reactor chamber using electronic flow meter/controllers (Vacuum General Inc.) and a 'shower head' gas distributor at flow rates of 15 and 20 standard cubic centimeters per minute (sccm), respectively.

This gas ratio ( $R = F_{\text{NH}_3} / F_{\text{C}_2\text{H}_4} = 0.75$ ) was chosen since it was previously found to create coatings with the best compromise in terms of primary amine concentration and stability in aqueous media. XPS analysis showed a high concentration of nitrogen ( $[\text{N}] = 14\%$ ) and primary amines ( $[\text{NH}_2] = 7.5\%$ , determined by chemical derivatization using 4-[trifluoromethyl] benzaldehyde [TFBA] followed by F content measurement) in the resulting coating, as detailed previously (Ruiz et al., 2010). Moreover, these coatings were found to be very stable in aqueous solutions, with less than 10% decrease in thickness when immersed in Milli-Q water or PBS solution for up to one week, as assessed by Dektak profilometry. (Ruiz et al., 2010). LP deposition using these conditions led to a smooth and homogeneous layer,

without detectable porosity and with a roughness ( $R_q$ ) of 0.2-0.3 nm, as observed by scanning electron microscopy (SEM) and atomic force microscopy (AFM) (Ruiz et al., 2010), respectively. In the present study, a plasma deposition time of 10 min was chosen for all experiments, leading to 80 to 90 nm-thick LP coatings.

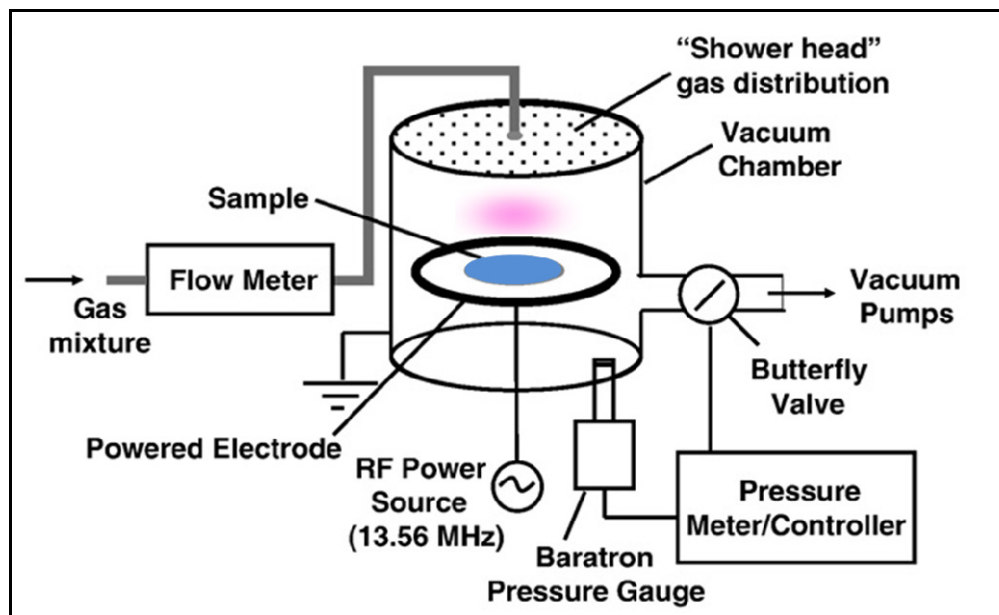


Figure 3.1. Schematic views of the low-pressure, capacitively coupled radio-frequency plasma reactor. Taken from (Truica-Marasescu et al., 2008).

### 3.1.3 Chemical grafting of PEG, CMD and CS

Three different macromolecules were covalently grafted on LP as well as on amino-coated glass surfaces to create low-fouling surfaces, namely star PEG, CMD and CS. The chemical structures of these molecules are presented in Figure 3.2. The PEG grafting method was first optimized by estimating low-fouling properties of various PEG coupling concentrations (for objective 1). A 4-arm PEG with N-hydroxy succinimide (NHS) terminal functional groups (PEG-NHS;  $M_w = 10$  kDa, Creative PEG Works Inc., Winston Salem, NC, USA) was chosen for this work. The terminal NHS groups allow simple reaction with primary amine groups (on LP or amino-coated glass) to form stable amide bonds as shown in Figure 3.3. The optimized PEG coating method was then compared with the CMD coating

for their ability to immobilize KQAGDV peptide and/or EGF (for objective 2). Finally, the low-fouling, non-thrombogenic and cell-adhesive properties of PEG, CMD and CS coatings were compared (for objective 3). Therefore, CMD and CS coating methods are also described in this section.

CMD is a highly flexible polysaccharide, an anionic derivative of dextran, which contains various carboxyl groups on the chain as shown in Figure 3.2. CMD chains were generated from commercially available dextran (Pharmacosmos, Holbaek, Denmark), and the carboxymethylation degree of the dextran chains (70 kDa) was previously estimated as approximately 60% (Liberelle et al., 2010). Similarly, CS (Sigma-Aldrich Canada Ltd., Oakville, ON, Canada) contains carboxyl terminal groups as shown in Figure 3.2. This polymer is a member of the glycosaminoglycan (GAG) family and a sulfated polysaccharide containing repetitive units of glucuronic acid and galactosamine.

Both CMD and CS polymers were covalently grafted on amine-functionalized surfaces (LP-coated or amino-coated glass surfaces) via NHS/EDC chemistry by following protocols that were previously developed in Lerouge's and De Crescenzo's laboratories (Charbonneau et al., 2011; Liberelle et al., 2010). In this procedure, EDC reacts with carboxyl terminal groups on the polymer to form an O-acylisourea intermediate and, followed by NHS reaction, forms a stable amine-reactive NHS ester, which enables stable amide bonding.

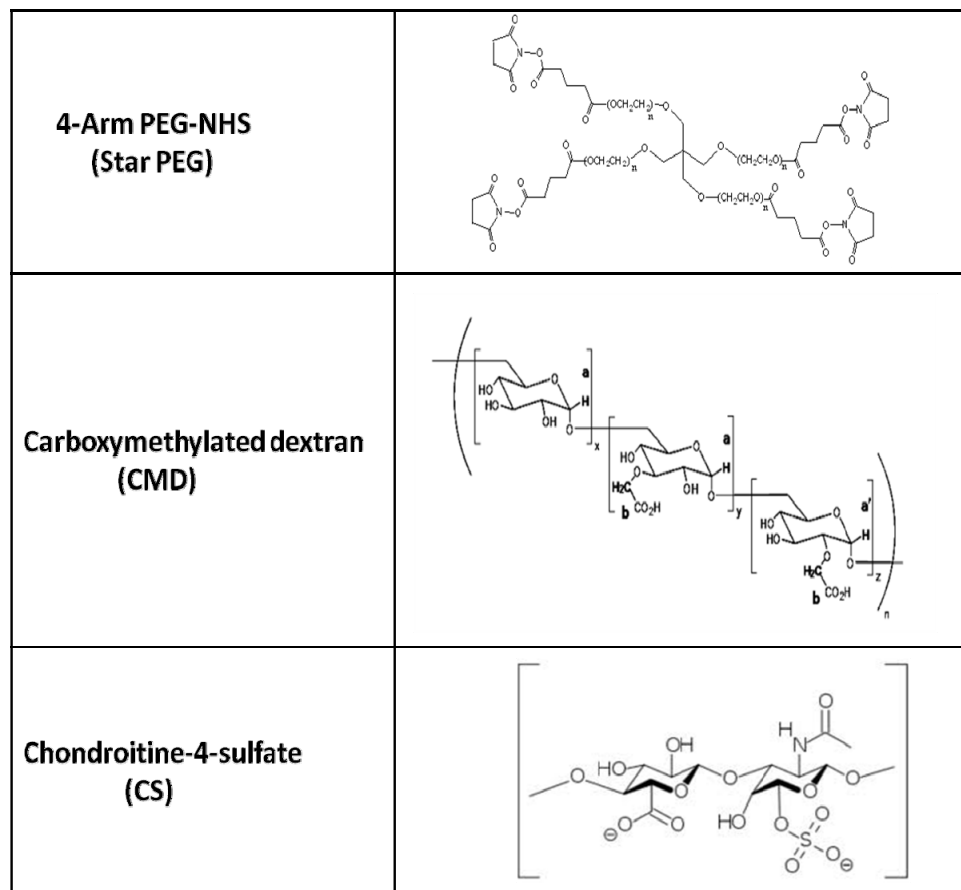


Figure 3.2. Chemical structure of polyethyleneglycol (PEG), carboxymethyl dextran (CMD) and chondroitin-4-sulfate (CS).

### 3.1.3.1 Optimizing star PEG Grafting

Star PEG-NHS reaction scheme is presented in Figure 3.3. PEG-NHS solutions at different concentrations (0.55, 1.66, 5, and 15% w/v) were prepared by dissolving in 25 mM phosphate buffer (25 mM  $\text{NaH}_2\text{PO}_4$  + 25 mM  $\text{Na}_2\text{HPO}_4$ , with drops of 0.01 M NaOH to adjust to pH 8.5) (Nakajima et Ikada, 1995). In order to prevent hydrolysis of NHS terminal groups, the PEG solution was immediately deposited on aminated surfaces for 2 h at room temperature (RT). The surfaces were then rinsed and dried as described in the cleaning samples section. Since there is no significant improvement in low-fouling properties by increasing PEG coupling concentration (See results section 4.1.2), 5 % (w/v) PEG was used for comparing low-fouling properties of PEG, CMD and CS surfaces.

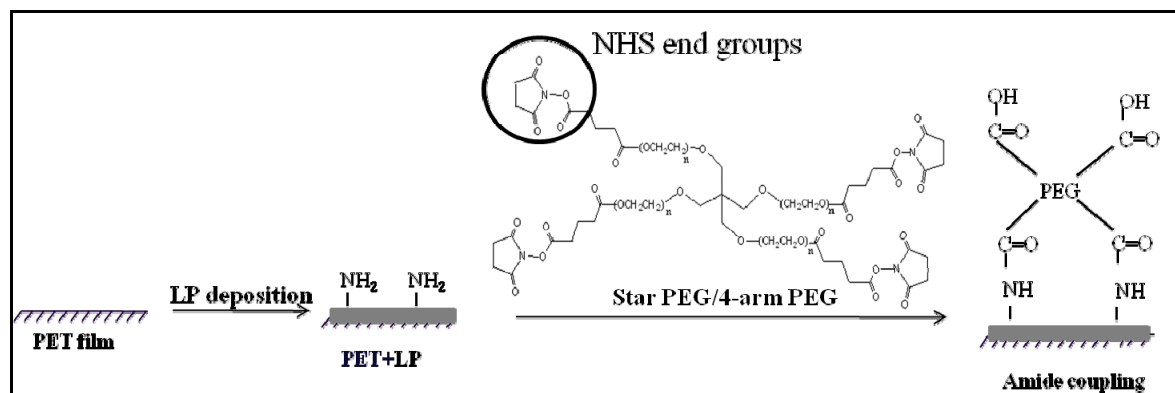


Figure 3.3. Schematic diagram of star PEG covalent binding reaction. Either one or two N- hydroxyl succinamide (NHS) terminal groups of star PEG react directly with primary amines through ester-amine reactions to form stable amide bonds; the remaining terminal groups do not participate in coupling, due to steric constraints (Park, Mao et Park, 1990) and hydrolyze to carboxylic acid groups during the reaction.

### 3.1.3.2 CMD grafting

The CMD solution was prepared in Milli-Q water (2 mg/mL). Once dissolved, CMD was activated by preparation of a solution containing (for a total volume of 1 mL) 800  $\mu\text{L}$  of CMD solution, 100  $\mu\text{L}$  of 0.4 M EDC in Milli-Q water and 100  $\mu\text{L}$  of 0.1 M NHS in Milli-Q water. The NHS-activated CMD solution was allowed to react with  $\text{NH}_2$  displaying surface for 1h at RT. The surfaces were finally rinsed and dried as described above.

### 3.1.3.3 CS grafting

The CS solution was prepared by dissolving 0.1 g in 1 mL of Milli-Q water, and was filtered (0.2  $\mu\text{m}$  PTFE filter) to remove aggregates. CS was then activated by preparation of a solution containing (for 1 mL) 400  $\mu\text{L}$  of EtOH, 347  $\mu\text{L}$  of Milli-Q water, 50  $\mu\text{L}$  of 1 M MES, 57  $\mu\text{L}$  of 0.4 M EDC, 46  $\mu\text{L}$  of 0.1 M NHS, and 100  $\mu\text{L}$  of CS solution. These conditions were shown to provide the best CS-covered surface as assessed by contact angle, XPS and ellipsometry, detailed in (Charbonneau et al., 2011). The NHS-activated solution was reacted with  $\text{NH}_2$  displaying surfaces for 1 h at RT. Rinsing steps and drying were performed as described above.

### 3.1.4 Covalent immobilization of peptides and epidermal growth factor (EGF)

Immobilization of peptide and tethering of EGF was performed on low-fouling surfaces (PEG or CMD) to investigate the possibilities of improving VSMC adhesion, growth and survival on biomaterial surfaces. Therefore, the immobilization procedure for these biomolecules is described in this section.

**Peptide immobilization:** The adhesive peptides such as KQAGDV (CGG-KQAGDV;  $M_w = 876$  Da) and RGD (CGG-RGD;  $M_w = 563$  Da) were produced with three additional residues at their C terminus, i.e. CGG, in order to immobilize them by taking advantage of the unique thiol (R-SH) group in their sequence. These peptides were synthesized by the peptide facility at the University of Colorado (Denver, CO, USA).

Peptides were immobilized on carboxyl terminal groups of PEG or CMD using a heterobifunctional cross linker, i.e., 3,3'-N-[ $\epsilon$ -Maleimidocaproic acid] hydrazide, trifluoroacetic acid salt (EMCH; Fisher Scientific Co., Ottawa, ON, Canada), as shown in Figure 3.4 (b --> d1). This linker readily reacts with cysteine containing molecules through sulfhydryl bonding (Trail et al., 1993). The carboxyl terminal groups of PEG or CMD were reacted with EMCH for 2.5 h using a solution containing (for a total volume of 1 mL) 100  $\mu$ L of EMCH (3.4 mg/mL in DMSO) and 400  $\mu$ L of PBS and 500  $\mu$ L of 0.4 M EDC. The same protocol was used for PDPH (3-[2-Pyridyldithio] propionyl hydrazide; Fisher Scientific Co., Ottawa, ON, Canada) linker grafting, which was an alternative to EMCH. Surfaces were then rinsed once with PBS and twice with Milli-Q water and finally air-dried at RT. Various concentrations (38, 12.6, 4.2, 1.4 and 0.46  $\mu$ M) of peptide solutions were prepared in PBS and reacted with linker-activated surfaces for 2 h, and finally surfaces were rinsed as described above.

**EGF tethering:** EGF tethering was performed on low-fouling surfaces by taking advantage of the innovative oriented immobilization strategy based on the interactions of two high-affinity peptides: the E coil and the K coil. These peptides heterodimerize with high specificity and affinity through coiled-coil interactions, as detailed in the literature review section and as shown in Figure 3.4 (d2 --> e). This technique was previously developed by De Crescenzo's team at Ecole polytechnique (Boucher et al., 2008b; De Crescenzo et al.,

2003). In order to allow such oriented immobilization of EGF on a low-fouling surface, E coil tagged EGF ((EVSALEK)<sub>5</sub>-EGF, produced in human embryonic kidney (HEK293) cells as described in (Boucher et al., 2008a)) and K coil (CGG-(KVSALKE)<sub>5</sub>; *M<sub>w</sub>* = 4 kDa, chemically synthesized and purified by the peptide facility at the University of Colorado (Denver, CO, USA) ) were used. First, K coil (2 μM) solution in PBS was reacted with an EMCH-grafted surface for 2h (Figure 3.4 (c-->d2)). After 2h, the surface was rinsed with PBS and then directly incubated with E coil EGF (160 nM) solution in PBS for 1 h, which allows EGF capture via coiled-coil interactions (Figure 3.4 (d2 --> e)). Finally, surfaces were rinsed with PBS as well as Milli-Q water to remove an unbound E coil EGF protein. The combined immobilization of peptides and EGF was optimized using the QCM-D technique, which will be described in the QCM-D measurement section.

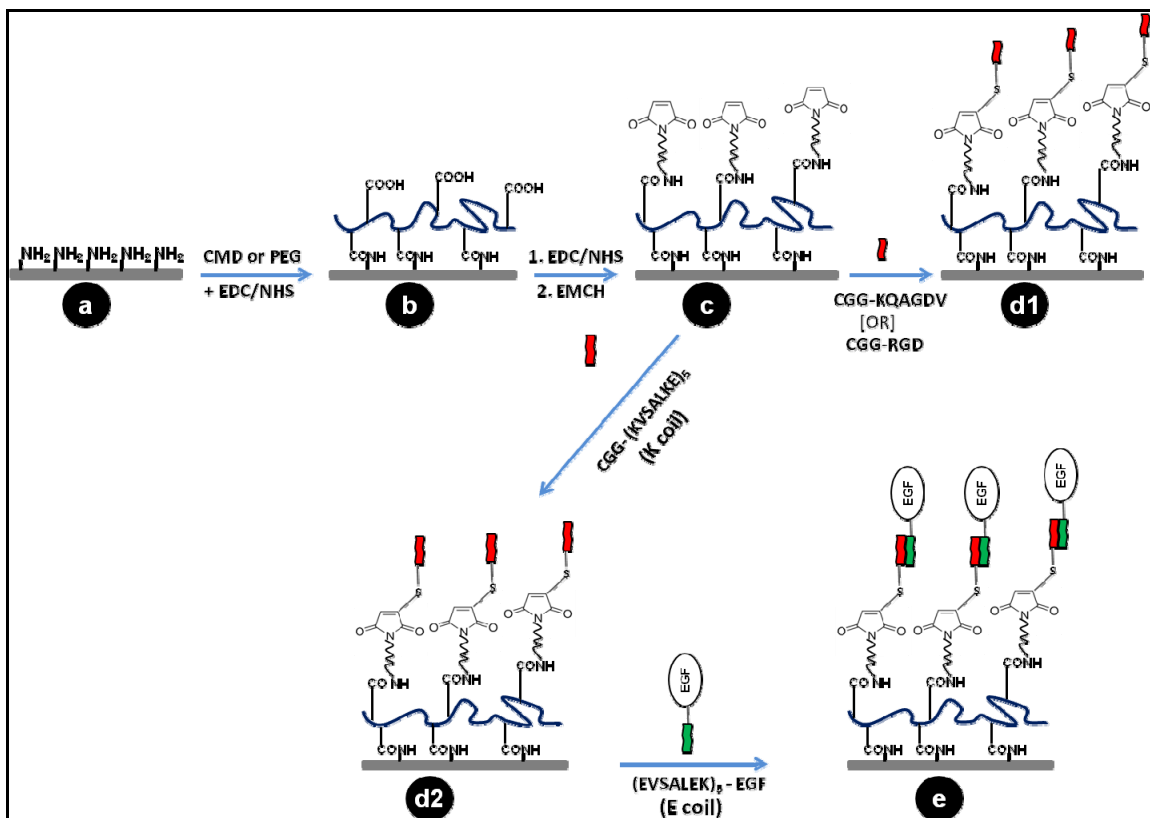


Figure 3.4. Schematic of KQAGDV and K coil peptide grafting using EMCH linker and E coil EGF tethering through coiled-coil interaction.

## 3.2 Surface characterization

### 3.2.1 X-ray photoelectron spectroscopy (XPS)

XPS is the most commonly used technique to analyze the composition of biomaterial surface coatings. In brief, it is accomplished by irradiating a sample with monoenergetic soft x-rays and analyzing the emitted electrons that have kinetic energies specific to the elements present as well as to their chemical state. Photons from the energy source have limited penetrating power in a solid on the order of 1-10  $\mu\text{m}$  and they interact with the atoms in the surface region, causing electrons to be emitted by the photoelectric effect (Hofmann, 2013). The emitted electrons can be measured in kinetic energies using the following equation Eq.2.1.

$$KE = h\nu - BE - \phi_s \quad (\text{Swingle, 1975}) \quad (2.1)$$

Where  $h\nu$  is the energy of the photon, BE is the binding energy, and  $\phi_s$  is the spectrometer work function.

Since each element has a unique set of binding energies, XPS can enable to determine the atomic concentration of elements on the surface, except hydrogen or helium, with a sensitivity of approximately 0.1 atom percent (Swingle, 1975). Variations in the elemental binding energies, also known as chemical shifts, arise from differences in the chemical potential and polarizability of the compounds. These changes can be used to identify the chemical state of the material being analyzed.

The chemical composition of PEG-modified surfaces was characterized by XPS using a VG ESCALAB 3MkII instrument with non-monochromatic Mg  $K\alpha$  radiation. The surface elemental composition was detected using survey scans and the chemical state of each element was evaluated by high-resolution scans. The curve fitting was applied to the peaks in the high-resolution scan for precise determination of binding energies. For each sample, survey (0-1200 eV) and high-resolution spectra for C1s and O1s were recorded at a pass energy of 100 eV and 20 eV, respectively. The take-off angle, defined as the angle between

the sample surface and the electron path to the analyzer, was adjusted to 70° in order to minimize the effect of the substrate. Charging was corrected by referencing all peaks with respect to the carbon (C1s) C-C, C-H peak at 285.0 eV. The Advantage v4.12 software (Thermo Electron Corporation, Waltham) was used to quantify the constituent elements after Shirley-type background subtraction by integrating the areas under relevant peaks. High resolution spectra of C1s and O1s were deconvoluted by full width half maximum (FWHM) factors of 1.6 and 1.8 respectively. Deconvoluted peak positions of chemical bonds such as C-Si, C-C, C-O and C=O in an amino-coated glass were kept constant for each subsequent analysis, in order to identify any new functional groups added after surface modification with PEG.

### 3.2.2 Static Water Contact Angle

Wettability measurements can provide a good understanding of surface properties, which can be determined from the measurement of contact angle of a pure liquid drop on that solid surface. When liquid is dropped onto a solid surface, it will spread over the surface depending on the surface properties. The angle formed between (as shown in Figure 3.5) solid surface and tangent of droplet is called the contact angle  $\theta$ , which can be referred by the following Young's Dupre equation. The measurement of contact angle indicates the degree of wetting when a solid and liquid interact. Small contact angles ( $< 90^\circ$ ) correspond to high wettability, while large contact angles ( $> 90^\circ$ ) correspond to low wettability.

$$\gamma_s = \gamma_L \cos \theta + \gamma_{sL} \quad (2.2)$$

Where  $\gamma_s$  = solid surface energy,  $\gamma_L$  = liquid surface tension and  $\gamma_{sL}$  = solid and liquid surface tension. The contact angle ( $\theta$ ) is indicative of the wettability of the surface.

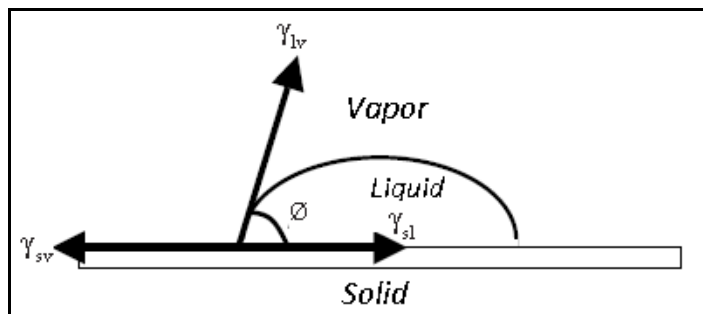


Figure 3.5. Schematic diagram of the contact angle and interfacial tensions at three phase boundaries.

In this work, the wettability of the amino-coated glass and LP-deposited surfaces before and after PEG grafting (of various coupling concentrations) was assessed by static water contact angle measurements, using a Ramé-Hart Inc., Model 100-00 115 goniometer. Three measurements were taken on each surface using Milli-Q water as probe liquid (2 $\mu$ L drop size), and experiments were repeated on three independent samples. The visual contact angle (VCA) Optima (AST Products, Billerica, MA) automated system was used to compare PEG, CMD and CS surfaces. A 2 $\mu$ L Milli-Q water (pH  $\approx$  6) drop was placed on each sample and the static contact angle measurements were performed on both sides of the drop within 5 s. Three measurements were taken on each surface and experiments were repeated on three independent samples.

### 3.3 QCM-D measurements

#### 3.3.1 QCM-D system

The QCM-D that has been used for the assays in this work is the Q-Sense E4 model (Q-Sense, Sweden). This system mainly consists of five parts (Figure 3.6):

1. **The sensor crystal:** The quartz crystal sensors are usually available pre-coated with, for example, metals, polymers or SAMs.
2. **The flow module chamber:** This is where the sensor crystal is mounted. This chamber provides a temperature-controlled environment for the crystal during the measurement. Four

flow modules can be arranged in parallel as shown in Figure 3.6, which allows the measurement of four different surfaces at a time.

3. **External peristaltic pump:** This pump enables solution to be injected through Teflon tubes and regulates flow rate (up to 500 $\mu$ L/min).

4. **The electronics unit:** This makes the QCM-D measurements possible and contains the temperature control system.

5. **The data acquisition software:** Q-soft 301 (Q-Sense, Sweden) records frequency and dissipation changes simultaneously and the data analysis software, Q-tool (Q-Sense, Sweden), allows data interpretation and analysis. Q tools software helps to use Sauerbrey relation as well as to apply Voigt mathematic model that calculates the adsorbed mass and viscoelastic properties considering frequency and dissipation changes. The conditions used for the experiments and data analysis using Q tools are described in M & M section.

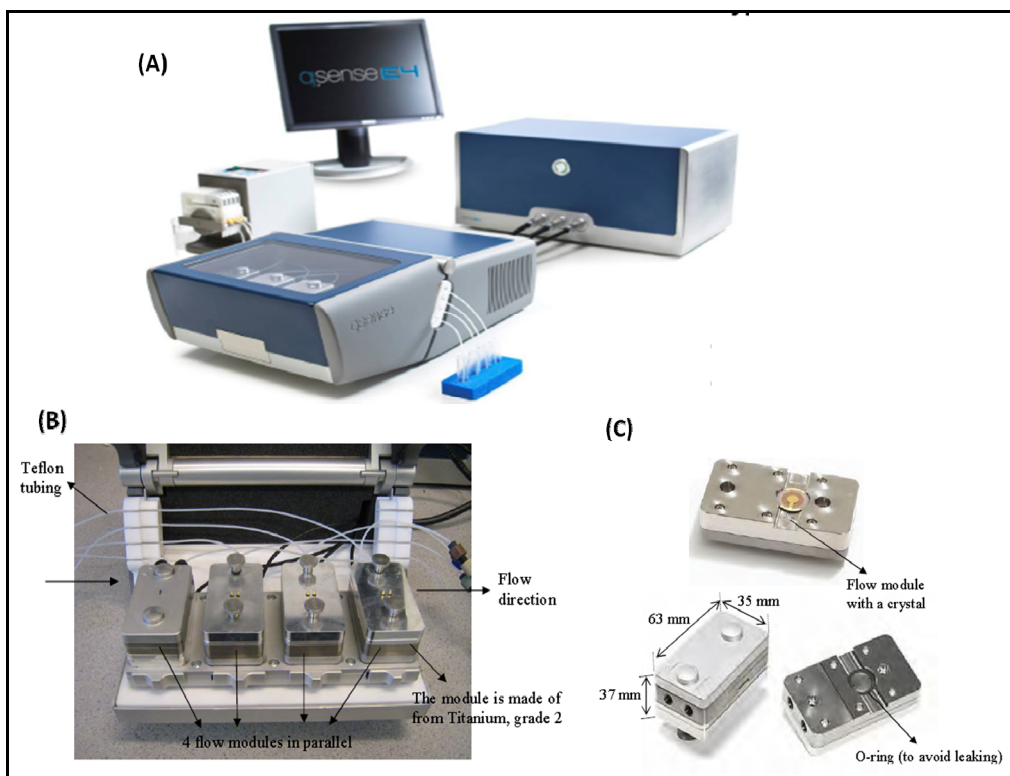


Figure 3.6. Schematic picture of (A) complete setup of the QCM-D equipment (B) four flow modules chamber and their setup and (C) flow module with a crystal, dimensions and o-ring position.

### 3.3.1.1 Overtone sensitivity

This QCM-D system allows simultaneous measurements of the resonance frequencies and the dissipation shift at different overtones (fundamental, third, fifth, seventh and up to thirteenth; i.e.,  $f=5$  MHz, 15 MHz, 25 MHz and so on.). As shown in Figure 3.7, the penetration depth varies as a function of overtone number. The fundamental overtone is too sensitive to environmental fluctuation and a higher overtone number is related to a lower penetration/detection depth (see Figure 3.7 for penetration depth depending overtone numbers). Therefore these two overtones should be excluded for data analysis (for both Sauerbrey and Voigt models). Simultaneous measurement of multiple overtones is required to model viscoelastic properties and extract correct thickness applying the Voigt model. Moreover, considering different overtones enables providing information about the homogeneity of applied layers as the detection range out from the crystal surface decreases with increasing overtone number.

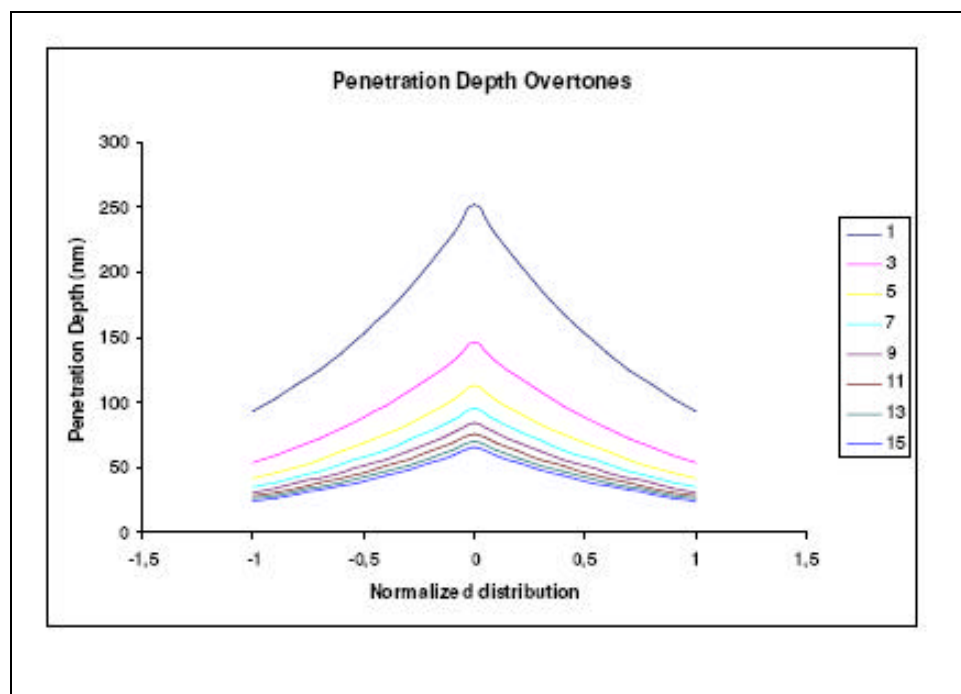


Figure 3.7. Schematic shows the viscous penetration depth as function of the overtone number (Q-Sense reported data).

### 3.3.2 QCM-D measurements

QCM-D measurements were performed with a Q-sense E4 system (Q-Sense AB, Sweden). This technique was used for different purposes in this thesis: (i) To optimize PEG grafting on LP surface by comparing protein adsorption (for objective 1). (ii) To compare the low-fouling properties of PEG, CMD and CS surfaces (for objective 3). (iii) To optimize the combined immobilization of adhesive peptides (KQAGDV and RGD) and EGF and to follow cell adhesion on KQAGDV and RGD grafted surfaces (for objective 2).

The Q-sense E4 system consists of four independent flow chambers, which allows measuring small masses for four different surfaces at a time. As detailed in the literature review section, this technique allows following of the changes in frequency ( $\Delta f$ ) and energy dissipation ( $\Delta D$ ) of an oscillating quartz crystal in response to mass changes on the crystal surface in real-time (Höök et al., 2002), as shown in Figure 3.8. The adsorbed mass of thin and non-dissipative layers can be calculated using the Sauerbrey relationship ( $\Delta m = C/n \Delta f$ ; where  $\Delta f$  is linearly related to the adsorbed mass ( $\Delta m$ ),  $n$  is the harmonic number and  $C$  is the mass sensitivity constant of the crystal) (Sauerbrey, 1959). In practice, most surface-adsorbed protein layers are hydrated, viscous, and cause significant energy dissipation. In such cases, the dissipation factor ( $D$ ) can be considered, which is defined as the ratio of the energy dissipated during one period of oscillation and the energy stored in the oscillating system ( $D = E_{\text{dissipated}}/2\pi E_{\text{stored}}$ ) (Voinova et al., 1999). In this study, depending on dissipation values, the adsorbed mass was calculated via the Sauerbrey equation (Sauerbrey, 1959) or by applying a viscoelastic, single-layer Voigt model implemented in the QCM software (Q tools, Q-sense AB, Sweden) (Voinova et al., 1999). The Voigt model was applied when dissipation shift was at least 5 % of the frequency shift of the respective surface (Höök et al., 2002).

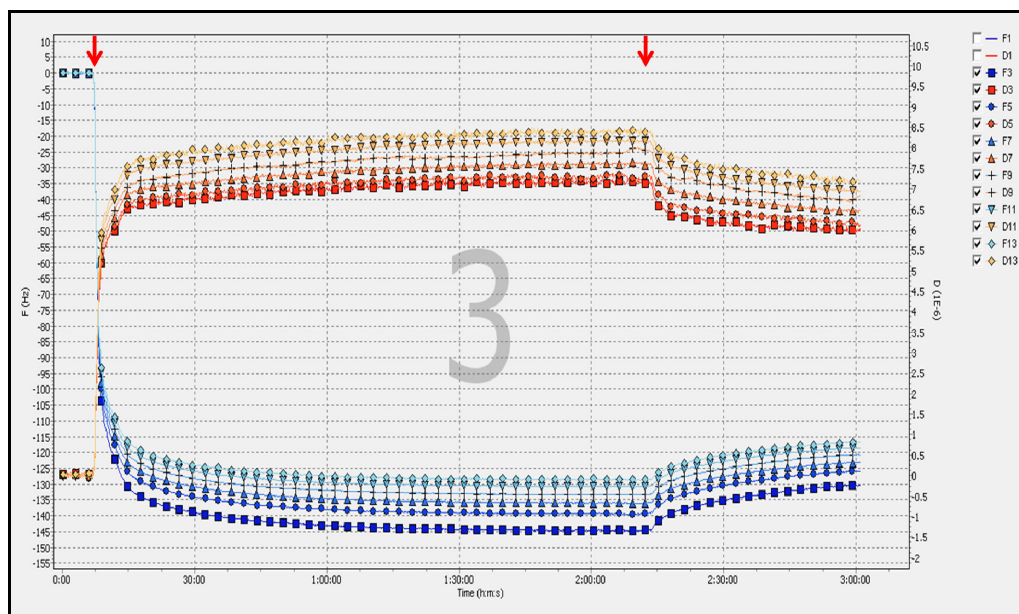


Figure 3.8. Example of QCM-D data for simultaneous measurements of frequency ( $\Delta f$ ) and ( $\Delta D$ ) dissipation changes (for various over tones) during fibrinogen (0.5 mg/mL) adsorption on LP deposited surface. Arrows refer to injection (left) of fibrinogen and rinsing (right) with PBS solution.

### 3.3.2.1 Protein adsorption studies to optimize star PEG coating for low-fouling properties

Gold-coated quartz crystals (5 MHz, Q-sense AB, Sweden) were coated with LP followed or not by star PEG grafting using PEG solutions of various concentrations (0.55, 1.66, 5 and 15% w/v) as described in the sample preparation section. QCM-D assay was performed at 37°C using human fibrinogen (340 kDa) solution (0.5 mg/mL in PBS). Crystals were first exposed to PBS with a flow rate of 50  $\mu\text{L}/\text{min}$  until a stable baseline was reached for frequency and dissipation. A fibrinogen solution was then flowed for 2 h followed by rinsing with PBS for 30 min. Protein adsorption on 4 different surfaces was compared each time by following changes in frequency ( $\Delta f$ ) and dissipation ( $\Delta D$ ) and each surface was tested at least three times. The Voigt viscoelastic modeling in QTools (Q tools, Q- sense AB, Sweden) was applied to estimate the adsorbed mass per surface unit by considering both frequency ( $\Delta f$ ) and dissipation ( $\Delta D$ ) shifts (Höök et al., 1998; Voinova et al., 1999). All the overtones except the first one were used to normalize the data and to estimate the adsorbed

mass of protein. It is important to note that the estimated mass included protein molecules in addition to water trapped in the layer. The following parameters were used for modeling the data as described by Weber et al. (Weber et al., 2007). The layer density was fixed at 1200 kg/m<sup>3</sup>. Parameters fitted were i) layer viscosity between 0.001 and 0.01 kg/ms and ii) layer thickness between 10<sup>-10</sup> and 10<sup>-7</sup> m.

In addition, QCM-D was used to assess the stability of the PEG coating. To that purpose, 5% PEG grafted crystals were incubated in PBS (37°C, pH 7.4, 5% CO<sub>2</sub>) for 4 weeks. Samples were then rinsed with Milli-Q water and dried with nitrogen gas. QCM-D assay was performed as described above to compare fibrinogen adsorption on LP, 5% PEG immersed for 1 day or for 4 weeks in PBS. This experiment was repeated three times. Between each experiment, gold crystals were extensively cleaned to remove LP and PEG for subsequent experiment. Crystals were cleaned by incubating them for 15 min in a solution containing Milli-Q water, ammonia and hydrogen peroxide (ratio of 5: 1: 1, 75 °C), followed by extensive rinsing with Milli-Q water. Then they were dried with nitrogen gas stream and exposed to UV and ozone for 10 min in an UV/ozone ProCleaner (Bioforce Nanosciences, Inc. Model ProCleaner 110), as reported in (Rodahl et al., 1997a).

### **3.3.2.2 Comparing PEG, CMD and CS low-fouling properties**

In this experiment, the gold-plated sensor surfaces were pre-coated with LP followed by PEG or CMD or CS. Protein adsorption kinetics were compared between these surfaces, as well as on a LP control surface. First, adsorption of human fibrinogen (0.5 mg/mL; 340kDa) and BSA (0.2 mg/mL; 66kDa) were studied independently. Then the surfaces were subjected to FBS (10% v/v), which contains a wide range of proteins of various size and affinity. The adsorbed mass was calculated as described above.

### **3.3.3 Combined immobilization**

As mentioned earlier, the potential of combined immobilization of adhesive peptides (KQAGDV and RGD) and EGF to achieve confluent VSMC adhesion and growth on low-

fouling surfaces was tested. In this section, the use of QCM-D to follow and analyze the immobilization peptides with/without coiled EGF is described. Gold-plated sensor surfaces were pre-coated with LP followed by PEG or CMD grafting, and followed by EMCH linker grafting as described in the peptide immobilization section. The linker-grafted surface can enable grafting of cysteine-tagged K coil and/or KQAGDV peptide via disulfide bonding (Trail et al., 1993), as shown in Figure 3.4. The sensor surfaces were inserted into the QCM-D system equipped with 4 parallel flow modules to follow the serial immobilization of KQAGDV peptide, K coil and the tethering of E coil EGF *in situ*. Since the biomolecule solutions were prepared using PBS, the stable baseline for frequency and dissipation was first created using the same solution. For combined immobilization, as shown in Figure 3.9, KQAGDV peptide solution at various concentrations (38, 12.6, 4.2, 1.4 and 0.46  $\mu\text{M}$ ) was allowed to flow for 2 h and followed or not by injection of K coil (2  $\mu\text{M}$ ) solution. Then cysteine solution was flowed for 1 h to block possible unreacted sites of EMCH linker. Finally, E coil EGF solution (160 nM) was injected (1h) to tether E coil EGF onto K coil derivatized surfaces through coiled-coil interactions. For all experiments, at the end of each grafting step, surfaces were rinsed with PBS to remove unbound biomolecules and we waited until reaching the stable baseline before injecting another biomolecule solution. K coil and cysteine-only grafted surfaces were used as positive and negative controls, respectively. The frequency and dissipation changes due to the immobilization of biomolecules were recorded at each step. Since the dissipation values were very low, the grafted mass was calculated from frequency changes using the Sauerbrey equation.

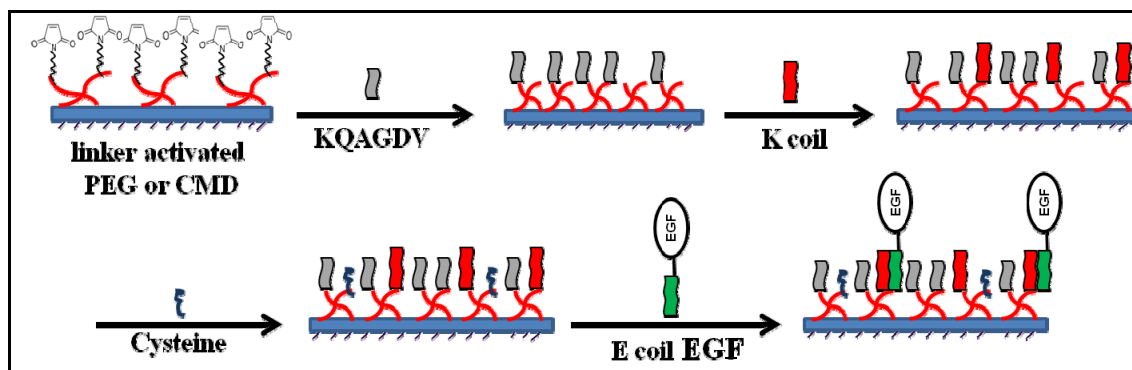


Figure 3.9. Schematic diagram of serial immobilization of KQAGDV peptide, K coil, Cysteine and E coil EGF, with QCM-D.

### 3.3.4 Measuring cell adhesion

QCM-D was also used to study VSMC adhesion kinetics in flow condition on various surfaces deposited on the gold sensors. Cells were routinely cultured in DMEM and used between passages 6 and 14. Cell suspension was prepared using DMEM (without serum) at a density of  $1 \times 10^5$  cells/mL. For QCM-D experiments, first peptide grafting on a CMD surface was confirmed by following frequency changes (as described above) and cell suspension was then allowed to flow over the surfaces. Peptide-modified (LP + CMD + peptide) and unmodified LP surfaces were allowed to flow with the cell suspension at the flow rate of  $50 \mu\text{L}/\text{min}$ . After 1 h adhesion, surfaces were rinsed with DMEM for 1 h (or until reaching a stable baseline) to remove weakly adhered cells. Cell adhesion was evaluated by recording changes in frequency and dissipation shifts.

### 3.4 Protein adsorption studies by fluorescence measurements

Fluorescence measurements were performed using Texas Red conjugated BSA (66 kDa; Sigma-Aldrich Canada Ltd., Oakville, ON, Canada) to confirm the results obtained with QCM-D and compare the coatings to pristine PET. Fluorescence measurements were used to demonstrate star PEG low-fouling properties as well as to compare BSA adsorption on PEG, CMD and CS surfaces. The fluorescence detection of adsorbed proteins was also used to

differentiate fouling and non-fouling patterns that were created using star PEG and LP coating on PET surfaces.

### **3.4.1 Protein adsorption studies on PEG, CMD and CS surfaces**

Each surface was covered with labeled BSA solution (0.2 mg/mL in PBS) for 2 h in static condition at room temperature (surfaces were protected from light exposure). The surfaces were washed thoroughly with PBS to remove unbound proteins, dried with a stream of nitrogen, and examined under a fluorescence microscope (Nikon Eclipse E600) at 10x magnification. The fluorescence intensity was assumed to be directly proportional to the amount of adsorbed albumin on the surface. The background auto-fluorescence was subtracted for each sample.

### **3.4.2 Micro -patterning**

In addition to developing low-fouling surfaces using star PEG coating, the ability of generating fouling and non-fouling micro-scale patterns was also investigated using LP and star PEG coating on PET surfaces. Micro-patterns were generated by placing electron microscopy grids (consisting of 184  $\mu\text{m}$  wide parallel bars separated by 92  $\mu\text{m}$ ; Electron Microscopy Sciences, Hatfield, PA, USA; see Figure 3.10) over PET substrates before LP deposition. Then PEG grafting was performed by covalent binding and unbound PEG was removed by rinsing with PBS in an ultrasonic bath as explained above. Samples were then immersed in Albumin Texas Red conjugate (0.2 mg/mL in PBS) for 2 h at room temperature and surfaces were washed thoroughly with PBS to remove unbound protein. Finally, substrates were examined by fluorescence microscopy to differentiate the fouling and non-fouling regions on PET surfaces.



Figure 3.10. Image of electron microscopy grids consisting of 184- $\mu\text{m}$  wide parallel bars separated by 92  $\mu\text{m}$ .

### 3.5 Platelet adhesion assays

Platelet adhesion and activation assays are typically used to evaluate the thrombogenicity of biomaterials. In this PhD, platelet adhesion assays were used first to estimate the anti-platelet property of star PEG and then to compare platelet adhesion on CS with PEG, CMD and bare PET surfaces. In both cases, platelet aggregation and morphology was also observed by scanning electron microscopy (SEM). Platelet adhesion in this study was evaluated by conducting perfusion tests using fresh human blood. This part of the study was approved by the human ethical committee of the Montreal Heart Institute. All subjects gave informed consent and were free from drugs interfering with platelet function for at least two weeks before blood sampling. Two different techniques were used to evaluate the amount of adhered platelets. First, radio-labeled platelets were used to demonstrate the anti-platelet properties of star PEG, following a protocol previously used and validated by Merhi (Merhi, King et Guidoin, 1997). However, when comparing PEG, CMD and CS surfaces a different protocol was used, which was developed by H. Fadlallah (Master student at ETS) at Merhi's lab using direct immunostaining of platelets by FITC. This was chosen due to the limitations of using radio-labeling at Merhi's lab, i.e. to reduce the cost and to allow double staining in the presence of endothelial cells. The perfusion system and platelet staining method are described in detail in the following paragraphs.

### 3.5.1 Perfusion system

All the perfusion assays were performed using plexiglas perfusion chambers that mimic the tube-like cylindrical shape of blood vessels (Diener et al., 2009; Merhi, King et Guidoin, 1997). The perfusion chambers were used to place the samples as shown in Figure 3.11 (a & b), which allows direct exposure of the samples to a blood flow. For each perfusion assay, two chambers were connected in parallel and one sample placed in each chamber. The connection between the chambers and the peristaltic pump (Masterflex L/S 7518-10, Cole-Parmer Inc.) has been made using non-toxic flexible surgical tubing (Tygon R-100, Fisher Scientific, Canada), and a thermostatically controlled water bath was used to maintain the perfusion system at 37° C, as shown in Figure 3.11 c. The perfusion time (15 min) and flow rate (40 mL/min) was fixed for blood flow.

The hemodynamic conditions inside the blood vessels lead to the development of shear stress, which is applied against the inner layer of vessel wall. Shear rate is the velocity gradient calculated across the diameter of a blood-flow channel, which is defined as the rate at which adjacent layers of fluid move with respect to each other. In physiological conditions, the shear stress at the arterial wall ranges between 10 and 70 dynes/cm<sup>2</sup> (Papaioannou et Stefanadis, 2005). The shear rate or shear stress of perfusion in this study corresponds to 840 s<sup>-1</sup> or 29 dyn/cm<sup>2</sup>. This is calculated using Poiseuille's law with the following approximation: the blood is an ideal Newtonian fluid, the blood flow is steady and laminar and the blood vessel is straight, cylindrical and inelastic (Papaioannou et Stefanadis, 2005).

$$\tau = 32 \cdot \mu \cdot Q / \pi \cdot d^3 \quad (2.3)$$

Where  $\tau$  = shear stress,  $\mu$  = viscosity of blood ( $3.5 \times 10^{-3}$  Pa s), Q = mean volumetric flow rate (40 mL/min), d = chamber internal diameter (2mm).

Therefore,  $\tau = 32 \times 3.5 \times 10^{-3} \times 0.66 / 0.025 = 29.4 \text{ dyne/cm}^2$  and Shear rate ( $\dot{\gamma}$ ) =  $\frac{\tau}{\mu} = 840 \text{ s}^{-1}$

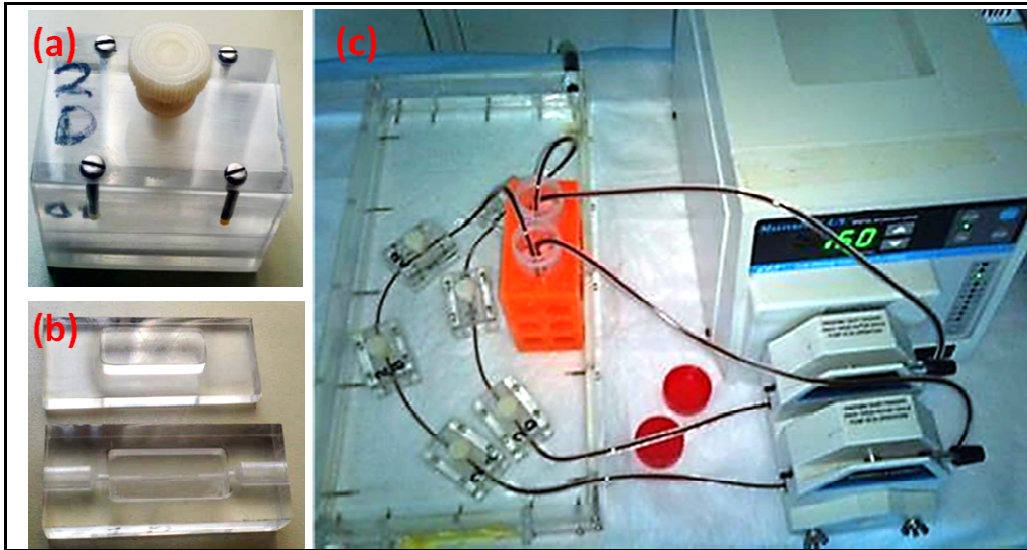


Figure 3.11. Schematic picture of (a) perfusion chamber (b) sample holder and (c) perfusion system setup along with thermostatically controlled water bath.

### 3.5.2 Platelet adhesion assay with radio-labeled platelets

#### 3.5.2.1 Platelet isolation and labeling

Platelet isolation and labeling as well as the perfusion experiments were conducted by following the previously developed method in Merhi's lab (Diener et al., 2009). A 60-mL sample of venous blood from each subject was anti-coagulated with 6 mL of D-Phenylalanyl-L-prolyl-L-arginine chloromethyl ketone (PPACK; Calbiochem, QC, Canada) in saline (50 nM final concentration) and a 30-mL sample with anticoagulant citrate dextrose (ACD, Baxter, Mississauga, Canada). PPACK was used in this study instead of heparin, because it is effective in preventing fibrin- and surface- bound thrombin (Bernd, Jens et Maria, 2006). The ACD blood was used to isolate and radio-label platelets. Briefly, platelet-rich plasma (PRP) was isolated by centrifugation for 15 min at 1800 rpm. PRP was then centrifuged for 10 min at 2200 rpm to separate platelets from platelet-poor plasma (PPP). The pellet of platelets was suspended with Hanks' Balanced Salt Solution (HBSS; Sigma-Aldrich Canada Ltd., Oakville, ON, Canada) containing 0.5  $\mu\text{g}/\mu\text{L}$  of prostaglandin E1 (PGE<sub>1</sub>; Sigma-Aldrich Canada Ltd., Oakville, ON, Canada) and centrifuged for 10 min at 2200 rpm. The

platelet pellet was re-suspended with 2 mL of HBSS containing PGE<sub>1</sub>, and incubated with 250 µCi of Indium<sup>111</sup> Oxine (GE Healthcare Canada inc. Burlington, Ontario) for 15 min at room temperature, followed by centrifugation for 8 min at 2100 rpm. The supernatant was removed and the radio-labeled platelet pellet re-suspended in 10 mL of PPP and finally mixed with the 60 mL of the PPACK blood. Platelet count of each sample was measured using the Coulter Act Diff cell counter (Beckman Coulter, Canada). For reference, 10 µL of blood containing labeled platelets was measured using a gamma counter (Minaxi 5000, Packard Instruments).

### 3.5.2.2 Platelet adhesion

Various samples (bare PET, LP-coated PET, and PEG-coated PET (prepared with 5% w/v PEG) were placed in the perfusion chambers that contained a window of 2 mm internal diameter x 10 mm long, permitting direct exposure of the samples to the blood. The samples within the perfusion chambers were directly exposed to the blood containing <sup>111</sup>In labeled platelets for 15 min at a flow rate of 40 mL/min and shear rate of 853 s<sup>-1</sup> (29 dyne/cm<sup>2</sup>), followed by rinsing with a buffered formalin solution for fixation. At the end of each experiment, the radioactivity on the exposed surfaces was measured using a gamma counter (Minaxi 5000, Packard Instruments). Platelet adhesion on each test surface was calculated from the known radioactivity of reference and platelet count in the blood in count per minute (cpm), using the following equation (Eq. 2.4). The experiment was repeated for each test surface using three different healthy blood donors. Results were also compared to intact (with endothelium) and injured (scrapped endothelium) arterial surfaces from pigs.

$$\text{Platelet adhesion} = \frac{\left\{ {}^{111}\text{In cpm in exposed segment} \right\} \times (\text{No. of platelets/mL blood}) / {}^{111}\text{In cpm/mL blood}}{\text{exposed surface (cm}^2\text{)}} \quad (2.4)$$

### 3.5.3 Platelet adhesion assay using fluorescence staining

This technique is not required for platelet isolation prior to perfusion assay. A 60 mL sample of venous blood from each subject was anticoagulated with 6 mL of D-Phenylalanyl-

L-prolyl-L-arginine chloromethyl ketone (PPACK) in saline (50 nM final concentration), as described above. The samples (bare PET, PET coated with LP +/- PEG, CMD and CS) were mounted in perfusion chambers and perfusion conducted for 15 min, as explained above. After perfusion, the surfaces were rinsed with saline for 10 s to remove weakly adhered platelets. Surfaces were then removed from the chambers and rinsed with PBS for three times. Platelets adhered to the surface were then stained with fluorescein isothiocyanate (FITC)-labeled anti-CD61 (DAKO, Burlington, Ontario, Canada), which is specific to CD61, a platelet membrane glycoprotein (Chou et al., 2003). The staining solution was prepared by dissolving FITC-labeled anti-CD61 (20  $\mu\text{g}/\text{mL}$ ) in 1% BSA. Each surface was covered with 100  $\mu\text{L}$  of this solution for 15 min, followed by three rinses with PBS to remove non-specific adsorption of the antibody. Finally, surfaces were fixed with 1% paraformaldehyde for 25 min and transferred to microscope slides with a mounting medium (DABCO, Fisher Scientific, Canada). Confocal microscopy images (Carl Zeiss LSM 510) were taken in the central zone of the exposed surface while areas out of the edges were excluded. The percentage of surface area covered by platelets was calculated using Image J software.

#### **3.5.4 Scanning electron microscopy**

After platelet adhesion assay, each surface was observed by scanning electron microscopy (SEM) to confirm platelet adhesion and morphology to assess aggregation and activation. The specimens were dehydrated through a series of graded ethanol solutions (30%, 50%, 70%, 95% and 2x 100% v/v) and subjected to CO<sub>2</sub> critical point drying (E3000, Polaron, Quorum Technologies). The dried specimens were sputter-coated with gold for 2 min (~15 nm layer) and then observed using a Hitachi S-3600N (Hitachi High-Technologies, Canada) operating at an acceleration voltage of 5 kV under high vacuum.

A brief description about platelets and their morphology is provided here for understanding SEM images in the following sections. Platelets are the smallest corpuscular components of human blood with a diameter of 2-4  $\mu\text{m}$ , which does not contain a nucleus (Harrison, 2005). The typical shape of adhered platelets is discoid (see Figure 3.12), but, upon activation, their shape changes to a spherical form with pseudopodia up to 5  $\mu\text{m}$  long.

The adhesive proteins such as collagen, fibronectin, laminin, vitronectin, fibrinogen and von Willebrand factor (vWF) are known to promote platelet adhesion (Harrison, 2005). Platelets activation leads to actin polymerization, cytoskeleton reorganization and finally secretion of storage granules (calcium, vWF, ADP, P-selectin). The secretion of storage granules amplifies activation and aggregation, exposure of phosphatidylserins that enhance pro-coagulant activity and contribute to thrombus stability (Harrison, 2005).



Figure 3.12. Typical smooth discoid shape of platelets (left) and spherical shape of activated platelets (right) (Harrison, 2005).

### 3.6 Cell culture experiments

Cell culture experiments were performed in various situations. Simple HUVEC adhesion and growth experiments were carried out to compare low-fouling properties of PEG, CMD and CS surfaces as well as to estimate HUVEC retention on various surfaces under blood flow. In order to confirm cell adhesion results obtained with QCM-D, VSMC adhesion assay was also performed in static condition to determine the KQAGDV or RGD bioactivity after grafting on a CMD surface.

#### 3.6.1 HUVEC adhesion and growth

Various surfaces (bare PET, PET coated with LP +/- CS, PEG and CMD; 1 cm<sup>2</sup> each) were placed at the bottom of 24-well plates. Cloning cylinders (internal diameter= 0.8 cm; Corning, Lowell, MA, USA) were used to limit the area and to retain the films at the bottom of the wells. HUVECs (Lonza, Shawinigan, Canada) were routinely cultured in Lonza EGM-

2 medium (containing growth factors and 2 % (v/v) FBS) and used between passages 2 and 6.

For cell adhesion and growth assays, cells were suspended in an EGM-2 culture medium at a density of  $0.75 \times 10^5$  cells/mL. A volume of 200  $\mu$ L (15,000 cells) was deposited on each surface and cells were left to adhere for 4 h. The cloning cylinders were then removed and surfaces were washed with PBS (1x) to remove non-adherent cells. Cells were stained with a 0.75% (w/v) crystal violet solution (Sigma- Aldrich, Oakville, Canada) for 15 min and rinsed three times with Milli-Q water before drying at RT. For growth assays, after removal of the cloning cylinders, cells were left to grow for 2 d in complete medium at 37 °C and 5% CO<sub>2</sub> before being stained as described above. Three images per sample were captured by optical microscopy to evaluate cell density. A minimum of four samples was tested per condition and the experiment was repeated three times.

**Focal adhesion assay:** Focal contact formation was evaluated by immunostaining for vinculin and actin fibers after 24 h adhesion of HUVEC (15,000 cells/well) on the various surfaces (PET, LP, LP + CS and LP + CMD) in presence as well as in absence of serum in order to determine the advantage of using CS coating. To that purpose, substrates were rinsed with PBS, fixed with 4% paraformaldehyde for 10 min, permeabilized with 0.4% Triton X-100 for 10 min and blocked 1 h with 2% BSA in PBS. Samples were then incubated overnight with a mouse anti-vinculin antibody (diluted 1:200 in PBS/2% BSA; MAB3574, Millipore, USA) at 4°C, followed by incubation with a secondary Goat Anti-Mouse IgG Alexa 546 (diluted 1:600 in PBS/2% BSA; Molecular probes, Invitrogen, Canada)) for 1 h at RT. To stain actin, samples were then incubated with Phalloidin-Alexa 488 (1:40 in PBS; Molecular probes, Invitrogen, Canada)) for 1 h, and finally counterstained for the nucleus with Hoechst 33258 (0.5 $\mu$ g/mL in PBS; Sigma-Aldrich Canada Ltd., Oakville, ON, Canada) which was added for the last 10 min of incubation. Samples were then mounted on glass slides using the DABCO mounting medium and images of stained samples were acquired using confocal microscopy (Olympus FV1000MPE).

### **3.6.2 VSMC adhesion assay on peptide grafted surfaces**

To confirm results obtained with QCM-D, VSMC adhesion assay was performed in static condition. Various surfaces (bare PET, PET+LP, LP +CMD, LP +CMD + Peptide; 1 cm<sup>2</sup> each) were placed at the bottom of 24 well plates and cloning cylinders were used to limit the area and to retain the films at the bottom of the wells. Cells were suspended in DMEM (without serum) at a density of  $0.75 \times 10^5$  cells/mL. A volume of 200  $\mu$ L (15,000 cells) was deposited on each surface and left to adhere for 4 h. The cloning cylinders were then removed and surfaces were washed with PBS (1x) to remove non-adherent cells. Cell staining procedure was followed as described above using a 0.75% (w/v) crystal violet solution. Three images per sample were captured by optical microscopy to observe cell adhesion and a minimum of four samples were tested per condition.

### **3.7 Statistical Analysis**

All the results are expressed as mean  $\pm$  standard deviation. Statistical analysis was carried out using one-way ANOVA analysis followed by Tukey's post-hoc analysis. The student's *t* test was used when comparing two groups and  $p < 0.05$  was considered to be statistically significant.



## CHAPTER 4

### RESULTS AND DISCUSSION

This section is divided into three different subsections, according to the three specific objectives. Results and discussion sections are presented separately for each specific objective.

#### **4.1 Develop a low-fouling and low-thrombogenic coating that can be applicable to a wide variety of biomaterial surfaces.**

##### **4.1.1 Rationale**

The first objective of this thesis was to develop a low-fouling and low-thrombogenic coating using PEG that can be applicable to a wide variety of biomaterial surfaces and allows subsequent coupling of bioactive molecules. Indeed the current PEG coating methods lack versatility. The stable plasma polymerized coatings (LP) with very high primary amine density have been created, which can be deposited on a large variety of biomaterials. LP coatings allow the stable chemical coupling of desired molecules and therefore are able to reach high surface coverage. On the other hand, multi-arm PEG coating is known to offer higher grafting densities and better low-fouling properties compared to linear PEG due to its molecular architecture, long chain length and presence of several terminal groups (Hoffmann et al., 2006).

We hypothesize that together LP and star PEG could be an interesting and novel method for stable star PEG grafting, which can be applied to a large variety of biomaterials (polymers, ceramics, metals and semiconductors used in biomedical applications); it can also enable one to create various deposit geometries such as micro-patterns. In this part of the thesis, the ability of LP coating combined with star PEG to create protein and platelet-repellent surfaces has been studied. To optimize this PEG grafting method, first covalent

coupling of star PEG on amino-coated glass substrates was assessed by static contact angle and XPS analysis (as a function of PEG coupling concentration), and then protein adsorption studies by QCM-D using LP coated substrates were carried out. Finally, the ability of PEG coatings to decrease protein adsorption and platelet adhesion on PET films was confirmed by fluorescence measurements and an *in vitro* perfusion platelet adhesion assay, respectively.

## 4.1.2 Results

### 4.1.2.1 Surface characterization

In order to confirm the presence of PEG, water contact angles were first measured on amino-coated glass before and after PEG coating (Figure 4.1). While amino-coated glass exhibited a relatively hydrophilic surface ( $54.9 \pm 1.1^\circ$ ), the contact angle significantly decreased after star PEG grafting as a function of its coupling concentration. As can be seen in Figure 4.1, no significant difference was observed between 5 and 15%; very similar results were obtained for PEG grafting on LP deposited PET films. LP coatings, on their side, exhibited a contact angle of about  $56.1 \pm 0.6^\circ$ .

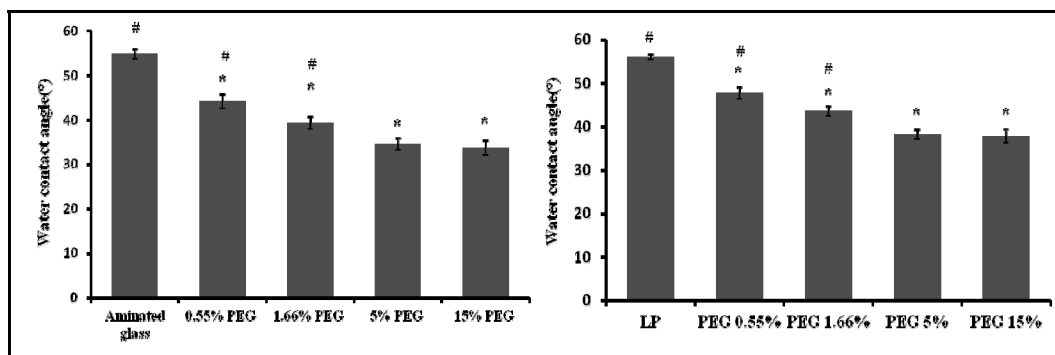


Figure 4.1. Static water contact angles on unmodified amino-coated glass (left) and LP (right), and after PEG coating at various coupling concentrations (0.55, 1.66, 5, and 15% w/v). Results are expressed as mean  $\pm$  SD, n=9-12. \*Significantly different from amino-coated glass and LP surfaces ( $P < 0.001$ ), # significantly different from 5% PEG ( $P < 0.001$ ).

XPS measurements further confirmed star PEG presence after the covalent coupling procedure on amino-coated glass surfaces. Survey scans were used to study changes in

elemental composition of modified and unmodified substrates. Table 4.1 shows the decrease of silicon (Si) and nitrogen (N) concentration, in parallel to the increase in carbon (C) on all PEG-modified surfaces, indicating the presence of PEG. However, in case of PEG 15%, we did not observe further increase in C or decrease in Si, which suggest that using PEG 15% may not help to further increase the grafting density. These results were further confirmed by high-resolution C1s and O1s scans. As shown in Figure 4.2, four different peaks were identified on the aminated glass control: the main two peaks (binding energies of 285 eV and 284 eV) corresponded to carbon-carbon (C-C) and carbon-silicon (C-Si) bonding, respectively. The low intensity peak around 286.3 eV was attributed to a mixture of C-N and C-O bonds, for which binding energies are too close to be discriminated. This peak most likely came from the amination process used by the manufacturer since commercial amino-coated glass substrates are generally produced by amino silylation using amino propyl triethoxy/methoxy silane. Therefore it is probable that this peak combines C-O (from triethoxy) and C-N (from C-NH<sub>2</sub> end groups) groups. The other small intensity peak at a higher energy level (288.4 eV) was attributed to the presence of carboxyl groups resulting from surface contamination (Sofia Susan et Merrill Edward, 1997). High-resolution scans of all star PEG grafted surfaces presented a large increase of the peak around 286.5 eV, in agreement with the presence of C-O bond in PEG. As can be seen in Figure 4.2, the relative intensity of this peak increased with star PEG coupling concentration, hence highly suggesting that the density and/or thickness of PEG coating increased with PEG concentration. XPS analysis was also performed on PEG-coated LP surfaces. However due to the complexity of LP composition, in particular the presence of C-N bond, whose binding energy is close to that of C-O groups in PEG (Wagner, 1979), we were unable to reach a conclusion about C-O increase on these substrates.

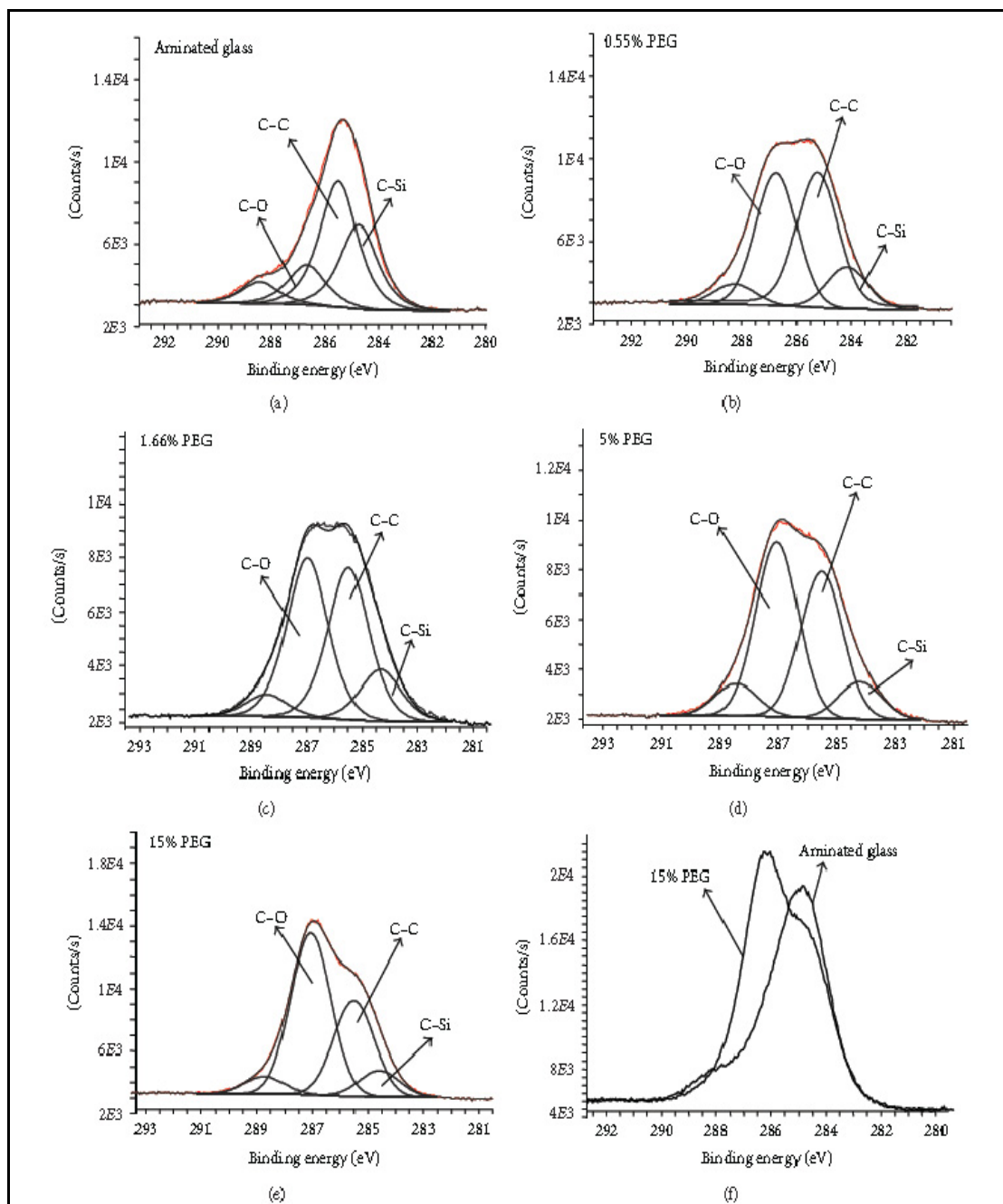


Figure 4.2. XPS high-resolution C1s scans of amino-coated glass (a) before and (b-e) after star PEG grafting at various coupling concentrations (0.55, 1.66, 5, and 15% w/v). Note that the relative intensity of the C-O peak increased with the PEG coupling concentration; (f) Overlay spectra of 15% PEG-modified on unmodified amino-coated surface.

Table 4.1. Surface elemental concentration (in At. %) of C, O, Si and N, as determined by XPS on amino-coated glass and PEG-modified surfaces using various star PEG coupling concentrations.

<b>Surface</b>	<b>O %</b>	<b>C %</b>	<b>Si %</b>	<b>N %</b>
Aminated glass	<b>40.9</b>	<b>36.6</b>	<b>17.0</b>	<b>4.8</b>
0.55% PEG	<b>38.3</b>	<b>44.5</b>	<b>12.7</b>	<b>3.7</b>
1.66% PEG	<b>37.4</b>	<b>46.8</b>	<b>11.8</b>	<b>3.3</b>
5% PEG	<b>36.1</b>	<b>50.3</b>	<b>10.1</b>	<b>3.1</b>
15% PEG	<b>37.4</b>	<b>48.1</b>	<b>11.1</b>	<b>2.8</b>

#### 4.1.2.2 Protein adsorption studies

The non-fouling properties of our LP-PEG-coatings were first investigated by monitoring fibrinogen adsorption using QCM-D. Figure 4.3 presents an example of change in resonance frequency ( $\Delta f$ ) and dissipation ( $\Delta D$ ) when LP and PEG (5%) coated quartz crystals were exposed to a solution of fibrinogen (0.5 mg/mL). On LP surfaces, introduction of the fibrinogen solution led to rapid decrease of the resonance frequency, indicative of fibrinogen adsorption, while the related increase in dissipation indicated that the adsorbed protein layer was viscous. A subsequent rinse with PBS (pH 7.4) induced only slight changes, indicating that only a small amount of bound fibrinogen was dissociated when rinsing with buffer and most of the protein was irreversibly adsorbed (Höök et al., 2002).  $\Delta f$  and  $\Delta D$  were much reduced on the PEG-modified surface.

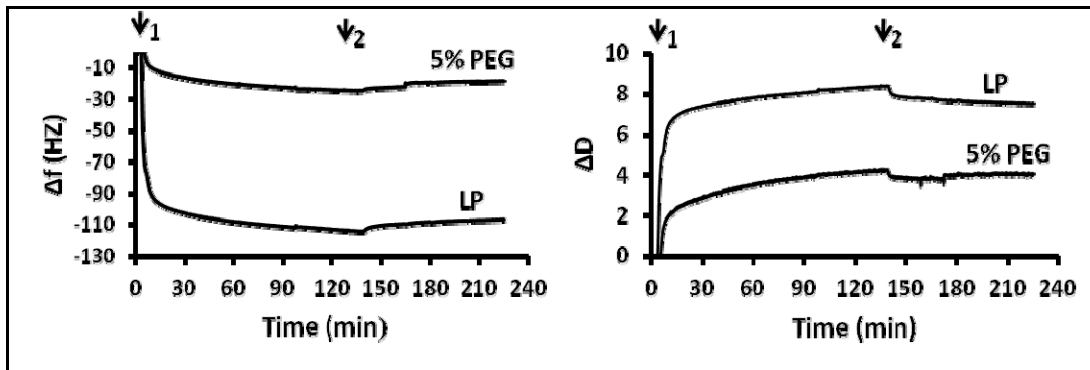


Figure 4.3. QCM-D real-time change in resonance frequency ( $\Delta f$ ) and dissipation ( $\Delta D$ ) related to modified (5% PEG) and unmodified LP surfaces upon exposure to fibrinogen solution (0.5 mg/mL; (1)) followed by rinsing with PBS (2).

Typical mass variation over time with the various PEG concentrations is presented in Figure 4.4, which is an example figure that presents data from one experiment, and the summarized data from several experiments were presented in Figure 4.5. As expected, fibrinogen adsorption decreased with rising PEG concentration, reaching a maximum reduction of  $79 \pm 11\%$  for 5% w/v PEG solution. Increasing PEG concentration from 5 to 15% did not result in a significant difference in subsequent fibrinogen adsorption ( $p=0.78$ ). Finally, after 4 weeks' immersion in PBS, the 5% PEG-coated surface still exhibited strong reduction of fibrinogen adsorption ( $89 \pm 7\%$ ) compared to LP (Figure 4.6.).

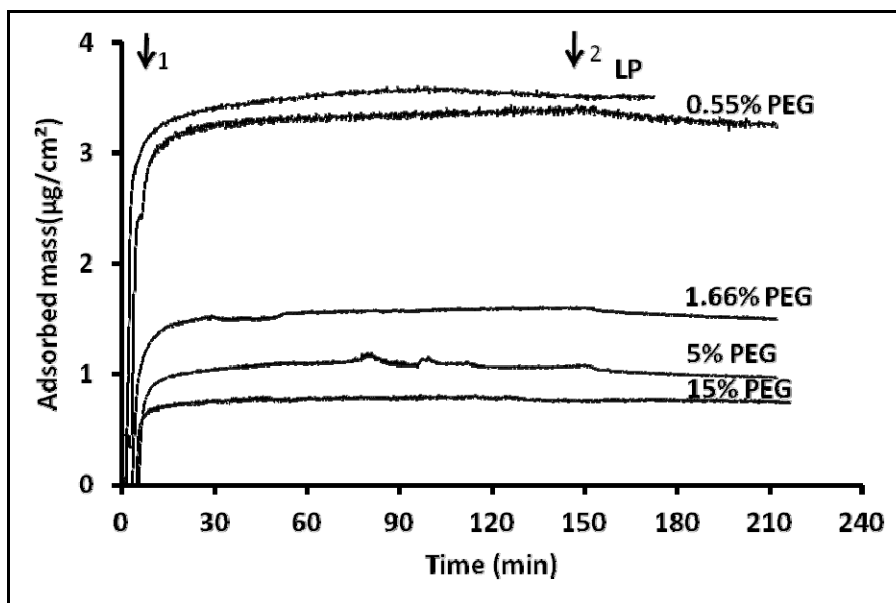


Figure 4.4. Time-resolved effect of various PEG coupling concentrations on fibrinogen (0.5 mg/mL) adsorption. QCM-D data were analyzed according to the Voigt model. Time of fibrinogen injection (1) and rinsing with PBS (2) are indicated. This is an example figure that shows data from one experiment.

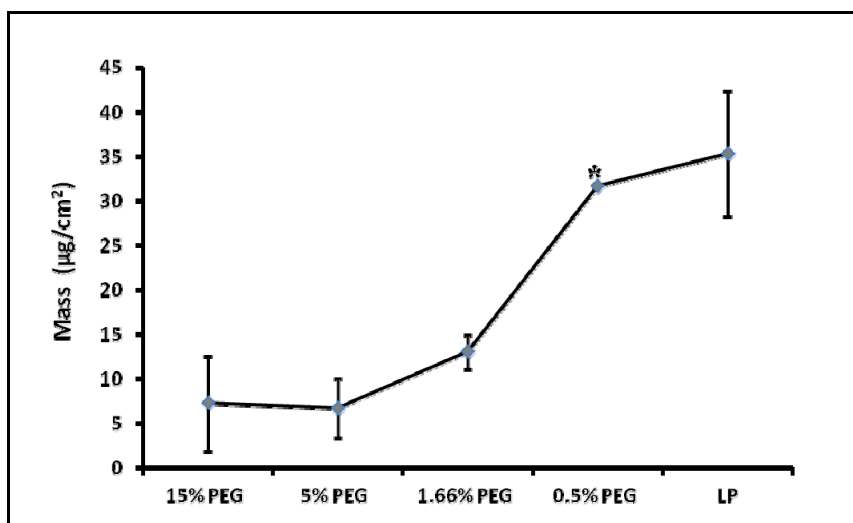


Figure 4.5. Calculated mass of adsorbed fibrinogen (0.5mg/mL) on LP and after PEG grafting at various coupling concentrations. QCM-D data were analyzed using the Voigt model. Results are expressed as mean  $\pm$  SD,  $n=4$  (\* result expressed as a mean;  $n=2$  only).

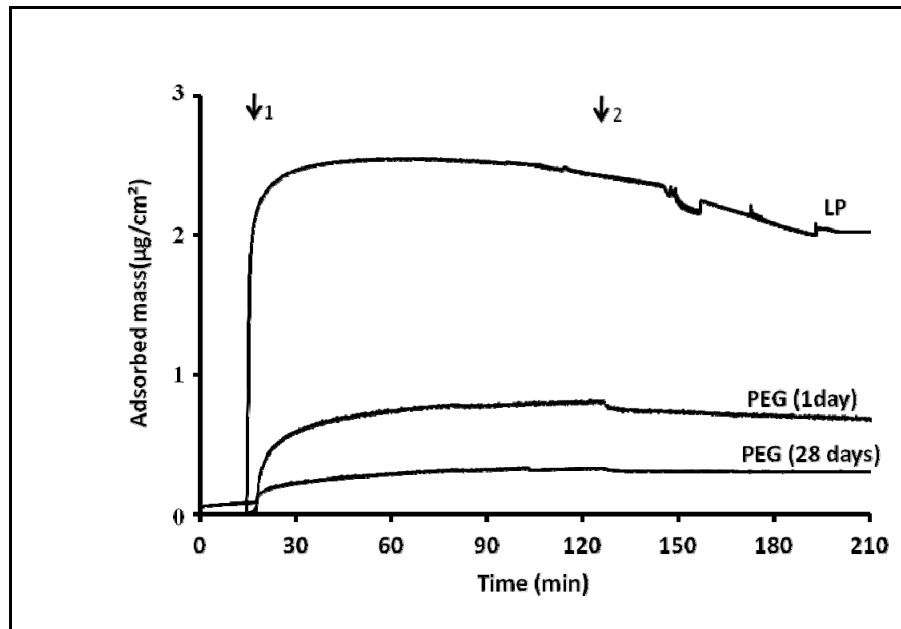


Figure 4.6. Example curves for fibrinogen (0.5 mg/mL) adsorption on LP and on PEG modified surfaces immersed in PBS over a period of 1 or 28 days. QCMD data were analyzed according to the Voigt model. Time of fibrinogen injection (1) and rinsing with PBS (2) are indicated.

In parallel, Texas-red conjugated albumin (66kDa, 0.2 mg/mL) adsorption in static condition was also investigated using fluorescence microscopy in order to allow comparison with PET surfaces (Figure 4.7). Since no significant difference had been observed by QCMD between 5 and 15% PEG conditions, only coatings obtained with in-solution concentrations of PEG up to 5% were compared to LP and to bare PET surfaces. While LP coating increased albumin adsorption compared to bare PET films, further PEG grafting strongly decreased protein adsorption. PEG coatings were even effective at low in-solution PEG concentrations and the amount of albumin adsorption decreased as PEG coupling concentrations were increased. Of interest, all PEG concentrations enabled decreasing albumin adsorption below PET control ( $P < 0.001$ ). On 5% PEG, fluorescence was decreased by 92% and 88% compared to LP and PET, respectively.

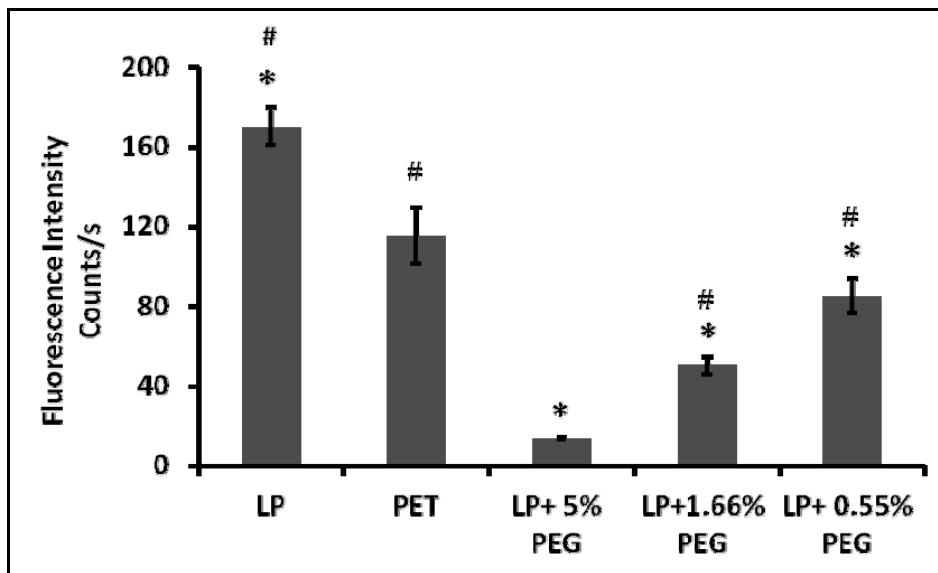


Figure 4.7. Fluorescence detection of adsorbed Texas red labeled albumin (0.2 mg/mL) on bare PET, LP alone and LP-PEG coated PET.

Results are expressed as mean  $\pm$  SD (n=12). Background was subtracted from each surface. \*Significantly different from PET ( $P < 0.001$ ), # significantly different from LP+ 5% PEG ( $P < 0.001$ ).

Texas red conjugated albumin was also used to demonstrate the applicability of our LP deposition method to the generation non-fouling micro-patterns (Figure 4.8). While only a slight difference was observed between PET and PET+LP coated regions (Figure 4.8 a), subsequent PEG grafting led to non-fouling areas clearly distinct from bare PET regions that manifested strong adsorption (Figure 4.8 b).

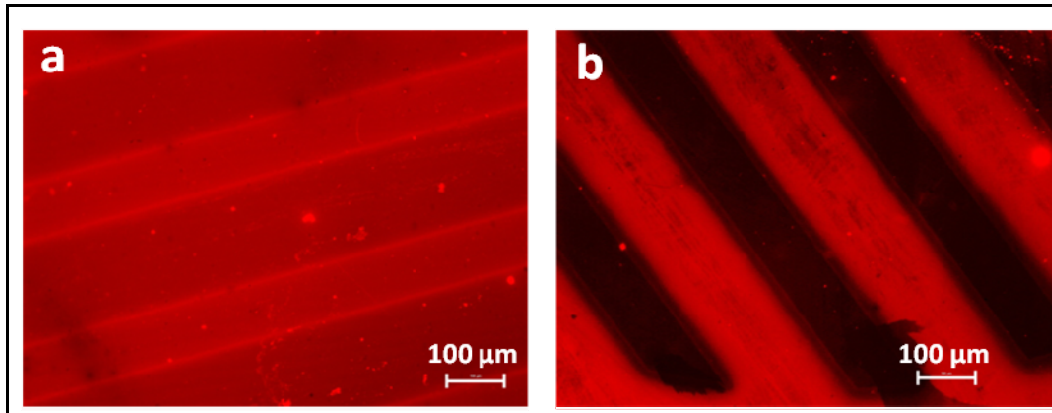


Figure 4.8. Fluorescence microscopy images of LP micro-patterns on PET surfaces after exposure to albumin Texas red conjugate. Parallel pattern surface (a) without PEG grafting and (b) modified with PEG.

#### 4.1.2.3 Platelet adhesion

The levels of platelet adhesion on the various surfaces after 15 minutes of perfusion with whole blood containing radiolabeled platelets (see section 3.5.2) are presented in Figure 4.9. As expected, LP coating on PET significantly increased platelet adhesion when compared to pristine PET ( $2060 \times 10^3$  versus  $244 \times 10^3$  platelets/cm<sup>2</sup>). These levels were, however, much lower than those corresponding to injured arterial tissues ( $15,195 \times 10^3$  platelets/cm<sup>2</sup>). Of interest, PEG grafting (5% PEG solution) on LP drastically decreased LP surface thrombogenicity, reaching levels about 10 times lower than those determined for bare PET control surfaces ( $25 \times 10^3$  versus  $244 \times 10^3$  platelets/cm<sup>2</sup>;  $p < 0.001$ ).

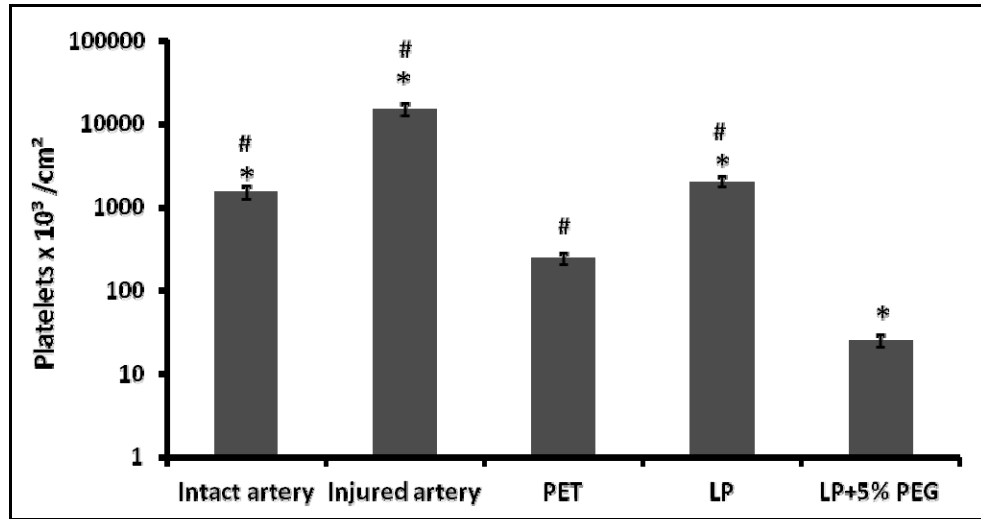


Figure 4.9. Platelet adhesion on an intact artery, injured artery, PET film, LP and 5% PEG- modified substrates. Results are expressed on a logarithmic scale, as mean  $\pm$  SD (n=12). \* significantly different from PET ( $P < 0.001$ ), # significantly different from LP + 5% PEG ( $P < 0.001$ ).

Direct observation of each individual surface using SEM (Figure 4.10) confirmed that platelet adhesion was almost abolished on PEG surfaces, since no platelets were observed on these surfaces. In contrast, a high level of platelet adhesion and aggregation was noticed after LP treatment and platelet morphology indicated that many of them were activated. Finally, although only a few platelets were identified on PET surfaces, their morphology corresponded to elongated pseudopodia and leading to platelet activation (Park, Mao et Park, 1990), which has been reported to contribute to the recruitment of other platelets and blood cells such as leukocytes during long-term contact with blood.

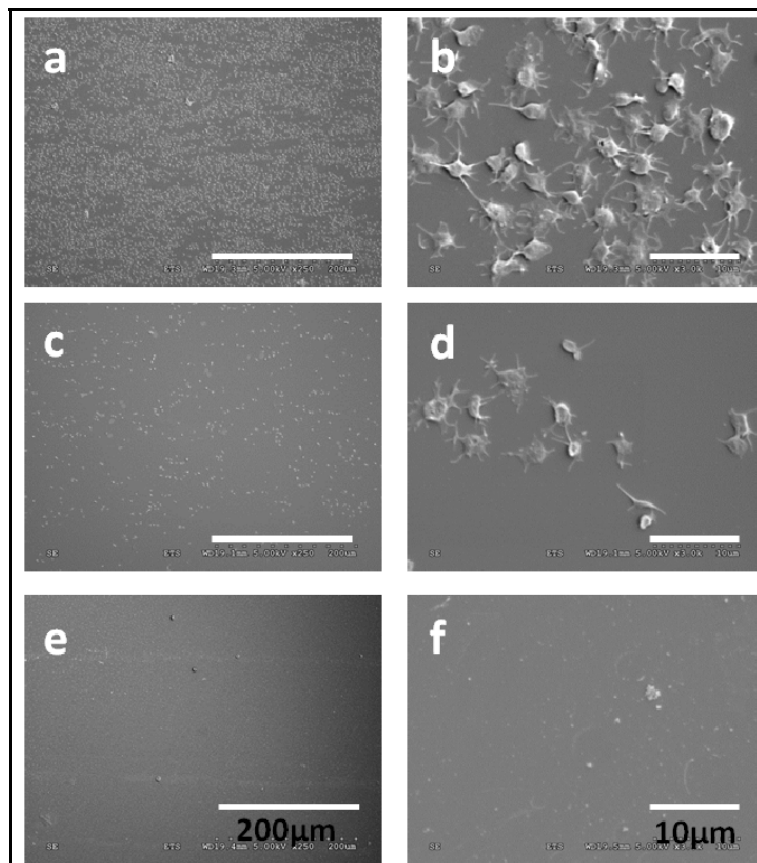


Figure 4.10. SEM visualization of platelet adhesion on LP (a, b), PET (c, d) and LP + 5% PEG (e, f) grafted surfaces.

### 4.1.3 Discussion

In this study, we have successfully grafted star PEG in a covalent fashion onto amino-coated surfaces, as indicated by contact angle measurements and by XPS. The presence of surface-adsorbed PEG cannot be completely excluded, although unlikely because rinsing in the ultrasonic bath most probably removed loosely bound PEG from the surface. Increasing PEG concentration during coupling greatly increased its density of the final coating, up to 15% PEG. While contact angle measurements showed no difference between 5 and 15% PEG, the relative intensity of the C-O peak was higher for 15% PEG. This suggests a higher density of the PEG coating that may in turn reduce protein adsorption, especially for small proteins such as albumin. However, owing to the high cost of star-shaped PEG and the modest improvement according to QCM-D assay when increasing concentration from 5 to

15%, we chose to evaluate the 5% PEG coating only, assuming that it would sufficiently reduce protein and platelet adhesion for the achievement of the other objectives of this thesis.

Fibrinogen and albumin were chosen for protein adsorption studies due to the fact that they are two major constituents of blood plasma. Fibrinogen (340 kDa), in particular, plays a key role in platelet adhesion and aggregation (Ratner Buddy, 2000). Albumin, a smaller protein (66 kDa), was also tested. 5% PEG coating strongly decreased protein adsorption compared to LP surfaces, fibrinogen adsorption was reduced by 79% and albumin by 92%, as deduced from QCM-D and fluorescence measurements, respectively. The slight discrepancy between QCM-D and fluorescent labeling results may be attributable to an overestimation of wet mass adsorption by QCM-D, in addition to inherent differences between dynamic (QCM-D) and static (fluorescence) assays for protein adsorption. Indeed, it has already been reported that QCM-D leads to 1.4 to 4-fold overestimation of adsorbed mass when compared to labeling or optical methods, depending on the type of protein (Weber, Wendel et Kohn, 2005b). However, protein adsorption could not be completely abrogated, even at high PEG coupling concentration. This result is most likely due to protein adsorption occurring at open spaces between the star PEG molecules (Sofia Susan et Merrill Edward, 1997), a process that can be favored by protein conformation changes initiated by steric constraints (Huang et al., 2011). Studies have also shown that protein adsorption decreases as PEG chain length and density increase (Gombotz et al., 1991; Groll et Moeller, 2010; Zhu et al., 2001). Hence, increasing PEG molecular weight and concentration may further decrease or completely inhibit protein adsorption with our amine-rich deposited polymer. Other teams showed that even more complete protein repellency can be achieved with PEG-containing copolymers (bulk modification) (Weber et al., 2007). However, these particular cases are very different from the method that we propose here, since the latter is much more versatile and can be translated to any type of surface without modifying the bulk properties of biomaterials.

Another interesting feature of the present method is its use to create fouling / non-fouling micro-patterns, as shown by experiments with electron microscopy grids (Figure 4.8).

Finally, the present PEG grafting method was demonstrated to exhibit excellent stability, as evidenced by strong reduction of fibrinogen adsorption over periods close to one month. Interestingly, results suggest that PEG is even more protein-resistant after 4 weeks of incubation in PBS than after 1 day in PBS. The reason for this observation is unclear and further investigation would be needed using complementary surface analysis techniques such as XPS and ellipsometry dry thickness measurements at different incubation times to better assess PEG stability on the surfaces.

The low level of fibrinogen adsorption on PEG surfaces can be directly related to their ability to prevent platelet adhesion (Zhang, Desai et Ferrari, 1998). This was confirmed with our perfusion model using fresh human blood, which mimics physiological conditions. This perfusion model is believed to better estimate the non-thrombogenic potential of PEG-grafted surfaces compared to platelet adhesion tests performed under static condition because it better mimics the hemodynamic conditions inside the blood vessels (Dimitrievska et al., 2011) as the contact of platelets with a given surface is a dynamic process that involves adhesion, activation, secretion and spreading. The relatively high level of platelet adhesion after LP treatment and its morphology by SEM indicate that LP attracts blood elements such as proteins and platelets. PEG grafted surface led to negligible number of platelet adhesion, as determined in our platelet adhesion assay and further confirmed by SEM observations.

The star PEG grafting method developed here is versatile and was shown to possess good stability in PBS, but how long PEG coated implants would consistently exhibit protein resistance and prevent thrombosis *in vivo* needs further investigation since PEG long-term stability and efficiency to prevent thrombus formation *in vivo* has shown to be limited (Akbar et al., 2011; Hubbell, 1993). As will be discussed later, the sole use of low-fouling coatings to prevent thrombus formation has been shown to exhibit disappointing results, due to the lack of active process to inhibit coagulation. Other methods proposed in the literature will be described in the section 1.3.2, but the sole completely long-term anti-thrombogenic surface that is known so far is a stable confluent endothelium lining. This could be achieved by immobilizing peptide and/or growth factor on star PEG or other low-fouling polymers to

promote confluent cell adhesion and growth. Indeed PEG derivatives have been shown to be interesting potential molecular linker/spacers for such bioactive molecules. Moreover, due to the steric constraints, either one or two terminal groups of star PEG are grafted to the surface, while the remaining groups do not participate in amide coupling and emanate outside of the surface. Hence, these terminal groups will be available for subsequent coupling of biomolecules. More importantly, star PEG increases the bioactivity of immobilized biomolecules and helps to achieve optimal interactions with the cells.

## **4.2 Develop a bioactive coating with the combination of peptide and GF on low-fouling background.**

### **4.2.1 Rationale**

We just showed that low-fouling PEG surfaces that strongly decrease protein adsorption and platelet adhesion can be created on any kind of biomaterial surface using nitrogen-rich plasma polymers (LP). Such low-fouling surfaces are believed to have several advantages in developing bioactive coatings.

- They prevent non-specific protein adsorption and platelet adhesion, but their terminal groups allow the immobilization of bioactive molecules to generate specific interactions with cells.
- They could enhance the bioactivity of immobilized biomolecules by offering conformational flexibility and motility.

The second aim of this thesis was to generate bioactive surfaces on low-fouling backgrounds and demonstrate their advantages for promoting optimal cell interactions. For several reasons, the bioactive coatings developed during this part of the thesis were created not to generate an EC layer on VG but for another clinical application, i.e. to improve VSMC adhesion and growth around stent-grafts (see section 1.1.3 in the literature review). Thus the peptides and EGF were chosen for their adhesive properties and proliferative and anti-apoptotic properties on VSMC, respectively. Based on the literature review, adhesive peptides such as RGD or KQAGDV could help to improve VSMC adhesion (Bellis, 2011; Dong et al., 2012a; Mann et al., 2001; Sabra et Vermette, 2011), while EGF immobilization

on biomaterials was shown to enhance VSMC survival and proliferation (Charbonneau et al., 2011; Lequoy et al., 2014). However, it was observed that EGF immobilization alone is not sufficient to achieve confluent cell growth on low-fouling backgrounds (Klenkler et al., 2008; Lequoy et al., 2014). Therefore we hypothesize that combined immobilization of integrin-binding peptide and growth factor (EGF) could lead to positive synergistic effects and help to achieve optimal cell interactions on low-fouling background.

In this project we combined the immobilization of KQAGDV/RGD peptide and EGF on PEG or CMD surfaces. To that end we take advantage of coiled-coil immobilization (Boucher et al., 2008b), which enables oriented immobilization of EGF. Since we aimed to develop a versatile method which could be applied on any biomaterial surface, LP films were first deposited and then used to graft a low-fouling polymer followed by peptide and EGF tethering. A secondary objective of this part of the PhD thesis was to demonstrate the ability of QCM-D to follow and optimize the sequential grafting of peptides and EGF on the surface. First, two different linkers (EMCH and PDPH) and two low-fouling substrates (PEG and CMD) were tested to choose the most appropriate ones. Then the peptide coupling solution concentration was varied while keeping that of EGF constant. The frequency and dissipation shifts were recorded for each immobilization step. The adsorbed mass was calculated using the Sauerbrey equation, since the dissipation values were too low to be considered for the Voigt model. Finally, the impact of the adhesive peptides on cells was evaluated by performing cell culture experiments in flow as well as in static conditions.

## 4.2.2 Results

### 4.2.2.1 Choosing a linker

EMCH and PDPH linkers were pre-coated on CMD surfaces and their efficiency for immobilization was verified by comparing K coil followed by E coil EGF immobilization *in situ* using QCM-D. Frequency shifts were observed as shown in Figure 4.11. A K coil solution injection on an EMCH-modified surface yielded a significantly higher frequency shift compared to that of a PDPH-modified surface. Subsequent E coil injection on these

surfaces further confirmed that EMCH allows more EGF recruitment than a PDPH surface. It is important to note that E coil EGF immobilization occurred only through coiled-coil interaction, since the unreacted EMCH sites were blocked with cysteine after K coil immobilization. These observations suggest that an EMCH linker is a better choice for further steps.

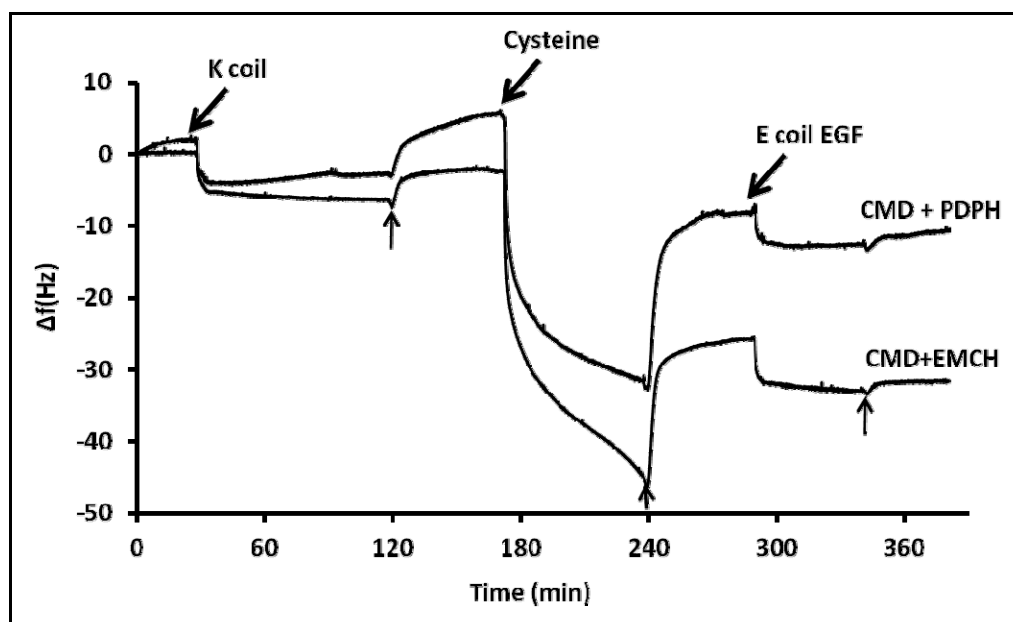


Figure 4.11. QCM-D frequency shift due to K coil, cysteine and E coil EGF serial injections on EMCH and PDPH modified CMD surfaces. Arrows refer to the PBS rinsing.

#### 4.2.2.2 PEG vs. CMD

PEG and CMD are both known to reduce non-specific protein adsorption and both contained carboxyl groups that allow subsequent protein/peptide grafting. However, the concentration of these carboxylic groups may vary between PEG and CMD. It was thus important to assess possible differences in K coil/EGF immobilization between two surfaces. Since an EMCH linker allowed better K coil/EGF grafting, it was used to compare PEG and CMD surfaces. A significant frequency shift was observed on both PEG and CMD surfaces after K coil immobilization, but the frequency shift was slightly higher on the CMD surface,

as shown in Figure 4.12. This difference was very significant after E coil EGF injection, which indicates that CMD allows higher levels of immobilization than PEG. Cysteine only grafted PEG and CMD surfaces neither allow immobilization of K coil nor subsequent E coil EGF recruitment (top two curves in Figure 4.12), which indicates that the reactive sites had reacted with cysteine and non-specific adsorption of K coil and E coil EGF is completely prevented on these surfaces. These observations also indicate that K coil is grafted only through the EMCH linker and accessible for coiled-coil immobilization of E coil EGF. CMD was chosen for future steps, since it allowed better immobilization.

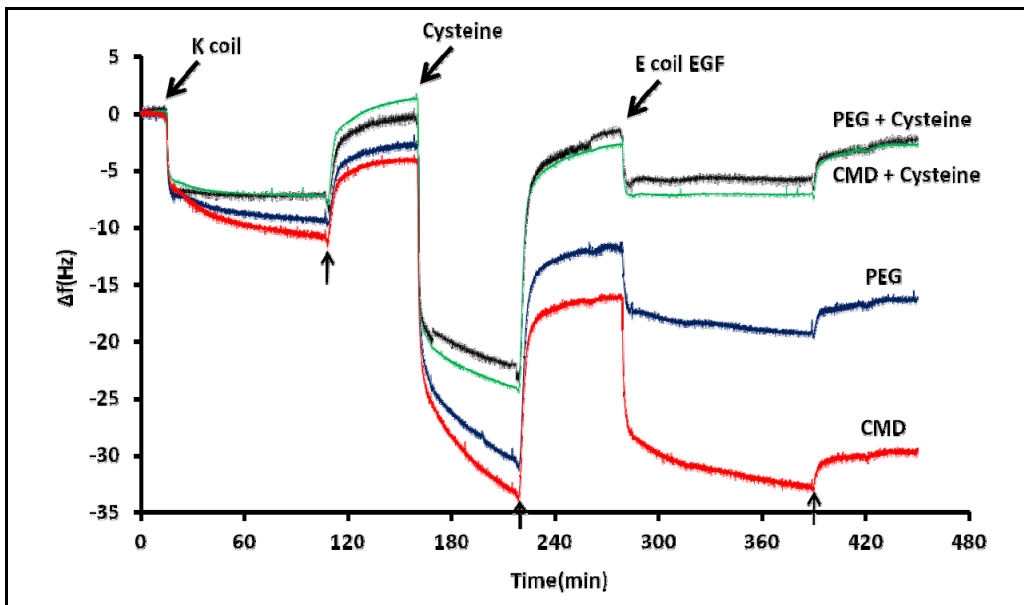


Figure 4.12. QCM-D frequency shift due to K coil, cysteine and E coil EGF serial injections on EMCH activated PEG and CMD surfaces. PEG + Cysteine and CMD + cysteine control surfaces corresponds to surface where K coil had not been immobilized. Arrows refer to the PBS rinsing.

#### 4.2.2.3 Combined immobilization of KQAGDV peptide and growth factor

Figure 4.13 presents one typical QCM-D result corresponding to the injections of various concentrations of peptide (0.15, 0.46 and 38  $\mu\text{M}$ ) on an EMCH + CMD surface, followed by K coil and E coil EGF injections. As expected, the frequency shifts increased with peptide concentrations and the highest frequency shift was observed for 38  $\mu\text{M}$ . K coil,

cysteine (to block available sites), and E coil-EGF injections led to a further decrease in frequency.

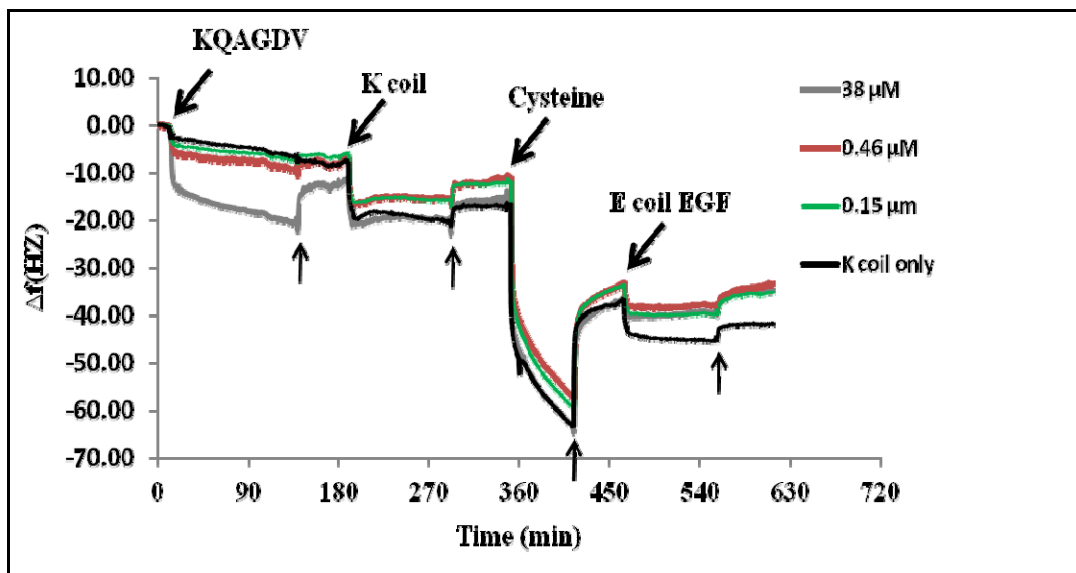


Figure 4.13. QCM-D frequency changes due to immobilization of various concentrations of KQAGDV and serial immobilization of K coil, Cysteine and E coil EGF on CMD surfaces. Arrows refer to PBS rinsing.

Experiments were repeated at least three times for each condition. Figure 4.14 summarizes the mean mass changes due to peptide, K coil and EGF immobilization. An increase in peptide grafted mass was observed from 0.15  $\mu\text{M}$  to 38  $\mu\text{M}$  input concentrations. Subsequent K coil grafting mass was influenced by the initial peptide grafted mass, with a clear increase in K coil and E coil grafted mass as the initial peptide grafting mass decreases. However, this trend was not observed for data corresponding to 0.46 and 0.15  $\mu\text{M}$  peptide concentration. This can be at least partly explained by the limitation of using QCM-D, which allows comparison of only four surfaces at a time. The resulting variability of results from one experiment to another may explain why there is no clear trend at such low peptide concentration. Overall, these results indicate that E coil EGF mass can be increased by decreasing peptide concentration and vice versa. This is due to the fact that both molecules use the same functional groups for immobilization, so that surfaces with low peptide concentration have more available sites for K coil immobilization. More generally, results

show that it is possible to capture both the peptide and growth factor at different ratios using CMD surfaces.

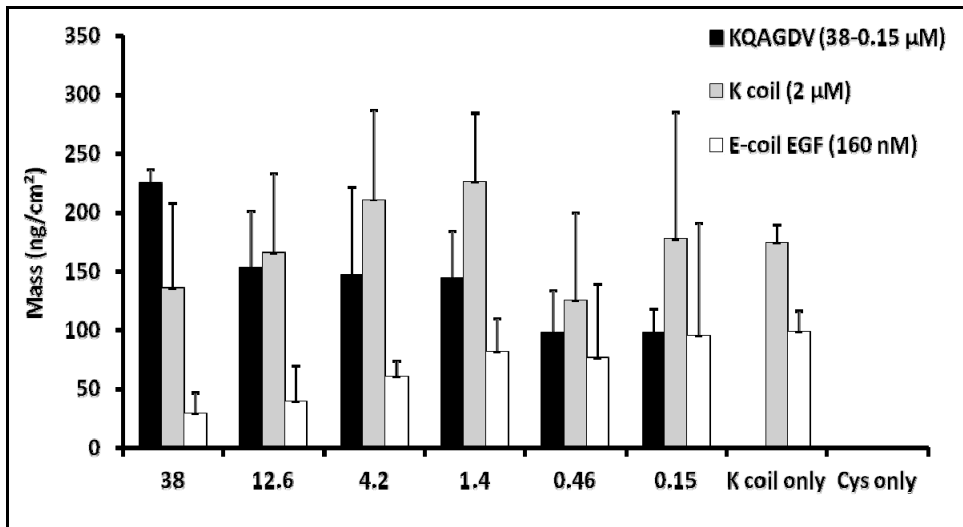


Figure 4.14. Mass increase corresponding to KQAGDV, K coil grafting and E coil EGF recruitment on CMD surfaces (previously modified with EMCH linker), as a function of KQADGV concentration that had been initially injected (n=3-6). Cys only surface corresponds to negative control surface, on which reactive sites are blocked with cysteine.

#### 4.2.2.4 Following VSMC adhesion using QCM-D

The effect of bioactive coating on cells was studied by QCM-D and cell adhesion tests. First, a preliminary experiment was performed to verify the feasibility of using the QCM-D technique for the detection of cell adhesion. VSMC adhesion (in a serum-free medium) was studied on LP, PEG and CMD surfaces in flow condition by following frequency and dissipation changes. PEG and CMD surfaces were known to be low-fouling, whereas the LP surface was known to exhibit fouling properties. As shown in Figure 4.15, there was a strong decrease in resonance frequency on the LP-coated gold electrode. This is believed to be essentially due to the VSMC adhesion, since the cells are suspended in DMEM (a serum-free medium) and a baseline was created using the same medium prior to VSMC injection. In strong contrast, neither frequency nor dissipation changes were

significant for PEG and CMD surfaces, which is indicative of prevention of VSMC adhesion on these surfaces. Interestingly, frequency change on LP was accompanied with a strong increase in dissipation. Rinsing with DMEM was started after 1 h to remove non-adherent cells and this was continued for 3 h to observe the behavior of frequency and dissipation shifts. After 1.5 h, a sudden increase in dissipation shift (from 3 to 6) was observed and reached a stable line after 2 h. This observation is similar to the results obtained in another study when measuring fibroblast cell adhesion on a collagen-modified surface using QCM-D (Tymchenko et al., 2012). According to Tymchenko et al studies, the increase in dissipation shift could be due to cell spreading on the surface.

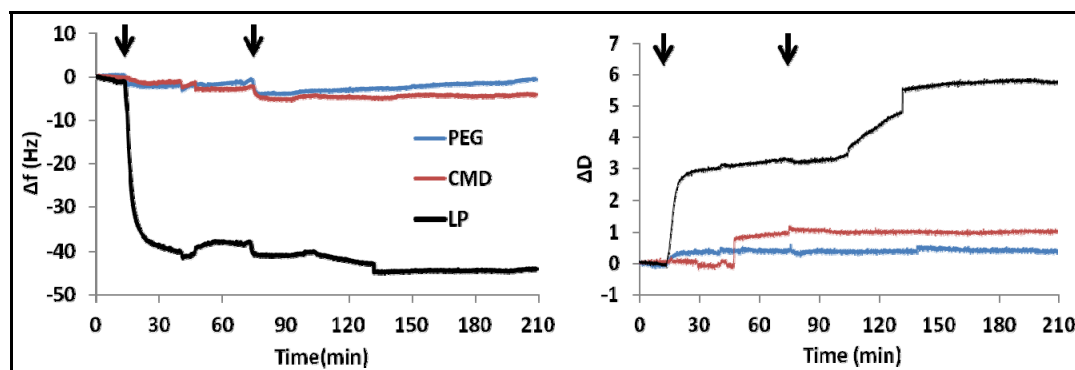


Figure 4.15. The frequency (left panel) and dissipation (right panel) changes due to VSMC adhesion on LP, PEG and CMD. Arrows refer to the injection of VSMCs (left) and DMEM rinsing (right).

In the next experiment, the ability of a peptide grafted surface to promote cell adhesion was evaluated using QCM-D by comparing bare CMD surfaces, CMD grafted with peptides (38  $\mu$ M) and an LP surface as positive control. Once again VSMC adhesion was investigated in a serum-free medium (DMEM) to minimize the influence of non-specific protein adsorption during the experiment. Before injecting cell suspension, peptide immobilization on the EMCH + CMD surface was confirmed by following the frequency changes, which were similar to those presented in Figure 4.13 (for 38  $\mu$ M).

In the following step, VSMC adhesion on these surfaces was compared with that on the LP surface, as shown in Figure 4.16. QCM-D behavior demonstrated similar trends to

those in Figure 4.15 despite some discrepancies. Thus a significant frequency shift was found for the LP surface after VSMC injection, with an almost stable baseline reached after 1 h adhesion. The decrease in frequency shift was observed on this surface after rinsing with DMEM, which is probably indicative of detachment of weakly adhered cells. Also as expected, (Figure 4.16), the frequency shift was much lower on the CMD surface than on LP. Yet, surprisingly, no improvement in VSMC adhesion was observed on the peptide grafted CMD surface, the frequency shift (and dissipation) being nearly similar to that of the bare CMD surface. The same trends were observed when using an RGD grafted CMD surface (Figure 4.17). Overall, these results indicate that peptide grafting on a CMD surface did not improve VSMC adhesion, as confirmed later in a conventional cell culture assay (see section 4.2.2.5).

The unconventional shape of the dissipation shift curve after VSMC injection on LP surfaces (Figure 4.16, right panel) is also worth mentioning. The rapid increase in dissipation is an indication of immediate cell adhesion on the LP surface, but it then decreased and was further decreased after rinsing with DMEM. No stable baseline could be observed even after 3 h. It is difficult to interpret the shape of these curves. According to published scientific reports (Tymchenko et al., 2012) and dissipation curves in Figure 4.15, the dissipation slightly decreases when cells start spreading on a surface. However, in this case it is not clear whether cells are spreading on the LP surface or detaching from it. Another possible explanation is that these changes are due to degradation or detachment of the LP underlying coating. We have observed in the lab that, while this coating is generally stable, some degradation may appear and change the composition and therefore the stability of this coating.

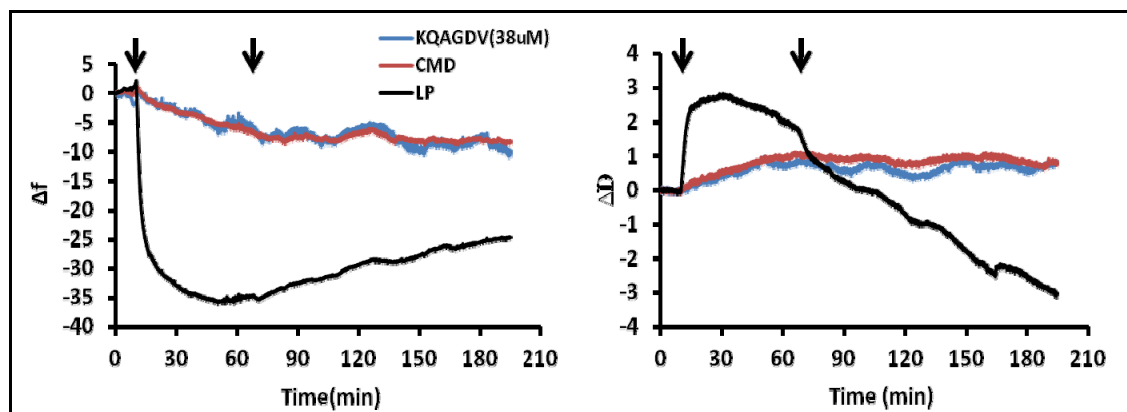


Figure 4.16. The frequency (left) and dissipation (right) changes due to VSMC adhesion on LP, CMD and CMD + KQAGDV surfaces.

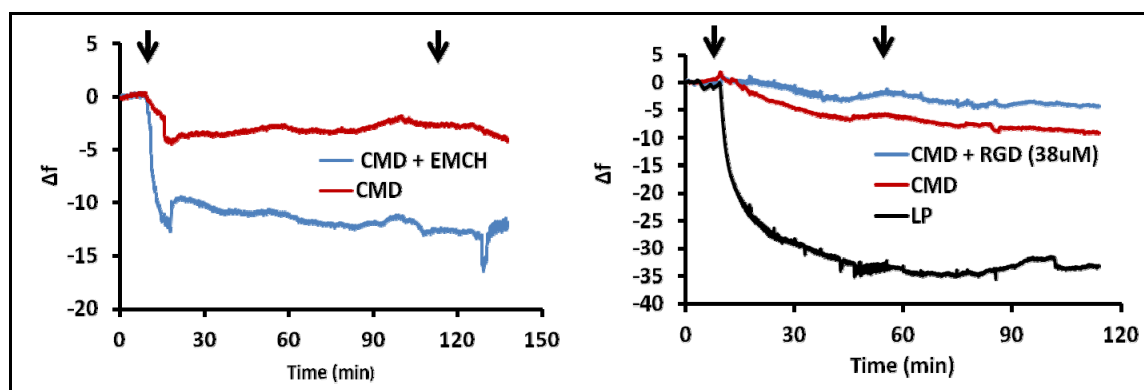


Figure 4.17. The frequency changes due to RGD (38  $\mu$ M) grafting (first arrow) on CMD + EMCH and CMD surfaces (left). VSMC adhesion on LP, CMD and CMD + RGD surfaces (right).

#### 4.2.2.5 VSMC adhesion in static condition

VSMC adhesion in static condition was performed to verify peptide influence on cell adhesion under various conditions. First, a VSMC adhesion assay was performed in the presence of serum using amino-coated 96 well plates. This experiment did not allow us to differentiate the cell adhesion between peptide-modified (various concentrations) and unmodified PEG/CMD or amino-coated surfaces, which might be due to the influence of serum. It was therefore decided to use a serum-free medium to evaluate peptide influence on promoting VSMC adhesion in the following experiment. In a serum-free medium, both PEG

and CMD were able to prevent VSMC adhesion. However, peptide immobilization (on PEG or CMD) did not show any improvement in VSMC adhesion. Finally, in order to confirm the results obtained with QCM-D, complementary VSMC adhesion assays were performed in static condition using LP-deposited PET films as a substrate for low-fouling and peptide grafting. The results were similar to those observed using QCM-D (Figure 4.18). Either KQAGDV or RGD grafting on CMD surfaces did not improve VSMC adhesion. The summarized results are presented in the Table 4.2.

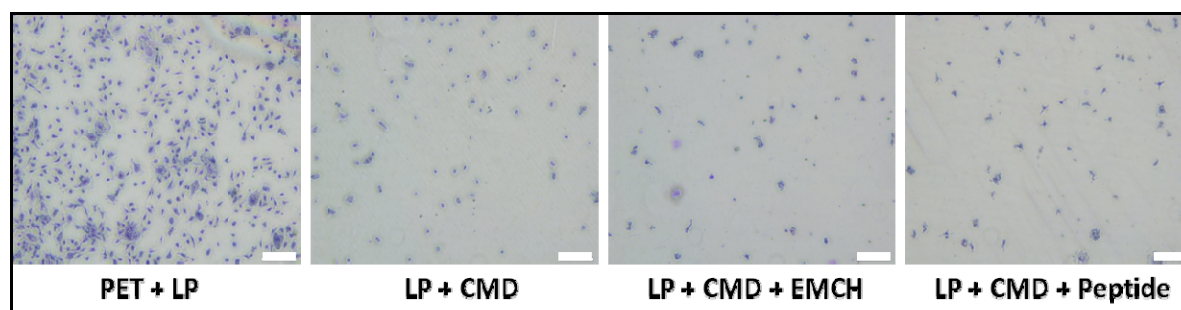


Figure 4.18. VSMC density observed (after 4 h adhesion in serum-free medium) by crystal violet staining on KQAGDV peptide modified and unmodified LP, CMD and EMCH surfaces. Scale bar corresponds to 200  $\mu\text{m}$ .

Table 4.2. Summarized observations of various experiments (at least 4 samples tested for each condition) performed to investigate the influence of immobilized peptides on VSMC adhesion.

Experiments	Observations
<p>1) VSMC adhesion (20,000 cells/well) assay on various surfaces in complete medium using amino coated 96 well plates.</p> <ul style="list-style-type: none"> <li>• KQAGDV modified (0.15-12 <math>\mu</math>M) and unmodified PEG, CMD (70 kDa) and CMD (500 kDa) surfaces</li> <li>• EMCH linker, cysteine grafted surfaces and bare amino-coated wells</li> </ul> <p>2) Experiment was repeated using different cell seeding densities (5,000 - 15,000 cells/well) on peptide modified and unmodified PEG and CMD (70 KDa) surfaces.</p>	<ul style="list-style-type: none"> <li>• No difference in VSMC adhesion was observed on KQAGDV modified (0.46-12.6<math>\mu</math>M) and unmodified surfaces, including EMCH linker and control (cysteine grafted) surfaces .</li> <li>• PEG and CMD (70kDa) surfaces were not effective in preventing VSMC adhesion in complete medium</li> <li>• However, VSMC adhesion was completely prevented by CMD (500 KDa). Surprisingly, peptide immobilization on this did not show any improvement in cell adhesion.</li> <li>• Same trends were observed when using different cell seeding densities.</li> </ul>
<p>1) VSMC adhesion assay (15,000 cells/well) on various surfaces in serum free medium and 0.5% FBS, using amino-coated 96 well plates. Experiment repeated 2 times.</p> <ul style="list-style-type: none"> <li>• KQAGDV modified (1.4 and 12 <math>\mu</math>M) and unmodified PEG and CMD (70 kDa) surfaces.</li> </ul> <p>EMCH linker, cysteine grafted surfaces and bare amino-coated wells</p>	<ul style="list-style-type: none"> <li>• VSMC adhesion was not improved on peptide modified surfaces.</li> <li>• PEG and CMD (70kDa) surfaces were able to prevent VSMC adhesion. Very few cells were adhered on these surfaces.</li> <li>• Significantly higher cell adhesion was observed on PCP as well as amino-coated positive control surfaces</li> </ul>
<p>1) VSMC adhesion (15,000 cells/well) assay in serum free medium on various surfaces using LP deposited PET films.</p> <ul style="list-style-type: none"> <li>• LP + CMD + EMCH + KQAGDV (38 <math>\mu</math>M)</li> <li>• LP + CMD+ EMCH , LP + CMD + EMCH + Cysteine, CMD, LP , PET and PCP.</li> </ul> <p>2) VSMC adhesion assay was repeated using RGD peptide</p> <ul style="list-style-type: none"> <li>• LP + CMD + EMCH + RGD (38 <math>\mu</math>M) and LP + CMD + EMCH + KQAGDV (38 <math>\mu</math>M)</li> <li>• LP + CMD+ EMCH, LP + CMD + EMCH + Cysteine, CMD, LP, PET and PCP.</li> </ul>	<ul style="list-style-type: none"> <li>• VSMC adhesion did not improved either on KQAGDV or RGD peptide immobilized CMD surfaces</li> <li>• Significantly higher cell adhesion was observed on LP and PCP surfaces, whereas CMD surface prevented VSMC adhesion.</li> </ul>

### 4.2.3 Discussion

In this study, we hypothesized that the combination of peptides and growth factor could help overcome the lack of cell adhesion on low-fouling backgrounds and thus take advantage of these low-fouling backgrounds to obtain better bioactivity of the growth factor or observed synergistic effect of peptide and GF. Frequency changes, measured by the QCM-D technique, were used to optimize the combined immobilization method. Although the calculated mass value using this technique is a wet mass and cannot be used to calculate the amount of peptide or GF used, it gives an idea of the total amount of mass on the surface and allows comparison between different surfaces. We confirm here that the QCM-D technique enables detection of mass changes despite the fact that peptide mass is only a few hundred Daltons and detection can occur even at very low peptide concentrations. It is worth noting that the limit of detection for a QCM-D sensor is about  $0.9 \text{ ng/cm}^2$  for a frequency resolution of 0.1 Hz, for a response time of 1 s (Biolin, 2014; Ogi et al., 2009).

This study was performed on CMD because it offers several advantages: 1) we have observed that CMD coatings present low-fouling properties that are as good as or even better than PEG (see objective 3), 2) it is less expensive than PEG and 3) most importantly it allowed a higher grafting mass of peptide and growth factor compared to that observed on star PEG during preliminary experiments. Since a CMD surface prevented non-specific adsorption of E coil EGF (Lequoy et al., 2014), and since the unreacted sites of EMCH on the CMD surface were already blocked with cysteine, the mass accumulation (after E coil EGF injection) is solely due to coiled-coil interactions between K coil and E coil EGF. It was previously demonstrated that such a coiled-coil system offers stable, bioactive and oriented immobilization of EGF (Boucher et al., 2008a). Although QCM-D data did not allow quantitative analysis, the mass changes due to sequential immobilization of peptide, K coil and E coil EGF confirms the presence of both the peptide and E coil EGF on the CMD surface. However, peptide immobilization on CMD, even at the highest coupling concentration tested here ( $38 \mu\text{M}$ ), did not improve VSMC adhesion. Cell adhesion assay results, performed under flow (QCM-D) and static (conventional cell culture) conditions, showed no improvement in VSMC adhesion. Yet, in general, several studies reported

improved cell attachment on peptide-functionalized surfaces (Groll et al., 2005b; Hubbell, Massia et Drumheller, 1992; Ito, Kajihara et Imanishi, 1991; Kämmerer et al., 2011; Li et al., 2008; Massia et Stark, 2001; Tugulu et al., 2007).

In the present study, the lack of improvement in cell adhesion on peptide-modified surfaces could be explained by several reasons that can be divided mainly into three categories: (i) the impact of peptide immobilization method and experimental conditions (ii) the impact of peptide surface concentration and (iii) the influence of peptide conformation and accessibility to the receptor. The possible reasons will be discussed in the following section.

#### **(i) Impact of peptide immobilization method and experimental conditions**

The use of a spacer for peptide immobilization allows peptide to stand out from the surface and freely extend outward from it, and therefore helps to reach the integrin-binding site on the cell. However, whether a spacer is needed or not is still not clear, as some studies also developed peptide-modified surfaces without using any spacers to investigate their interaction with cells and to enhance cell adhesion (Dee, Andersen et Bizios, 1998; Dee, Anderson et Bizios, 1999; Mann et West, 2002). Most systems are, however, using some form of soft polymeric matrix (e.g. hydrogels, brushes and SAMs) as a background for peptide immobilization to minimize non-specific protein adsorption and thus at least to offer some flexibility and motility (Petersen, Gattermayer et Biesalski, 2011).

Some studies have successfully used low-fouling polymers (such as PEG and Dextran) for peptide immobilization and thus to enhance cell adhesion (Groll et al., 2005b; Sabra et Vermette, 2011; Tugulu et al., 2007). However, it is difficult to compare results emanating from a small number of studies because several parameters such as the immobilization method, the type of substrate, the type of polymer and its molecular weight, the type of peptide and conditions used for the cell culture experiment can greatly influence

the outcomes of the studies. Nonetheless, we did a comparison here with the studies that are closely related to our work.

Both Sabra et al. and Massia et al. used dextran or CMD (70 kDa) for the immobilization of RGD and cyclic RGD peptides, respectively. (Massia et Stark, 2001; Sabra et Vermette, 2011). They both showed an increase in endothelial cell adhesion compared to an unmodified dextran surface. Although these studies used the same polymer as we did in our study, there are two main differences. Firstly, the peptide immobilization method is different, where RGD was immobilized on CMD or dextran through its N-terminus (without using a cross-linker). In our study KQAGDV/RGD peptide was immobilized using an EMCH cross-linker, which allows disulfide bonding between thiol groups (present on cysteine molecule of CGG-KQAGDV) and maleimide groups (present on EMCH cross-linker). Normally this would not be a problem, but some studies indicated that the optimal spacer length should be around 3-4 nm, as further increase in spacer length was shown to impede cell adhesion (Beer, Springer et Coller, 1992). This might be due to the increasing entropy of longer flexible spacer chains, which opposes strong binding with integrin receptors (Mammen, Choi et Whitesides, 1998; Wong et al., 1997). In our case the length of PEG and CMD is already in the range of 10-20 nm and the use of an EMCH linker can add a further 1.3 nm to the length of these polymers. Although this increase is not considerably high, the overall spacer length is much higher than optimal spacer length (3-4 nm), as suggested in (Beer, Springer et Coller, 1992). Thus, in future studies it would be worth verifying cell response by immobilizing peptide through its N-terminus without using a linker or using shorter spacer lengths.

Secondly, the conditions used for cell culture experiments are different in our study compared to other studies. Sabra et al., Massia et al. and others (Groll et al., 2005b; Tugulu et al., 2007; Wang et al., 2011b) performed cell adhesion assays in the presence of serum in order to show the improvement of cell adhesion on RGD-immobilized CMD or dextran surfaces. Wang et al. performed similar experiments to test the RGD impact on cell adhesion when it is immobilized on PEG-based materials. In this study, cell viability results (after 1

day) showed no significant difference in cell attachment when they tested various coatings on Poly(3-hydroxybutyrate-co-3-hydroxyvalerate) (PHBV) films (PHBV, PHBV + NH<sub>2</sub>, PHBV + PEG and PHBV + PEG + RGD). We observed a similar trend when we tested VSMC response (in the presence of serum) on KQAGDV-modified and unmodified PEG or CMD surfaces. Another important observation from Wang's studies is that after 3 days, some improvement in cell attachment on a PHBV + PEG + RGD surface compared to bare PHBV were noted, but cell adhesion on a PHBV + PEG surface was as good as a PHBV + PEG + RGD surface. It was concluded that the maleimide groups were responsible for good cell attachment on a PHBV + PEG surface. However, this was not true in our case when we tested cell adhesion on an EMCH-activated CMD (see Figure 4.18) or a PEG surface. The adsorption of serum proteins seems to be responsible for the variable results reported by Wang and colleagues.

Generally speaking, the influence of adhesive peptide on cell adhesion should be verified in the absence of serum, otherwise it is difficult to know whether the increase in cell response is due to immobilized peptide itself or through the combined effect of peptide and adsorbed proteins (Shin, Jo et Mikos, 2003). Recent results suggest a possible synergy between immobilized peptides and proteins. Thus the presence of a PHSRN sequence in the fibronectin-III domain of fibronectin can act synergistically with RGD to increase  $\alpha 5\beta 1$  binding, and therefore it enhances cell adhesion and spreading (Benoit et Anseth, 2005; Ebara et al., 2008; Nakaoka et al., 2013). In our case we did not observe any difference in terms of VSMC adhesion in the presence of serum when we tested peptide-modified and unmodified surfaces (PEG/CMD or amine-displaying surfaces). Therefore we performed further experiments in the absence of serum in order to investigate the impact of peptide. However, unfortunately, peptide-modified PEG or CMD surfaces did not show improved VSMC adhesion.

## **(ii) Peptide surface concentration**

Peptide density can play a key role in promoting cell adhesion. Cell adhesion as a function of peptide density showed a sigmoidal increase (Danilov et Juliano, 1989; Jeschke et

al., 2002; Kantlehner et al., 2000; Neff, Tresco et Caldwell, 1999). Some studies also reported a required minimum peptide concentration to enhance cell adhesion, spreading and focal contact formation (Drumheller, P. D. and Hubbell, J. A. 1994, Hubbell, J. A., Massia, S. P. et al. 1992, Massia, S. P. and Hubbell, J. A. 1991). The required minimum peptide density was indicated as 12 fmol/cm<sup>2</sup> for cell-spreading and 66 fmol/cm<sup>2</sup> for focal contact formation when using a PEG spacer (Drumheller, Elbert et Hubbell, 1994). However, cell attachment and spreading depend not only on peptide density but also on the hydrophilic/hydrophobic nature of the substrate/material. Moreover, it is not possible to generalize the impact of density to all peptides, because different peptides have different integrin-binding affinity and selectivity. Finally, high peptide density also has drawbacks since it was shown to impede cell migration and proliferation (Mann et West, 2002).

Although we were not able to compare our QCM-D data with these peptide densities, the input peptide concentrations used in the present work are comparable to several other studies (Patel et al., 2007; Sabra et Vermette, 2011; Wang et al., 2011b). Very low E coil EGF grafting was observed at the highest peptide input concentration (38 μM), which indicates that the surface was almost completely occupied by the peptide. Therefore, we do not believe that further increase in peptide concentration would improve cell adhesion. Moreover, this could make it impossible for combined immobilization of peptide and GF, which was the ultimate goal of this study. The absence of direct measurement of peptide density is, however, the main limitation of this study. Ideally, it should be performed by ELISA or by quantification of immobilized peptides using radio-labeled peptides.

### **(iii) Peptide conformation and accessibility**

The objective of this study was to promote VSMC-specific adhesion and growth on a low-fouling background. To meet this requirement KQAGDV peptide was chosen, which is known to mediate VSMC-specific adhesion through α2β3 integrin (Dong et al., 2012b; Mann et West, 2002). Since the poor results with KQAGDV could be explained by the absence of bioactivity on the peptide on rat VSMC, other experiments were also performed

with RGD for comparison purposes. RGD peptide is known to promote adhesion of several cell types through several different integrins ( $\alpha3\beta1$ ;  $\alpha5\beta1$ ;  $\alpha8\beta1$ ;  $\alpha11\beta3$ ;  $\alpha\nu\beta1$ ;  $\alpha\nu\beta3$ ;  $\alpha\nu\beta5$ ;  $\alpha\nu\beta6$ ;  $\alpha\nu\beta8$ ,  $\alpha2\beta1$  and  $\alpha4\beta1$ ) (Hersel, Dahmen et Kessler, 2003; Ruoslahti, 1996). Since low-fouling backgrounds offer some flexibility and mobility, these peptides are supposed to be accessible to integrin receptors present on cells. However, a lack of improvement in cell adhesion was observed. One possible reason might be an inaccessibility of the peptide to integrin receptors. Some ligands on PEG and CMD may not be accessible to cell receptors, and accessible ligands may not be sufficient for strong cell adhesion and spreading.

Some studies indicated that the presentation of ligands in a way that allows or triggers integrin clustering could enhance cell interactions with the surface (Irvine et al., 2001; Maheshwari et al., 2000). Studies by Maheshwari and colleagues reported enhanced fibroblast cell adhesion, spreading and focal contact formation when RGD was presented in clusters (9 RGD/star PEG molecule) versus individual format. In our case, star PEG has 4 arms, and at least 2 arms are available for peptide immobilization (see Figure 3.2 and Figure 3.3). In the case of CMD, we are unsure of the number of side chains per molecule, but it might have a higher density of carboxyl terminal groups than star PEG, as suggested by the higher amount of peptide grafting and EGF recruitment on CMD versus star PEG (Figure 4.12). Nevertheless, this may be insufficient to form clusters. In our case, both PEG and CMD are branched polymers and they would have promoted integrin clustering and therefore VSMC adhesion, as showed in Maheshwari et al.'s work. However, this did not occur when using both PEG and CMD polymers. Possible reasons for lack of cell adhesion in our case might be due to two reasons: (i) With regard to CMD, although it has several branches, the chain conformation may not be same as star PEG. The side chains or arms in star-shaped molecules always emanate towards the surface (see Figure 3.3) due to the steric hindrance effect of the core of the PEG molecule; (ii) In the case of our star PEG, the number of side chain groups or arms (only 4 arms per molecule as explained above) per molecule may not be sufficient to form integrin clustering, which could be further verified using star PEG molecules that have at least nine arms.

Conformation of the peptide is another important concern. It has been recognized that the specificity and binding ability of small peptide sequences are limited compared to ECM proteins (Kantlehner et al., 2000; Pierschbacher et Ruoslahti, 1984), since ECM proteins have multiple binding sites for cell adhesion receptors or integrin receptors. RGD peptide in looped conformation was shown to be more effective towards cell adhesion receptors compared to linear peptide, because looped confirmation closely mimics the natural structure of fibronectin and offers several binding sites for integrin binding (Kämmerer et al., 2011; Kantlehner et al., 2000; Verrier et al., 2002; Zhu et al., 2009). Moreover, since looped structures are large in size compared to linear peptide, there are chances to overcome the influence of the steric hindrance effect of low-fouling surfaces.

Overall, this study enabled us to investigate the possibilities for combined immobilization of peptide and GF on non-fouling surfaces. QCM-D data allowed us to follow the changes in mass resulting from combined immobilization. These results indicated that it is possible to modulate EGF immobilization by varying peptide input concentrations. However, this system did not allow us to compare the peptide surface concentration with other studies. Several other surface characterization techniques (XPS, FTIR, contact angle etc.) and direct or indirect quantification methods (BCA assay, ELISA, UV detection and radio-labeling etc) are available to determine peptide densities (Hersel, Dahmen et Kessler, 2003). Most systems used radio-labeled peptides for quantification of immobilized peptide and it was believed to be more reliable than other techniques. In our case it was difficult to use such a technique due to the inaccessibility and unavailability of these radio-labeled peptides. Most research teams did not perform complementary studies to confirm the presence of immobilized peptide, relying instead on cell culture experiments to show the impact of peptide on cell response. In our case, the QCM-D technique allowed to follow peptide immobilization in real time and confirmed the presence of the peptide, but the absence of improvement in cell adhesion did not allow us to prove the concept. We did not verify cell adhesion on peptide- and EGF-immobilized surfaces for two reasons: (i) our aim was to promote initial cell adhesion with the help of peptide and then to promote cell growth with the help of growth factor; (ii) we observed poor VSMC growth on EGF-immobilized

CMD surfaces in recent studies in our lab (Lequoy et al., 2014). Therefore, we anticipate that the presence of EGF may not benefit improvement of cell proliferation response on low-fouling backgrounds. In future studies, the cell response could be verified by changing several parameters such as peptide conformation, spacer length, immobilization method and combination with other peptide sequences such as PHSRN. At the same time, other hydrophilic polymers can be foreseen that would exhibit favorable properties for promoting cell adhesion (with or without the need for peptide/GF immobilization) while preventing protein adsorption. Overall, the strategy of improving cell adhesion by peptide immobilization on low-fouling surfaces is not as good as we expected and seen in the literature. Most probably, the combination of the steric hindrance effect and the hydrophilic nature of low-fouling polymers is strongly opposing cell adhesion. However, this could be further verified by changing several parameters as discussed above.

### **4.3 Evaluate the advantages and limitations of using CS coating for vascular grafts**

#### **4.3.1 Rationale**

Section 4.2 highlighted the limitation of using peptide grafting on low-fouling surfaces to promote cell adhesion. Recently, chondroitin sulfate (CS)-based surfaces have been developed in our laboratory to tether growth factors (GF) in a random (Charbonneau et al., 2011; Charbonneau et al., 2012; Lequoy et al., 2014) or oriented fashion. (Lequoy et al., 2014). This polymer presented a huge advantage when we compared VSMC behavior on CS and CMD surfaces on which EGF had been grafted. We hypothesize that this is mainly due to CS cell pro-adhesive properties despite good protein resistance. Moreover, sulfated polysaccharides can improve hemocompatibility by means of electrostatic repulsion towards negatively charged blood components (Keuren et al., 2003). This suggests that CS could combine several advantages as a coating on vascular implants. Therefore in this part of thesis, we investigated the advantages and limitations of CS for the creation of low-fouling and non-thrombogenic surfaces by comparing CS to well-known low-fouling polymers, i.e. multi-arm PEG and CMD.

In order to achieve this objective, LP coatings (Ruiz et al., 2010; Truica-Marasescu et al., 2008) were used once again for covalent coupling of the three (PEG, CMD and CS) carboxyl-functionalized polymers. The low-fouling properties were first assessed by following adsorption of fibrinogen, bovine serum albumin (BSA) and fetal bovine serum (FBS) in real time using QCM-D and further confirmed using labeled BSA in static incubation. The functionalized surfaces were also evaluated for their ability to promote endothelial cell adhesion, retention and growth *in vitro*. Finally, platelet adhesion during blood perfusion was also assessed on bare and endothelial cell grown surfaces.

## **4.3.2 Results**

### **4.3.2.1 Physical characterization of coatings**

The chemical grafting protocols for PEG have been already optimized, as presented in section 3.1. PEG grafting was confirmed with an XPS survey and high resolution scans of C1s and O1s. In addition, CMD and CS grafting on aminated surfaces had been recently optimized to maximize surface density. These surfaces were characterized using various techniques such as XPS, ToF-SIMS and ellipsometry dry thickness measurements, as detailed in previous publications (Charbonneau et al., 2011; Liberelle et al., 2010). In brief, XPS analysis confirmed the presence of sulphur (0.3%) indicative of CS on the surface, (Charbonneau et al., 2012) while ToF-SIMS demonstrated its uniform distribution on the surface (Charbonneau et al., 2011). The dry thickness of the CS layer was estimated by ellipsometry to be around 0.8 nm ( $n \geq 5$ ) and slightly higher for CMD (about 1.3 nm;  $n=5$ ) (Liberelle et al., 2010). In both cases, the surface was almost completely covered since adsorption of a 6 kDa molecule (epidermal growth factor) was reduced by 93% according to ELISA measurement, as published by Lequoy et al. (Lequoy et al., 2014).

In this part of the thesis, optimized protocols were applied to LP-coated PET and amino-coated glass substrates to prepare PEG, CMD and CS coatings. Contact angle measurements were performed to rapidly confirm chemical grafting and compare the three surfaces. As shown in Figure 4.19, all modified surfaces (PEG, CMD and CS) exhibited contact angles

significantly lower than those observed on LP ( $62 \pm 1^\circ$ ) or PET ( $66 \pm 3^\circ$ ) surfaces, the lowest contact angle corresponding to CMD ( $40 \pm 2^\circ$ ). The same trend was observed when grafting these polymers on aminated glass surfaces (see Figure 4.20).

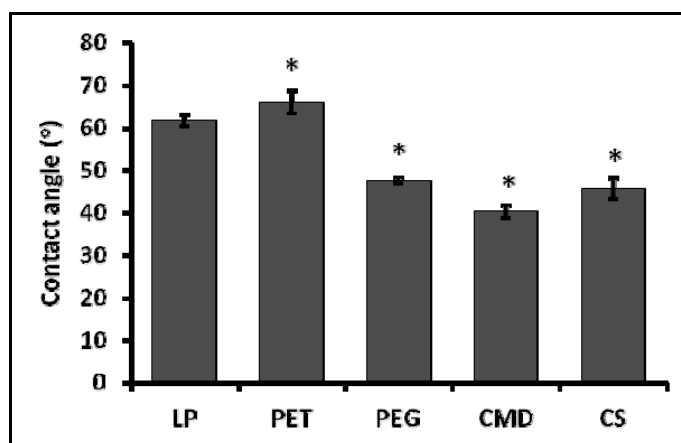


Figure 4.19. Static water contact angle measurements of unmodified LP and LP coated with PEG, CMD and CS (mean  $\pm$  SD;  $n = 10-12$ ); \*  $p < 0.0001$  vs. LP.

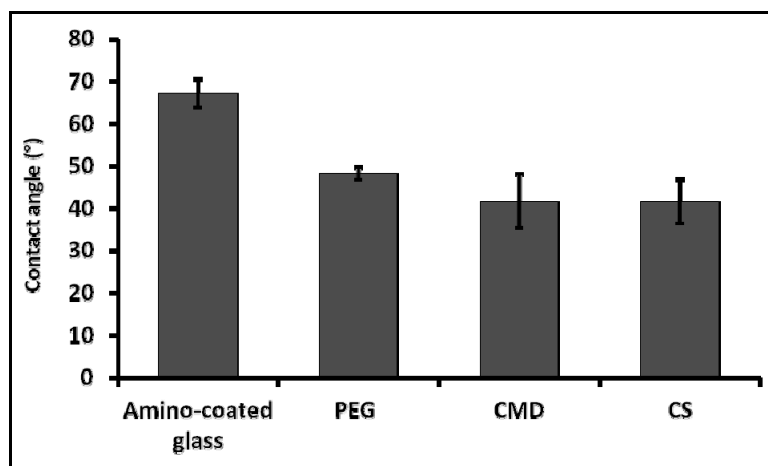


Figure 4.20. Static water contact angle measurements of unmodified and modified amino-coated glass surfaces with PEG, CMD and CS (mean  $\pm$  SD;  $n = 7$ ).

#### 4.3.2.2 Protein adsorption

Low-fouling properties of PEG-, CMD- and CS-coated LP surfaces were assayed by QCM-D, and compared to those of LP. First, fibrinogen injections were performed on the different surfaces. Examples of frequency and dissipation curves obtained for LP and CMD coatings are presented in Figure 4.21. Fibrinogen adsorption occurred rapidly on LP surfaces, yielding a significant negative frequency shift (Figure 4.21 a) and positive dissipation shift (Figure 4.21 b). As expected, these shifts were largely reduced on CMD-coated surfaces, indicating almost complete prevention of protein adsorption.

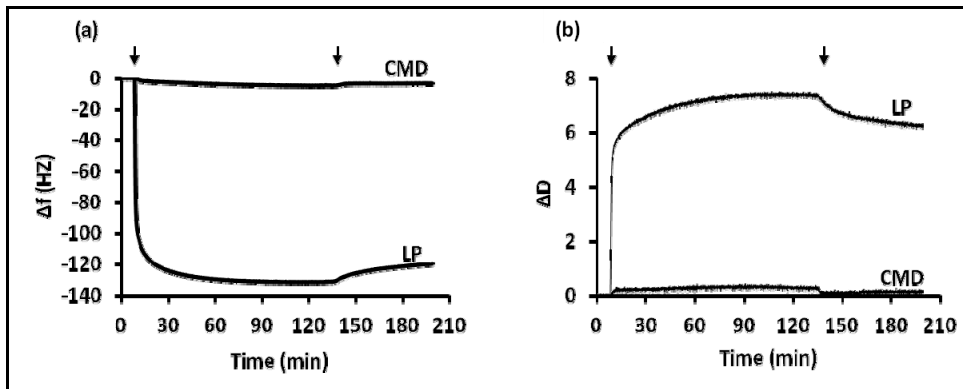


Figure 4.21. QCM-D frequency ( $\Delta f$ , panel a) and dissipation ( $\Delta D$ , panel b) versus time for fibrinogen (0.5 mg/mL) adsorption on a CMD modified and an LP surface. The arrows refer to the injection of the protein solution (left) and PBS rinsing (right).

Similar adsorption assays were performed for each surface using BSA and FBS. In each case, frequency and dissipation values were used to calculate the mass of adsorbed material (Figure 4.22). The average reduction of adsorbed mass on PEG, CMD and CS compared to LP surfaces is presented in Table 4.3. LP surfaces induced a large amount of fibrinogen adsorption that was almost suppressed by CMD (98%) and PEG (90%) coatings, as expected. Interestingly, results for CS-coated surfaces were comparable to those of PEG (87%). In the case of BSA, PEG and CMD also exhibited very good resistance to adsorption, while CS was somewhat less efficient (72% compared to 85% and 84% for PEG and CMD, respectively; Table 4.3 and Figure 4.22 a). The small number of samples that were assayed

did not permit conclusions to be drawn on the significance of these differences. Finally, when FBS was injected (Figure 4.22 b), the same trend was observed (Figure 4.22 and Table 4.3).

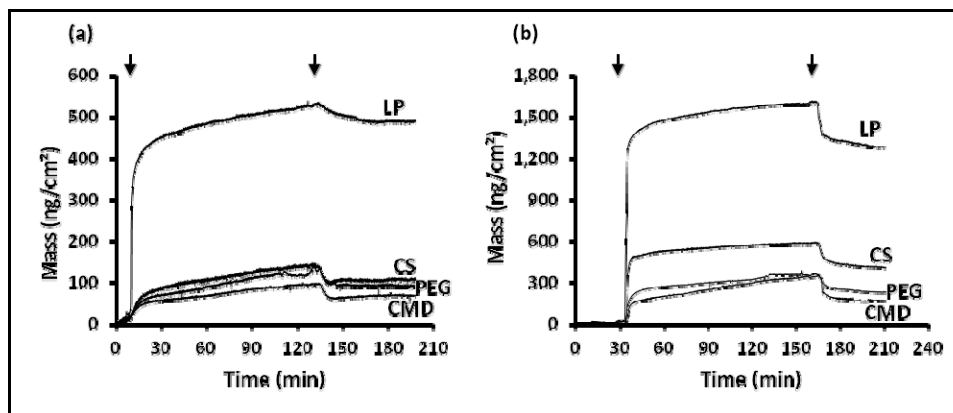


Figure 4.22. The adsorption and desorption kinetics of BSA (a) and 10% (w/v) FBS (b) on PEG, CMD and CS modified and unmodified LP surfaces. Arrows indicate the start of the protein (left) and PBS (right) injections.

Table 4.3. Mean percentage reduction of protein-adsorbed mass compared to LP surface, based on QCM-D results (mean  $\pm$  SD;  $n = 3-5$ ).

Coating	% Reduction of fibrinogen	% Reduction of BSA	% Reduction of FBS (10% v/v)
PEG	90 $\pm$ 3	85 $\pm$ 2.5	88 $\pm$ 5
CMD	98 $\pm$ 0.1	84 $\pm$ 3.6	89 $\pm$ 5
CS	87 $\pm$ 9	72 $\pm$ 4.2	66 $\pm$ 9

For validation purposes, under static conditions, BSA adsorption on various surfaces was also directly evaluated using fluorescent-labeled albumin. Results (Figure 4.23) were in excellent agreement with those obtained by QCM-D. The reductions of BSA adsorption mediated by PEG and CMD coatings (85  $\pm$  3% and 84  $\pm$  4% reduction, respectively) was significantly ( $p < 0.0001$ ) better than that mediated by CS coating (71  $\pm$  4%). The difference

was also significant compared to bare PET surface ( $p < 0.0001$ ), with a reduction of  $81 \pm 4$  %,  $80 \pm 3$  % and  $64 \pm 8$  % on PEG, CMD and CS, respectively.

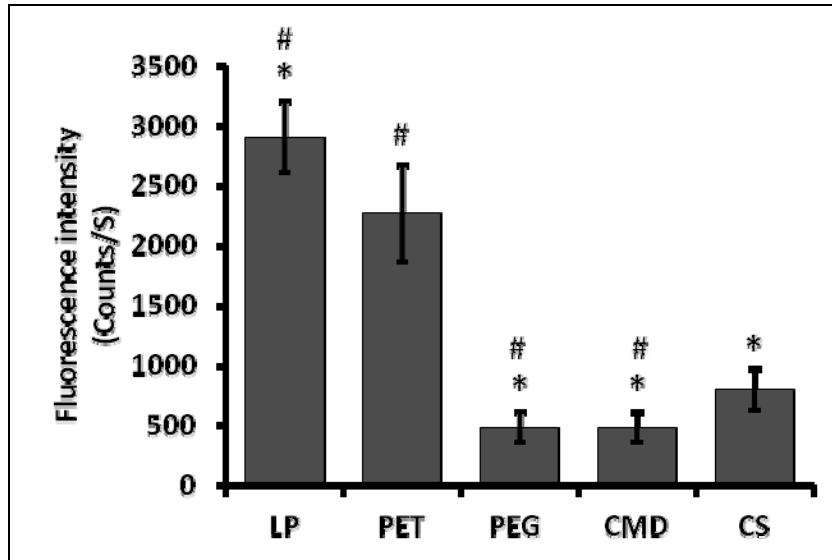


Figure 4.23. Fluorescence intensity of adsorbed Texas Red labeled albumin (0.2 mg/mL) on PEG-, 2 CMD- and CS-modified and unmodified LP surfaces, as well as on bare PET control (mean  $\pm$  3 SD;  $n = 8-12$ ); \*  $p < 0.0001$  vs. PET; #  $p < 0.0001$  vs. CS.

#### 4.3.2.3 Cell adhesion and growth

HUVEC adhesion and growth was investigated on PEG, CMD and CS surfaces and compared to growth on LP, bare PET and polystyrene culture plates (PCP) (Figure 4.25). HUVEC adhesion and growth were excellent on LP and PCP positive control, but relatively poor on PET as already observed in previous studies (Gigout et al., 2011). Grafting of PEG and CMD to the surfaces led to even lower adhesion and no growth. Cells displayed a round shape and spreading was limited (see Figure 4.24). These observations are consistent with previous investigations with low-fouling polymer surfaces (Desai et Hubbell, 1991; Zhang, Desai et Ferrari, 1998). In stark contrast, cells adhered well on CS and showed rapid growth similar to that observed on LP and PCP surfaces.

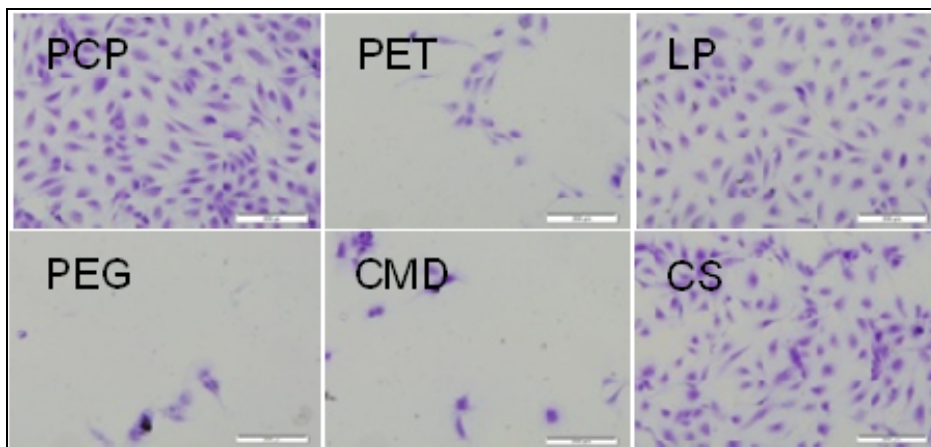


Figure 4.24. Typical images of crystal violet staining after 2 day HUVEC growth on each surface (scale bar = 200  $\mu\text{m}$ ).

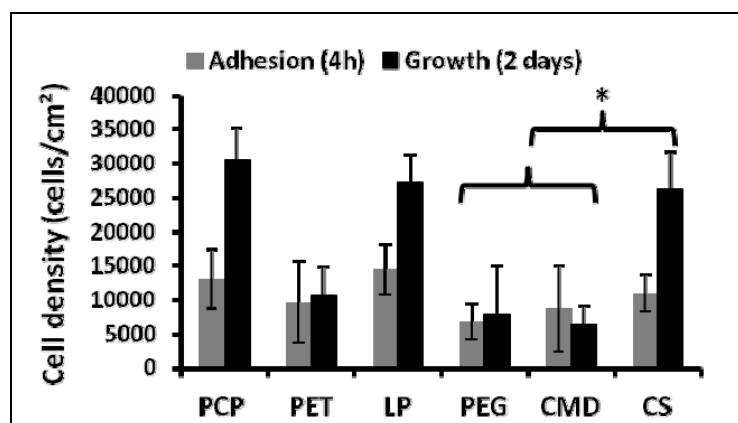


Figure 4.25. HUVEC density after 4h (adhesion) and 2 days (growth) (mean  $\pm$  SD ;  $n = 12$ ); \*  $p < 0.0001$ .

The presence of HUVEC focal adhesion after 24h on CS was confirmed by actin and vinculin immunostaining, as shown in Figure 4.26. HUVECs on CS and LP surfaces exhibited a spread morphology, with well defined actin fibers (in green) throughout the cytoplasm and termini clustered at vinculin rich sites (red color spots mainly at the edges). These observations are indicative of integrin-mediated anchorage on CS and LP surfaces and suggest strong cell attachment and adequate signaling for cell growth and survival. On bare PET, fewer cells were observed. Some exhibited a rounded morphology (data not shown) while others were spread but exhibited only a few stress fibers and the actin cytoskeleton did

not appear to be well organized. Only rare focal adhesion points could be observed. Finally, as expected, very few cells were observed after 24h on CMD and they generally presented a rounded morphology, without any focal contact formation. Absence of spreading and focal adhesion of HUVEC on CMD suggests that there is a strong risk of cell detachment and cell death and correlates well with the very low cell number after 2 days of growth in Figure 4.25.

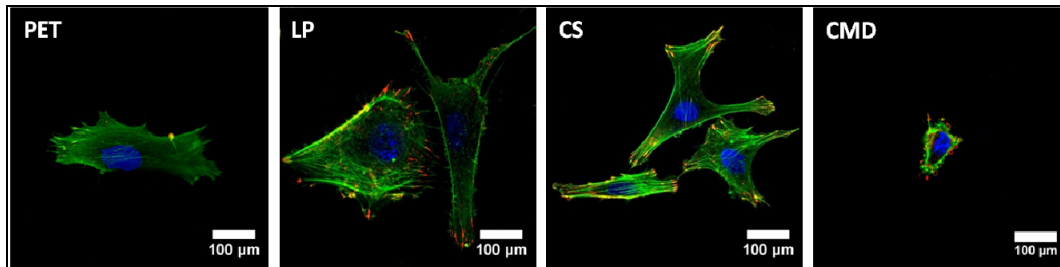


Figure 4.26. Immunostaining of vinculin (red), actin (green), and the nucleus (blue) after 24 h of HUVEC adhesion on PET, LP, LP-CS and LP-CMD surfaces.

#### 4.3.2.4 Platelet adhesion

Since the hemocompatibility of the surface is particularly important for vascular graft application, platelet adhesion was assayed on our different coatings using the previously described device and protocols developed at Dr. Merhi's laboratory (Merhi, King et Guidoin, 1997). Figure 4.27 presents the average percentages of LP, PET, PEG, CMD and CS surfaces covered by platelets after whole blood perfusion for 15 min. Representative images from confocal microscopy after platelet labeling using CD61/FITC labeling and from SEM for LP, PET and CS are shown in Figure 4.28. The platelets adhered on LP surfaces, appeared as activated and changed in shape with pseudopod extrusions. The LP surface also became prone to platelet-platelet interaction and aggregation, most likely due to the positively charged amine groups present in aqueous media. Although platelet adhesion on PET was significantly lower than on the LP surface, the adhesion on PET surfaces varied considerably from one experiment to another, probably due to the variability in platelet reactivity between different blood donors. However, on PET surfaces, platelets presented filopodia typical of an activated phenotype (Figure 4.28 c). In contrast, platelet adhesion was almost abolished on

PEG, CMD and CS surfaces. Interestingly, CS grafted surfaces were as efficient as PEG and CMD surfaces in resisting platelet adhesion as no significant difference was observed between these three surfaces.

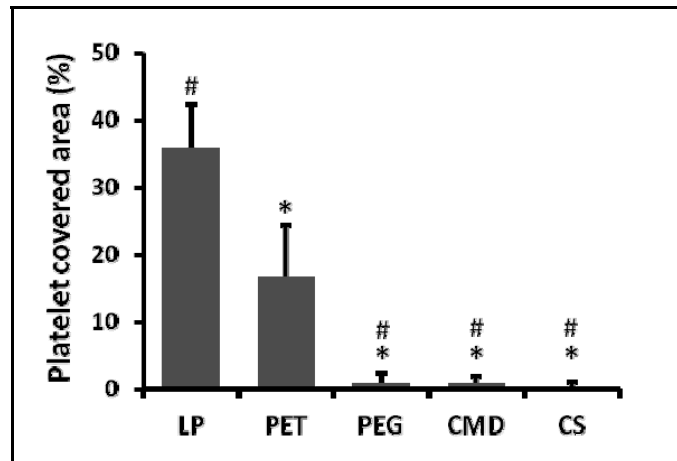


Figure 4.27. Percentage of surface area covered by platelets after perfusion with whole blood for 15 min (mean  $\pm$  SD;  $n = 5-9$ ); \*  $p < 0.0001$  vs. LP; #  $p < 0.0001$  vs. PET.

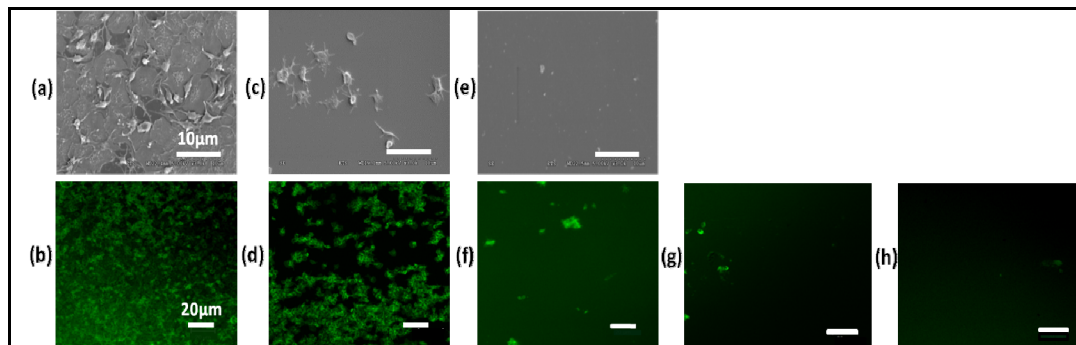


Figure 4.28. Representative images of SEM (a, c, e) and confocal microscopy (b, d, f, g, h: labeling with CD 61/FITC) for platelet adhesion on LP (a, b), PET (c, d), CS (e, f), PEG (g) and CMD (h) surfaces after perfusion with whole blood.

Since CS surfaces exhibited very low platelet adhesion and favorable HUVEC growth, they appeared as promising surfaces for creating a complete endothelial layer on a non-thrombogenic underlayer. To that purpose, HUVEC must present a non-thrombogenic

phenotype and must be resistant to the shear induced by blood flow. As a first assessment of these properties, cells grown for 7 days on the various surfaces were subjected to blood flow for 15 min. HUVEC density and platelet adhesion were measured.

Figure 4.29 presents the results of Fadlallah's work, showing the HUVEC density on each type of surface that had been submitted or not to blood flow, thus enabling estimation of HUVEC retention. Despite relatively similar initial HUVEC densities on all three surfaces (PET, LP, CS), cell density on PET was shown to decrease dramatically during perfusion, with only 25% retention on the surface. In contrast, cells strongly adhered on LP and CS, on which cell densities before and after perfusion were not significantly different.

With respect to platelet adhesion on HUVEC-grown surfaces, platelet adhesion on CS was very low, both on HUVEC-grown and bare CS surfaces (Figure 4.30). On HUVEC-grown LP surfaces, the presence of numerous cells significantly reduced platelet adhesion compared to LP alone ( $p < 0.0001$ ). However, platelet adhesion was still visible in regions (of green color) where no cells were present (Figure 4.30 b), which might be either due to the lack of complete coverage after 7 days of growth or to cell detachment during perfusion. Altogether, even with HUVEC, LP surfaces tended to be more thrombogenic than CS surfaces, though the difference was not statistically significant ( $p = 0.16$ ;  $n=7$ ).

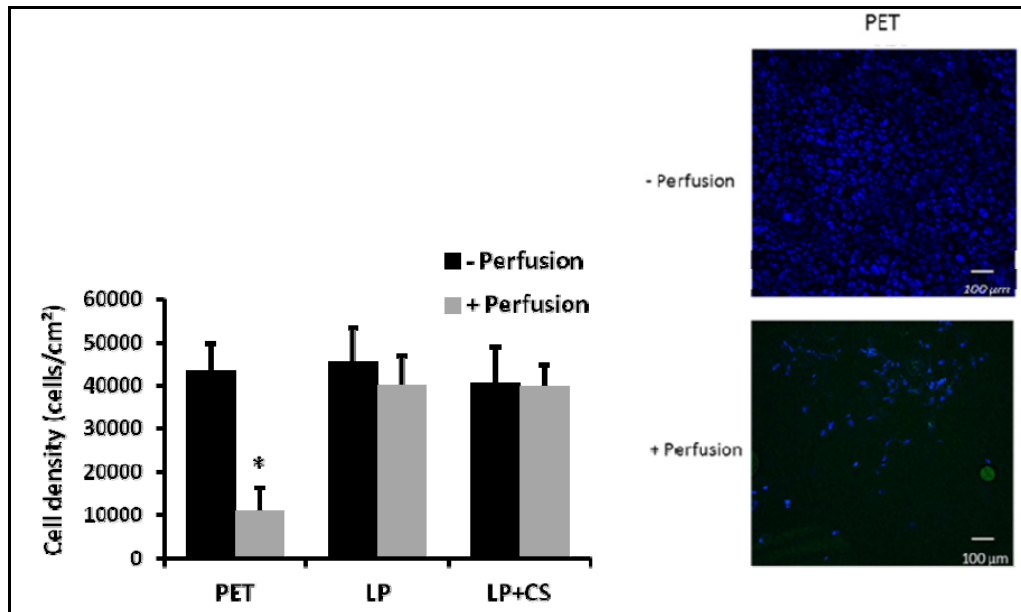


Figure 4.29. Cell density on the different surfaces (bare PET and LP +/-CS coating) not perfused (-Perfusion) and after perfusion (+Perfusion) of whole blood (mean  $\pm$  SD;  $n = 7$ ); \*  $p < 0.0001$  vs. all other surfaces. Confocal microscopy images (right side) of HUVEC growth (7 d; labeled with CellVue Maroon (in blue color)) on PET, before and after 15 min of perfusion. Data adapted from Fadlallah's thesis (Fadlallah, 2013).

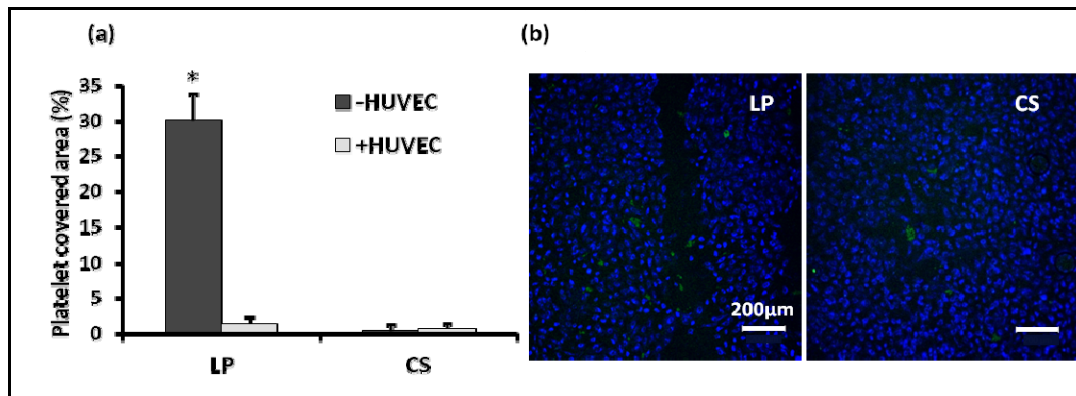


Figure 4.30. (a) Percentage of LP and CS surfaces covered by platelets after perfusion with whole blood in the absence (-HUVEC) and presence (+HUVEC) of previously seeded HUVEC (mean  $\pm$  SD;  $n = 7$ ; \*  $p < 0.0001$  vs. other surfaces). (b) Representative images of HUVECs and platelets on LP and CS surfaces after perfusion (HUVEC membranes colored with CellVue® Maroon (blue) and platelets stained with anti-CD61/FITC antibody (green)). Scale bar corresponds to 200  $\mu$ m. Data adapted from Fadlallah's thesis (Fadlallah, 2013).

### 4.3.3 Discussion

The aim of this part of the thesis was to study whether CS could be an interesting alternative to PEG or CMD as an underlayer for vascular implants, to be used alone or combined with GF immobilization. Therefore the low-fouling and cell-adhesive properties of CS were compared with well-known low-fouling polymers such as PEG and CMD, as well as with an LP coating and pristine PET as controls. CS was as efficient as PEG and CMD in limiting fibrinogen adsorption, a key protein in the cascade leading to thrombus formation (Ratner Buddy, 2000). However, CS was less effective than PEG and CMD in limiting the adsorption of albumin and FBS (containing hormones, ECM proteins (collagen, fibrinogen, fibronectin, etc.) and growth factors). In a previous study, it was demonstrated that CS surfaces prevented EGF non-specific adsorption as efficiently as CMD (Lequoy et al., 2014). In contrast, CS has also been reported to interact strongly with fibroblast growth factor and heparin-binding growth factors (Deepa et al., 2002; Freeman, Kedem et Cohen, 2008). Altogether, these observations strongly suggest that CS presents selective protein resistance. QCM-D enables study of the adsorption kinetics of proteins from complex mixtures, but it allows neither identification of the adsorbed proteins nor determination of whether these proteins are denatured once adsorbed. This could be further investigated by conducting competitive protein adsorption studies (Hlady, Buijs et Jennissen, 1999) using serum containing the mixture of several different fluorescent labeled proteins and GFs. This will help to identify which proteins are selectively recruited by CS and thus gain a better understanding of its mode of action.

Interestingly, although protein adsorption was not completely abrogated on CS surfaces, platelet adhesion was almost abolished and comparable to that observed on PEG and CMD surfaces. The perfusion assay in this work mimicked physiological conditions (Papaioannou et Stefanadis, 2005), and therefore it is believed to give a better estimate of the anti-platelet property of our surfaces as compared to static assays because the shear stress induced by blood flow causes qualitative and quantitative differences in adhesion (Engbers et al., 1987). Moreover, platelets have a relatively low density and do not settle easily in static conditions. One limitation of our platelet adhesion test is the short perfusion time (15 min),

which was chosen due to the limited lifetime of the anticoagulant as well as to allow comparison of several surfaces with blood from the same donor. However, 15 min perfusion was sufficient to observe a significant decrease in platelet adhesion on PEG, CMD and CS surfaces as compared to PET. Almost no platelets were observed on both HUVEC grown and bare CS and none were activated. This suggests that HUVEC growth on CS exhibited a non-thrombogenic phenotype. However, further studies would be required to confirm this point, including the assay of released pro- and anti-thrombogenic molecules by cells (Thébaud et al., 2010) and of longer perfusion times. These observations are consistent with some previous results (Keuren et al., 2003) and are probably due to the electrostatic repulsion of the negative charges on sulfated CS, and the additive effect of highly hydrophilic properties of CS surfaces. Indeed, platelet adhesion and complement system activation are known to decrease with increasing surface hydrophilicity (Rodrigues et al., 2006).

Overall, resistance to fibrinogen adsorption and the absence of platelet adhesion on CS suggest that it can prevent thrombus formation. Vascular grafts fail due to several reasons, but the most prevalent is occlusion due to blood coagulation. Therefore, additional studies such as using a whole blood kinetic clotting time method (Motlagh et al., 2006) or plasma coagulation tests based on turbidity measurements (Sask et al., 2011) and measurement of thrombin generation in flowing blood (Keuren et al., 2003) could be performed to confirm the blood compatibility of CS.

More importantly, in stark contrast to PEG and CMD, CS was shown to support and promote endothelial cell adhesion and growth leading to the formation of a complete and flow-resistant endothelium, whereas most cells detached from the PET surface during perfusion. Focal adhesion points and strong cell attachment suggest integrin-mediated anchorage on CS surfaces. CS probably promotes the adsorption of some proteins and/or growth factors present in the culture medium (containing 2% FBS) that are favorable to HUVEC adhesion and proliferation. Since CS has negatively charged sulfate groups, it may preferentially interact with proteins that have basic amino acids (Lys and Arg) whose positive charges presumably interact with the negatively charged sulfates and carboxylates of the GAG chains (Esko et al., 2009). The cell-adhesive proteins and (fibronectin (Fn),

laminin (Ln) and Vitronectin ) (Faucheux et al., 2006; Sottile, 2004; Underwood, Steele et Dalton, 1993) and GFs, particularly VEGF and FGF-2 (Byzova et al., 2000; Koenig, Gambillara et Grainger, 2003a), possess binding domains for endothelial cells. Of these proteins, vitronectin is a positively charged protein at physiological pH conditions, and it seems CS interacts with this protein to promote EC adhesion. The role of adsorbed proteins in the performance of CS coating are demonstrated by the fact that previous work in our lab showed that CS by itself did not exhibit proliferative properties (Charbonneau et al., 2012). Moreover, during focal adhesion assays, we observed much lower cell adhesion when cells were incubated on the CS surface in a serum-free medium.

Despite the fact that other factors could explain the difference in results between CS and CMD or PEG coatings (density, length of free mobile chains and compliance of the coating), we believe that these differences are mostly due to CS composition. Other studies also showed that sulfated GAG-modified surfaces were able to promote EC adhesion in the presence of FBS (but not in the absence of FBS) due to the interaction of selective FBS proteins and/or growth factors with negatively charged sulfate groups (Wang et Luo, 2013). Indeed, heparin-binding proteins and GF were shown to bind to sulfated HA and sulfated alginate but not to HA or alginate (Freeman, Kedem et Cohen, 2008).

Moreover, CS shares structural similarities with heparin, which is well known for its anticoagulant activity. Both are sulfated polysaccharides with repeating units of uronate and hexosamine saccharides (Kjellen et Lindahl, 1991). Their net negative charge due to the presence of sulfate groups allows them to interact with a large number of proteins and basic molecules through ionic and hydrogen bonding interactions (Kidane et al., 1999; Li et Henry, 2011a). In terms of anti-coagulant effect, heparin has an advantage since it binds specifically to the enzyme inhibitor antithrombin III (AT), which inactivates thrombin. On the other hand, CS is more effective in preventing protein adsorption (including fibrinogen) and platelet adhesion (Keuren et al., 2003). Keuren et al. also concluded that CS leads to almost as little thrombin generation as heparin, thanks to its higher protein-repelling property. Moreover, CS has the advantage of exhibiting an anti-apoptotic effect on vascular cells, including endothelial cells and mesenchymal stem cells (Raymond et al., 2004). This anti-

apoptotic activity is conserved when CS is grafted by covalent coupling on biomaterial surfaces (Charbonneau et al., 2011). Furthermore, the hydrophilic and low-fouling properties of CS are believed to be important to ensuring good access and presentation of GF to the cells (Lequoy et al., 2014). Overall, the results from this part of the work suggest that CS as a sublayer favors selective low-fouling properties, which lead to low thrombogenicity combined with cell adhesive properties.



## CHAPTER 5

### GENERAL DISCUSSION

#### **General discussion, limitations and perspectives**

Cardiovascular diseases are the leading cause of mortality and morbidity in the aging population and they are expected to increase in the future. There is an urgent clinical need for improved vascular implants, mainly vascular grafts and vascular stents, that will promote desirable blood-biomaterial interactions with a high patency. The current vascular grafts made of polyethylene terephthalate (PET) and polytetrafluoroethylene (PTFE) have failed due to two main reasons: (i) when in contact with blood, implants are subject to the risks of coagulation and thrombosis, which are especially problematic when using small-diameter vascular grafts (<6mm); (ii) the lack of favorable surface properties to induce endothelialization *in vivo* on the lumen of vascular grafts; and similarly for stent grafts, the lack of vascular smooth muscle cell growth that promotes healing and SG incorporation into the surrounding vessel wall. Therefore, recent research efforts have aimed to develop surface physical, chemical and biological modification methods to improve the patency of vascular implants. Several attempts were already made to develop surface modification methods to minimize surface thrombogenicity and promote desirable cell interactions, as described in the literature review section.

Currently there is a strong trend toward using low-fouling surfaces for bioactive coatings, thanks to their advantages (prevent non-specific protein adsorption and interactions with cells, as described in the literature review section). However, based on the literature review, we realized that two major issues need to be resolved: (i) the current bioactive coating methods fail to find a good compromise between preventing protein adsorption and promoting desirable cell adhesive properties. Moreover, (ii) most techniques lack versatility, which compromises their commercial use since the coating process must be optimized for each new material and application.

Therefore, in this PhD thesis we proposed developing an innovative and versatile bioactive coating for vascular grafts and stent grafts that can induce desired cell interactions while preventing protein adsorption and platelet adhesion. This proposal has been divided into three different steps: (i) Develop a versatile PEG coating method to offer low-fouling and non-thrombogenic properties. (ii) Subsequently immobilize adhesive peptides (here KQAGDV or RGD) and growth factor (here EGF) to create a bioactive coating which promotes specific and optimal cell interactions. (iii) Evaluate the potential of CS as a possible ideal compromise between low-fouling and cell-adhesive properties, in comparison with conventional low-fouling coatings, for developing biocompatible vascular implants.

### **A versatile PEG low-fouling coating**

The primary aim of this thesis was to develop a versatile low-fouling coating, using PEG and LP plasma polymer, for further grafting of biomolecules in order to create bioactive coatings. Protein-resistant coatings such as those made of polyethylene glycol (PEG) have already been extensively investigated, since they can reduce platelet adhesion and the risk of thrombus formation (Kidane et al., 1999; Li et Henry, 2011b). PEG low-fouling properties are attributed to steric repulsion and a highly hydrated surface layer (Hoffmann et al., 2006; Kidane et al., 1999; Ratner Buddy, 2000; Zhang, Desai et Ferrari, 1998). Several strategies previously used for PEG immobilization on biomaterial surfaces include simple direct adsorption (Davis et Illum, 1988), radiation and chemical cross-linking approaches (Graham et McNeill, 1984), and self-assembled monolayers (Yang, Galloway et Yu, 1999). Simple adsorption is flexible and convenient, but its efficacy is limited by the tendency of PEG to elute off the surface (Gombotz et al., 1991). Stable PEG coatings generated by direct covalent chemical coupling to substrates have already been reported (Demming et al., 2011). However, this approach is far from being versatile since it relies on the availability of compatible functional groups on both PEG and the host surface, as well as on their respective surface densities.

*The main originality of the first part of this thesis consists in the versatility of the star PEG low-fouling coating, which was created by exploiting LP coatings. This versatile PEG coating method is applicable to a wide variety of biomaterials used for vascular implants and other biomedical and bio-analytical applications. This part of the work was published in the journal BioMed Research International (Thalla et al., 2012).*

Star-shaped (multi-arm) PEG was used in this study for two reasons: (i) star PEG's molecular architecture and long chain length enable a higher grafting density than linear PEG (Groll et Moeller, 2010; Kuhl et Griffith-Cima, 1996; Sofia Susan et Merrill Edward, 1997) and therefore a highly protein-resistant surface can be created. Indeed, for similar chain lengths and molecular weights, star-shaped polymer brush variants have been demonstrated to possess higher density and greater steric repulsive forces against adsorbing proteins when compared to linear PEGs (Satulovsky, Carignano et Szleifer, 2000). (ii) Star PEG offers a high density of functional groups that allow subsequent grafting of selected biomolecules designed to further tailor surface properties (Groll et Moeller, 2010; Kuhl et Griffith-Cima, 1996).

As expected, protein adsorption studies carried out in this project showed that the efficiency of the star PEG low-fouling coating increased as a function of its coupling concentration. XPS analysis (of survey and high-resolution scans) and contact angle measurement results also indicate an increase in PEG surface concentration as a function of its coupling concentration. However, complete prevention of protein adsorption was not achieved and led to some cell adhesion in the presence of serum (as seen later during the second part of this study). To better understand the reasons for this result, other surface characterization methods such as ellipsometry dry thickness measurements, ToF-SIMS and AFM techniques could be performed to study grafting densities and coating uniformity. The main limitation of this part of the study was a lack of studies comparing grafting densities and low-fouling properties using different molecular weights of star PEG, which could have helped to achieve a complete low-fouling surface. We did not perform these studies for several reasons: (i) Although protein adsorption was not prevented by 100% on star PEG,

platelet adhesion was almost completely abolished on 5% PEG-coated surface. We believed that it would be sufficient to create a versatile non-thrombogenic surface. (ii) Our ultimate goal was to tether biomolecules to promote confluent cell adhesion and growth on a low-fouling underlayer. We believed that this star PEG coating method would be enough to create such a surface, since it has at least two or three available functional groups per star molecule for further coupling. (iii) Finally, the star PEG grafting method is not economical, which is also encouraged us to look for other alternatives for bioactive coatings in the next steps.

**Recommendation 1:** *Since the current PEG grafting did not prevent complete protein adsorption, in future work the low-fouling properties of star PEGs could be investigated by changing several parameters such as PEG molecular weight, number of arms, chain length and grafting conditions on surface density, uniformity and thickness.*

Alone, this star PEG coating exhibits low-fouling and anti-platelet adhesion properties, which suggests that this surface could be non-thrombogenic. However, most *in vivo* studies of PEG-modified implants have been unsuccessful in limiting blood clot formation (Akbar et al., 2011; Hubbell, 1993; Nojiri et al., 1990a). This is in part due to the poor stability of PEG coatings and might be due to the fact the PEG layers limit only individual platelet adhesion but not platelet aggregates that might form in blood away from the material surface (Park et al., 2000). Although PEGylated surfaces showed prolonged circulation profiles in the vasculature (Moghimi, Hunter et Andresen, 2012), they can still trigger complement activation through all three known pathways (Andersen et al., 2013a). Some studies also showed that PEG is effective in preventing protein adsorption when using 10% serum, but it is not effective when using full serum or 100% plasma (Zhang et Horbett, 2009; Zhang et al., 2008b). Moreover, unlike anticoagulants such as heparin and hirudin, PEG is not able to inhibit thrombin generation. The star PEG grafted in this study presented stable low-fouling properties for up to one month in PBS, but this is clearly insufficient to demonstrate its long-term stability *in vivo*.

Dextran-based coatings were developed as an alternative to PEG coatings since their low-fouling properties were demonstrated to be as good as PEG (Dubois, Gaudreault et

Vermette, 2009; Massia, Stark et Letbetter, 2000). However, they face the same stability issues as PEG. More generally, approaches involving only low-fouling surfaces are limited due to the absence of active mechanisms to prevent coagulation and induce thrombolysis. Several authors thus used low-fouling surfaces to further immobilize anti-thrombogenic molecules such as heparin, hirudin, or other direct thrombin inhibitors (Akbar et al., 2011; Gorbet et Sefton, 2004) to create active anti-thrombogenic surfaces. We will not further discuss these approaches in detail here since it is outside the scope of the present thesis. Moreover, despite interesting results, the long-term durability of these approaches is also a concern and the only demonstrated long-term anti-thrombogenic surface to date is a stable complete endothelial layer. Low-fouling coatings can be used to create such bioactive surfaces by subsequent immobilization of biomolecules.

### **Bioactive coating on low-fouling backgrounds**

The second objective of this thesis was to co-immobilize adhesive peptides and growth factor on low-fouling backgrounds and demonstrate their benefit. Due to the availability of the coil-coil technique only for EGF (which has quite limited benefit on endothelial cells), we decided to focus this part of the study on the combination of adhesive peptides and growth factor to promote VSMC adhesion and growth for SG application. Immobilization of adhesive peptide could promote initial cell attachment on low-fouling surfaces while growth factor could further support cell growth and survival, and therefore enable achievement of a confluent cell layer. The literature demonstrates that integrin and growth factor receptors share common signaling pathways within the focal adhesion complex (Plopper et al., 1995) and the mutual activation of both the receptors through their association results in signaling synergism and reciprocal potentiation (see literature review section 1.5.4 for more details) (Comoglio, Boccaccio et Trusolino, 2003; Yamada et Even-Ram, 2002). According to some recent studies, enhanced cell migration and proliferation was observed when a variety of growth factors (such as EGF (Gobin et West, 2003b) and FGF (DeLong, Moon et West, 2005; Kolodziej et al., 2011)) co-immobilized with RGD-like peptides on PEG hydrogels. Therefore, combined immobilization of peptide and growth factors not only offers an additive effect but also possible synergistic effects, and thus there is great interest in

surfaces which combine both biomolecules. The optimization of cell-surface interaction, however, requires optimization of the ratio of both molecules. Here, the same linker was used to graft peptides and growth factor (through the coiled-coil immobilization technique) in order to modulate the relative density of these two biomolecules on the surface and study their influence on cells.

In this study, both CMD and PEG were used as an underlayer for combined immobilization, but the probable higher density of carboxyl functional groups of CMD enabled higher peptide mass on CMD compared to PEG-modified surfaces. We first demonstrated that the QCM-D technique can be used to follow changes in mass due to immobilization of biomolecules in real time and then confirmed the presence of peptide and growth factor on low-fouling surfaces. This technique has several advantages as it allows: i) using label-free biomolecules, ii) following reaction kinetics of biomolecules at the surface, iii) using flow conditions and iv) using a very low concentration of biomolecules (in the range of nM concentrations) with the mass sensitivity of  $0.9\text{ng}/\text{cm}^2$ . The QCM-D technique also enabled us to follow changes in frequency due to cell adhesion on different types of surfaces. However, there were some limitations when using this technique:

- It did not allow for quantitative analysis to compare peptide surface concentration with other studies. In addition, the conformation of grafted peptide and its availability to the cells could not be confirmed, which may explain the poor results in terms of cell adhesion. Moreover, the Q-sense E4 system did not allow us to compare more than four surfaces at a time, which makes it difficult to interpret and compare data from one set of experiments to another when using several different concentrations.
- Reproducing the results for cell adhesion experiments seemed to be difficult because the changes in resonant frequency are related not only to changes in mass but also to changes in the fractional surface coverage by the cells (Lord et al., 2006; Modin et al., 2006; Wegener et al., 2000). Another limitation was the difficulty in understanding the behavior of dissipation changes during cell adhesion and spreading on the surface. The relationship between cell attachment and energy dissipation has not been fully understood, and several authors have expressed different opinions. Rodahl and

colleagues reported that the changes in energy dissipation are due to the liquid trapped between the cell and the surface, in the cell membrane, and in the interior of each cell (Rodahl et al., 1997b), whereas Marx and coworkers suggested that the dissipation arises due to the remodeling of actin filaments (Marx et al., 2005) and Wegner et al. suggested that it is related to changes in the ECM, the actin cytoskeleton and the cell-substrate separation distance (Wegener et al., 2000).

- In addition, we were not able to draw conclusions about dissipation and frequency changes for cell experiments in the presence of serum. The reasons were unclear, but we suspect that the complex reactions and conformational changes due to the adsorption of serum proteins make it difficult to understand the trends in frequency and dissipation changes.

Unexpectedly, peptide immobilization on the CMD surface did not improve cell attachment and did not allow us to achieve the objective. These disappointing results contradict several other studies (Massia et Stark, 2001; Sabra et Vermette, 2011). Several factors influence prevention of cell adhesion when using low-fouling backgrounds, as discussed in section 4.2.3. However, we suspect two main reasons for these unfavorable results. The non-adhesive nature and strong low-fouling effect of CMD could be one reason, because previous studies and recent studies in our lab observed poor cell growth on EGF-tethered PEG (Klenkler et al., 2008) or CMD surfaces (Lequoy et al., 2014). Our QCM-D results confirmed the presence of peptide, but a lack of improvement in cell adhesion was observed. Therefore, the other possible reason could be inaccessibility of immobilized peptide to cell adhesion receptors.

**Recommendation 2:** *Peptide surface concentration may be verified using other methods such as ELISA or quantification of immobilized peptides using radio-labeled peptides. Deep understanding of peptide influence on cell response when it is immobilized on low-fouling surfaces would be required. This could be further investigated by changing several parameters such as peptide confirmation, spacer length, peptide immobilization method and combination with other peptide sequences such as PHSRN.*

Due to the lack of cell adhesion on the peptide modified PEG or CMD surfaces, it was not possible to draw a conclusion about the possible increase in bioactivity of biomolecules when grafted on a low-fouling background or on the possible additive effect or synergy between adhesive peptides and EGF. More generally, our results and the careful critical review of the literature on biomolecule grafting on low-fouling backgrounds emphasize the difficulty of achieving good cell coverage on such surfaces, probably due to the steric hindrance of the non-fouling background (Klenkler et al., 2005).

Since the creation of bioactive coating using conventional low-fouling polymers such as PEG and CMD and thereby promoting confluent cell adhesion did not work in our case, we moved on to next step to find an alternative polymer that would offer favorable properties for endothelialization on vascular graft materials. Several strategies have already been proposed to increase endothelial cell adhesion and retention on the lumen of vascular grafts, particularly through the use of RGD peptides. Although these studies in general, with or without using low-fouling polymers, showed enhanced cell adhesion and resistance to shear stress *in vitro* (Rémy et al., 2012; Tugulu et al., 2007), their *in vivo* efficiency still remains uncertain. Indeed, some studies have reported enhanced tissue response (Ferris et al., 1999; Li et al., 2003) while others showed no benefit (Petrie et al., 2008; Schliephake et al., 2002). These mitigated results may be explained by the difficulty in finding a compromise between (i) preventing non-specific protein adsorption when RGD peptides are grafted on fouling surfaces directly; and (ii) achieving sufficient RGD peptide density when using a non-fouling underlayer (Bellis, 2011). Moreover, native ECM proteins are known to stimulate a more robust integrin signaling than the isolated RGD domain and can engage multiple ligands at different time-points (Williams, 2008). However, as mentioned earlier, they increase not only endothelial cell adhesion but also the risk of thrombosis through the recruitment of platelets.

**Is CS coating an ideal compromise between low-fouling and pro- cell adhesive properties?**

The final objective of this thesis was therefore to study the possible advantages and limitations of using CS coating for developing vascular grafts. CS coating was already shown to enhance resistance to apoptosis in vascular cells (Raymond et al., 2004), prevent EGF non-specific adsorption (Lequoy et al., 2014) and improve hemocompatibility by means of electrostatic repulsion towards negatively charged blood components (Keuren et al., 2003). These interesting properties of CS coatings motivated us to evaluate its low-fouling and low-thrombogenic properties by comparing it with well-known low-fouling polymers such as PEG and CMD.

Again, the use of nitrogen-rich plasma polymerized thin film coatings (LP) (Ruiz et al., 2010; Truica-Marasescu et al., 2008) enabled us to create and achieve good surface coverage of PEG, CMD and CS. The low-fouling potential of PEG and CMD compares well with those reported in the literature. Unsworth and colleagues reported an 80% reduction of fibrinogen adsorption on surfaces with high PEG chain density (Unsworth, Sheardown et Brash, 2005), where PEG had been grafted on a gold surface through the chemisorption method. Indeed, our CMD coating almost completely prevented fibrinogen adsorption (98% reduction), whereas PEG coating reduced it by 90%. The reduction of albumin adsorption on both PEG and CMD (~ 85%) assessed by fluorescence is comparable to the results obtained by covalent coupling of PEG on silicone surfaces (Chen et al., 2005a).

Interestingly, CS low-fouling properties towards fibrinogen adsorption and platelet adhesion were as efficient as PEG and CMD, but less effective in preventing BSA and FBS adsorption. Therefore, it is believed that selective protein adsorption is responsible for good HUVEC adhesion and growth on CS surfaces. However, it is not clear which specific proteins and GFs are involved in promoting HUVEC adhesion and growth, and this could be further investigated.

The low-platelet adhesion on CS can be explained in large part by its chemical structure and composition, as detailed previously. In a way, the CS coating is a biomimetic approach to prevent platelet adhesion. Indeed, native endothelium exerts its antithrombogenic activity by expressing proteoglycans (such as heparin sulfate proteoglycans (HSPGs),

chondroitin sulfate (CS) and hyaluronic acid/hyaluronan (HA)), which serve as cofactors for antithrombin-III (AT-III) to facilitate thrombin inhibition. Moreover, these macromolecules in glycocalyx, including CS, are negatively charged, which effectively retains water and forms a lubrication layer on the EC surface and can resist platelet adhesion (Hashi et al., 2007).

*The originality of this part of the work is to highlight the selective low-fouling properties of CS and to demonstrate for the first time the ability of CS coating to promote confluent endothelium while preventing fibrinogen and platelet adhesion, thus minimizing the risks of thrombosis and occlusion in vascular grafts. This part of the work was published in the journal Biomacromolecules (Thalla et al., 2014).*

In comparison with CS coating, coatings with cell-adhesive proteins such as fibronectin, collagen or laminin (Assmann et al., 2013; De Visscher et al., 2012; Kapadia, Popowich et Kibbe, 2008; Parikh et Edelman, 2000; Wissink et al., 2000b) were also shown to enhance endothelial cell adhesion and growth, but they increase the risk of thrombosis through the recruitment of platelets. This same risk applies to LP coating, which has been shown previously to strongly improve endothelial cell adhesion and retention (Gigout et al., 2011), but was found here to be highly thrombogenic. A thrombogenic underlayer is not recommended for vascular grafts as it could lead to thrombosis if cells detach from the surface under blood flow.

The high resistance to flow-induced shear stress observed on CS coatings is also important since the *in vitro* pre-seeding of VG by ECs or EPCs has shown success (Bordenave et al., 2005; Deutsch et al., 1999), but is known to be limited by poor cell adhesion and retention under blood flow (Feugier et al., 2005). Early attempts to seed autologous ECs on ePTFE/PET-based vascular grafts showed that the majority of ECs are lost within 24 h after exposure to physiological shear stress (Herring et al., 1994; Walluscheck et al., 1996) and has led to poor clinical outcomes. Long-term outcomes of EC-seeded implants depend on the type of seeding protocol as well as the synthetic material

used. Therefore, surface coating must favor strong EC attachment and bear fluid shear stress for a long period.

Thus, the main advantage of using CS coating over other low-fouling polymers is that CS promotes strong endothelial cell attachment and growth while preventing protein adsorption and platelet adhesion and activation. Research in our lab has also shown that CS allows GF immobilization (via the coil-coil technique) with an excellent adhesion and proliferation effect on VSMC (Lequoy et al., 2014). CS may therefore be an ideal compromise for promoting endothelialization of vascular and stent and grafts. Yet CS promotes not only HUVEC but also VSMC adhesion (Charbonneau et al., 2012) and is therefore more suitable as a coating for cell pre-seeding on vascular implants.

This part of the study is limited by a lack of information regarding CS anticoagulant properties and long-term anti-platelet properties. This could be further investigated by comparing it with other anticoagulants such as heparin. However, the long-term hemocompatibility of CS coating is of less concern once the CS coating is covered by confluent endothelium, since endothelium acts as an active anti-thrombogenic surface. Further work could also be done to ensure that EC present their normal anti-thrombogenic on CS surface and do not enhance inflammation. Since endothelial cells contribute to the inflammatory process through the expression of adhesion molecules (platelet endothelial cell adhesion molecule-1 (PECAM-1), intercellular adhesion molecule-1(ICAM-1), Integrin  $\alpha$ v $\beta$ 3; vascular cell adhesion molecule-1 (VCAM-1), E-selectin, P-selectin and L-selectin), it would be important to examine whether their expression is modified by the interaction with our coating. For example, ammonia plasma treated PET and PTFE surfaces shown to improve EC adhesion and growth but also slightly up regulated expression of adhesion molecules (Pu et al., 2002a). However, on the other hand, a number of studies noted that the effect of underlying substrate on EC function is insignificant when cell confluence is reached (Kottke-Marchant, Veenstra et Marchant, 1996; McGuigan et Sefton, 2007; Wissink et al., 2001; Wissink et al., 2000a). All of these aspects could be further verified using our CS coatings.

**Recommendation 3:** *CS interactions with several heparin-binding proteins and growth factors could be investigated and compared with heparin coating in order to understand the molecular mechanism by which CS governs cell adhesion. To demonstrate whether CS has additional advantages over heparin coating, CS long-term stability, anti-clotting and thrombin generation properties could be investigated and compared with heparin coatings. These studies could also be extended to HUVEC-grown CS surfaces. Some studies highlighted neointima formation due to heparin coatings; this can be verified on CS coatings since it has structural similarities to heparin.*

## CONCLUSION

The long-term goal of this PhD thesis was to develop bioactive coatings on vascular biomaterials to either promote a stable endothelium to limit vascular graft occlusion or to favor VSMC growth to promote healing around endovascular stent grafts. Extensive research has previously been conducted on improving surface properties for the development of vascular implants, however the current coating methods lack versatility and failed to promote optimal cell interactions with the biomaterial surface. The coating methods presented in this thesis are versatile and transferable to a wide variety of biomaterials used in designing vascular implants. To allow such versatility, we took advantage of stable nitrogen-rich plasma polymerized thin film coatings (LP) that can be deposited on any biomaterial surface.

The primary aim of this project was to create a low-fouling and low-thrombogenic underlayer for bioactive coatings. The PEG-coated surfaces were not completely protein-repellent and could be further optimized. However, platelet adhesion study suggests that star PEG-modified surfaces may prevent thrombus formation. Subsequent immobilization of peptide (KQAGDV or RGD) on low-fouling polymers (PEG and CMD) did not show improvement of VSMC adhesion and therefore did not allow us to prove the concept of bioactive coating. However, this part of the work showed the potential of the QCM-D technique as a tool to follow and optimize grafting on surfaces and opened new avenues for developing bioactive coatings on low-fouling backgrounds using a combination of peptide and growth factors. Further studies would be required to understand the mechanisms involved in poor cell adhesion on peptide-immobilized low-fouling surfaces. The disappointing results obtained with low-fouling surfaces, also partly due to methodological problems, emphasize the limitations of this approach due to the difficult compromise to be found between the prevention of protein adsorption and the promotion of cell attachments on the surface.

Based on previous results obtained in the lab, we proposed CS as a potential candidate for finding this compromise and designing a non-thrombogenic coating. The final objective of

this thesis was to develop a coating that would promote a stable endothelium while preventing protein adsorption and platelet adhesion. In this context, the properties of CS coatings were compared with other low-fouling polymers such as PEG and CMD. This study demonstrates the advantages of CS as an underlayer with selective low-fouling properties that result in low fibrinogen adsorption and platelet adhesion combined with HUVEC adhesive properties. CS thus exhibits very favorable properties as a coating for vascular implants. Alone or combined with other biomolecules such as growth factors, it may promote formation of a complete and stable endothelium, and therefore prevent graft occlusion. Further studies are however required to assess CS stability, long-term non-thrombogenic properties, and the molecular mechanisms by which CS governs cell adhesion. Although there are some issues that still need to be clarified and optimization of coating methods is required, the multidisciplinary work presented in this thesis and our promising results are essential to the development of vascular implants.

## BIBLIOGRAPHY

- Absolom, D. R., L. A. Hawthorn et G. Chang. 1988. « Endothelialization of polymer surfaces ». *Journal of Biomedical Materials Research*, vol. 22, n° 4, p. 271-285.
- Adam van der Vliet, J., et Albert P. M. Boll. 1997. « Abdominal aortic aneurysm ». *The Lancet*, vol. 349, n° 9055, p. 863-866.
- Akbar, H., X. Shang, R. Perveen, M. Berryman, K. Funk, J. F. Johnson, N. N. Tandon et Y. Zheng. 2011. « Gene targeting implicates Cdc42 GTPase in GPVI and non-GPVI mediated platelet filopodia formation, secretion and aggregation ». *PloS One*, vol. 6, n° 7, p. e22117.
- Allaire, Eric, Béatrice Muscatelli-Groux, Chantal Mandet, Anne-Marie Guinault, Patrick Bruneval, Pascal Desgranges, Alexander Clowes, Didier Méllière et Jean-Pierre Becquemin. 2002. « Paracrine effect of vascular smooth muscle cells in the prevention of aortic aneurysm formation ». *Journal of Vascular Surgery*, vol. 36, n° 5, p. 1018-1026.
- Altankov, G., F. Grinnell et T. Groth. 1996. « Studies on the biocompatibility of materials: fibroblast reorganization of substratum-bound fibronectin on surfaces varying in wettability ». *Journal of Biomedical Materials Research*, vol. 30, n° 3, p. 385-91.
- Andersen, Alina J., Joshua T. Robinson, Hongjie Dai, A. Christy Hunter, Thomas L. Andresen et S. Moein Moghimi. 2013a. « Single-Walled Carbon Nanotube Surface Control of Complement Recognition and Activation ». *ACS Nano*, vol. 7, n° 2, p. 1108-1119.
- Andersen, Alina J., Barbara Windschiegl, Sibel Ilbasmis-Tamer, Ismail T. Degim, Alan Christy Hunter, Thomas L. Andresen et Seyed Moein Moghimi. 2013b. « Complement activation by PEG-functionalized multi-walled carbon nanotubes is independent of PEG molecular mass and surface density ». *Nanomedicine: Nanotechnology, Biology and Medicine*, vol. 9, n° 4, p. 469-473.
- Andersson, M., J. Andersson, A. Sellborn, M. Berglin, B. Nilsson et H. Elwing. 2005. « Quartz crystal microbalance-with dissipation monitoring (QCM-D) for real time measurements of blood coagulation density and immune complement activation on artificial surfaces ». *Biosensors and Bioelectronics*, vol. 21, n° 1, p. 79-86.
- Andrade, J. D., et V. Hlady. 1986. « Protein adsorption and materials biocompatibility: A tutorial review and suggested hypotheses ». *Biopolymers/Non-Exclusion HPLC*. Vol. 79, p. 1-63. Coll. « Advances in Polymer Science »: Springer Berlin Heidelberg.

- Assmann, Alexander, Christofer Delfs, Hiroshi Munakata, Franziska Schiffer, Kim Horstkötter, Khon Huynh, Mareike Barth, Volker R. Stoldt, Hiroyuki Kamiya, Udo Boeken, Artur Lichtenberg et Payam Akhyari. 2013. « Acceleration of autologous in vivo recellularization of decellularized aortic conduits by fibronectin surface coating ». *Biomaterials*, vol. 34, n° 25, p. 6015-6026.
- Badimon, L., V. Turitto, J. A. Rosemark, J. J. Badimon et V. Fuster. 1987. « Characterization of a tubular flow chamber for studying platelet interaction with biologic and prosthetic materials: deposition of indium 111-labeled platelets on collagen, subendothelium, and expanded polytetrafluoroethylene ». *Journal of Laboratory and Clinical Medicine*, vol. 110, n° 6, p. 706-18.
- Baldwin, Aaron D., et Kristi L. Kiick. 2010. « Polysaccharide-modified synthetic polymeric biomaterials ». *Peptide Science*, vol. 94, n° 1, p. 128-140.
- Barnthip, Naris, Hyeran Noh, Evan Leibner et Erwin A. Vogler. 2008. « Volumetric interpretation of protein adsorption: Kinetic consequences of a slowly-concentrating interphase ». *Biomaterials*, vol. 29, n° 21, p. 3062-3074.
- Barnthip, Naris, Purnendu Parhi, Avantika Golas et Erwin A. Vogler. 2009. « Volumetric interpretation of protein adsorption: Kinetics of protein-adsorption competition from binary solution ». *Biomaterials*, vol. 30, n° 33, p. 6495-6513.
- Beer, J. H., K. T. Springer et B. S. Coller. 1992. « Immobilized Arg-Gly-Asp (RGD) peptides of varying lengths as structural probes of the platelet glycoprotein IIb/IIIa receptor ». *Blood*, vol. 79, n° 1, p. 117-28.
- Bellis, Susan L. 2011. « Advantages of RGD peptides for directing cell association with biomaterials ». *Biomaterials*, vol. 32, n° 18, p. 4205-4210.
- Bennett, J. S., B. W. Berger et P. C. Billings. 2009. « The structure and function of platelet integrins ». *Journal of Thrombosis and Haemostasis*, vol. 7 Suppl 1, p. 200-5.
- Benoit, D. S., et K. S. Anseth. 2005. « The effect on osteoblast function of colocalized RGD and PHSRN epitopes on PEG surfaces ». *Biomaterials*, vol. 26, n° 25, p. 5209-20.
- Bentz, H., J. A. Schroeder et T. D. Estridge. 1998. « Improved local delivery of TGF-beta2 by binding to injectable fibrillar collagen via difunctional polyethylene glycol ». *Journal of Biomedical Materials Research*, vol. 39, n° 4, p. 539-48.
- Bernacca, G. M., M. J. Gulbransen, R. Wilkinson et D. J. Wheatley. 1998. « In vitro blood compatibility of surface-modified polyurethanes ». *Biomaterials*, vol. 19, n° 13, p. 1151-65.

- Bernd, Potzsch, Muller Jens et Rox Jutta Maria. 2006. « Developmental strategies of novel anticoagulants ». *Transfusion Med Hemotherapy*, vol. 33, p. 200-204.
- Bernfield, M., M. Gotte, P. W. Park, O. Reizes, M. L. Fitzgerald, J. Lincecum et M. Zako. 1999. « Functions of cell surface heparan sulfate proteoglycans ». *Annual Review of Biochemistry*, vol. 68, p. 729-77.
- Bernfield, M., R. Kokenyesi, M. Kato, M. T. Hinkes, J. Spring, R. L. Gallo et E. J. Lose. 1992. « Biology of the syndecans: a family of transmembrane heparan sulfate proteoglycans ». *Annual Review of Cell Biology*, vol. 8, p. 365-93.
- Besselink, G. A. J., T. Beugeling et A. Bantjes. 1993. « N-Hydroxysuccinimide-activated glycine-sepharose ». *Applied Biochemistry and Biotechnology*, vol. 43, n° 3, p. 227-246.
- Best, L. C., T. J. Martin, R. G. G. Russell et F. E. Preston. 1977. « Prostacyclin increases cyclic AMP levels and adenylate cyclase activity in platelets ». *Nature*, vol. 267, n° 5614, p. 850-852.
- Biolin, Scientific. 2014. « QCM-D technology ». < <http://www.biolinscientific.com/q-sense/technologies/> >.
- Biotextiles. 2014. « Biotextiles product development ». < <http://biotextiles2014.wordpress.com/vascular-prosthesis-for-coronary-artery-bypass/> >.
- Blackburn, Jonathan M., et Aubrey Shoko. 2011. « Protein Function Microarrays for Customised Systems-Oriented Proteome Analysis ». *Protein Microarrays*, sous la dir. de Korf, Ulrike. Vol. 785, p. 305-330. Humana Press.
- Blockmans, D., H. Deckmyn et J. Vermynen. 1995. « Platelet actuation ». *Blood Reviews*, vol. 9, n° 3, p. 143-156.
- Boland, Genevieve M., et Ronald J. Weigel. 2006. « Formation and Prevention of Postoperative Abdominal Adhesions ». *The Journal of surgical research*, vol. 132, n° 1, p. 3-12.
- Bordenave, L., Ph Fernandez, M. Rémy-Zolghadri, S. Villars, R. Daculsi et D. Midy. 2005. « In vitro endothelialized ePTFE prostheses: Clinical update 20 years after the first realization ». *Clinical Hemorheology and Microcirculation*, vol. 33, n° 3, p. 227-234.
- Boss, A., et P. Stierli. 1993. « [Dacron prosthesis dilatation. Case report and review of the literature] ». *Helvetica Chirurgica Acta*, vol. 60, n° 1-2, p. 153-6.

- Boucher, C., G. St-Laurent, M. Loignon, M. Jolicoeur, G. De Crescenzo et Y. Durocher. 2008a. « The bioactivity and receptor affinity of recombinant tagged EGF designed for tissue engineering applications is defined by the nature and position of the tags ». *Tissue Engineering: Part A*, vol. 14, n° 12, p. 2069-77.
- Boucher, Cyril, Benoît Liberelle, Mario Jolicoeur, Yves Durocher et Gregory De Crescenzo. 2009. « Epidermal Growth Factor Tethered through Coiled-Coil Interactions Induces Cell Surface Receptor Phosphorylation ». *Bioconjugate Chemistry*, vol. 20, n° 8, p. 1569-1577.
- Boucher, Cyril, Gilles St-Laurent, Martin Loignon et Mario Jolicoeur. 2008b. « The Bioactivity and Receptor Affinity of Recombinant Tagged EGF Designed for Tissue Engineering ApIs Defined by the Nature and Position of the Tagsplifications ». *Tissue Engineering: Part A*, vol. 14, n° 12.
- Boura, C., S. Muller, D. Vautier, D. Dumas, P. Schaaf, J. Claude Voegel, J. Francois Stoltz et P. Menu. 2005. « Endothelial cell--interactions with polyelectrolyte multilayer films ». *Biomaterials*, vol. 26, n° 22, p. 4568-75.
- Boxus, T., R. Touillaux, G. Dive et J. Marchand-Brynaert. 1998. « Synthesis and evaluation of RGD peptidomimetics aimed at surface bioderivatization of polymer substrates ». *Bioorganic and Medicinal Chemistry*, vol. 6, n° 9, p. 1577-95.
- Brash, J. L., et P. Ten Hove. 1993. « Protein adsorption studies on 'standard' polymeric materials ». *Journal of Biomaterials Science, Polymer Edition*, vol. 4, n° 6, p. 591-9.
- Brash, John L. 1996. « Behavior of proteins at interfaces ». *Current Opinion in Colloid & Interface Science*, vol. 1, n° 5, p. 682-688.
- Brewer, Scott H., Wilhelm R. Glomm, Marcus C. Johnson, Magne K. Knag et Stefan Franzen. 2005. « Probing BSA Binding to Citrate-Coated Gold Nanoparticles and Surfaces ». *Langmuir*, vol. 21, n° 20, p. 9303-9307.
- Brooks, P. C., R. A. Clark et D. A. Cheresh. 1994. « Requirement of vascular integrin alpha v beta 3 for angiogenesis ». *Science*, vol. 264, n° 5158, p. 569-71.
- Burkel, W. E. 1988. « The challenge of small diameter vascular grafts ». *Medical Progress Through Technology*, vol. 14, n° 3-4, p. 165-75.
- Burman, J. F., H. I. Chung, D. A. Lane, H. Philippou, A. Adami et J. C. Lincoln. 1994. « Role of factor XII in thrombin generation and fibrinolysis during cardiopulmonary bypass ». *Lancet*, vol. 344, n° 8931, p. 1192-3.
- Burmeister, Jeffrey S., Valerie Z. McKinney, William M. Reichert et George A. Truskey. 1999. « Role of endothelial cell-substrate contact area and fibronectin-receptor

- affinity in cell adhesion to HEMA/EMA copolymers ». *Journal of Biomedical Materials Research*, vol. 47, n° 4, p. 577-584.
- Byun, Y., H. A. Jacobs et S. W. Kim. 1994. « Heparin surface immobilization through hydrophilic spacers: thrombin and antithrombin III binding kinetics ». *Journal of Biomaterials Science, Polymer Edition*, vol. 6, n° 1, p. 1-13.
- Byzova, Tatiana V., Wes Kim, Ronald J. Midura et Edward F. Plow. 2000. « Activation of Integrin  $\alpha V\beta 3$  Regulates Cell Adhesion and Migration to Bone Sialoprotein ». *Experimental Cell Research*, vol. 254, n° 2, p. 299-308.
- Cao, L., P. R. Arany, Y. S. Wang et D. J. Mooney. 2009. « Promoting angiogenesis via manipulation of VEGF responsiveness with notch signaling ». *Biomaterials*, vol. 30, n° 25, p. 4085-93.
- Carpenter, G., et S. Cohen. 1979. « Epidermal growth factor ». *Annual Review of Biochemistry*, vol. 48, p. 193-216.
- Carpenter, G., et S. Cohen. 1990. « Epidermal growth factor ». *Journal of Biological Chemistry*, vol. 265, n° 14, p. 7709-7712.
- Carrell, Tom W.G., Kevin G. Burnand, Graham M.A. Wells, John M. Clements et Alberto Smith. 2002. « Stromelysin-1 (Matrix Metalloproteinase-3) and Tissue Inhibitor of Metalloproteinase-3 Are Overexpressed in the Wall of Abdominal Aortic Aneurysms ». *Circulation*, vol. 105, n° 4, p. 477-482.
- Cavalcanti-Adam, E. A., I. M. Shapiro, R. J. Composto, E. J. Macarak et C. S. Adams. 2002. « RGD Peptides Immobilized on a Mechanically Deformable Surface Promote Osteoblast Differentiation ». *Journal of Bone and Mineral Research*, vol. 17, n° 12, p. 2130-2140.
- Chao, H., D. L. Bautista, J. Litowski, R. T. Irvin et R. S. Hodges. 1998. « Use of a heterodimeric coiled-coil system for biosensor application and affinity purification ». *Journal of Chromatography. B: Biomedical Sciences and Applications*, vol. 715, n° 1, p. 307-29.
- Chao, Heman, Michael E. Houston, Suzanne Grothe, Cyril M. Kay, Maureen O'Connor-McCourt, Randall T. Irvin et Robert S. Hodges. 1996. « Kinetic Study on the Formation of a de Novo Designed Heterodimeric Coiled-Coil: Use of Surface Plasmon Resonance To Monitor the Association and Dissociation of Polypeptide Chains† ». *Biochemistry*, vol. 35, n° 37, p. 12175-12185.
- Chapman, Robert G., Emanuele Ostuni, Shuichi Takayama, R. Erik Holmlin, Lin Yan et George M. Whitesides. 2000. « Surveying for Surfaces that Resist the Adsorption of Proteins ». *Journal of the American Chemical Society*, vol. 122, n° 34, p. 8303-8304.

- Charbonneau, Cindy, Benoît Liberelle, Marie-Josée Hébert, Gregory De Crescenzo et Sophie Lerouge. 2011. « Stimulation of cell growth and resistance to apoptosis in vascular smooth muscle cells on a chondroitin sulfate/epidermal growth factor coating ». *Biomaterials*, vol. 32, n° 6, p. 1591-1600.
- Charbonneau, Cindy, Juan-Carlos Ruiz, Pauline Lequoy, Marie-Josée Hébert, Gregory De Crescenzo, Michael R. Wertheimer et Sophie Lerouge. 2012. « Chondroitin Sulfate and Epidermal Growth Factor Immobilization after Plasma Polymerization: A Versatile Anti-Apoptotic Coating to Promote Healing Around Stent Grafts ». *Macromolecular Bioscience*, vol. 12, n° 6, p. 812-821.
- Chen, Hong, Yang Chen, Heather Sheardown et Michael A. Brook. 2005a. « Immobilization of heparin on a silicone surface through a heterobifunctional PEG spacer ». *Biomaterials*, vol. 26, n° 35, p. 7418-7424.
- Chen, Hong, Zheng Zhang, Yang Chen, Michael A. Brook et Heather Sheardown. 2005b. « Protein repellent silicone surfaces by covalent immobilization of poly(ethylene oxide) ». *Biomaterials*, vol. 26, n° 15, p. 2391-2399.
- Chen, Shengfu, Lingyan Li, Christina L. Boozer et Shaoyi Jiang. 2000. « Controlled Chemical and Structural Properties of Mixed Self-Assembled Monolayers of Alkanethiols on Au(111) ». *Langmuir*, vol. 16, n° 24, p. 9287-9293.
- Chlupac, J., E. Filova et L. Bacakova. 2009. « Blood vessel replacement: 50 years of development and tissue engineering paradigms in vascular surgery ». *Physiological Research*, vol. 58 Suppl 2, p. S119-39.
- Chou, Tz-Chong, Earl Fu, Chang-Jer Wu et Jeng-Hsien Yeh. 2003. « Chitosan enhances platelet adhesion and aggregation ». *Biochemical and Biophysical Research Communications*, vol. 302, n° 3, p. 480-483.
- Chuang, W. H., et J. C. Lin. 2007. « Surface characterization and platelet adhesion studies for the mixed self-assembled monolayers with amine and carboxylic acid terminated functionalities ». *Journal of Biomedical Materials Research, Part A*, vol. 82, n° 4, p. 820-30.
- Cohen, George B., Ruibao Ren et David Baltimore. « Modular binding domains in signal transduction proteins ». *Cell*, vol. 80, n° 2, p. 237-248.
- Comoglio, Paolo M., Carla Boccaccio et Livio Trusolino. 2003. « Interactions between growth factor receptors and adhesion molecules: breaking the rules ». *Current Opinion in Cell Biology*, vol. 15, n° 5, p. 565-571.

- Conte, M. S., M. J. Mann, H. F. Simosa, K. K. Rhyhart et R. C. Mulligan. 2002. « Genetic interventions for vein bypass graft disease: a review ». *Journal of Vascular Surgery*, vol. 36, n° 5, p. 1040-52.
- Coughlin, Shaun R. 2000. « Thrombin signalling and protease-activated receptors ». *Nature*, vol. 407, n° 6801, p. 258-264.
- Courtney, J. M., et C. D. Forbes. 1994. « Thrombosis on foreign surfaces ». *British Medical Bulletin*, vol. 50, n° 4, p. 966-81.
- Crombez, M., P. Chevallier, R. C. Gaudreault, E. Petitclerc, D. Mantovani et G. Laroche. 2005. « Improving arterial prosthesis neo-endothelialization: Application of a proactive VEGF construct onto PTFE surfaces ». *Biomaterials*, vol. 26, n° 35, p. 7402-7409.
- Currie, E. P. K., W. Norde et M. A. Cohen Stuart. 2003. « Tethered polymer chains: surface chemistry and their impact on colloidal and surface properties ». *Advances in Colloid and Interface Science*, vol. 100–102, n° 0, p. 205-265.
- Dai, W., J. Belt et W. M. Saltzman. 1994. « Cell-binding peptides conjugated to poly(ethylene glycol) promote neural cell aggregation ». *Bio/Technology*, vol. 12, n° 8, p. 797-801.
- Danilov, Y. N., et R. L. Juliano. 1989. « (Arg-Gly-Asp)<sub>n</sub>-albumin conjugates as a model substratum for integrin-mediated cell adhesion ». *Experimental Cell Research*, vol. 182, n° 1, p. 186-96.
- David Richard Schmidt, Heather Waldeck, Weiyuan John Kao (1-18). 2009. *Biological Interactions on Materials Surfaces*. Coll. « Understanding and Controlling Protein, Cell, and Tissue Responses ». Springer US.
- Davie, Earl W., Kazuo Fujikawa et Walter Kisiel. 1991. « The coagulation cascade: initiation, maintenance, and regulation ». *Biochemistry*, vol. 30, n° 43, p. 10363-10370.
- Davis, Stanley S., et Lisbeth Illum. 1988. « Polymeric microspheres as drug carriers ». *Biomaterials*, vol. 9, n° 1, p. 111-112, IN5, 113-115.
- De Crescenzo, Gregory, Jennifer R. Litowski, Robert S. Hodges et Maureen D. O'Connor-McCourt. 2003. « Real-Time Monitoring of the Interactions of Two-Stranded de Novo Designed Coiled-Coils: Effect of Chain Length on the Kinetic and Thermodynamic Constants of Binding† ». *Biochemistry*, vol. 42, n° 6, p. 1754-1763.
- De, Crescenzo, Suzanne Grothe, Robert Lortie, Maria T. Debanne et Maureen O'Connor-McCourt. 2000. « Real-Time Kinetic Studies on the Interaction of Transforming

- Growth Factor  $\alpha$  with the Epidermal Growth Factor Receptor Extracellular Domain Reveal a Conformational Change Model† ». *Biochemistry*, vol. 39, n° 31, p. 9466-9476.
- De Giglio, E., L. Sabbatini, S. Colucci et G. Zambonin. 2000. « Synthesis, analytical characterization, and osteoblast adhesion properties on RGD-grafted polypyrrole coatings on titanium substrates ». *Journal of Biomaterials Science, Polymer Edition*, vol. 11, n° 10, p. 1073-83.
- de Graaf, J. C., J. D. Banga, S. Moncada, R. M. Palmer, P. G. de Groot et J. J. Sixma. 1992. « Nitric oxide functions as an inhibitor of platelet adhesion under flow conditions ». *Circulation*, vol. 85, n° 6, p. 2284-90.
- De Scheerder, I., K. Wang, K. Wilczek, D. Meuleman, R. Van Amsterdam, G. Vogel, J. Piessens et F. Van de Werf. 1997. « Experimental study of thrombogenicity and foreign body reaction induced by heparin-coated coronary stents ». *Circulation*, vol. 95, n° 6, p. 1549-53.
- De Visscher, G., L. Mesure, B. Meuris, A. Ivanova et W. Flameng. 2012. « Improved endothelialization and reduced thrombosis by coating a synthetic vascular graft with fibronectin and stem cell homing factor SDF-1alpha ». *Acta Biomaterialia*, vol. 8, n° 3, p. 1330-8.
- Dee, K. C., T. T. Andersen et R. Bizios. 1998. « Design and function of novel osteoblast-adhesive peptides for chemical modification of biomaterials ». *Journal of Biomedical Materials Research*, vol. 40, n° 3, p. 371-7.
- Dee, K. C., T. T. Anderson et R. Bizios. 1999. « Osteoblast population migration characteristics on substrates modified with immobilized adhesive peptides ». *Biomaterials*, vol. 20, n° 3, p. 221-7.
- Deepa, Sarama Sathyaseelan, Yuko Umehara, Shigeki Higashiyama, Nobuyuki Itoh et Kazuyuki Sugahara. 2002. « Specific Molecular Interactions of Oversulfated Chondroitin Sulfate E with Various Heparin-binding Growth Factors: Implications as a physiological binding partner in the brain and other tissues ». *Journal of Biological Chemistry*, vol. 277, n° 46, p. 43707-43716.
- Defawe, Olivier D, Alain Colige, Charles A Lambert, Carine Munaut, Philippe Delvenne, Charles M Lapière, Raymond Limet, Betty V Nusgens et Natzi Sakalihasan. 2003. « TIMP-2 and PAI-1 mRNA levels are lower in aneurysmal as compared to atherosclerotic abdominal aortas ». *Cardiovascular Research*, vol. 60, n° 1, p. 205-213.
- Deible, C. R., P. Petrosko, P. C. Johnson, E. J. Beckman, A. J. Russell et W. R. Wagner. 1999. « Molecular barriers to biomaterial thrombosis by modification of surface proteins with polyethylene glycol ». *Biomaterials*, vol. 20, n° 2, p. 101-9.

- Del Campo, Aránzazu, et IanJ Bruce. 2005. « Substrate Patterning and Activation Strategies for DNA Chip Fabrication ». *Immobilisation of DNA on Chips I*, sous la dir. de Wittmann, Christine. Vol. 260, p. 77-111. Coll. « Topics in Current Chemistry »: Springer Berlin Heidelberg.
- DeLong, Solitaire A., James J. Moon et Jennifer L. West. 2005. « Covalently immobilized gradients of bFGF on hydrogel scaffolds for directed cell migration ». *Biomaterials*, vol. 26, n° 16, p. 3227-3234.
- Demming, Stefanie, Claudia Lesche, Hannah Schmolke, Claus-Peter Klages et Stephanus Büttgenbach. 2011. « Characterization of long-term stability of hydrophilized PEG-grafted PDMS within different media for biotechnological and pharmaceutical applications ». *physica status solidi (a)*, vol. 208, n° 6, p. 1301-1307.
- Desai, Mital, Alexander M. Seifalian et George Hamilton. 2011. « Role of prosthetic conduits in coronary artery bypass grafting ». *European Journal of Cardio-Thoracic Surgery*, vol. 40, n° 2, p. 394-398.
- Desai, Neil P., et Jeffrey A. Hubbell. 1991. « Biological responses to polyethylene oxide modified polyethylene terephthalate surfaces ». *Journal of Biomedical Materials Research*, vol. 25, n° 7, p. 829-843.
- Deutsch, Manfred, Johann Meinhart, Teddy Fischlein, Petra Preiss et Peter Zilla. 1999. « Clinical autologous in vitro endothelialization of infrainguinal ePTFE grafts in 100 patients: A 9-year experience ». *Surgery*, vol. 126, n° 5, p. 847-855.
- Diener, J. L., H. A. Daniel Lagasse, D. Duerschmied, Y. Merhi, J. F. Tanguay, R. Hutabarat, J. Gilbert, D. D. Wagner et R. Schaub. 2009. « Inhibition of von Willebrand factor-mediated platelet activation and thrombosis by the anti-von Willebrand factor A1-domain aptamer ARC1779 ». *Journal of Thrombosis and Haemostasis*, vol. 7, n° 7, p. 1155-62.
- Dillow, Angela K., Sarah E. Ochsenhirt, James B. McCarthy, Gregg B. Fields et Matthew Tirrell. 2001. « Adhesion of  $\alpha 5\beta 1$  receptors to biomimetic substrates constructed from peptide amphiphiles ». *Biomaterials*, vol. 22, n° 12, p. 1493-1505.
- Dimitrievska, S., M. Maire, G. A. Diaz-Quijada, L. Robitaille, A. Ajji, L. Yahia, M. Moreno, Y. Merhi et M. N. Bureau. 2011. « Low thrombogenicity coating of nonwoven PET fiber structures for vascular grafts ». *Macromolecular Bioscience*, vol. 11, n° 4, p. 493-502.
- Dinbergs, Iveta D., Larry Brown et Elazer R. Edelman. 1996. « Cellular Response to Transforming Growth Factor- $\beta 1$  and Basic Fibroblast Growth Factor Depends on Release Kinetics and Extracellular Matrix Interactions ». *Journal of Biological Chemistry*, vol. 271, n° 47, p. 29822-29829.

- Discher, Dennis E., Paul Janmey et Yu-li Wang. 2005. « Tissue Cells Feel and Respond to the Stiffness of Their Substrate ». *Science*, vol. 310, n° 5751, p. 1139-1143.
- Dong, C. L., S. Y. Li, Y. Wang, Y. Dong, J. Z. Tang, J. C. Chen et G. Q. Chen. 2012a. « The cytocompatibility of polyhydroxyalkanoates coated with a fusion protein of PHA repressor protein (PhaR) and Lys-Gln-Ala-Gly-Asp-Val (KQAGDV) polypeptide ». *Biomaterials*, vol. 33, n° 9, p. 2593-9.
- Dong, Cui-Ling, Shi-Yan Li, Yang Wang, Ying Dong, James Zhenggui Tang, Jin-Chun Chen et Guo-Qiang Chen. 2012b. « The cytocompatibility of polyhydroxyalkanoates coated with a fusion protein of PHA repressor protein (PhaR) and Lys-Gln-Ala-Gly-Asp-Val (KQAGDV) polypeptide ». *Biomaterials*, vol. 33, n° 9, p. 2593-2599.
- Douglas A. Lauffenburger, Jennifer J. Linderman. 1993. *Receptors: Models for Binding, Trafficking and signaling*. New York: Oxford University Press.
- Drumheller, P. D., D. L. Elbert et J. A. Hubbell. 1994. « Multifunctional poly(ethylene glycol) semi-interpenetrating polymer networks as highly selective adhesive substrates for bioadhesive peptide grafting ». *Biotechnology and Bioengineering*, vol. 43, n° 8, p. 772-80.
- Drumheller, P. D., et J. A. Hubbell. 1994. « Polymer networks with grafted cell adhesion peptides for highly biospecific cell adhesive substrates ». *Analytical Biochemistry*, vol. 222, n° 2, p. 380-8.
- Dubiel, Evan A., et Patrick Vermette. 2012. « Solution composition impacts fibronectin immobilization on carboxymethyl-dextran surfaces and INS-1 insulin secretion ». *Colloids and Surfaces B: Biointerfaces*, vol. 95, n° 0, p. 266-273.
- Dubois, Justin, Charles Gaudreault et Patrick Vermette. 2009. « Biofouling of dextran-derivative layers investigated by quartz crystal microbalance ». *Colloids and Surfaces B: Biointerfaces*, vol. 71, n° 2, p. 293-299.
- E. Niklason, Laura, et Robert S. Langer. 1997. « Advances in tissue engineering of blood vessels and other tissues ». *Transplant Immunology*, vol. 5, n° 4, p. 303-306.
- Earp, H. S., T. L. Dawson, X. Li et H. Yu. 1995. « Heterodimerization and functional interaction between EGF receptor family members: a new signaling paradigm with implications for breast cancer research ». *Breast Cancer Research and Treatment*, vol. 35, n° 1, p. 115-32.
- Ebara, Mitsuhiro, Masayuki Yamato, Takao Aoyagi, Akihiko Kikuchi, Kiyotaka Sakai et Teruo Okano. 2008. « A Novel Approach to Observing Synergy Effects of PHSRN on Integrin-RGD Binding Using Intelligent Surfaces ». *Advanced Materials*, vol. 20, n° 16, p. 3034-3038.

- Eckmann, David M., Irene Y. Tsai, Nancy Tomczyk, John W. Weisel et Russell J. Composto. 2013. « Hyaluronan and dextran modified tubes resist cellular activation with blood contact ». *Colloids and Surfaces B: Biointerfaces*, vol. 108, n° 0, p. 44-51.
- Edwards, W. S., W. F. Holdefer et M. Mohtashemi. 1966. « The importance of proper caliber of lumen in femoral-popliteal artery reconstruction ». *Surgery, Gynecology and Obstetrics*, vol. 122, n° 1, p. 37-40.
- Elbert, Donald L., et Jeffrey A. Hubbell. 2001. « Conjugate Addition Reactions Combined with Free-Radical Cross-Linking for the Design of Materials for Tissue Engineering ». *Biomacromolecules*, vol. 2, n° 2, p. 430-441.
- Ellis, H., B. J. Moran, J. N. Thompson, M. C. Parker, M. S. Wilson, D. Menzies, A. McGuire, A. M. Lower, R. J. Hawthorn, F. O'Brien, S. Buchan et A. M. Crowe. 1999. « Adhesion-related hospital readmissions after abdominal and pelvic surgery: a retrospective cohort study ». *Lancet*, vol. 353, n° 9163, p. 1476-80.
- Engbers, G. H. M., L. Dost, W. E. Hennink, P. A. M. M. Aarts, J. J. Sixma et J. Feijen. 1987. « An in vitro study of the adhesion of blood platelets onto vascular catheters. Part I ». *Journal of Biomedical Materials Research*, vol. 21, n° 5, p. 613-627.
- Ertel, S. I., B. D. Ratner et T. A. Horbett. 1990. « Radiofrequency plasma deposition of oxygen-containing films on polystyrene and poly(ethylene terephthalate) substrates improves endothelial cell growth ». *Journal of Biomedical Materials Research*, vol. 24, n° 12, p. 1637-59.
- Esko, JD, et RJ linhardt. 2009. « Proteins that bind Glycosaminoglycans ». *Essentials of Glycobiology*, sous la dir. de A, Varki, et Cummings RD. New York: Cold Spring Harbor Laboratory Press.
- Fadlallah, Hicham. 2013. « Influence de revêtements bioactifs sur les cellules endothéliales: vers des prothèse vasculaires non thrombotiques ». École de technologie supérieure.
- Fairbrother, Wayne J., Mark A. Champe, Hans W. Christinger, Bruce A. Keyt et Melissa A. Starovasnik. 1998. « Solution structure of the heparin-binding domain of vascular endothelial growth factor ». *Structure*, vol. 6, n° 5, p. 637-648.
- Faucheux, N., R. Tzoneva, M. D. Nagel et T. Groth. 2006. « The dependence of fibrillar adhesions in human fibroblasts on substratum chemistry ». *Biomaterials*, vol. 27, n° 2, p. 234-45.
- Ferris, D. M., G. D. Moodie, P. M. Dimond, C. W. D. Giorani, M. G. Ehrlich et R. F. Valentini. 1999. « RGD-coated titanium implants stimulate increased bone formation in vivo ». *Biomaterials*, vol. 20, n° 23-24, p. 2323-2331.

- Feugier, P., R. A. Black, J. A. Hunt et T. V. How. 2005. « Attachment, morphology and adherence of human endothelial cells to vascular prosthesis materials under the action of shear stress ». *Biomaterials*, vol. 26, n° 13, p. 1457-66.
- Fields, G. B., J. L. Lauer, Y. Dori, P. Forns, Y. C. Yu et M. Tirrell. 1998. « Protein-like molecular architecture: biomaterial applications for inducing cellular receptor binding and signal transduction ». *Biopolymers*, vol. 47, n° 2, p. 143-51.
- Fittkau, M. H., P. Zilla, D. Bezuidenhout, M. P. Lutolf, P. Human, J. A. Hubbell et N. Davies. 2005. « The selective modulation of endothelial cell mobility on RGD peptide containing surfaces by YIGSR peptides ». *Biomaterials*, vol. 26, n° 2, p. 167-74.
- Freeman, Inbar, Alon Kedem et Smadar Cohen. 2008. « The effect of sulfation of alginate hydrogels on the specific binding and controlled release of heparin-binding proteins ». *Biomaterials*, vol. 29, n° 22, p. 3260-3268.
- Fressinaud, E., A. B. Federici, G. Castaman, C. Rothschild, F. Rodeghiero, H. R. Baumgartner, P. M. Mannucci et D. Meyer. 1994. « The role of platelet von Willebrand factor in platelet adhesion and thrombus formation: a study of 34 patients with various subtypes of type I von Willebrand disease ». *British Journal of Haematology*, vol. 86, n° 2, p. 327-32.
- Furie, B., et B. C. Furie. 2008. « Mechanisms of thrombus formation ». *New England Journal of Medicine*, vol. 359, n° 9, p. 938-49.
- Garcia, A. J., M. D. Vega et D. Boettiger. 1999. « Modulation of cell proliferation and differentiation through substrate-dependent changes in fibronectin conformation ». *Molecular Biology of the Cell*, vol. 10, n° 3, p. 785-98.
- Gasteier, Peter, Anna Reska, Petra Schulte, Jochen Salber, Andreas Offenhäusser, Martin Moeller et Jürgen Groll. 2007. « Surface Grafting of PEO-Based Star-Shaped Molecules for Bioanalytical and Biomedical Applications ». *Macromolecular Bioscience*, vol. 7, n° 8, p. 1010-1023.
- Geiger, B., et A. Bershadsky. 2001a. « Assembly and mechanosensory function of focal contacts ». *Current Opinion in Cell Biology*, vol. 13, n° 5, p. 584-92.
- Geiger, Benjamin, et Alexander Bershadsky. 2001b. « Assembly and mechanosensory function of focal contacts ». *Current Opinion in Cell Biology*, vol. 13, n° 5, p. 584-592.
- Giesen, P. L., U. Rauch, B. Bohrmann, D. Kling, M. Roque, J. T. Fallon, J. J. Badimon, J. Himber, M. A. Riederer et Y. Nemerson. 1999. « Blood-borne tissue factor: another

- view of thrombosis ». *Proceedings of the National Academy of Sciences of the United States of America*, vol. 96, n° 5, p. 2311-5.
- Gigout, Anne, Juan-Carlos Ruiz, Michael R. Wertheimer, Mario Jolicoeur et Sophie Lerouge. 2011. « Nitrogen-Rich Plasma-Polymerized Coatings on PET and PTFE Surfaces Improve Endothelial Cell Attachment and Resistance to Shear Flow ». *Macromolecular Bioscience*, vol. 11, n° 8, p. 1110-1119.
- Gobin, A. S., et J. L. West. 2003a. « Effects of epidermal growth factor on fibroblast migration through biomimetic hydrogels ». *Biotechnology Progress*, vol. 19, n° 6, p. 1781-5.
- Gobin, Andrea S., et Jennifer L. West. 2003b. « Effects of Epidermal Growth Factor on Fibroblast Migration through Biomimetic Hydrogels ». *Biotechnology Progress*, vol. 19, n° 6, p. 1781-1785.
- Gombotz, Wayne R., Wang Guanghui, Thomas A. Horbett et Allan S. Hoffman. 1991. « Protein adsorption to poly(ethylene oxide) surfaces ». *Journal of Biomedical Materials Research*, vol. 25, n° 12, p. 1547-1562.
- Goodwin, S. C., H. C. Yoon, G. Chen, P. Abdel-Sayed, M. M. Costantino, S. M. Bonilla et E. Nishimura. 2003. « Intense inflammatory reaction to heparin polymer coated intravascular Palmaz stents in porcine arteries compared to uncoated Palmaz stents ». *Cardiovascular and Interventional Radiology*, vol. 26, n° 2, p. 158-67.
- Gorbet, Maud B., et Michael V. Sefton. 2004. « Biomaterial-associated thrombosis: roles of coagulation factors, complement, platelets and leukocytes ». *Biomaterials*, vol. 25, n° 26, p. 5681-5703.
- Gorman, R. C., N. Ziats, A. K. Rao, N. Gikakis, L. Sun, M. M. Khan, N. Stenach, S. Sapatnekar, V. Chouhan, J. H. Gorman, 3rd, S. Niewiarowski, R. W. Colman, J. M. Anderson et L. H. Edmunds, Jr. 1996. « Surface-bound heparin fails to reduce thrombin formation during clinical cardiopulmonary bypass ». *Journal of Thoracic and Cardiovascular Surgery*, vol. 111, n° 1, p. 1-11; discussion 11-2.
- Graham, N. B., et M. E. McNeill. 1984. « Hydrogels for controlled drug delivery ». *Biomaterials*, vol. 5, n° 1, p. 27-36.
- Gray, Jeffrey J. 2004. « The interaction of proteins with solid surfaces ». *Current Opinion in Structural Biology*, vol. 14, n° 1, p. 110-115.
- Greisler, H. P. 1990. « Interactions at the blood/material interface ». *Annals of Vascular Surgery*, vol. 4, n° 1, p. 98-103.

- Grigoriou, V., I. M. Shapiro, E. A. Cavalcanti-Adam, R. J. Composto, P. Ducheyne et C. S. Adams. 2005. « Apoptosis and survival of osteoblast-like cells are regulated by surface attachment ». *Journal of Biological Chemistry*, vol. 280, n° 3, p. 1733-9.
- Groll, J., Z. Ademovic, T. Ameringer, D. Klee et M. Moeller. 2004a. « Biofunctional coatings from star PEG - A comparison to linear PEG and applications ». In. (Sydney, NSW 2001, Australia), p. 21. Coll. « Transactions - 7th World Biomaterials Congress »: Biomaterials 2004 Congress Managers.
- Groll, Juergen, Thomas Ameringer, Joachim P. Spatz et Martin Moeller. 2005a. « Ultrathin coatings from isocyanate-terminated star PEG prepolymers: Layer formation and characterization ». *Langmuir*, vol. 21, n° 5, p. 1991-1999.
- Groll, Juergen, Joerg Fiedler, Erika Engelhard, Thomas Ameringer, Stefano Tugulu, Harm-Anton Klok, Rolf E. Brenner et Martin Moeller. 2005b. « A novel star PEG-derived surface coating for specific cell adhesion ». *Journal of Biomedical Materials Research Part A*, vol. 74A, n° 4, p. 607-617.
- Groll, Juergen, Wulf Haubensak, Thomas Ameringer et Martin Moeller. 2005c. « Ultrathin Coatings from Isocyanate Terminated Star PEG Prepolymers: Patterning of Proteins on the Layers ». *Langmuir*, vol. 21, n° 7, p. 3076-3083.
- Groll, Jürgen, Elza V. Amirgoulova, Thomas Ameringer, Colin D. Heyes, Carlheinz Röcker, G. Ulrich Nienhaus et Martin Möller. 2004b. « Biofunctionalized, Ultrathin Coatings of Cross-Linked Star-Shaped Poly(ethylene oxide) Allow Reversible Folding of Immobilized Proteins ». *Journal of the American Chemical Society*, vol. 126, n° 13, p. 4234-4239.
- Groll, Jürgen, et Martin Moeller. 2010. « Star Polymer Surface Passivation for Single-Molecule Detection ». *Methods in Enzymology*, vol. Volume 472, p. 1-18.
- Grutter, M. G., J. P. Priestle, J. Rahuel, H. Grossenbacher, W. Bode, J. Hofsteenge et S. R. Stone. 1990. « Crystal structure of the thrombin-hirudin complex: a novel mode of serine protease inhibition ». *EMBO Journal*, vol. 9, n° 8, p. 2361-5.
- Guidoin, R., N. Chakfe, S. Maurel, T. How, M. Batt, M. Marois et C. Gosselin. 1993. « Expanded polytetrafluoroethylene arterial prostheses in humans: histopathological study of 298 surgically excised grafts ». *Biomaterials*, vol. 14, n° 9, p. 678-93.
- Hackeng, T. M., L. F. Maurissen, E. Castoldi et J. Rosing. 2009. « Regulation of TFPI function by protein S ». *Journal of Thrombosis and Haemostasis*, vol. 7 Suppl 1, p. 165-8.

- Hadjizadeh, Afra, et Charles J. Doillon. 2010. « Directional migration of endothelial cells towards angiogenesis using polymer fibres in a 3D co-culture system ». *Journal of Tissue Engineering and Regenerative Medicine*, vol. 4, n° 7, p. 524-531.
- Hadjizadeh, Afra, Charles J. Doillon et Patrick Vermette. 2007. « Bioactive Polymer Fibers to Direct Endothelial Cell Growth in a Three-Dimensional Environment ». *Biomacromolecules*, vol. 8, n° 3, p. 864-873.
- Hansson, K. M., S. Tosatti, J. Isaksson, J. Wettero, M. Textor, T. L. Lindahl et P. Tengvall. 2005a. « Whole blood coagulation on protein adsorption-resistant PEG and peptide functionalised PEG-coated titanium surfaces ». *Biomaterials*, vol. 26, n° 8, p. 861-72.
- Hansson, Kenny M., Samuele Tosatti, Joakim Isaksson, Jonas Wetterö, Marcus Textor, Tomas L. Lindahl et Pentti Tengvall. 2005b. « Whole blood coagulation on protein adsorption-resistant PEG and peptide functionalised PEG-coated titanium surfaces ». *Biomaterials*, vol. 26, n° 8, p. 861-872.
- Harrison, P. 2005. « Platelet function analysis ». *Blood Reviews*, vol. 19, n° 2, p. 111-23.
- Hashi, Craig K., Nikita Derugin, Randall Raphael R. Janairo, Randall Lee, David Schultz, Jeffrey Lotz et Song Li. 2010. « Antithrombogenic Modification of Small-Diameter Microfibrous Vascular Grafts ». *Arteriosclerosis, Thrombosis, and Vascular Biology*, vol. 30, n° 8, p. 1621-1627.
- Hashi, Craig K., Yiqian Zhu, Guo-Yuan Yang, William L. Young, Benjamin S. Hsiao, Karin Wang, Benjamin Chu et Song Li. 2007. « Antithrombogenic property of bone marrow mesenchymal stem cells in nanofibrous vascular grafts ». *Proceedings of the National Academy of Sciences*, vol. 104, n° 29, p. 11915-11920.
- Hemmersam, A. G., M. Foss, J. Chevallier et F. Besenbacher. 2005. « Adsorption of fibrinogen on tantalum oxide, titanium oxide and gold studied by the QCM-D technique ». *Colloids and Surfaces B: Biointerfaces*, vol. 43, n° 3-4, p. 208-15.
- Hermanson, Greg T. 2008. « Chapter 28 - Bioconjugation in the Study of Protein Interactions ». *Bioconjugate Techniques (Second Edition)*, sous la dir. de Hermanson, Greg T., p. 1003-1039. New York: Academic Press.
- Hern, D. L., et J. A. Hubbell. 1998. « Incorporation of adhesion peptides into nonadhesive hydrogels useful for tissue resurfacing ». *Journal of Biomedical Materials Research*, vol. 39, n° 2, p. 266-76.
- Herring, Malcolm, John Smith, Michael Dalsing, John Glover, Rebecca Compton, Karen Etchberger et Terrell Zollinger. 1994. « Endothelial seeding of polytetrafluoroethylene femoral popliteal bypasses: The failure of low-density seeding to improve patency ». *Journal of Vascular Surgery*, vol. 20, n° 4, p. 650-655.

- Herron, G. S., E. Unemori, M. Wong, J. H. Rapp, M. H. Hibbs et R. J. Stoney. 1991. « Connective tissue proteinases and inhibitors in abdominal aortic aneurysms. Involvement of the vasa vasorum in the pathogenesis of aortic aneurysms ». *Arteriosclerosis and Thrombosis*, vol. 11, n° 6, p. 1667-77.
- Herrwerth, Sascha, Wolfgang Eck, Sven Reinhardt et Michael Grunze. 2003. « Factors that Determine the Protein Resistance of Oligoether Self-Assembled Monolayers – Internal Hydrophilicity, Terminal Hydrophilicity, and Lateral Packing Density ». *Journal of the American Chemical Society*, vol. 125, n° 31, p. 9359-9366.
- Hersel, Ulrich, Claudia Dahmen et Horst Kessler. 2003. « RGD modified polymers: biomaterials for stimulated cell adhesion and beyond ». *Biomaterials*, vol. 24, n° 24, p. 4385-4415.
- Higuchi, Akon, Kazunobu Shirano, Masaharu Harashima, Boo Ok Yoon, Mariko Hara, Mitsuo Hattori et Kazuo Imamura. 2002. « Chemically modified polysulfone hollow fibers with vinylpyrrolidone having improved blood compatibility ». *Biomaterials*, vol. 23, n° 13, p. 2659-2666.
- Hirano, Y., M. Okuno, T. Hayashi, K. Goto et A. Nakajima. 1993. « Cell-attachment activities of surface immobilized oligopeptides RGD, RGDS, RGDV, RGDV, and YIGSR toward five cell lines ». *Journal of Biomaterials Science, Polymer Edition*, vol. 4, n° 3, p. 235-43.
- Hlady, V., J. Buijs et H. P. Jennissen. 1999. « Methods for studying protein adsorption ». *Methods in Enzymology*, vol. 309, p. 402-29.
- Hlady, V. V., et J. Buijs. 1996. « Protein adsorption on solid surfaces ». *Current Opinion in Biotechnology*, vol. 7, n° 1, p. 72-7.
- Hoening, M. R., G. R. Campbell, B. E. Rolfe et J. H. Campbell. 2005. « Tissue-engineered blood vessels: alternative to autologous grafts? ». *Arteriosclerosis, Thrombosis, and Vascular Biology*, vol. 25, n° 6, p. 1128-34.
- Hoffmann, Jan, Jurgen Groll, Jean Heuts, Haitao Rong, Doris Klee, Gerhard Ziemer, Martin Moeller et Hans P. Wendel. 2006. « Blood cell and plasma protein repellent properties of Star-PEG-modified surfaces ». *Journal of Biomaterials Science, Polymer Edition*, vol. 17, n° 9, p. 985-996.
- Hofmann, Siegfried. 2013. « Qualitative Analysis (Principle and Spectral Interpretation) ». *Auger- and X-Ray Photoelectron Spectroscopy in Materials Science*. Vol. 49, p. 43-76. Coll. « Springer Series in Surface Sciences »: Springer Berlin Heidelberg.

- Holladay, L. A., C. R. Savage, Jr., S. Cohen et D. Puett. 1976. « Conformation and unfolding thermodynamics of epidermal growth factor and derivatives ». *Biochemistry*, vol. 15, n° 12, p. 2624-33.
- Holmer, E., K. Kurachi et G. Soderstrom. 1981. « The molecular-weight dependence of the rate-enhancing effect of heparin on the inhibition of thrombin, factor Xa, factor IXa, factor XIa, factor XIIa and kallikrein by antithrombin ». *Biochemical Journal*, vol. 193, n° 2, p. 395-400.
- Holmes, Dennis R., Shixiong Liao, William C. Parks et Robert W. Hompson. « Medial neovascularization in abdominal aortic aneurysms: A histopathologic marker of aneurysmal degeneration with pathophysiologic implications ». *Journal of Vascular Surgery*, vol. 21, n° 5, p. 761-772.
- Hook, F., B. Kasemo, T. Nylander, C. Fant, K. Sott et H. Elwing. 2001. « Variations in coupled water, viscoelastic properties, and film thickness of a Mefp-1 protein film during adsorption and cross-linking: a quartz crystal microbalance with dissipation monitoring, ellipsometry, and surface plasmon resonance study ». *Analytical Chemistry*, vol. 73, n° 24, p. 5796-804.
- Höök, F., M. Rodahl, P. Brzezinski et B. Kasemo. 1998. « Energy Dissipation Kinetics for Protein and Antibody–Antigen Adsorption under Shear Oscillation on a Quartz Crystal Microbalance ». *Langmuir*, vol. 14, n° 4, p. 729-734.
- Höök, F., J. Vörös, M. Rodahl, R. Kurrat, P. Böni, J. J. Ramsden, M. Textor, N. D. Spencer, P. Tengvall, J. Gold et B. Kasemo. 2002. « A comparative study of protein adsorption on titanium oxide surfaces using in situ ellipsometry, optical waveguide lightmode spectroscopy, and quartz crystal microbalance/dissipation ». *Colloids and Surfaces B: Biointerfaces*, vol. 24, n° 2, p. 155-170.
- Höök, Fred Chalmers tekniska högskola Department of Applied Physics Chalmers tekniska högskola Department of Biochemistry, et Biophysics. 1997. *Development of a novel QCM technique for protein adsorption studies*. Göteborg: Department of Biochemistry and Biophysics and Department of Applied Physics, Chalmers University of Technology.
- Höök, Fredrik, Bengt Kasemo, Tommy Nylander, Camilla Fant, Kristin Sott et Hans Elwing. 2001. « Variations in Coupled Water, Viscoelastic Properties, and Film Thickness of a Mefp-1 Protein Film during Adsorption and Cross-Linking: A Quartz Crystal Microbalance with Dissipation Monitoring, Ellipsometry, and Surface Plasmon Resonance Study ». *Analytical Chemistry*, vol. 73, n° 24, p. 5796-5804.
- Huang, He, Jing Xie, Xiaoli Liu, Lin Yuan, Shasha Wang, Songxi Guo, Haoran Yu, Hong Chen, Yanliang Zhang et Xiaohu Wu. 2011. « Conformational Changes of Protein

- Adsorbed on Tailored Flat Substrates with Different Chemistries ». *Chemphyschem*, vol. 12, n° 18, p. 3642-3646.
- Hubbell, J. A., S. P. Massia et P. D. Drumheller. 1992. « Surface-grafted cell-binding peptides in tissue engineering of the vascular graft ». *Annals of the New York Academy of Sciences*, vol. 665, p. 253-8.
- Hubbell, Jeffrey A. 1993. « Chapter 11 Pharmacologic modification of materials ». *Cardiovascular Pathology*, vol. 2, n° 3, Supplement, p. 121-127.
- Huynh, T., G. Abraham, J. Murray, K. Brockbank, P. O. Hagen et S. Sullivan. 1999. « Remodeling of an acellular collagen graft into a physiologically responsive neovessel ». *Nature Biotechnology*, vol. 17, n° 11, p. 1083-6.
- Hyman, William A. 1985. « Contemporary biomaterials ». *Annals of Biomedical Engineering*, vol. 13, n° 5, p. 469-471.
- Irvine, D. J., A. M. Mayes et L. Griffith-Cima. 1996. « Self-Consistent Field Analysis of Grafted Star Polymers ». *Macromolecules*, vol. 29, n° 18, p. 6037-6043.
- Irvine, D. J., A. M. Mayes, S. K. Satija, J. G. Barker, S. J. Sofia-Allgor et L. G. Griffith. 1998. « Comparison of tethered star and linear poly(ethylene oxide) for control of biomaterials surface properties ». *Journal of Biomedical Materials Research*, vol. 40, n° 3, p. 498-509.
- Irvine, Darrell J., Kerri-Ann Hue, Anne M. Mayes et Linda G. Griffith. 2002. « Simulations of Cell-Surface Integrin Binding to Nanoscale-Clustered Adhesion Ligands ». *Biophysical Journal*, vol. 82, n° 1, p. 120-132.
- Irvine, Darrell J., Anne M. Mayes et Linda G. Griffith. 2000. « Nanoscale Clustering of RGD Peptides at Surfaces Using Comb Polymers. 1. Synthesis and Characterization of Comb Thin Films ». *Biomacromolecules*, vol. 2, n° 1, p. 85-94.
- Irvine, Darrell J., Anne-Valerie G. Ruzette, Anne M. Mayes et Linda G. Griffith. 2001. « Nanoscale Clustering of RGD Peptides at Surfaces Using Comb Polymers. 2. Surface Segregation of Comb Polymers in Polylactide ». *Biomacromolecules*, vol. 2, n° 2, p. 545-556.
- Ito, Y., M. Kajihara et Y. Imanishi. 1991. « Materials for enhancing cell adhesion by immobilization of cell-adhesive peptide ». *Journal of Biomedical Materials Research*, vol. 25, n° 11, p. 1325-37.
- Ito, Yoshihiro. 1998. « Tissue engineering by immobilized growth factors ». *Materials Science and Engineering: C*, vol. 6, n° 4, p. 267-274.

- Iuliano, D. J., S. S. Saavedra et G. A. Truskey. 1993. « Effect of the conformation and orientation of adsorbed fibronectin on endothelial cell spreading and the strength of adhesion ». *Journal of Biomedical Materials Research*, vol. 27, n° 8, p. 1103-13.
- Jain, G., M. Allon, S. Saddekni, J. F. Barker et I. D. Maya. 2009. « Does heparin coating improve patency or reduce infection of tunneled dialysis catheters? ». *Clinical Journal of the American Society of Nephrology*, vol. 4, n° 11, p. 1787-90.
- Jao, Win-Chun, Chien-Hong Lin, Jui-Yuan Hsieh, Yi-Hsing Yeh, Chia-Yi Liu et Ming-Chien Yang. 2010. « Effect of immobilization of polysaccharides on the biocompatibility of poly(butyleneadipate-co-terephthalate) films ». *Polymers for Advanced Technologies*, vol. 21, n° 8, p. 543-553.
- Jensen, L. P., M. Lepantalo, J. E. Fossdal, O. C. Roder, B. S. Jensen, M. S. Madsen, O. Grenager, H. Fasting, H. O. Myhre, N. Baekgaard, O. M. Nielsen, U. Helgstrand et T. V. Schroeder. 2007. « Dacron or PTFE for above-knee femoropopliteal bypass. a multicenter randomised study ». *European Journal of Vascular and Endovascular Surgery*, vol. 34, n° 1, p. 44-9.
- Jeon, S. I., et J. D. Andrade. 1991. « Protein—surface interactions in the presence of polyethylene oxide: II. Effect of protein size ». *Journal of Colloid and Interface Science*, vol. 142, n° 1, p. 159-166.
- Jeon, S. I., J. H. Lee, J. D. Andrade et P. G. De Gennes. 1991. « Protein—surface interactions in the presence of polyethylene oxide: I. Simplified theory ». *Journal of Colloid and Interface Science*, vol. 142, n° 1, p. 149-158.
- Jeschke, B., J. Meyer, A. Jonczyk, H. Kessler, P. Adamietz, N. M. Meenen, M. Kantlehner, C. Goepfert et B. Nies. 2002. « RGD-peptides for tissue engineering of articular cartilage ». *Biomaterials*, vol. 23, n° 16, p. 3455-63.
- Jin, Z., W. Feng, S. Zhu, H. Sheardown et J. L. Brash. 2009. « Protein-resistant polyurethane via surface-initiated atom transfer radical polymerization of oligo(ethylene glycol) methacrylate ». *Journal of Biomedical Materials Research, Part A*, vol. 91, n° 4, p. 1189-201.
- Jo, S., P. S. Engel et A. G. Mikos. 2000. « Synthesis of poly(ethylene glycol)-tethered poly(propylene fumarate) and its modification with GRGD peptide ». *Polymer*, vol. 41, n° 21, p. 7595-7604.
- Jonasson, L., J. Holm, O. Skalli, G. Bondjers et G. K. Hansson. 1986. « Regional accumulations of T cells, macrophages, and smooth muscle cells in the human atherosclerotic plaque ». *Arteriosclerosis*, vol. 6, n° 2, p. 131-8.

- Jones, S. M., et A. Kazlauskas. 2000. « Connecting signaling and cell cycle progression in growth factor-stimulated cells ». *Oncogene*, vol. 19, n° 49, p. 5558-67.
- Jorissen, Robert N., Francesca Walker, Normand Pouliot, Thomas P. J. Garrett, Colin W. Ward et Antony W. Burgess. 2003. « Epidermal growth factor receptor: mechanisms of activation and signalling ». *Experimental Cell Research*, vol. 284, n° 1, p. 31-53.
- Jung, I. K., J. W. Bae, W. S. Choi, J. H. Choi et K. D. Park. 2009. « Surface graft polymerization of poly(ethylene glycol) methacrylate onto polyurethane via thiol-ene reaction: preparation and characterizations ». *Journal of Biomaterials Science, Polymer Edition*, vol. 20, n° 10, p. 1473-82.
- Kakisis, J. D., C. D. Liapis, C. Breuer et B. E. Sumpio. 2005. « Artificial blood vessel: the Holy Grail of peripheral vascular surgery ». *Journal of Vascular Surgery*, vol. 41, n° 2, p. 349-54.
- Kämmerer, P. W., M. Heller, J. Brieger, M. O. Klein, B. Al-Nawas et M. Gabriel. 2011. « Immobilisation of linear and cyclic RGD-peptides on titanium surfaces and their impact on endothelial cell adhesion and proliferation ». *European cells & materials*, vol. 21, p. 364-372.
- Kannan, R. Y., H. J. Salacinski, P. E. Butler, G. Hamilton et A. M. Seifalian. 2005. « Current status of prosthetic bypass grafts: a review ». *Journal of Biomedical Materials Research, Part B: Applied Biomaterials*, vol. 74, n° 1, p. 570-81.
- Kantlehner, M., P. Schaffner, D. Finsinger, J. Meyer, A. Jonczyk, B. Diefenbach, B. Nies, G. Holzemann, S. L. Goodman et H. Kessler. 2000. « Surface coating with cyclic RGD peptides stimulates osteoblast adhesion and proliferation as well as bone formation ». *ChemBioChem*, vol. 1, n° 2, p. 107-14.
- Kapadia, Muneera R., Daniel A. Popowich et Melina R. Kibbe. 2008. « Modified Prosthetic Vascular Conduits ». *Circulation*, vol. 117, n° 14, p. 1873-1882.
- Katz, B. Z., E. Zamir, A. Bershadsky, Z. Kam, K. M. Yamada et B. Geiger. 2000. « Physical state of the extracellular matrix regulates the structure and molecular composition of cell-matrix adhesions ». *Molecular Biology of the Cell*, vol. 11, n° 3, p. 1047-60.
- Keselowsky, Benjamin G., David M. Collard et Andrés J. García. 2003. « Surface chemistry modulates fibronectin conformation and directs integrin binding and specificity to control cell adhesion ». *Journal of Biomedical Materials Research Part A*, vol. 66A, n° 2, p. 247-259.
- Keselowsky, Benjamin G., David M. Collard et Andrés J. García. 2005. « Integrin binding specificity regulates biomaterial surface chemistry effects on cell differentiation ». *Proceedings of the National Academy of Sciences*, vol. 102, n° 17, p. 5953-5957.

- Keuren, Jeffrey F. W., Simone J. H. Wielders, George M. Willems, Marco Morra, Linda Cahalan, Patrick Cahalan et Theo Lindhout. 2003. « Thrombogenicity of polysaccharide-coated surfaces ». *Biomaterials*, vol. 24, n° 11, p. 1917-1924.
- Keys, Kelley Britton, Fotios M. Andreopoulos et Nikolaos A. Peppas. 1998. « Poly(ethylene glycol) Star Polymer Hydrogels ». *Macromolecules*, vol. 31, n° 23, p. 8149-8156.
- Kidane, Argaw, Gary C. Lantz, Seongbong Jo et Kinam Park. 1999. « Surface modification with PEO-containing triblock copolymer for improved biocompatibility: In vitro and ex vivo studies ». *Journal of Biomaterials Science, Polymer Edition*, vol. 10, n° 10, p. 1089-1105.
- Kingshott, Peter, et Hans J. Griesser. 1999. « Surfaces that resist bioadhesion ». *Current Opinion in Solid State and Materials Science*, vol. 4, n° 4, p. 403-412.
- Kjellen, L, et U Lindahl. 1991. « Proteoglycans: Structures and Interactions ». *Annual Review of Biochemistry*, vol. 60, n° 1, p. 443-475.
- Klenkler, B. J., H. Chen, Y. Chen, M. A. Brook et H. Sheardown. 2008. « A high-density PEG interfacial layer alters the response to an EGF tethered polydimethylsiloxane surface ». *Journal of Biomaterials Science, Polymer Edition*, vol. 19, n° 11, p. 1411-24.
- Klenkler, B. J., M. Griffith, C. Becerril, J. A. West-Mays et H. Sheardown. 2005. « EGF-grafted PDMS surfaces in artificial cornea applications ». *Biomaterials*, vol. 26, n° 35, p. 7286-7296.
- Knudsen, H. L., et J. A. Frangos. 1997. « Role of cytoskeleton in shear stress-induced endothelial nitric oxide production ». *American Journal of Physiology*, vol. 273, n° 1 Pt 2, p. H347-55.
- Koenig, A. L., V. Gambillara et D. W. Grainger. 2003a. « Correlating fibronectin adsorption with endothelial cell adhesion and signaling on polymer substrates ». *Journal of Biomedical Materials Research, Part A*, vol. 64, n° 1, p. 20-37.
- Koenig, Andrea L., Veronica Gambillara et David W. Grainger. 2003b. « Correlating fibronectin adsorption with endothelial cell adhesion and signaling on polymer substrates ». *Journal of Biomedical Materials Research Part A*, vol. 64A, n° 1, p. 20-37.
- Kolodziej, Christopher M., Sung Hye Kim, Rebecca M. Broyer, Sina S. Saxer, Caitlin G. Decker et Heather D. Maynard. 2011. « Combination of Integrin-Binding Peptide and Growth Factor Promotes Cell Adhesion on Electron-Beam-Fabricated Patterns ». *Journal of the American Chemical Society*, vol. 134, n° 1, p. 247-255.

- Koo, L. Y., D. J. Irvine, A. M. Mayes, D. A. Lauffenburger et L. G. Griffith. 2002. « Co-regulation of cell adhesion by nanoscale RGD organization and mechanical stimulus ». *Journal of Cell Science*, vol. 115, n° 7, p. 1423-1433.
- Kottke-Marchant, K., A. A. Veenstra et R. E. Marchant. 1996. « Human endothelial cell growth and coagulant function varies with respect to interfacial properties of polymeric substrates ». *Journal of Biomedical Materials Research*, vol. 30, n° 2, p. 209-20.
- Krishnan, A., C. A. Siedlecki et E. A. Vogler. 2004. « Mixology of protein solutions and the Vroman effect ». *Langmuir*, vol. 20, n° 12, p. 5071-8.
- Kuhl, Philip R., et Linda G. Griffith-Cima. 1996. « Tethered epidermal growth factor as a paradigm for growth factor-induced stimulation from the solid phase ». *Nature Medicine*, vol. 2, n° 9, p. 1022-1027.
- L'Heureux, N., N. Dusserre, A. Marini, S. Garrido, L. de la Fuente et T. McAllister. 2007. « Technology Insight: The evolution of tissue-engineered vascular grafts - From research to clinical practice ». *Nature Clinical Practice Cardiovascular Medicine*, vol. 4, n° 7, p. 389-395.
- Lahann, Jörg, Wilhelm Plüster, Doris Klee, Hans-Gregor Gattner et Hartwig Höcker. 2001. « Immobilization of the thrombin inhibitor r-hirudin conserving its biological activity ». *Journal of Materials Science: Materials in Medicine*, vol. 12, n° 9, p. 807-810.
- Lamallice, Laurent, Fabrice Le Boeuf et Jacques Huot. 2007. « Endothelial Cell Migration During Angiogenesis ». *Circulation Research*, vol. 100, n° 6, p. 782-794.
- Larm, O, R Larsson et P Olsson. 1983. « A New Non-Thrombogenic Surface Prepared by Selective Covalent Binding of Heparin Via a Modified Reducing Terminal Residue. ». *Biomaterials Medical Devices and Artificial Organs*, vol. 11, p. 161-73.
- Lateef, S. S., S. Boateng, T. J. Hartman, C. A. Crot, B. Russell et L. Hanley. 2002. « GRGDSP peptide-bound silicone membranes withstand mechanical flexing in vitro and display enhanced fibroblast adhesion ». *Biomaterials*, vol. 23, n° 15, p. 3159-68.
- Lax, I., A. K. Mitra, C. Ravera, D. R. Hurwitz, M. Rubinstein, A. Ullrich, R. M. Stroud et J. Schlessinger. 1991. « Epidermal growth factor (EGF) induces oligomerization of soluble, extracellular, ligand-binding domain of EGF receptor. A low resolution projection structure of the ligand-binding domain ». *Journal of Biological Chemistry*, vol. 266, n° 21, p. 13828-33.
- LeBaron, R. G., et K. A. Athanasiou. 2000. « Extracellular matrix cell adhesion peptides: functional applications in orthopedic materials ». *Tissue Engineering*, vol. 6, n° 2, p. 85-103.

- Leckband, D., S. Sheth et A. Halperin. 1999. « Grafted poly(ethylene oxide) brushes as nonfouling surface coatings ». *Journal of Biomaterials Science, Polymer Edition*, vol. 10, n° 10, p. 1125-1147.
- Lee, H., et T. G. Park. 2002. « Preparation and characterization of mono-PEGylated epidermal growth factor: evaluation of in vitro biologic activity ». *Pharmaceutical Research*, vol. 19, n° 6, p. 845-51.
- Lee, Jin Ho, Hai Bang Lee et Joseph D. Andrade. 1995. « Blood compatibility of polyethylene oxide surfaces ». *Progress in Polymer Science*, vol. 20, n° 6, p. 1043-1079.
- Lee, K., E. A. Silva et D. J. Mooney. 2011. « Growth factor delivery-based tissue engineering: general approaches and a review of recent developments ». *J R Soc Interface*, vol. 8, n° 55, p. 153-70.
- Leonard, E. F., et L. Vroman. 1991. « Is the Vroman effect of importance in the interaction of blood with artificial materials? ». *Journal of Biomaterials Science, Polymer Edition*, vol. 3, n° 1, p. 95-107.
- Lequoy, Pauline, Benoît Liberelle, Gregory De Crescenzo et Sophie Lerouge. 2014. « Additive Benefits of Chondroitin Sulfate and Oriented Tethered Epidermal Growth Factor for Vascular Smooth Muscle Cell Survival ». *Macromolecular Bioscience*, vol. 10.1002/mabi.201300443.
- Lerouge, Sophie, Annie Major, Pierre-Luc Girault-Lauriault, Marc-André Raymond, Patrick Laplante, Gilles Soulez, Fackson Mwale, Michael R. Wertheimer et Marie-Josée Hébert. 2007. « Nitrogen-rich coatings for promoting healing around stent-grafts after endovascular aneurysm repair ». *Biomaterials*, vol. 28, n° 6, p. 1209-1217.
- Lewandowska, K., E. Pergament, C. N. Sukenik et L. A. Culp. 1992. « Cell-type-specific adhesion mechanisms mediated by fibronectin adsorbed to chemically derivatized substrata ». *Journal of Biomedical Materials Research*, vol. 26, n° 10, p. 1343-63.
- Lhoest, J. B., E. Detrait, P. van den Bosch de Aguilar et P. Bertrand. 1998. « Fibronectin adsorption, conformation, and orientation on polystyrene substrates studied by radiolabeling, XPS, and ToF SIMS ». *Journal of Biomedical Materials Research*, vol. 41, n° 1, p. 95-103.
- Li, F., D. Carlsson, C. Lohmann, E. Suuronen, S. Vascotto, K. Kobuch, H. Sheardown, R. Munger, M. Nakamura et M. Griffith. 2003. « Cellular and nerve regeneration within a biosynthetic extracellular matrix for corneal transplantation ». *Proceedings of the National Academy of Sciences of the United States of America*, vol. 100, n° 26, p. 15346-15351.

- Li, J., M. Ding, Q. Fu, H. Tan, X. Xie et Y. Zhong. 2008. « A novel strategy to graft RGD peptide on biomaterials surfaces for endothelialization of small-diameter vascular grafts and tissue engineering blood vessel ». *Journal of Materials Science: Materials in Medicine*, vol. 19, n° 7, p. 2595-603.
- Li, S., et J. J. Henry. 2011a. « Nonthrombogenic approaches to cardiovascular bioengineering ». *Annual Review of Biomedical Engineering*, vol. 13, p. 451-75.
- Li, Song, et Jeffrey J.D. Henry. 2011b. « Nonthrombogenic Approaches to Cardiovascular Bioengineering ». *Annual Review of Biomedical Engineering*, vol. 13, n° 1, p. 451-475.
- Liberelle, Benoit, Cyril Boucher, Jingkui Chen, Mario Jolicoeur, Yves Durocher et Gregory De Crescenzo. 2010. « Impact of Epidermal Growth Factor Tethering Strategy on Cellular Response ». *Bioconjugate Chemistry*, vol. 21, n° 12, p. 2257-2266.
- Liberelle, Benoît, Abderrazzak Merzouki et Gregory De Crescenzo. 2013. « Immobilized carboxymethylated dextran coatings for enhanced ELISA ». *Journal of Immunological Methods*, vol. 389, n° 1-2, p. 38-44.
- Lin, H. B., W. Sun, D. F. Mosher, C. Garcia-Echeverria, K. Schaufelberger, P. I. Lelkes et S. L. Cooper. 1994. « Synthesis, surface, and cell-adhesion properties of polyurethanes containing covalently grafted RGD-peptides ». *Journal of Biomedical Materials Research*, vol. 28, n° 3, p. 329-42.
- Lin, H. B., Z. C. Zhao, C. Garcia-Echeverria, D. H. Rich et S. L. Cooper. 1992. « Synthesis of a novel polyurethane co-polymer containing covalently attached RGD peptide ». *Journal of Biomaterials Science, Polymer Edition*, vol. 3, n° 3, p. 217-27.
- Lin, Y. S., S. S. Wang, T. W. Chung, Y. H. Wang, S. H. Chiou, J. J. Hsu, N. K. Chou, K. H. Hsieh et S. H. Chu. 2001. « Growth of endothelial cells on different concentrations of Gly-Arg-Gly-Asp photochemically grafted in polyethylene glycol modified polyurethane ». *Artificial Organs*, vol. 25, n° 8, p. 617-21.
- Lopez-Candales, A., D. R. Holmes, S. Liao, M. J. Scott, S. A. Wickline et R. W. Thompson. 1997. « Decreased vascular smooth muscle cell density in medial degeneration of human abdominal aortic aneurysms ». *American Journal of Pathology*, vol. 150, n° 3, p. 993-1007.
- Lord, M. S., C. Modin, M. Foss, M. Duch, A. Simmons, F. S. Pedersen, B. K. Milthorpe et F. Besenbacher. 2006. « Monitoring cell adhesion on tantalum and oxidised polystyrene using a quartz crystal microbalance with dissipation ». *Biomaterials*, vol. 27, n° 26, p. 4529-37.

- Love, J. Christopher, Lara A. Estroff, Jennah K. Kriebel, Ralph G. Nuzzo et George M. Whitesides. 2005. « Self-Assembled Monolayers of Thiolates on Metals as a Form of Nanotechnology ». *Chemical Reviews*, vol. 105, n° 4, p. 1103-1170.
- Ludwig, Nicholas S., Colin Yoder, Michael McConney, Terrence G. Vargo et Khalid N. Kader. 2006. « Directed type IV collagen self-assembly on hydroxylated PTFE ». *Journal of Biomedical Materials Research Part A*, vol. 78A, n° 3, p. 615-619.
- Lytle, B. W., F. D. Loop, D. M. Cosgrove, N. B. Ratliff, K. Easley et P. C. Taylor. 1985. « Long-term (5 to 12 years) serial studies of internal mammary artery and saphenous vein coronary bypass grafts ». *Journal of Thoracic and Cardiovascular Surgery*, vol. 89, n° 2, p. 248-58.
- Mackman, Nigel. 2008. « Triggers, targets and treatments for thrombosis ». *Nature*, vol. 451, n° 7181, p. 914-918.
- Maheshwari, G., G. Brown, D. A. Lauffenburger, A. Wells et L. G. Griffith. 2000. « Cell adhesion and motility depend on nanoscale RGD clustering ». *Journal of Cell Science*, vol. 113 ( Pt 10), p. 1677-86.
- Major, Terry C., et Joan A. Keiser. 1997. « Inhibition of Cell Growth: Effects of the Tyrosine Kinase Inhibitor CGP 53716 ». *Journal of Pharmacology and Experimental Therapeutics*, vol. 283, n° 1, p. 402-410.
- Maldonado, B A, et L T Furcht. 1995. « Epidermal growth factor stimulates integrin-mediated cell migration of cultured human corneal epithelial cells on fibronectin and arginine-glycine-aspartic acid peptide ». *Investigative Ophthalmology and Visual Science*, vol. 36, n° 10, p. 2120-6.
- Mammen, Mathai, Seok-Ki Choi et George M. Whitesides. 1998. « Polyvalent Interactions in Biological Systems: Implications for Design and Use of Multivalent Ligands and Inhibitors ». *Angewandte Chemie International Edition*, vol. 37, n° 20, p. 2754-2794.
- Mann, B. K., A. S. Gobin, A. T. Tsai, R. H. Schmedlen et J. L. West. 2001. « Smooth muscle cell growth in photopolymerized hydrogels with cell adhesive and proteolytically degradable domains: synthetic ECM analogs for tissue engineering ». *Biomaterials*, vol. 22, n° 22, p. 3045-51.
- Mann, B. K., R. H. Schmedlen et J. L. West. 2001. « Tethered-TGF-beta increases extracellular matrix production of vascular smooth muscle cells ». *Biomaterials*, vol. 22, n° 5, p. 439-44.
- Mann, B. K., et J. L. West. 2002. « Cell adhesion peptides alter smooth muscle cell adhesion, proliferation, migration, and matrix protein synthesis on modified surfaces and in

- polymer scaffolds ». *Journal of Biomedical Materials Research*, vol. 60, n° 1, p. 86-93.
- Marchant, R. E., S. Yuan et G. Szakalas-Gratzl. 1994. « Interactions of plasma proteins with a novel polysaccharide surfactant physisorbed to polyethylene ». *Journal of biomaterials science. Polymer edition*, vol. 6, n° 6, p. 549-564.
- Marconi, W., F. Benvenuti et A. Piozzi. 1997. « Covalent bonding of heparin to a vinyl copolymer for biomedical applications ». *Biomaterials*, vol. 18, n° 12, p. 885-890.
- Marx, K. A., T. Zhou, A. Montrone, D. McIntosh et S. J. Braunhut. 2005. « Quartz crystal microbalance biosensor study of endothelial cells and their extracellular matrix following cell removal: Evidence for transient cellular stress and viscoelastic changes during detachment and the elastic behavior of the pure matrix ». *Analytical Biochemistry*, vol. 343, n° 1, p. 23-34.
- Massia, S. P., et J. A. Hubbell. 1990a. « Covalent surface immobilization of Arg-Gly-Asp- and Tyr-Ile-Gly-Ser-Arg-containing peptides to obtain well-defined cell-adhesive substrates ». *Analytical Biochemistry*, vol. 187, n° 2, p. 292-301.
- Massia, S. P., et J. A. Hubbell. 1990b. « Covalently attached GRGD on polymer surfaces promotes biospecific adhesion of mammalian cells ». *Annals of the New York Academy of Sciences*, vol. 589, p. 261-70.
- Massia, S. P., et J. A. Hubbell. 1991. « An RGD spacing of 440 nm is sufficient for integrin alpha V beta 3-mediated fibroblast spreading and 140 nm for focal contact and stress fiber formation ». *Journal of Cell Biology*, vol. 114, n° 5, p. 1089-100.
- Massia, S. P., et J. Stark. 2001. « Immobilized RGD peptides on surface-grafted dextran promote biospecific cell attachment ». *Journal of Biomedical Materials Research*, vol. 56, n° 3, p. 390-9.
- Massia, Stephen P. 1999. « Cell-extracellular matrix interactions relevant to vascular tissue engineering ». *Tissue Engineering of Vascular Prosthetic Grafts*.
- Massia, Stephen P., John Stark et David S. Letbetter. 2000. « Surface-immobilized dextran limits cell adhesion and spreading ». *Biomaterials*, vol. 21, n° 22, p. 2253-2261.
- McArthur, Sally L., Keith M. McLean, Peter Kingshott, Heather A. W. St John, Ronald C. Chatelier et Hans J. Griesser. 2000. « Effect of polysaccharide structure on protein adsorption ». *Colloids and Surfaces B: Biointerfaces*, vol. 17, n° 1, p. 37-48.
- McCarty, O. J., Y. Zhao, N. Andrew, L. M. Machesky, D. Staunton, J. Frampton et S. P. Watson. 2004. « Evaluation of the role of platelet integrins in fibronectin-dependent

spreading and adhesion ». *Journal of Thrombosis and Haemostasis*, vol. 2, n° 10, p. 1823-33.

McGuigan, A. P., et M. V. Sefton. 2007. « The influence of biomaterials on endothelial cell thrombogenicity ». *Biomaterials*, vol. 28, n° 16, p. 2547-71.

McInnes, C., et B. D. Sykes. 1997. « Growth factor receptors: structure, mechanism, and drug discovery ». *Biopolymers*, vol. 43, n° 5, p. 339-66.

Merck. 2014. « Treatment of Atherosclerosis ». < <http://www.pharmaceutical-networking.com/merck-mk-0524b-treatment-of-atherosclerosis/> >.

Merhi, Yahye, Martin King et Robert Guidoin. 1997. « Acute thrombogenicity of intact and injured natural blood conduits versus synthetic conduits: Neutrophil, platelet, and fibrin(ogen) adsorption under various shear-rate conditions ». *Journal of Biomedical Materials Research*, vol. 34, n° 4, p. 477-485.

Michel, E. C., V. Montano, P. Chevallier, A. Labbe-Barrere, D. Letourneur et D. Mantovani. 2014. « Dextran grafting on PTFE surface for cardiovascular applications ». *Biomatter*, vol. 4, n° 1.

Michiels, C. 2003. « Endothelial cell functions ». *Journal of Cellular Physiology*, vol. 196, n° 3, p. 430-43.

Mikulikova, R., S. Moritz, T. Gumpenberger, M. Olbrich, C. Romanin, L. Bacakova, V. Svorcik et J. Heitz. 2005. « Cell microarrays on photochemically modified polytetrafluoroethylene ». *Biomaterials*, vol. 26, n° 27, p. 5572-80.

Miyagawa, J., S. Higashiyama, S. Kawata, Y. Inui, S. Tamura, K. Yamamoto, M. Nishida, T. Nakamura, S. Yamashita, Y. Matsuzawa et al. 1995. « Localization of heparin-binding EGF-like growth factor in the smooth muscle cells and macrophages of human atherosclerotic plaques ». *Journal of Clinical Investigation*, vol. 95, n° 1, p. 404-11.

Modin, C., A. L. Stranne, M. Foss, M. Duch, J. Justesen, J. Chevallier, L. K. Andersen, A. G. Hemmersam, F. S. Pedersen et F. Besenbacher. 2006. « QCM-D studies of attachment and differential spreading of pre-osteoblastic cells on Ta and Cr surfaces ». *Biomaterials*, vol. 27, n° 8, p. 1346-54.

Veillez sélectionner un type de document autre que « Generic » afin de faire afficher la référence bibliographique.

Monchaux, Emmanuelle, et Patrick Vermette. 2007. « Development of Dextran-Derivative Arrays To Identify Physicochemical Properties Involved in Biofouling from Serum ». *Langmuir*, vol. 23, n° 6, p. 3290-3297.

- Morpurgo, M., E. A. Bayer et M. Wilchek. 1999. « N-hydroxysuccinimide carbonates and carbamates are useful reactive reagents for coupling ligands to lysines on proteins ». *Journal of Biochemical and Biophysical Methods*, vol. 38, n° 1, p. 17-28.
- Motlagh, D., J. Yang, K. Y. Lui, A. R. Webb et G. A. Ameer. 2006. « Hemocompatibility evaluation of poly(glycerol-sebacate) in vitro for vascular tissue engineering ». *Biomaterials*, vol. 27, n° 24, p. 4315-24.
- Mulloy, B., P. A. S. Mourão et E. Gray. 2000. « Structure/function studies of anticoagulant sulphated polysaccharides using NMR ». *Journal of Biotechnology*, vol. 77, n° 1, p. 123-135.
- Murray, Christopher J. L., et Alan D. Lopez. 1997. « Global mortality, disability, and the contribution of risk factors: Global Burden of Disease Study ». *The Lancet*, vol. 349, n° 9063, p. 1436-1442.
- Murschel, Frederic, Benoit Liberelle, Gilles St-Laurent, Mario Jolicoeur, Yves Durocher et Gregory De Crescenzo. 2013. « Coiled-coil-mediated grafting of bioactive vascular endothelial growth factor ». *Acta Biomaterialia*, vol. 9, n° 6, p. 6806-6813.
- Murugesan, G., M. A. Ruegsegger, F. Kligman, R. E. Marchant et K. Kottke-Marchant. 2002. « Integrin-dependent interaction of human vascular endothelial cells on biomimetic peptide surfactant polymers ». *Cell Commun Adhes*, vol. 9, n° 2, p. 59-73.
- « Muscle anatomy of the body ». 2014. < <http://physiologie-musculaire.cwebh.org/anatomie-musculaire-du-corps> >.
- Nakajima, Naoki, et Yoshito Ikada. 1995. « Mechanism of Amide Formation by Carbodiimide for Bioconjugation in Aqueous Media ». *Bioconjugate Chemistry*, vol. 6, n° 1, p. 123-130.
- Nakaoka, Ryusuke, Yoshiaki Hirano, DavidJ Mooney, Toshie Tsuchiya et Atsuko Matsuoka. 2013. « Study on the potential of RGD- and PHSRN-modified alginates as artificial extracellular matrices for engineering bone ». *Journal of Artificial Organs*, vol. 16, n° 3, p. 284-293.
- Neff, J. A., K. D. Caldwell et P. A. Tresco. 1998. « A novel method for surface modification to promote cell attachment to hydrophobic substrates ». *Journal of Biomedical Materials Research*, vol. 40, n° 4, p. 511-9.
- Neff, J. A., P. A. Tresco et K. D. Caldwell. 1999. « Surface modification for controlled studies of cell-ligand interactions ». *Biomaterials*, vol. 20, n° 23-24, p. 2377-2393.
- Neufeld, G., T. Cohen, S. Gengrinovitch et Z. Poltorak. 1999a. « Vascular endothelial growth factor (VEGF) and its receptors ». *FASEB Journal*, vol. 13, n° 1, p. 9-22.

- Neufeld, Gera, Tzafra Cohen, Stela Gengrinovitch et Zoya Poltorak. 1999b. « Vascular endothelial growth factor (VEGF) and its receptors ». *The FASEB Journal*, vol. 13, n° 1, p. 9-22.
- Noh, Hyeran, et Erwin A. Vogler. 2007. « Volumetric interpretation of protein adsorption: Competition from mixtures and the Vroman effect ». *Biomaterials*, vol. 28, n° 3, p. 405-422.
- Nojiri, C., T. Okano, H. A. Jacobs, K. D. Park, S. F. Mohammad, D. B. Olsen et S. W. Kim. 1990a. « Blood compatibility of PEO grafted polyurethane and HEMA/styrene block copolymer surfaces ». *Journal of Biomedical Materials Research*, vol. 24, n° 9, p. 1151-71.
- Nojiri, C., K. D. Park, D. W. Grainger, H. A. Jacobs, T. Okano, H. Koyanagi et S. W. Kim. 1990b. « In vivo nonthrombogenicity of heparin immobilized polymer surfaces ». *ASAIO Transactions*, vol. 36, n° 3, p. M168-72.
- Nolan, Timothy M., Nick Di Girolamo, Minas T. Coroneo et Denis Wakefield. 2004. « Proliferative Effects of Heparin-Binding Epidermal Growth Factor-like Growth Factor on Pterygium Epithelial Cells and Fibroblasts ». *Investigative Ophthalmology and Visual Science*, vol. 45, n° 1, p. 110-113.
- Nomura, T., et O. Hattori. 1980. « Determination of micromolar concentrations of cyanide in solution with a piezoelectric detector ». *Analytica Chimica Acta*, vol. 115, n° 0, p. 323-326.
- Norde, Willem. 1996. « Driving forces for protein adsorption at solid surfaces ». *Macromolecular Symposia*, vol. 103, n° 1, p. 5-18.
- Normanno, N., C. Bianco, L. Strizzi, M. Mancino, M. R. Maiello, A. De Luca, F. Caponigro et D. S. Salomon. 2005. « The ErbB receptors and their ligands in cancer: An overview ». *Current Drug Targets*, vol. 6, n° 3, p. 243-257.
- O'Shannessy, D. J., M. Brigham-Burke et K. Peck. 1992. « Immobilization chemistries suitable for use in the BIAcore surface plasmon resonance detector ». *Analytical Biochemistry*, vol. 205, n° 1, p. 132-6.
- Ogi, H., H. Nagai, Y. Fukunishi, M. Hirao et M. Nishiyama. 2009. « 170-MHz electrodeless quartz crystal microbalance biosensor: capability and limitation of higher frequency measurement ». *Analytical Chemistry*, vol. 81, n° 19, p. 8068-73.
- Ohl, A., et K. Schröder. 1999. « Plasma-induced chemical micropatterning for cell culturing applications: a brief review ». *Surface and Coatings Technology*, vol. 116-119, n° 0, p. 820-830.

- Olayioye, M. A., R. M. Neve, H. A. Lane et N. E. Hynes. 2000. « The ErbB signaling network: Receptor heterodimerization in development and cancer ». *EMBO Journal*, vol. 19, n° 13, p. 3159-3167.
- Osterberg, E., K. Bergstrom, K. Holmberg, T. P. Schuman, J. A. Riggs, N. L. Burns, J. M. Van Alstine et J. M. Harris. 1995. « Protein-rejecting ability of surface-bound dextran in end-on and side-on configurations: comparison to PEG ». *Journal of Biomedical Materials Research*, vol. 29, n° 6, p. 741-7.
- Österberg, Eva, Karin Bergström, Krister Holmberg, Jennifer A. Riggs, J. M. Van Alstine, Thomas P. Schuman, Norman L. Burns et J. Milton Harris. 1993. « Comparison of polysaccharide and poly(ethylene glycol) coatings for reduction of protein adsorption on polystyrene surfaces ». *Colloids and Surfaces A: Physicochemical and Engineering Aspects*, vol. 77, n° 2, p. 159-169.
- Ostuni, Emanuele, Robert G. Chapman, R. Erik Holmlin, Shuichi Takayama et George M. Whitesides. 2001. « A Survey of Structure–Property Relationships of Surfaces that Resist the Adsorption of Protein ». *Langmuir*, vol. 17, n° 18, p. 5605-5620.
- Owen, G. R., D. O. Meredith, I. ap Gwynn et R. G. Richards. 2005. « Focal adhesion quantification - a new assay of material biocompatibility? Review ». *Eur Cell Mater*, vol. 9, p. 85-96; discussion 85-96.
- Pakalns, T., K. L. Haverstick, G. B. Fields, J. B. McCarthy, D. L. Mooradian et M. Tirrell. 1999a. « Cellular recognition of synthetic peptide amphiphiles in self-assembled monolayer films ». *Biomaterials*, vol. 20, n° 23-24, p. 2265-79.
- Pakalns, Teika, Kraig L. Haverstick, Gregg B. Fields, James B. McCarthy, Daniel L. Mooradian et Matthew Tirrell. 1999b. « Cellular recognition of synthetic peptide amphiphiles in self-assembled monolayer films ». *Biomaterials*, vol. 20, n° 23-24, p. 2265-2279.
- Palatianos, G. M., L. H. Edmunds, Jr., D. J. Cohen et L. W. Stephenson. 1983. « Extracorporeal left ventricular assistance with prostacyclin and heparinized centrifugal pump ». *Annals of Thoracic Surgery*, vol. 35, n° 5, p. 504-15.
- Palmaz, Julio C. 1998. « Review of Polymeric Graft Materials for Endovascular Applications ». *Journal of Vascular and Interventional Radiology*, vol. 9, n° 1, p. 7-13.
- Pande, Gopal. 2000. « The role of membrane lipids in regulation of integrin functions ». *Current Opinion in Cell Biology*, vol. 12, n° 5, p. 569-574.
- Panetti, T. S., D. F. Hannah, C. Avraamides, J. P. Gaughan, C. Marcinkiewicz, A. Huttenlocher et D. F. Mosher. 2004. « Extracellular matrix molecules regulate

- endothelial cell migration stimulated by lysophosphatidic acid ». *Journal of Thrombosis and Haemostasis*, vol. 2, n° 9, p. 1645-1656.
- Papaioannou, T. G., et C. Stefanadis. 2005. « Vascular wall shear stress: basic principles and methods ». *Hellenic Journal of Cardiology. Hellenike Kardiologike Epitheorese*, vol. 46, n° 1, p. 9-15.
- Pardee, A. B. 1989. « G1 events and regulation of cell proliferation ». *Science*, vol. 246, n° 4930, p. 603-8.
- Parikh, Sahil A., et Elazer R. Edelman. 2000. « Endothelial cell delivery for cardiovascular therapy ». *Advanced Drug Delivery Reviews*, vol. 42, n° 1-2, p. 139-161.
- Park, K., F. W. Mao et H. Park. 1990. « Morphological characterization of surface-induced platelet activation ». *Biomaterials*, vol. 11, n° 1, p. 24-31.
- Park, K., H. S. Shim, M. K. Dewanjee et N. L. Eigler. 2000. « In vitro and in vivo studies of PEO-grafted blood-contacting cardiovascular prostheses ». *Journal of Biomaterials Science, Polymer Edition*, vol. 11, n° 11, p. 1121-34.
- Patel, S., J. Tsang, G. M. Harbers, K. E. Healy et S. Li. 2007. « Regulation of endothelial cell function by GRGDSP peptide grafted on interpenetrating polymers ». *Journal of Biomedical Materials Research, Part A*, vol. 83, n° 2, p. 423-33.
- Pearson, J. D., J. S. Carleton et J. L. Gordon. 1980. « Metabolism of adenine nucleotides by ectoenzymes of vascular endothelial and smooth-muscle cells in culture ». *Biochemical Journal*, vol. 190, n° 2, p. 421-9.
- Petersen, S., M. Gattermayer et M. Biesalski. 2011. « Hold on at the Right Spot: Bioactive Surfaces for the Design of Live-Cell Micropatterns ». *Bioactive Surfaces*, sous la dir. de Börner, Hans G., et Jean-Francois Lutz. Vol. 240, p. 35-78. Coll. « Advances in Polymer Science »: Springer Berlin Heidelberg.
- Petit, V., et J. P. Thiery. 2000. « Focal adhesions: structure and dynamics ». *Biology of the Cell*, vol. 92, n° 7, p. 477-94.
- Petrie, Timothy A., Jenny E. Raynor, Catherine D. Reyes, Kellie L. Burns, David M. Collard et Andrés J. García. 2008. « The effect of integrin-specific bioactive coatings on tissue healing and implant osseointegration ». *Biomaterials*, vol. 29, n° 19, p. 2849-2857.
- Pfaff, Martin. 1997. « Recognition Sites of RGD-Dependent Integrins ». *Integrin-Ligand Interaction*. p. 101-121. Springer US.

- Phaneuf, Matthew D., Scott A. Berceli, Martin J. Bide, William G. Quist et Frank W. LoGerfo. 1997. « Covalent linkage of recombinant hirudin to poly(ethylene terephthalate) (Dacron): creation of a novel antithrombin surface ». *Biomaterials*, vol. 18, n° 10, p. 755-765.
- Pierschbacher, M. D., et E. Ruoslahti. 1984. « Cell attachment activity of fibronectin can be duplicated by small synthetic fragments of the molecule ». *Nature*, vol. 309, n° 5963, p. 30-3.
- Plopper, G. E., H. P. McNamee, L. E. Dike, K. Bojanowski et D. E. Ingber. 1995. « Convergence of integrin and growth factor receptor signaling pathways within the focal adhesion complex ». *Molecular Biology of the Cell*, vol. 6, n° 10, p. 1349-65.
- Plow, Edward F., Thomas A. Haas, Li Zhang, Joseph Loftus et Jeffrey W. Smith. 2000. « Ligand Binding to Integrins ». *Journal of Biological Chemistry*, vol. 275, n° 29, p. 21785-21788.
- Pompe, Tilo, Kristin Keller, Gisela Mothes, Mirko Nitschke, Mark Teese, Ralf Zimmermann et Carsten Werner. 2007. « Surface modification of poly(hydroxybutyrate) films to control cell-matrix adhesion ». *Biomaterials*, vol. 28, n° 1, p. 28-37.
- Pompe, Tilo, Fritz Kobe, Katrin Salchert, Birgitte Jørgensen, Joachim Oswald et Carsten Werner. 2003. « Fibronectin anchorage to polymer substrates controls the initial phase of endothelial cell adhesion ». *Journal of Biomedical Materials Research Part A*, vol. 67A, n° 2, p. 647-657.
- Pu, F. R., R. L. Williams, T. K. Markkula et J. A. Hunt. 2002a. « Effects of plasma treated PET and PTFE on expression of adhesion molecules by human endothelial cells in vitro ». *Biomaterials*, vol. 23, n° 11, p. 2411-28.
- Pu, F. R., R. L. Williams, T. K. Markkula et J. A. Hunt. 2002b. « Effects of plasma treated PET and PTFE on expression of adhesion molecules by human endothelial cells in vitro ». *Biomaterials*, vol. 23, n° 11, p. 2411-2428.
- Qu, Xiang-Hua, Qiong Wu, Juan Liang, Xue Qu, Shen-Guo Wang et Guo-Qiang Chen. 2005. « Enhanced vascular-related cellular affinity on surface modified copolyesters of 3-hydroxybutyrate and 3-hydroxyhexanoate (PHBHHx) ». *Biomaterials*, vol. 26, n° 34, p. 6991-7001.
- Quirk, R. A., W. C. Chan, M. C. Davies, S. J. Tendler et K. M. Shakesheff. 2001. « Poly(L-lysine)-GRGDS as a biomimetic surface modifier for poly(lactic acid) ». *Biomaterials*, vol. 22, n° 8, p. 865-72.
- Raab, G., et M. Klagsbrun. 1997. « Heparin-binding EGF-like growth factor ». *Biochimica et Biophysica Acta (BBA) - Bioenergetics*, vol. 1333, n° 3, p. F179-99.

- Radomski, M. W., P. Vallance, G. Whitley, N. Foxwell et S. Moncada. 1993. « Platelet adhesion to human vascular endothelium is modulated by constitutive and cytokine induced nitric oxide ». *Cardiovascular Research*, vol. 27, n° 7, p. 1380-2.
- Ramirez, Francesco, et Daniel B. Rifkin. 2003. « Cell signaling events: a view from the matrix ». *Matrix Biology*, vol. 22, n° 2, p. 101-107.
- Ranieri, J. P., R. Bellamkonda, E. J. Bekos, T. G. Vargo, J. A. Gardella, Jr. et P. Aebischer. 1995. « Neuronal cell attachment to fluorinated ethylene propylene films with covalently immobilized laminin oligopeptides YIGSR and IKVAV. II ». *Journal of Biomedical Materials Research*, vol. 29, n° 6, p. 779-85.
- Rao, Srinivasa K., Krishna V. Reddy et Jon R. Cohen. 1996. « Role of Serine Proteases in Aneurysm Development ». *Annals of the New York Academy of Sciences*, vol. 800, n° 1, p. 131-137.
- Rathore, Animesh, Muriel Cleary, Yuji Naito, Kevin Rocco et Christopher Breuer. 2012. « Development of tissue engineered vascular grafts and application of nanomedicine ». *Wiley Interdisciplinary Reviews: Nanomedicine and Nanobiotechnology*, vol. 4, n° 3, p. 257-272.
- Ratner, B. D. 1993. « New ideas in biomaterials science--a path to engineered biomaterials ». *Journal of Biomedical Materials Research*, vol. 27, n° 7, p. 837-50.
- Ratner, Buddy D. 1995. « Surface modification of polymers: chemical, biological and surface analytical challenges ». *Biosensors and Bioelectronics*, vol. 10, n° 9-10, p. 797-804.
- Ratner Buddy, D. 2000. « Blood compatibility - a perspective ». *Journal of Biomaterials Science, Polymer Edition*, vol. 11, n° 11, p. 1107-1119.
- Ratner, Buddy D., et Stephanie J. Bryant. 2004. « Biomaterials: Where We Have Been and Where We are Going ». *Annual Review of Biomedical Engineering*, vol. 6, n° 1, p. 41-75.
- Raymond, M. A., A. Desormeaux, P. Laplante, N. Vigneault, J. G. Filep, K. Landry, A. V. Pshezhetsky et M. J. Hebert. 2004. « Apoptosis of endothelial cells triggers a caspase-dependent anti-apoptotic paracrine loop active on VSMC ». *FASEB Journal*, vol. 18, n° 6, p. 705-7.
- Reape, T. J., V. J. Wilson, J. M. Kanczler, J. P. Ward, K. G. Burnand et C. R. Thomas. 1997. « Detection and cellular localization of heparin-binding epidermal growth factor-like growth factor mRNA and protein in human atherosclerotic tissue ». *Journal of Molecular and Cellular Cardiology*, vol. 29, n° 6, p. 1639-48.

- Rechendorff, K., M. B. Hovgaard, M. Foss, V. P. Zhdanov et F. Besenbacher. 2006. « Enhancement of Protein Adsorption Induced by Surface Roughness ». *Langmuir*, vol. 22, n° 26, p. 10885-10888.
- Rémy, Murielle, Reine Bareille, Vincent Rerat, Chantal Bourget, Jacqueline Marchand-Brynaert et Laurence Bordenave. 2012. « Polyethylene terephthalate membrane grafted with peptidomimetics: endothelial cell compatibility and retention under shear stress ». *Journal of Biomaterials Science, Polymer Edition*, vol. 24, n° 3, p. 269-286.
- Reynolds, Cherilynn M., Satoru Eguchi, Gerald D. Frank et Evangeline D. Motley. 2002. « Signaling Mechanisms of Heparin-Binding Epidermal Growth Factor-Like Growth Factor in Vascular Smooth Muscle Cells ». *Hypertension*, vol. 39, n° 2, p. 525-529.
- Rezania, Alireza, Robert Johnson, Anthony R. Lefkow et Kevin E. Healy. 1999. « Bioactivation of Metal Oxide Surfaces. 1. Surface Characterization and Cell Response ». *Langmuir*, vol. 15, n° 20, p. 6931-6939.
- Ritter, E. F., M. M. Fata, A. M. Rudner et B. Klitzman. 1998. « Heparin bonding increases patency of long microvascular prostheses ». *Plastic and Reconstructive Surgery*, vol. 101, n° 1, p. 142-6.
- Roach, Paul, David Farrar et Carole C. Perry. 2005. « Interpretation of Protein Adsorption: Surface-Induced Conformational Changes ». *Journal of the American Chemical Society*, vol. 127, n° 22, p. 8168-8173.
- Roach, Paul, David Farrar et Carole C. Perry. 2006. « Surface Tailoring for Controlled Protein Adsorption: Effect of Topography at the Nanometer Scale and Chemistry ». *Journal of the American Chemical Society*, vol. 128, n° 12, p. 3939-3945.
- Rodahl, Michael, Fredrik Hook, Claes Fredriksson, Craig A. Keller, Anatol Krozer, Peter Brzezinski, Marina Voinova et Bengt Kasemo. 1997a. « Simultaneous frequency and dissipation factor QCM measurements of biomolecular adsorption and cell adhesion ». *Faraday Discussions*, vol. 107, p. 229-246.
- Rodahl, Michael, Fredrik Hook, Claes Fredriksson, Craig A. Keller, Anatol Krozer, Peter Brzezinski, Marina Voinova et Bengt Kasemo. 1997b. « Simultaneous frequency and dissipation factor QCM measurements of biomolecular adsorption and cell adhesion ». *Faraday Discussions*, vol. 107, n° 0, p. 229-246.
- Rodahl, Michael, Fredrik Höök, Anatol Krozer, Peter Brzezinski et Bengt Kasemo. 1995. « Quartz crystal microbalance setup for frequency and Q-factor measurements in gaseous and liquid environments ». *Review of Scientific Instruments*, vol. 66, n° 7, p. 3924-3930.

- Rodrigues, Sofia N., Inês C. Gonçalves, M. C. L. Martins, Mário A. Barbosa et Buddy D. Ratner. 2006. « Fibrinogen adsorption, platelet adhesion and activation on mixed hydroxyl-/methyl-terminated self-assembled monolayers ». *Biomaterials*, vol. 27, n° 31, p. 5357-5367.
- Roll, S., J. Muller-Nordhorn, T. Keil, H. Scholz, D. Eidt, W. Greiner et S. N. Willich. 2008. « Dacron vs. PTFE as bypass materials in peripheral vascular surgery--systematic review and meta-analysis ». *BMC Surgery*, vol. 8, p. 22.
- Ruben Y. Kannan, Henryk J. Salacinski, Peter E. Butler, George Hamilton et Alexander M. Seifalian. 2005. « Current status of prosthetic bypass grafts: A review ». *Journal of Biomedical Materials Research Part B: Applied Biomaterials*, vol. 74B, n° 1, p. 570-581.
- Ruggeri, Z. M. 1997. « Mechanisms initiating platelet thrombus formation ». *Thrombosis and Haemostasis*, vol. 78, n° 1, p. 611-6.
- Ruggeri, Z. M. 2009. « Platelet adhesion under flow ». *Microcirculation*, vol. 16, n° 1, p. 58-83.
- Ruiz, Juan-Carlos, Amélie St-Georges-Robillard, Charles Thérésy, Sophie Lerouge et Michael R. Wertheimer. 2010. « Fabrication and Characterisation of Amine-Rich Organic Thin Films: Focus on Stability ». *Plasma Processes and Polymers*, vol. 7, n° 9-10, p. 737-753.
- Ruoslahti, E. 1996. « RGD and other recognition sequences for integrins ». *Annual Review of Cell and Developmental Biology*, vol. 12, p. 697-715.
- Sabra, Georges, et Patrick Vermette. 2011. « Endothelial cell responses towards low-fouling surfaces bearing RGD in a three-dimensional environment ». *Experimental Cell Research*, vol. 317, n° 14, p. 1994-2006.
- Sacks, M. S., F. J. Schoen et J. E. Mayer. 2009. « Bioengineering challenges for heart valve tissue engineering ». *Annual Review of Biomedical Engineering*, vol. 11, p. 289-313.
- Sagnella, S. M., F. Kligman, E. H. Anderson, J. E. King, G. Murugesan, R. E. Marchant et K. Kottke-Marchant. 2004. « Human microvascular endothelial cell growth and migration on biomimetic surfactant polymers ». *Biomaterials*, vol. 25, n° 7-8, p. 1249-59.
- Sakalihasan, N., R. Limet et O. D. Defawe. 2005. « Abdominal aortic aneurysm ». *The Lancet*, vol. 365, n° 9470, p. 1577-1589.

- Sakiyama-Elbert, S. E., et J. A. Hubbell. 2000. « Development of fibrin derivatives for controlled release of heparin-binding growth factors ». *Journal of Controlled Release*, vol. 65, n° 3, p. 389-402.
- Salacinski, H. J., S. Goldner, A. Giudiceandrea, G. Hamilton, A. M. Seifalian, A. Edwards et R. J. Carson. 2001. « The mechanical behavior of vascular grafts: a review ». *Journal of Biomaterials Applications*, vol. 15, n° 3, p. 241-78.
- Sask, Kyla N., W. Glenn McClung, Leslie R. Berry, Anthony K. C. Chan et John L. Brash. 2011. « Immobilization of an antithrombin–heparin complex on gold: Anticoagulant properties and platelet interactions ». *Acta Biomaterialia*, vol. 7, n° 5, p. 2029-2034.
- Satulovsky, J., M. A. Carignano et I. Szleifer. 2000. « Kinetic and thermodynamic control of protein adsorption ». *Proceedings of the National Academy of Sciences*, vol. 97, n° 16, p. 9037-9041.
- Sauerbrey, Günter. 1959. « Verwendung von Schwingquarzen zur Wägung dünner Schichten und zur Mikrowägung ». *Zeitschrift für Physik*, vol. 155, n° 2, p. 206-222.
- Schliephake, Henning, Dieter Scharnweber, Michael Dard, Sophie Rößler, Andreas Sewing, Jörg Meyer et Dennis Hoogestraat. 2002. « Effect of RGD peptide coating of titanium implants on periimplant bone formation in the alveolar crest ». *Clinical Oral Implants Research*, vol. 13, n° 3, p. 312-319.
- Schmaier, A. H. 1997. « Contact activation: a revision ». *Thrombosis and Haemostasis*, vol. 78, n° 1, p. 101-7.
- Schmitz, T., M. Rothe et J. Dodt. 1991. « Mechanism of the inhibition of alpha-thrombin by hirudin-derived fragments hirudin(1-47) and hirudin(45-65) ». *European Journal of Biochemistry*, vol. 195, n° 1, p. 251-6.
- Sebra, Robert P., Kristyn S. Masters, Christopher N. Bowman et Kristi S. Anseth. 2005. « Surface Grafted Antibodies: Controlled Architecture Permits Enhanced Antigen Detection ». *Langmuir*, vol. 21, n° 24, p. 10907-10911.
- Seifert, B., P. Romaniuk et Th Groth. 1997. « Covalent immobilization of hirudin improves the haemocompatibility of polylactide—polyglycolide in vitro ». *Biomaterials*, vol. 18, n° 22, p. 1495-1502.
- Shah, P. K. 1997. « Inflammation, metalloproteinases, and increased proteolysis: an emerging pathophysiological paradigm in aortic aneurysm ». *Circulation*, vol. 96, n° 7, p. 2115-7.
- Shen, Mingchao, Matthew S. Wagner, David G. Castner, Buddy D. Ratner et Thomas A. Horbett. 2003. « Multivariate Surface Analysis of Plasma-Deposited Tetraglyme for

- Reduction of Protein Adsorption and Monocyte Adhesion† ». *Langmuir*, vol. 19, n° 5, p. 1692-1699.
- Sherrill, Jennifer Miller, et Jack Kyte. 1996. « Activation of Epidermal Growth Factor Receptor by Epidermal Growth Factor† ». *Biochemistry*, vol. 35, n° 18, p. 5705-5718.
- Shi, Qun, Moses Hong-De Wu, Yoko Onuki, Rafik Ghali, Glenn C. Hunter, Kaj H. Johansen et Lester R. Sauvage. 1997. « Endothelium on the flow surface of human aortic Dacron vascular grafts ». *Journal of Vascular Surgery*, vol. 25, n° 4, p. 736-742.
- Shin, Heungsoo, Seongbong Jo et Antonios G. Mikos. 2003. « Biomimetic materials for tissue engineering ». *Biomaterials*, vol. 24, n° 24, p. 4353-4364.
- Sieg, D. J., C. R. Hauck, D. Ilic, C. K. Klingbeil, E. Schaefer, C. H. Damsky et D. D. Schlaepfer. 2000. « FAK integrates growth-factor and integrin signals to promote cell migration ». *Nature Cell Biology*, vol. 2, n° 5, p. 249-56.
- Siow, Kim Shyong, Leanne Britcher, Sunil Kumar et Hans J. Griesser. 2006. « Plasma Methods for the Generation of Chemically Reactive Surfaces for Biomolecule Immobilization and Cell Colonization - A Review ». *Plasma Processes and Polymers*, vol. 3, n° 6-7, p. 392-418.
- Smith, J. T., J. T. Elkin et W. M. Reichert. 2006. « Directed cell migration on fibronectin gradients: effect of gradient slope ». *Experimental Cell Research*, vol. 312, n° 13, p. 2424-32.
- Sofia Susan, J., et W. Merrill Edward. 1997. « Protein Adsorption on Poly(ethylene oxide)-Grafted Silicon Surfaces ». *Poly(ethylene glycol)*, vol. 680, n° 680, p. 342-360.
- Sofia, Susan J., V. Premnath et Edward W. Merrill. 1998. « Poly(ethylene oxide) Grafted to Silicon Surfaces: Grafting Density and Protein Adsorption ». *Macromolecules*, vol. 31, n° 15, p. 5059-5070.
- Soldi, R., S. Mitola, M. Strasly, P. Defilippi, G. Tarone et F. Bussolino. 1999. « Role of alphavbeta3 integrin in the activation of vascular endothelial growth factor receptor-2 ». *EMBO Journal*, vol. 18, n° 4, p. 882-92.
- Sorkin, A., et M. Von Zastrow. 2002. « Signal transduction and endocytosis: close encounters of many kinds ». *Nature Reviews: Molecular Cell Biology*, vol. 3, n° 8, p. 600-14.
- Sottile, J. 2004. « Regulation of angiogenesis by extracellular matrix ». *Biochimica et Biophysica Acta (BBA) - Bioenergetics*, vol. 1654, n° 1, p. 13-22.

- Sporn, E., K. Kubin, T. Hoblaj, M. Ploner, H. J. Böhmig, J. Nanobashvili, I. Huk, M. R. Prager et P. Polterauer. 2008. « Dacron grafts dilate more than Stretch PTFE grafts after abdominal aortic aneurysm repair – long-term results of a prospective randomized trial ». *European Surgery*, vol. 40, n° 2, p. 66-71.
- Srokowski, ElizabethM, et KimberlyA Woodhouse. 2013. « Surface and adsorption characteristics of three elastin-like polypeptide coatings with varying sequence lengths ». *Journal of Materials Science: Materials in Medicine*, vol. 24, n° 1, p. 71-84.
- Stary, Herbert C., A. Bleakley Chandler, Robert E. Dinsmore, Valentin Fuster, Seymour Glagov, William Insull, Michael E. Rosenfeld, Colin J. Schwartz, William D. Wagner et Robert W. Wissler. 1995. « A Definition of Advanced Types of Atherosclerotic Lesions and a Histological Classification of Atherosclerosis: A Report From the Committee on Vascular Lesions of the Council on Arteriosclerosis, American Heart Association ». *Circulation*, vol. 92, n° 5, p. 1355-1374.
- Stearns-Kurosawa, D. J., S. Kurosawa, J. S. Mollica, G. L. Ferrell et C. T. Esmon. 1996. « The endothelial cell protein C receptor augments protein C activation by the thrombin-thrombomodulin complex ». *Proceedings of the National Academy of Sciences of the United States of America*, vol. 93, n° 19, p. 10212-6.
- Steele, J. G., G. Johnson, C. McFarland, B. A. Dalton, T. R. Gengenbach, R. C. Chatelier, P. A. Underwood et H. J. Griesser. 1994. « Roles of serum vitronectin and fibronectin in initial attachment of human vein endothelial cells and dermal fibroblasts on oxygen- and nitrogen-containing surfaces made by radiofrequency plasmas ». *Journal of Biomaterials Science, Polymer Edition*, vol. 6, n° 6, p. 511-32.
- Stile, R. A., et K. E. Healy. 2001. « Thermo-responsive peptide-modified hydrogels for tissue regeneration ». *Biomacromolecules*, vol. 2, n° 1, p. 185-94.
- Stupack, D. G., et D. A. Cheresh. 2004. « Integrins and Angiogenesis ». *Current Topics in Developmental Biology*. Vol. Volume 64, p. 207-238. Academic Press.
- Sun, L. B., J. Utoh, S. Moriyama, H. Tagami, K. Okamoto et N. Kitamura. 2001. « Pretreatment of a Dacron graft with tissue factor pathway inhibitor decreases thrombogenicity and neointimal thickness: a preliminary animal study ». *ASAIO Journal*, vol. 47, n° 4, p. 325-8.
- Swingle, Robert S. 1975. « Quantitative surface analysis by x-ray photoelectron spectroscopy (ESCA) ». *Analytical Chemistry*, vol. 47, n° 1, p. 21-24.
- Tay, S. W., E. W. Merrill, E. W. Salzman et J. Lindon. 1989. « Activity toward thrombin-antithrombin of heparin immobilized on two hydrogels ». *Biomaterials*, vol. 10, n° 1, p. 11-5.

- Taylor, John M., William M. Mitchell et Stanley Cohen. 1972. « Epidermal Growth Factor: Physical and Chemical properties ». *Journal of Biological Chemistry*, vol. 247, n° 18, p. 5928-5934.
- Thalla, Pradeep K., Hicham Fadlallah, Benoit Liberelle, Pauline Lequoy, Gregory De Crescenzo, Yahye Merhi et Sophie Lerouge. 2014. « Chondroitin Sulfate Coatings Display Low Platelet but High Endothelial Cell Adhesive Properties Favorable for Vascular Implants ». *Biomacromolecules*, vol. 15, n° 7, p. 2512-2520.
- Thalla, Pradeep Kumar, Angel Contreras-Garcia, Hicham Fadlallah, Jeremie Barrette, Gregory De Crescenzo, Yahye Merhi et Sophie Lerouge. 2012. « A Versatile Star PEG Grafting Method for the Generation of Nonfouling and Nonthrombogenic Surfaces ». *BioMed Research International*, vol. 2013, p. 12.
- Thébaud, N. B., R. Bareille, R. Daculsi, Ch Bourget, M. Rémy, H. Kerdjoudj, P. Menu et L. Bordenave. 2010. « Polyelectrolyte multilayer films allow seeded human progenitor-derived endothelial cells to remain functional under shear stress in vitro ». *Acta Biomaterialia*, vol. 6, n° 4, p. 1437-1445.
- Thevenot, P., W. Hu et L. Tang. 2008. « Surface chemistry influences implant biocompatibility ». *Current Topics in Medicinal Chemistry*, vol. 8, n° 4, p. 270-80.
- Thomas, A. Horbett, et L. Brash John. 1987. « Proteins at Interfaces: Current Issues and Future Prospects ». *Proteins at Interfaces*. Vol. 343, p. 1-33. Coll. « ACS Symposium Series », 343: American Chemical Society.
- Thompson, Michael, Catherine L. Arthur et Gurbaksh K. Dhaliwal. 1986. « Liquid-phase piezoelectric and acoustic transmission studies of interfacial immunochemistry ». *Analytical Chemistry*, vol. 58, n° 6, p. 1206-1209.
- Thompson, Robert W., et William C. Parks. 1996. « Role of Matrix Metalloproteinases in Abdominal Aortic Aneurysms ». *Annals of the New York Academy of Sciences*, vol. 800, n° 1, p. 157-174.
- Tomizawa, Y. 1995. « Vascular prostheses for aortocoronary bypass grafting: a review ». *Artificial Organs*, vol. 19, n° 1, p. 39-45.
- Toufik, Jamila, Marie-Paule Carreno, Marcel Jozefowicz et Denis Labarre. 1995. « Activation of the complement system by polysaccharidic surfaces bearing carboxymethyl, carboxymethylbenzyl-amide and carboxymethylbenzylamide sulphonate groups ». *Biomaterials*, vol. 16, n° 13, p. 993-1002.
- Trail, PA, D Willner, SJ Lasch, AJ Henderson, S Hofstead, AM Casazza, RA Firestone, I Hellstrom et KE Hellstrom. 1993. « Cure of xenografted human carcinomas by BR96-doxorubicin immunoconjugates ». *Science*, vol. 261, n° 5118, p. 212-215.

- Truica-Marasescu, Florina, Pierre-Luc Girard-Lauriault, Andreas Lippitz, Wolfgang E. S. Unger et Michael R. Wertheimer. 2008. « Nitrogen-rich plasma polymers: Comparison of films deposited in atmospheric- and low-pressure plasmas ». *Thin Solid Films*, vol. 516, n° 21, p. 7406-7417.
- Tseng, Po-Yuan, Shyam S. Rele, Xue-Long Sun et Elliot L. Chaikof. 2006. « Membrane-mimetic films containing thrombomodulin and heparin inhibit tissue factor-induced thrombin generation in a flow model ». *Biomaterials*, vol. 27, n° 12, p. 2637-2650.
- Tugulu, Stefano, Paolo Silacci, Nikolaos Stergiopoulos et Harm-Anton Klok. 2007. « RGD—Functionalized polymer brushes as substrates for the integrin specific adhesion of human umbilical vein endothelial cells ». *Biomaterials*, vol. 28, n° 16, p. 2536-2546.
- Tymchenko, Nina, Erik Nilebäck, Marina V Voinova, Julie Gold, Bengt Kasemo et Sofia Svedhem. 2012. « Reversible Changes in Cell Morphology due to Cytoskeletal Rearrangements Measured in Real-Time by QCM-D ». *Biointerphases*, vol. 7, n° 1-4, p. 1-9.
- Ugarova, Tatiana P., Concepcion Zamarron, Yuri Veklich, Ron D. Bowditch, Mark H. Ginsberg, John W. Weisel et Edward F. Plow. 1995. « Conformational Transitions in the Cell Binding Domain of Fibronectin ». *Biochemistry*, vol. 34, n° 13, p. 4457-4466.
- Underwood, P. A., J. G. Steele et B. A. Dalton. 1993. « Effects of polystyrene surface chemistry on the biological activity of solid phase fibronectin and vitronectin, analysed with monoclonal antibodies ». *Journal of Cell Science*, vol. 104 ( Pt 3), p. 793-803.
- Underwood, P. Anne, et Frances A. Bennett. 1993. « The Effect of Extracellular Matrix Molecules on the in Vitro Behavior of Bovine Endothelial Cells ». *Experimental Cell Research*, vol. 205, n° 2, p. 311-319.
- Unsworth, Larry D., Heather Sheardown et John L. Brash. 2005. « Protein Resistance of Surfaces Prepared by Sorption of End-Thiolated Poly(ethylene glycol) to Gold: Effect of Surface Chain Density ». *Langmuir*, vol. 21, n° 3, p. 1036-1041.
- Unsworth, Larry D., Zin Tun, Heather Sheardown et John L. Brash. 2005. « Chemisorption of thiolated poly(ethylene oxide) to gold: surface chain densities measured by ellipsometry and neutron reflectometry ». *Journal of Colloid and Interface Science*, vol. 281, n° 1, p. 112-121.
- Vainionpaa, N., Y. Kikkawa, K. Lounatmaa, J. H. Miner, P. Rousselle et I. Virtanen. 2006. « Laminin-10 and Lutheran blood group glycoproteins in adhesion of human endothelial cells ». *American Journal of Physiology: Cell Physiology*, vol. 290, n° 3, p. C764-75.

- van Horssen, Remco, Niels Galjart, Joost A. P. Rens, Alexander M. M. Eggermont et Timo L. M. ten Hagen. 2006. « Differential effects of matrix and growth factors on endothelial and fibroblast motility: Application of a modified cell migration assay ». *Journal of Cellular Biochemistry*, vol. 99, n° 6, p. 1536-1552.
- van Wachem, P. B., C. M. Vreriks, T. Beugeling, J. Feijen, A. Bantjes, J. P. Detmers et W. G. van Aken. 1987. « The influence of protein adsorption on interactions of cultured human endothelial cells with polymers ». *Journal of Biomedical Materials Research*, vol. 21, n° 6, p. 701-718.
- Veith, F. J., C. M. Moss, S. Sprayregen et C. Montefusco. 1979. « Preoperative saphenous venography in arterial reconstructive surgery of the lower extremity ». *Surgery*, vol. 85, n° 3, p. 253-6.
- Vermette, Patrick, et Laurence Meagher. 2002. « Immobilization and Characterization of Poly(acrylic acid) Graft Layers ». *Langmuir*, vol. 18, n° 26, p. 10137-10145.
- Verrier, S., S. Pallu, R. Bareille, A. Jonczyk, J. Meyer, M. Dard et J. Amédée. 2002. « Function of linear and cyclic RGD-containing peptides in osteoprogenitor cells adhesion process ». *Biomaterials*, vol. 23, n° 2, p. 585-596.
- Vlahakis, Nicholas E., Bradford A. Young, Amha Atakilit, Anne E. Hawkrige, Rachel B. Issaka, Nancy Boudreau et Dean Sheppard. 2007. « Integrin  $\alpha 9 \beta 1$  Directly Binds to Vascular Endothelial Growth Factor (VEGF)-A and Contributes to VEGF-A-induced Angiogenesis ». *Journal of Biological Chemistry*, vol. 282, n° 20, p. 15187-15196.
- Voinova, M. V., M. Rodahl, M. Jonson et B. Kasemo. 1999. « Viscoelastic Acoustic Response of Layered Polymer Films at Fluid-Solid Interfaces: Continuum Mechanics Approach ». *Physica Scripta*, vol. 59, n° 5, p. 391.
- Vroman, Leo, et Ann L. Adams. 1969. « Identification of rapid changes at plasma–solid interfaces ». *Journal of Biomedical Materials Research*, vol. 3, n° 1, p. 43-67.
- Wagner, C.D. 1979. *Handbook of X-Ray and Ultraviolet Photoelectron Spectroscopy*, 1st Perkin-Elmer Corporation(Physical Electronics).
- Walluscheck, K. P., G. Steinhoff, S. Kelm et A. Haverich. 1996. « Improved endothelial cell attachment on ePTFE vascular grafts pretreated with synthetic RGD-containing peptides ». *Eur J Vasc Endovasc Surg*, vol. 12, n° 3, p. 321-30.
- Walpoth, B. H., R. Rogulenko, E. Tikhvinskaia, S. Gogolewski, T. Schaffner, O. M. Hess et U. Althaus. 1998. « Improvement of patency rate in heparin-coated small synthetic vascular grafts ». *Circulation*, vol. 98, n° 19 p. 11319-23; discussion 11324.

- Wang, Kai, et Ying Luo. 2013. « Defined Surface Immobilization of Glycosaminoglycan Molecules for Probing and Modulation of Cell–Material Interactions ». *Biomacromolecules*, vol. 14, n° 7, p. 2373-2382.
- Wang, Shudong, Youzhu Zhang, Hongwei Wang et Zhihui Dong. 2011a. « Preparation, characterization and biocompatibility of electrospinning heparin-modified silk fibroin nanofibers ». *International Journal of Biological Macromolecules*, vol. 48, n° 2, p. 345-353.
- Wang, Y. X., J. L. Robertson, W. B. Spillman, Jr. et R. O. Claus. 2004. « Effects of the chemical structure and the surface properties of polymeric biomaterials on their biocompatibility ». *Pharmaceutical Research*, vol. 21, n° 8, p. 1362-73.
- Wang, Yan-Yan, Lan-Xin Lü, Jun-Cai Shi, Hai-Feng Wang, Zhong-Dang Xiao et Ning-Ping Huang. 2011b. « Introducing RGD Peptides on PHBV Films through PEG-Containing Cross-Linkers to Improve the Biocompatibility ». *Biomacromolecules*, vol. 12, n° 3, p. 551-559.
- Wary, K. K., F. Mainiero, S. J. Isakoff, E. E. Marcantonio et F. G. Giancotti. 1996. « The adaptor protein Shc couples a class of integrins to the control of cell cycle progression ». *Cell*, vol. 87, n° 4, p. 733-43.
- Wary, K. K., A. Mariotti, C. Zurzolo et F. G. Giancotti. 1998. « A requirement for caveolin-1 and associated kinase Fyn in integrin signaling and anchorage-dependent cell growth ». *Cell*, vol. 94, n° 5, p. 625-34.
- Weber, N., H. P. Wendel et J. Kohn. 2005a. « Formation of viscoelastic protein layers on polymeric surfaces relevant to platelet adhesion ». *Journal of Biomedical Materials Research, Part A*, vol. 72, n° 4, p. 420-7.
- Weber, Norbert, Aaron Pesnell, Durgadas Bolikal, Joan Zeltinger et Joachim Kohn. 2007. « Viscoelastic Properties of Fibrinogen Adsorbed to the Surface of Biomaterials Used in Blood-Contacting Medical Devices ». *Langmuir*, vol. 23, n° 6, p. 3298-3304.
- Weber, Norbert, Hans Peter Wendel et Joachim Kohn. 2005b. « Formation of viscoelastic protein layers on polymeric surfaces relevant to platelet adhesion ». *Journal of Biomedical Materials Research Part A*, vol. 72A, n° 4, p. 420-427.
- Wegener, Joachim, Jochen Seebach, Andreas Janshoff et Hans-Joachim Galla. 2000. « Analysis of the Composite Response of Shear Wave Resonators to the Attachment of Mammalian Cells ». *Biophysical Journal*, vol. 78, n° 6, p. 2821-2833.
- Weis, Christine, Erich K. Odermatt, Jörg Kressler, Zofia Funke, Tim Wehner et Dorothee Freytag. 2004. « Poly(vinyl alcohol) membranes for adhesion prevention ». *Journal*

*of Biomedical Materials Research Part B: Applied Biomaterials*, vol. 70B, n° 2, p. 191-202.

Veillez sélectionner un type de document autre que « Generic » afin de faire afficher la référence bibliographique.

WHO. 2013. « Cardiovascular diseases (CVDs) ». < <http://www.who.int/mediacentre/factsheets/fs317/en/> >.

Wilcox, J N, K M Smith, S M Schwartz et D Gordon. 1989. « Localization of tissue factor in the normal vessel wall and in the atherosclerotic plaque ». *Proceedings of the National Academy of Sciences*, vol. 86, n° 8, p. 2839-2843.

Williams, David F. 2008. « On the mechanisms of biocompatibility ». *Biomaterials*, vol. 29, n° 20, p. 2941-2953.

Wissink, M. J. B., R. Beernink, A. A. Poot, G. H. M. Engbers, T. Beugeling, W. G. van Aken et J. Feijen. 2001. « Relation between cell density and the secretion of von Willebrand factor and prostacyclin by human umbilical vein endothelial cells ». *Biomaterials*, vol. 22, n° 16, p. 2283-2290.

Wissink, M. J. B., R. Beernink, N. M. Scharenborg, A. A. Poot, G. H. M. Engbers, T. Beugeling, W. G. van Aken et J. Feijen. 2000a. « Endothelial cell seeding of (heparinized) collagen matrices: effects of bFGF pre-loading on proliferation (after low density seeding) and pro-coagulant factors ». *Journal of Controlled Release*, vol. 67, n° 2-3, p. 141-155.

Wissink, M. J., M. J. van Luyn, R. Beernink, F. Dijk, A. A. Poot, G. H. Engbers, T. Beugeling, W. G. van Aken et J. Feijen. 2000b. « Endothelial cell seeding on crosslinked collagen: effects of crosslinking on endothelial cell proliferation and functional parameters ». *Thrombosis and Haemostasis*, vol. 84, n° 2, p. 325-31.

Wong, Joyce Y., Tonya L. Kuhl, Jacob N. Israelachvili, Nasreen Mullah et Samuel Zalipsky. 1997. « Direct Measurement of a Tethered Ligand-Receptor Interaction Potential ». *Science*, vol. 275, n° 5301, p. 820-822.

Wu, M. H., Y. Kouchi, Y. Onuki, Q. Shi, H. Yoshida, S. Kaplan, R. F. Viggers, R. Ghali et L. R. Sauvage. 1995. « Effect of differential shear stress on platelet aggregation, surface thrombosis, and endothelialization of bilateral carotid-femoral grafts in the dog ». *Journal of Vascular Surgery*, vol. 22, n° 4, p. 382-90; discussion 390-2.

Wu, Yuguang, Felix I. Simonovsky, Buddy D. Ratner et Thomas A. Horbett. 2005. « The role of adsorbed fibrinogen in platelet adhesion to polyurethane surfaces: A comparison of surface hydrophobicity, protein adsorption, monoclonal antibody

- binding, and platelet adhesion ». *Journal of Biomedical Materials Research Part A*, vol. 74A, n° 4, p. 722-738.
- Wyers, Mark C., Matthew D. Phaneuf, Eva M. Rzuclidlo, Mauricio A. Contreras, Frank W. LoGerfo et William C. Quist. 1999. « In Vivo Assessment of a Novel Dacron Surface with Covalently Bound Recombinant Hirudin ». *Cardiovascular Pathology*, vol. 8, n° 3, p. 153-159.
- Xu, F. J., Y. L. Li, E. T. Kang et K. G. Neoh. 2005. « Heparin-Coupled Poly(poly(ethylene glycol) monomethacrylate)-Si(111) Hybrids and Their Blood Compatible Surfaces ». *Biomacromolecules*, vol. 6, n° 3, p. 1759-1768.
- Yamada, Kenneth M., et Sharona Even-Ram. 2002. « Integrin regulation of growth factor receptors ». *Nature Cell Biology*, vol. 4, n° 4, p. E75-E76.
- Yanai, R., N. Yamada, N. Kugimiya, M. Inui et T. Nishida. 2002. « Mitogenic and antiapoptotic effects of various growth factors on human corneal fibroblasts ». *Investigative Ophthalmology and Visual Science*, vol. 43, n° 7, p. 2122-6.
- Yang, Zhihao, Jeffrey A. Galloway et Hyuk Yu. 1999. « Protein Interactions with Poly(ethylene glycol) Self-Assembled Monolayers on Glass Substrates: Diffusion and Adsorption ». *Langmuir*, vol. 15, n° 24, p. 8405-8411.
- Yeager, Anson, et Aalland Callow. 1988. « New Graft Materials and Current Approaches to an Acceptable Small Diameter Vascular Graft ». *American Society for Artificial Internal Organs*, vol. 34, n° 2, p. 88-94.
- Zamir, E., et B. Geiger. 2001a. « Molecular complexity and dynamics of cell-matrix adhesions ». *Journal of Cell Science*, vol. 114, n° Pt 20, p. 3583-90.
- Zamir, Eli, et Benjamin Geiger. 2001b. « Molecular complexity and dynamics of cell-matrix adhesions ». *Journal of Cell Science*, vol. 114, n° 20, p. 3583-3590.
- Zankl, A. R., H. Schumacher, U. Krumsdorf, H. A. Katus, L. Jahn et C. P. Tiefenbacher. 2007. « Pathology, natural history and treatment of abdominal aortic aneurysms ». *Clinical Research in Cardiology*, vol. 96, n° 3, p. 140-51.
- Zhang, Min, et Thomas A. Horbett. 2009. « Tetraglyme coatings reduce fibrinogen and von Willebrand factor adsorption and platelet adhesion under both static and flow conditions ». *Journal of Biomedical Materials Research Part A*, vol. 89A, n° 3, p. 791-803.
- Zhang, Miqin, Tejal Desai et Mauro Ferrari. 1998. « Proteins and cells on PEG immobilized silicon surfaces ». *Biomaterials*, vol. 19, n° 10, p. 953-960.

- Zhang, W. J., W. Liu, L. Cui et Y. Cao. 2007. « Tissue engineering of blood vessel ». *Journal of Cellular and Molecular Medicine*, vol. 11, n° 5, p. 945-57.
- Zhang, Z., M. Zhang, S. Chen, T. A. Horbett, B. D. Ratner et S. Jiang. 2008a. « Blood compatibility of surfaces with superlow protein adsorption ». *Biomaterials*, vol. 29, n° 32, p. 4285-91.
- Zhang, Zheng, Shengfu Chen, Yung Chang et Shaoyi Jiang. 2006. « Surface Grafted Sulfobetaine Polymers via Atom Transfer Radical Polymerization as Superlow Fouling Coatings ». *The Journal of Physical Chemistry B*, vol. 110, n° 22, p. 10799-10804.
- Zhang, Zheng, Min Zhang, Shengfu Chen, Thomas A. Horbett, Buddy D. Ratner et Shaoyi Jiang. 2008b. « Blood compatibility of surfaces with superlow protein adsorption ». *Biomaterials*, vol. 29, n° 32, p. 4285-4291.
- Zhao, Changsheng, Xiangdong Liu, Motoyoshi Nomizu et Norio Nishi. 2003. « Blood compatible aspects of DNA-modified polysulfone membrane - protein adsorption and platelet adhesion ». *Biomaterials*, vol. 24, n° 21, p. 3747-3755.
- Zheng, Jie, Lingyan Li, Heng-Kwong Tsao, Yu-Jane Sheng, Shenfu Chen et Shaoyi Jiang. 2005. « Strong Repulsive Forces between Protein and Oligo (Ethylene Glycol) Self-Assembled Monolayers: A Molecular Simulation Study ». *Biophysical Journal*, vol. 89, n° 1, p. 158-166.
- Zhou, Jun, Jiang Yuan, Xiaopeng Zang, Jian Shen et Sicong Lin. 2005. « Platelet adhesion and protein adsorption on silicone rubber surface by ozone-induced grafted polymerization with carboxybetaine monomer ». *Colloids and Surfaces B: Biointerfaces*, vol. 41, n° 1, p. 55-62.
- Zhu, Boru, Thomas Eurell, Rico Gunawan et Deborah Leckband. 2001. « Chain-length dependence of the protein and cell resistance of oligo(ethylene glycol)-terminated self-assembled monolayers on gold ». *Journal of Biomedical Materials Research*, vol. 56, n° 3, p. 406-416.
- Zhu, Junmin, Chad Tang, Kandice Kottke-Marchant et Roger E. Marchant. 2009. « Design and Synthesis of Biomimetic Hydrogel Scaffolds with Controlled Organization of Cyclic RGD Peptides ». *Bioconjugate Chemistry*, vol. 20, n° 2, p. 333-339.
- Zilla, P., U. von Oppell et M. Deutsch. 1993. « The endothelium: a key to the future ». *Journal of Cardiac Surgery*, vol. 8, n° 1, p. 32-60.